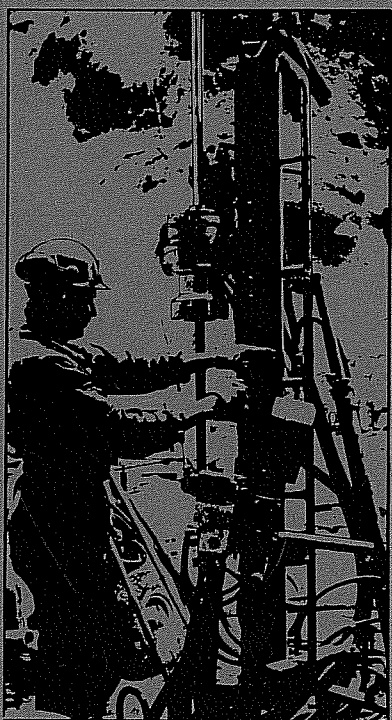


SWEDISH-AMERICAN COOPERATIVE PROGRAM ON RADIOACTIVE WASTE STORAGE IN MINED CAVERNS IN CRYSTALLINE ROCK



Technical Information Report No. 29

THERMAL AND THERMOMECHANICAL DATA FROM IN SITU HEATER EXPERIMENTS AT STRIPA, SWEDEN

Tin Chan, Eugene Binnall, Philip Nelson,
Robert Stolzman, Oliver Wan, Christopher Weaver,
Kam Ang, James Braley, and Maurice McEvoy

Lawrence Berkeley Laboratory
University of California
Berkeley, California 94720

September 1980

A Joint Project of

Swedish Nuclear Fuel Supply Co.
Fack 10240 Stockholm, Sweden

Operated for the Swedish
Nuclear Power Utility Industry

Lawrence Berkeley Laboratory
Earth Sciences Division
University of California
Berkeley, California 94720, USA

Operated for the U.S. Department of
Energy under Contract W-7405-ENG-48

This report was prepared as an account of work sponsored by the United States Government and/or the Swedish Nuclear Fuel Supply Company. Neither the United States nor the U.S. Department of Energy, nor the Swedish Nuclear Fuel Supply Company, nor any of their employees, nor any of their contractors, subcontractors, or their employees, makes any warranty, express or implied or assumes any legal liability or responsibility for the accuracy, completeness or usefulness of any information, apparatus, product or process disclosed, or represents that its use would not infringe privately owned rights.

Printed in the United States of America
Available from
National Technical Information Service
U.S. Department of Commerce
5285 Port Royal Road
Springfield, VA 22161
Price Code: A11

LBL-11477
SAC-29
UC-70

THERMAL AND THERMOMECHANICAL DATA FROM IN SITU
HEATER EXPERIMENTS AT STRIPA, SWEDEN

Tin Chan, Eugene Binnall, Philip Nelson, Robert Stolzman, Oliver Wan
Christopher Weaver, Kam Ang, James Braley, and Maurice McEvoy
Lawrence Berkeley Laboratory
University of California
Berkeley, California 94720

September, 1980

This report was prepared by Lawrence Berkeley Laboratory under the University of California Contract W-7405-ENG-48 with the Department of Energy. The contract is administered by the Office of Nuclear Waste Isolation at Battelle Memorial Institute, Columbus, Ohio.

PREFACE

This report is one of a series documenting the results of the Swedish-American cooperative research program in which the cooperating scientists explore the geological, geophysical, hydrological, geochemical, and structural effects anticipated from the use of a large crystalline rock mass as a geologic repository for nuclear waste. This program has been sponsored by the Swedish Nuclear Power Utilities through the Swedish Nuclear Fuel Supply Company (SKBF), and the U.S. Department of Energy (DOE) through the Lawrence Berkeley Laboratory.

The principal investigators are L.B. Nilsson and O. Degerman for SKBF, and N.G.W. Cook, P.A. Witherspoon, and J.E. Gale for LBL. Other participants will appear as authors of the individual reports.

Previous technical reports in this series are listed below.

1. Swedish-American Cooperative Program on Radioactive Waste Storage in Mined Caverns by P.A. Witherspoon and O. Degerman. (LBL-7049, SAC-01).
2. Large Scale Permeability Test of the Granite in the Stripa Mine and Thermal Conductivity Test by Lars Lundstrom and Haken Stille. (LBL-7052, SAC-02).
3. The Mechanical Properties of the Stripa Granite by Graham Swan (LBL-7074, SAC-03).
4. Stress Measurements in the Stripa Granite by Hans Carlsson (LBL-7078, SAC-04).
5. Borehole Drilling and Related Activities at the Stripa Mine by P.J. Kurfurst, T. Hugo-Persson, and G. Rudolph (LBL-7080, SAC-05).
6. A Pilot Heater Test in the Stripa Granite by Hans Carlsson (LBL-7086, SAC-06).
7. An Analysis of Measured Values for the State of Stress in the Earth's Crust by Dennis B. Jamison and Neville G.W. Cook (LBL-7071, SAC-07).
8. Mining Methods Used in the Underground Tunnels and Test Rooms at Stripa by B. Andersson and P.A. Halen (LBL-7081, SAC-08).
9. Theoretical Temperature Fields for the Stripa Heater Project by T. Chan, Neville G.W. Cook, and C.F. Tsang (LBL-7082, SAC-09).
10. Mechanical and Thermal Design Considerations for Radioactive Waste Repositories in Hard Rock. Part I: An Appraisal of Hard Rock for Potential Underground Repositories of Radioactive Waste by N.G.W. Cook; Part II: In Situ Heating Experiments in Hard Rock: Their Objectives and Design by N.G.W. Cook and P.A. Witherspoon (LBL-7073, SAC-10).
11. Full-Scale and Time-Scale Heating Experiments at Stripa: Preliminary Results by N.G.W. Cook and M. Hood (LBL-7072; SAC-11).

12. Geochemistry and Isotope Hydrology of Groundwaters in the Stripa Granite: Results and Preliminary Interpretation by P. Fritz, Barker, and J.E. Gale (LBL-8285, SAC-12).
13. Electrical Heaters for Thermo-Mechanical Tests at the Stripa Mine by R.H. Burleigh, E.P. Binnall, A.O. DuBois, D.O. Norgren, and A.R. Ortiz (LBL-7063, SAC-13).
14. Data Acquisition, Handling, and Display for the Heater Experiments at Stripa by Maurice B. McEvoy (LBL-7062, SAC-14).
15. An Approach to the Fracture Hydrology at Stripa: Preliminary Results by J.E. Gale and P.A. Witherspoon (LBL-7079, SAC-15).
16. Preliminary Report on Geophysical and Mechanical Borehole Measurements at Stripa by P. Nelson, B. Paulsson, R. Rachiele, L. Andersson, T. Schrauf, W. Hustrulid, O. Duran, and K.A. Magnussen (LBL-8280, SAC-16).
17. Observations of a Potential Size-Effect in Experimental Determination of the Hydraulic Properties of Fractures by P.A. Witherspoon, C.H. Amick, J.E. Gale, and K. Iwai (LBL-8571, SAC-17).
18. Rock Mass Characterization for Storage in Nuclear Waste in Granite by P.A. Witherspoon, P. Nelson, T. Doe, R. Thorpe, B. Paulsson, J.E. Gale, and C. Forster (LBL-8570, SAC-18).
19. Fracture Detection in Crystalline Rock Using Ultrasonic Shear Waves by K.H. Waters, S.P. Palmer, and W.F. Farrell (LBL-7051, SAC-19).
20. Characterization of Discontinuities in the Stripa Granite--Time Scale Heater Experiment by R. Thorpe (LBL-7083, SAC-20).
21. Geology and Fracture System at Stripa by A. Olkiewicz, J.E. Gale, R. Thorpe, and B. Paulsson (LBL-8907, SAC-21).
22. Calculated Thermally Induced Displacements and Stresses for Heater Experiments at Stripa by T. Chan and N.G.W. Cook (LBL-7061, SAC-22).
23. Validity of Cubic Law for Fluid Flow in a Deformable Rock Fracture by P.A. Witherspoon, J. Wang, K. Iwai and J.E. Gale (LBL-9557, SAC-23).
24. Determination of In-Situ Thermal Properties of Stripa Granite from Temperature Measurements in the Full-Scale Heater Experiments: Methods and Primary Results by J. Jeffry, T. Chan, N.G.W. Cook and P.A. Witherspoon (LBL-8424, SAC-24).
25. Instrumentation Evaluation, Calibration, and Installation for Heater Tests Simulating Nuclear Waste In Crystalline Rock, Sweden by T. Schrauf, H. Pratt, E. Simonson, W. Hustrulid, P. Nelson, A. DuBois, E. Binnall, and R. Haught (LBL-8313, SAC-25).

26. Part I: Some Results from a Field Investigation of Thermo-Mechanical Loading of a Rock Mass When Heater Canisters are Emplaced in the Rock by M. Hood. Part II: The Application of Field Data from Heater Experiments Conducted at Stripa, Sweden for Repository Design by M. Hood, H. Carlsson, and P.H. Nelson (LBL-9392, SAC-26).
27. Progress with Field Investigations at Stripa by P.A. Witherspoon, N.G.W. Cook, and J.E. Gale (LBL-10559, SAC-27).
28. A Laboratory Assessment of the Use of Borehole Pressure Transients to Measure the Permeability of Fractured Rock Masses by C. Forster and J.E. Gale (LBL-8674, SAC-28).

TABLE OF CONTENTS

	<u>Page</u>
AUTHORS' NOTE	ix
GLOSSARY	x
LIST OF FIGURES	xii
LIST OF TABLES	xv
ABSTRACT	1
1. INTRODUCTION	4
1.1 General Description of Heaters and Heater Layout	5
1.1.1 Experiments 1 and 2	5
1.1.2 Experiment 3	11
1.2 General Description of Instrumentation and Quantities Measured	17
1.2.1 Instruments for Experiments 1 and 2	17
1.2.2 Instruments for Experiment 3	19
2. DATA ACQUISITION AND TRANSFER PROCEDURES	20
2.1 Acquisition System	20
2.2 Transfer Procedures	23
3. DATA STORAGE AND REORGANIZATION AT LBL	25
3.1 Decoding	25
3.2 Reorganization	26
3.3 Storage	26
4. TYPES OF DATA AVAILABLE	27
4.1 Raw Data	27
4.2 Logger Data	28
4.3 Long-Term Data	29
4.4 Engineering Data	30
4.5 Sign Convention	31
5. DATA VERIFICATION PROCEDURES	33
6. DATA PROCESSING PROCEDURES	47
6.1 Correction for Voltage Errors	47
6.1.1 Thermocouples	50
6.1.2 USBM gauges	51
6.2 Conversion to Engineering Units	53
6.2.1 Heater Monitors	53
6.2.2 Thermocouples	53
6.2.3 Extensometers	54
6.2.4 USBM Gauges	60
7. VERIFICATION OF DATA PROCESSING PROCEDURES	67
7.1 Verification of Voltage Corrections	67
7.1.1 Thermocouples	67

	<u>Page</u>
7.1.2 USBM Gauges	70
7.2 Verification of Conversion to Engineering Units	70
7.2.1 Heater Monitors	70
7.2.2 Thermocouples	70
7.2.3 Extensometers	70
7.2.4 USBM Gauges	74
8. STRUCTURE AND FORMAT OF THE ENGINEERING DATA ON THE PUBLIC DOMAIN TAPES	79
8.1 Overall Structure	79
8.2 Structure and Format of Data for Experiments 1 and 2 (Full-Scale Experiments)	81
8.3 Structure and Format of Time-Scaled Experiment Data	90
9. PROCEDURES FOR ACQUIRING AND ACCESSING DATA	92
9.1 Acquiring Public Domain Tapes	92
9.2 Accessing other Available Data	92
9.2.1 Raw Data	92
9.2.2 Logger Data	96
9.2.3 Long-term Data	99
9.2.4 Engineering Data	99
ACKNOWLEDGMENTS	100
REFERENCES	101
APPENDIX A: USEFUL INFORMATION ON HEATER EXPERIMENTS (TABLES AND FIGURES)	A-1
APPENDIX B: PERFORMANCE OF STRIPA DATA ACQUISITION	B-1
APPENDIX C: SENSOR PARAMETERS	C-1
APPENDIX D: PLOTS AND LISTINGS OF ENGINEERING DATA ON MICROFICHE	D-1

AUTHORS' NOTE

For the purpose of quality assurance, responsibility for the contents of various portions of this report is given below.

Chan	Overall responsibility for data verification, processing procedures and algorithms, and writing of the main text.
Binnall	Data logger algorithms, part of Appendix B, and thermocouple calibration coefficients.
Nelson	Appendix B.
Stolzman	Execution of main-stream data processing programs.
Wan	Coding of data verification programs and writing of part of Section 9.
Weaver	Coding of main-stream data processing programs.
Ang	Public-domain tapes (Section 8) and Appendix D.
Braley	Coding of programs for verification of data conversion for thermocouples and USBM gauges.
McEvoy	Writing of Sections 2 and 3 and Appendix B.
DuBois	Extensometer calibration coefficients and sensor locations.
Lingle	USBM gauge calibration coefficients.
Littlestone	Coding of program for verification of data conversion for extensometer and computer graphics.

GLOSSARY

This glossary is included to provide the reader with a quick reference to uncommon terms, or terms which normally have wider meanings but are used in a restrictive sense in this report. It is by no means exhaustive.

Appendix B contains a further list of abbreviations.

AD-9	Acurex Autodata-Nine data logger
ARPA	Advanced Research Project Agency (Department of Defense)
ASCII	American Standard Code for Information Interchange
B&F	Data logger used for USBM gauges
BCD	Binary Coded Decimal
bpi	Bits per inch, the unit for density of information recorded on magnetic tape
C^1	A function that is continuous and has continuous first derivative
CDC	Control Data Corporation
DCDT	A special Linear Variable Differential Transformer (LVDT) transducer containing hybrid circuits that provide signal conditioning for direct current input and output. A DC-LVDT, hence, DCDT
Engineering data	Experimental data that were converted to engineering units using computer programs written at LBL. Data on the PDT are time-averaged engineering data
Experiment 1	Full-scale experiment with 3.6 kW heater
Experiment 2	Full-scale experiment with 5 kW heater and eight additional peripheral heaters
Experiment 3	Time-scaled experiment
Extensometer	Rod-type extensometer type 4 CSLT(R) with four superinvar rods, manufactured by Terrametrics, Inc. of Golden, Colorado
GSS	Gettape Stotape System, a system for information storage and retrieval designed by LBL's computer center staff. Refer to GSS writeup by LBL's computer center for detailed description and usage

Hand-shake circuitry	Electronics used to coordinate the asynchronous timing, control, and data flows between the IRAD data logger and the digital IOIS interface with the MODCOMP computer
IRAD gauge	Vibrating wire stressmeter, manufactured by IRAD Gage, Inc., Lebanon, New Hampshire
IOIS	MODCOMP's Input/Output Interface Subsystem
LBL	Lawrence Berkeley Laboratory, University of California, Berkeley, California
Logger data	Data printed on paper tapes by data loggers; also referred to as "data logger data"
Long-term data	Experimental data that were time-averaged and converted to engineering units using the computer programs implemented on the MODCOMP computer "on-site"
MODCOMP	Modular Computer Systems, Inc.
NBS	National Bureau of Standards, U.S.A.
PDT	Public-domain tapes - two 800 bpi, 2400 ft. magnetic tapes (for computer use) containing digital data from the Stripa heater experiments; available to the public
PSS	Program Storage System. Refer to PSS writeup by LBL's computer center for detailed description and usage
PWR	Pressurized Water Reactor
Raw data	Unprocessed experimental data recorded by the computer-based data acquisition system
REMAC	MODCOMP's Remote Data Acquisition Unit
SAC	Swedish-American Cooperative Program on Radioactive Waste Storage in Mined Caverns in Crystalline Rock
SPF	Sensor Parameter File
Superinvar	An alloy (64% Fe, 31% Ni, and 5% Co) with low thermal expansion coefficient
Thermocouple	Chromel-Alumel type K thermocouple
USBM gauge	U.S. Bureau of Mines borehole deformation gauge
WRR AIS	Wide Range-Relay Analog-Input Subsystem, manufactured by MODCOMP

LIST OF FIGURES

	<u>Page</u>
1. Location of experimental rooms	6
2. 3-D view of Experiments 1 and 2 (full-scale experiments) showing heater layout and some instrument holes	7
3. 3-D view of Experiment 3 (time-scaled experiment) showing heater layout	8
4. Plan (a) and elevation (b) views of Experiments 1 and 2 illustrating heater and extensometer locations	9
5. Nominal power histories of the full-scale heater experiments: (a) Experiment 1, (b) Experiment 2	13
6. Plan view of heater layout in Experiment 3 (time-scaled experiment)	15
7. Typical power history of one of the heaters (H1) in Experiment 3	16
8. Important milestones for the Stripa heater experiments	18
9. Block diagram of the Stripa data acquisition system	21
10. Scatter plot of raw data versus AD-9 logger data for a thermocouple	34
11. Scatter plot of raw data versus AD-9 logger data for an extensometer anchor point	35
12. Scatter plot of raw data versus IRAD logger data for an IRAD stressmeter	36
13. Scatter plot of raw data versus B&F logger data for USBM gauge	37
14. Scatter plot of raw data versus logger data at two values of time for all sensors: (a) AD-9 logger data for Experiments 1 and 2 (full-scale experiments), (b) AD-9 logger data for Experiment 3 (time-scaled experiment), (c) B&F logger data, and (d) IRAD logger data	41
15. Scatter plot of raw data versus AD-9 logger data for a thermocouple, showing poor correlation	43
16. Time history for voltage data for the thermocouple in Fig. 15: (a) raw data, (b) AD-9 logger data	44

	<u>Page</u>
17. Scatter plot of raw data versus AD-9 logger data for the thermocouple in Fig. 15, showing improved correlation after bad data points were removed	46
18. Scatter plot of the deviation (raw WRR AIS voltage minus AD-9 logger voltage) versus AD-9 logger voltage	48
19. Schematic illustration of the relationship between voltage (V), diametral displacement (U), and temperature (T) for a USBM gauge. See text for detailed information	64
20. Scatter plot of converted temperatures (engineering data) versus long-term temperatures for all thermocouples installed in USBM holes	71
21. Scatter plot of converted temperatures (engineering data) versus AD-9 logger temperatures for sampled thermocouples from (a) Experiment 1, (b) Experiment 2, (c) Experiment 3, and (d) all three experiments	72
22. Overall data structure on public-domain tapes	80
23. Sample sensor parameter record	85
24. Detailed file arrangement for public-domain tape; (a) tape 1 of 2, (b) tape 2 of 2	86
25. Detailed structure and format of sensor data within a borehole	91
A-1. Power history for Experiment 1 (H9)	A-29
A-2. Power history for Experiment 2 (H10 - H18)	A-30
A-3. Power history for Experiment 3 (H1 - H8)	A-34
A-4. Plan view of full-scale heater drift showing locations of heater and instrument boreholes	A-36
A-5. Vertical sections of full-scale heater drift and extensometer drift	A-37
A-6. Plan view of time-scaled drift showing locations of heater and instrument boreholes	A-39
A-7. Vertical section along axis of time-scaled drift	A-40
A-8. Extensometer anchor point designation	A-41

	<u>Page</u>
B-1 Block diagram of the Stripa data acquisition system	B-7
B-2 Block diagram of the analog input portion of the computer- controlled data acquisition system	B-11
B-3 History of circuit board changes between the full-scale and time-scale WRRAISS	B-17
B-4 Differences between WRRAIS and AD-9 voltages for: (A) Full- scale thermocouple 478 and (B) Time-scale thermocouple 910	B-20
B-5 Diagrams of the calibration setup: (A) General setup and (B) Detailed cabling	B-22
B-6 Reference voltage and shorted input for: (A) Time-scale AD-9 and (B) Full-scale AD-9	B-32
B-7 Difference between WRRAIS and AD-9 voltages from full-scale thermocouples on July 7, 1979	B-34
B-8 Calibrations of: (A) Full-scale and (B) Time-scale AD-9's in Aug. 79 and Apr. 80	B-37
B-9 Expanded scale for calibration of: (A) Time-scale and (B) Full- scale AD-9's in Aug. 79 and Apr. 80	B-39
B-10 Error counts vs: (A) Negative input voltages and (B) Postive input voltages for the full-scale WRRAIS with zero-offset board removed	B-41
B-11 Extensometer displacement error due to full-scale WRRAIS error, Feb. 80	B-43
B-12 USBM borehole deformation error due to the full-scale WRRAIS, for a typical (64 $\mu\text{m}/\text{mV}$) USBM gauge	B-44
B-13 Temperature measurement errors due to: (A) Full-scale and (B) Time-scale WRRAIS errors, for a typical (25°C/mV) thermocouple	B-45
B-14 Difference history between full-scale WRRAIS and AD-9 readings .	B-49
B-15 Difference history between time-scale WRRAIS and AD-9 readings .	B-52
B-16 Observed: (A) Probability of failure and (B) Probability of repair vs. time for the MODCOMP computer system	B-58
B-17 Data collection periods (shaded regions) for H10: (A) USBM gauges, (B) IRAD gauges, (C) Thermocouples, and (D) Extensometers	B-70

LIST OF TABLES

	<u>Page</u>
1. Dimensions of the heaters and heater layout	12
2. Number of heater and instrument holes in each experiment	19
3. Units used in engineering data	32
4. Cross-correlation coefficients (r) between raw data and data logger data for some sensors in the Stripa heater experiments	38
5. Free thermal strain of superinvar rod at various temperatures above 20°C	57
6. Deviation of raw voltage from AD-9 data logger voltage for thermocouple TE7D (sensor no. 160) before and after voltage correction	68
7. Root-mean-square (rms) deviation between raw voltage and AD-9 logger voltage for a number of thermocouples before and after voltage correction	69
8. Comparison of engineering data obtained for some extensometers using two different conversion programs	75
9. Comparison of engineering data obtained for two USBM gauges using two different conversion programs	78
10. Master sensor parameter file record structure	82
11. Master sensor parameter file description	83
12. Location of raw data and engineering data before averaging on magnetic tapes	93
13. Time period and access ID for raw data files	95
14. Format for a raw-data file	97
15. Format for a logger data file	98
A-1 Correspondence between calendar dates and experiment days for the Stripa heater experiments	A-3
A-2 Power histories for the Stripa heater experiments	A-10
A-3 Sensor locations in the Stripa heater experiments	A-13
B-1 Chronology of important events	B-9
B-2 WRRAS's analog input voltage ranges	B-12

	<u>Page</u>
B-3 Gain ranges and operating bands for the WRRAISs	B-14
B-4 Measurement resolution of thermocouples, extensometers, and USBM gauges imposed by the WRRAIS's 11-bit ADC	B-15
B-5 Significant voltage offsets for full scale thermocouple 478 . .	B-19
B-6 Significant voltage offsets for time scale thermocouple 910 . .	B-19
B-7 Specifications for the Fluke 343A DC voltage calibrator	B-25
B-8 Input characteristic specifications for the Fluke 8500A DVM . .	B-26
B-9 Accuracy specifications for the Fluke 8500A DVM	B-26
B-10 Specifications for the AD-9 data logger	B-27
B-11 General input specifications for the WRRAIS	B-27
B-12 Specifications for the WRRAIS's zero-offset feature	B-28
B-13 General output specifications for the WRRAIS	B-30
B-14 Peak 3-sigma output noise specification for the WRRAIS	B-31
B-15 Common mode rejection (CMR), from DC to 60 Hz, for the WRRAIS .	B-31
B-16 Reference output voltages, measured with the same Fluke 8500A DVM	B-31
B-17 B&F data logger and WRRAIS voltage readings	B-36
B-18 Selected voltage offsets and gain factors used to correct the full scale WRRAIS's raw voltage data	B-55
B-19 Selected voltage offsets and gain factors used to correct the time scale WRRAIS's raw voltage data	B-56
B-20 Gaps in the "raw" data collected by the MODCOMP computer	B-61
C-1 Grouping of thermocouples by peak temperature	C-2
C-2 Thermocouple polynomial coefficients from NBS calibration . . .	C-2
C-3 Sensor parameters for extensometers	C-3
C-4 Sensor parameters for USBM gauges	C-5
C-5 Time table for bad data for USBM gauges	C-8

ABSTRACT

Heater experiments were conducted in a granite body adjacent to a recently abandoned iron ore mine at Stripa, Sweden, to investigate the response of a hard rock mass to thermal loading. Heating commenced in June, 1978 and lasted for approximately one year. The rock was heavily instrumented to measure the temperature, displacement, and stress fields. Monitoring of the rock response continued for half a year after the heaters were deactivated. In-situ post-experiment calibrations of instrumentation were completed by June, 1980. The enormous data base (approximately 50 million measurements), recorded by a computer-based data acquisition system, has now been structured, verified, and converted to engineering units.

This report describes the types of data available and the procedures used for data acquisition, transfer, encoding-decoding, reorganization, storage, processing, and verification. Information is given on data structure and format and how potential users can access the computer-readable data.

The work presented in this report can be summarized as follows:

(i) To ensure that no gross error, such as misidentification of sensor or time, has been inadvertently introduced during data manipulation, the raw data (recorded by the computer on magnetic tapes) were verified by comparison with sampled back-up data recorded by data loggers. The comparison was made using scatter plots and cross-correlation coefficients.

(ii) A computer program has been written for reprocessing "raw voltage data" tapes to obtain heater power, currents, voltages, temperatures, displacements, borehole deformations. Important differences between this program and the original program implemented on the MODCOMP computer at Stripa to perform initial "on site" data conversion include:

- (a) correction for voltage errors caused by malfunctions in the MODCOMP computer's "Wide-Range Relay Analog-Input Subsystem,"
 - (b) use of NBS calibration coefficients for thermocouple data to circumvent the self-heating problem in the standard employed for field calibration of thermocouples,
 - (c) consistent adherence to rock mechanics sign convention for all thermal strains and displacements to avoid possible sign error in accounting for the thermal expansion of the extensometer rods or the body of the USBM gauge,
 - (d) improved numerical methods in correcting for the thermal expansion of the extensometer rods,
 - (e) more accurate computation of the temperature dependence of various calibration parameters for the USBM borehole deformation gauges,
 - (f) use of new calibration parameters which represent the results of the pre- and post-test instrument calibrations, with due account taken of the fact that some sensors had been removed and re-installed during the heater tests.
- (iii) The data processing procedures were verified by showing that:
- (a) the root-mean-square deviation between the raw voltages and data logger voltages were reduced by the voltage correction procedure;
 - (b) good correlation existed between temperatures recorded by the data loggers and those obtained by reprocessing the raw data with the computer program mentioned above;
 - (c) two different computer programs for converting raw voltage data to engineering units using either different numerical techniques (as for extensometer displacements) or the same algorithm but with

coding done by two different individuals (as for USBM borehole diametral displacements) produced practically identical results.

(iv) All the raw data were reprocessed and written on two standard magnetic tapes. The data on these tapes are logically ordered.

1. INTRODUCTION

Several concepts have been proposed for isolating radioactive wastes from the biosphere (U.S. Department of Energy, 1979). Among these, conventional geological disposal--burial in deep underground caverns in a geologically stable formation--appears to be the most practicable. One of the host rock types being considered is granite.

The heat generated by radioactive decay must be accounted for when assessing the structural integrity of a waste repository and when estimating the likelihood of any of the waste returning to the biosphere while still significantly radioactive. To study the thermal effects, heater experiments were conducted in a granite body at a depth of approximately 340 m in the Stripa mine in Sweden. These experiments were part of a Swedish - United States cooperative program to study radioactive waste storage (Witherspoon and Degerman, 1978; Witherspoon et al., 1980).

The Stripa heater experiments were conducted from June 1978 to June 1980 and yielded an enormous amount of data. This report describes these data as they appear on public-domain magnetic tapes to be released to the nuclear waste isolation research community. This is the first time that a comprehensive set of field data on the thermal and thermomechanical responses of a hard rock mass has been made available in digital form in the open literature.

Descriptions of the experiment configuration, heater power histories, and the procedures for data acquisition, handling, verification, and processing are included to ensure that the report is self-contained. Finally, the structure and format of the data on the public-domain tapes are described, along with information on acquiring the public-domain tapes and accessing

other available data.

Assessment of measurement errors resulting from uncertainties in calibration coefficients and other instrumentation limitations will be addressed in two future SAC reports. Errors introduced by hardware problems in the computer-based data acquisition system are discussed in one of the appendices. Statistical estimate of random errors is not possible because there is only one single data point of a particular type at each point in space and time.

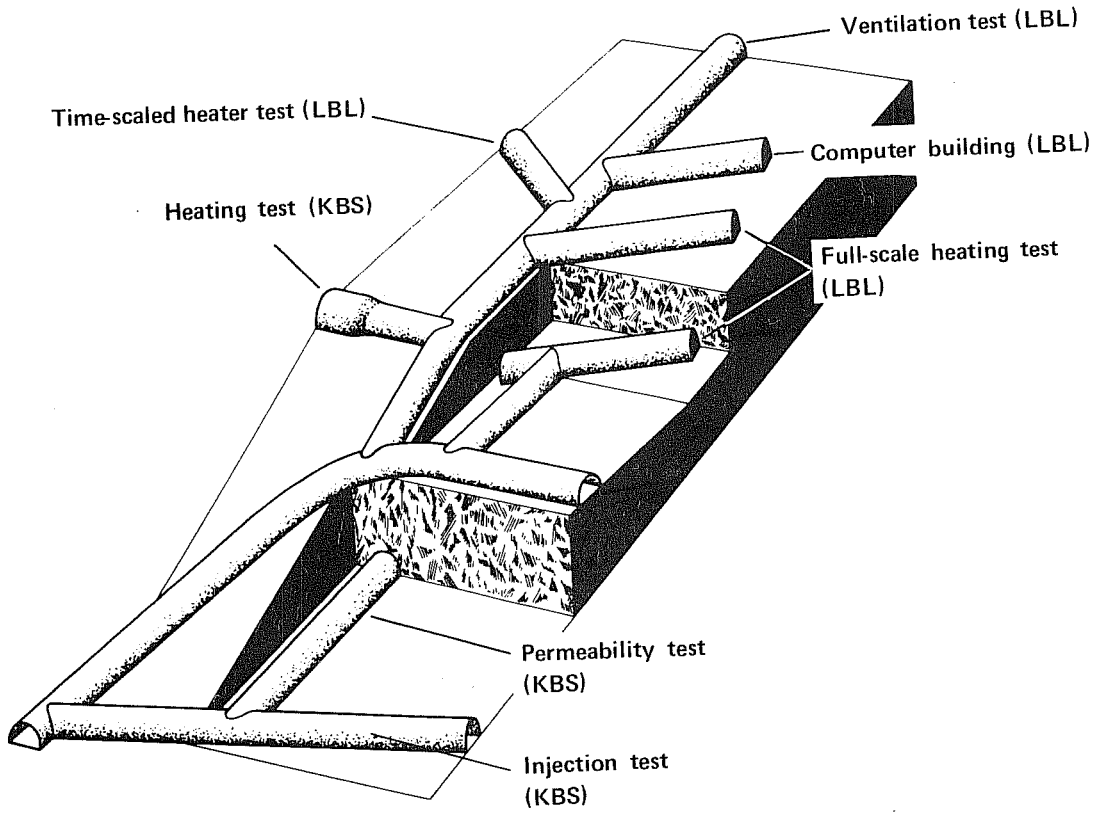
1.1 General Description of Heaters and Heater Layout

Two full-scale experiments and one time-scaled experiment were conducted. The primary objective of the full-scale experiments was to assess the short-term thermal and thermomechanical responses of the granite rock mass in the immediate vicinity of simulated nuclear waste canisters. The time-scaled experiment provided field data for the interaction between adjacent waste canisters for two different spacings over a period of time equivalent to about a decade. Figures 1-3 (taken from Witherspoon et al., 1980) illustrate, respectively, the locations of the experimental drifts and the general configurations of the full-scale and time-scaled experiments.

1.1.1 Experiments 1 and 2

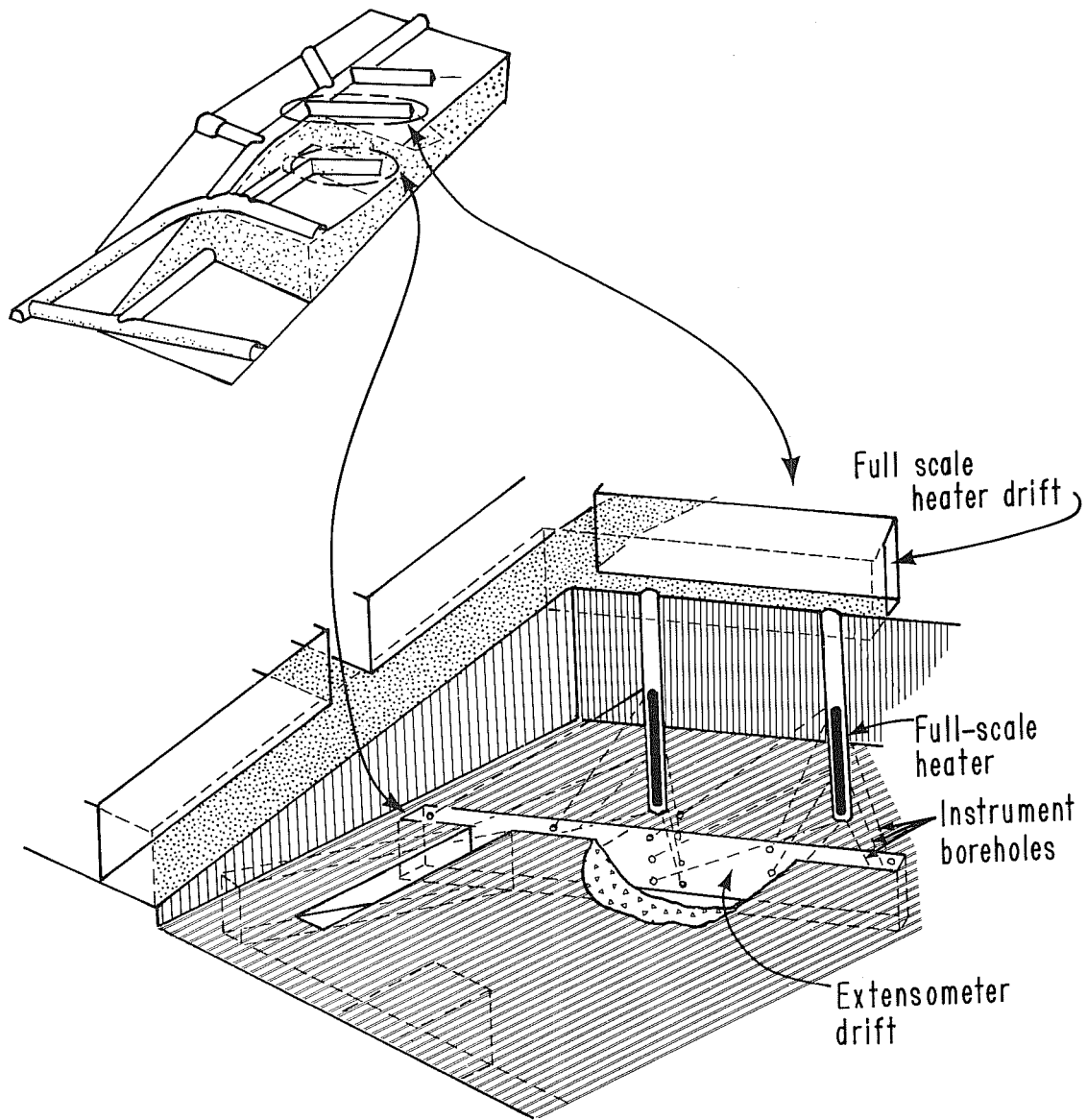
Full-scale electrical heater canisters, 0.32 m in diameter and 2.59 m long, were placed in vertical 0.406 m diameter boreholes as shown in Fig. 4, with their midplane approximately 4.25 m below the floor of the drift.

Experiment 1 consisted of a single heater canister operated at a constant electrical power of 3.6 kW which was supplied by four heating elements (see Burleigh et al., 1979 for details).



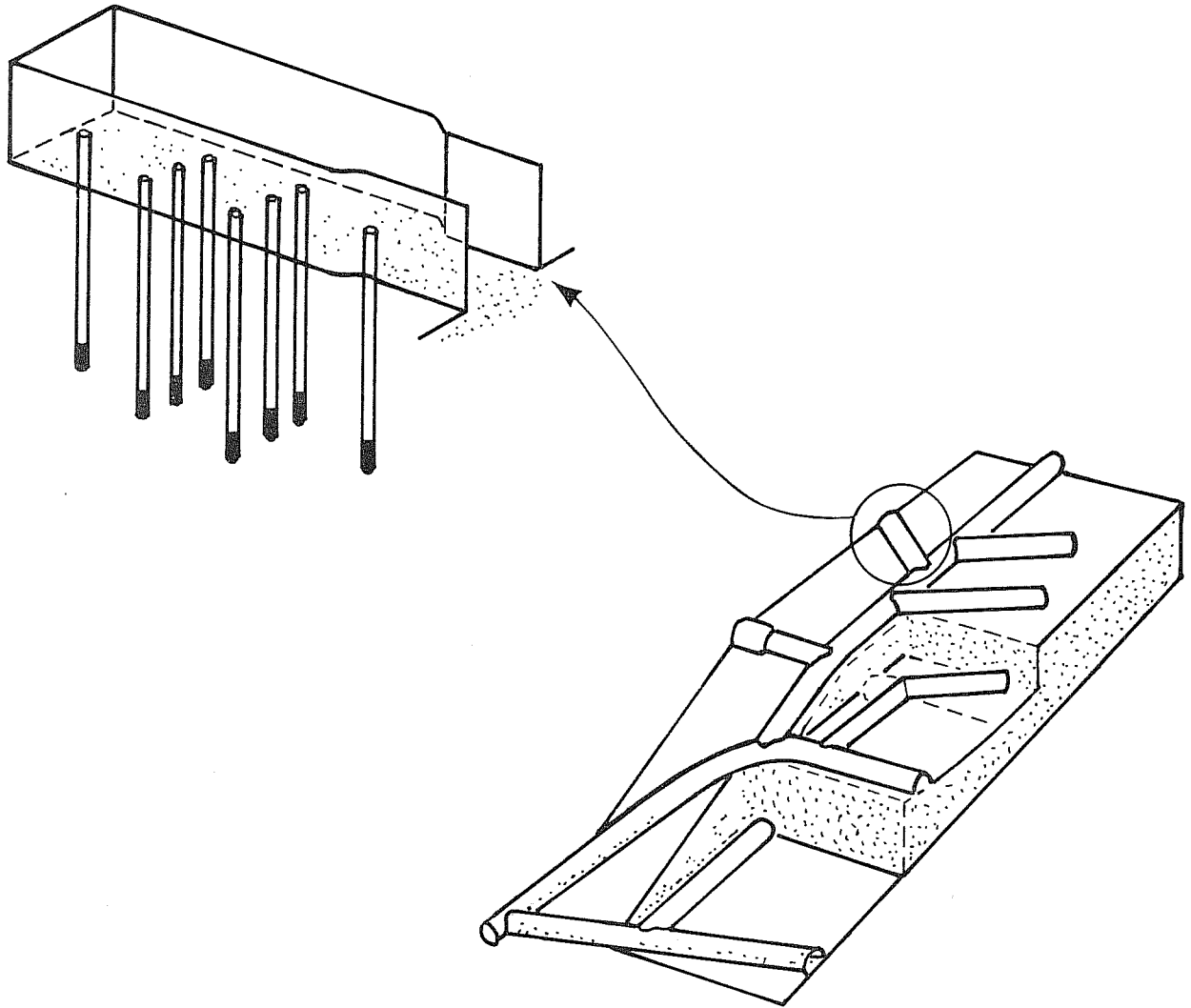
XBL787-2596 A

Fig. 1. Location of experimental rooms.



XBL 785-970 A

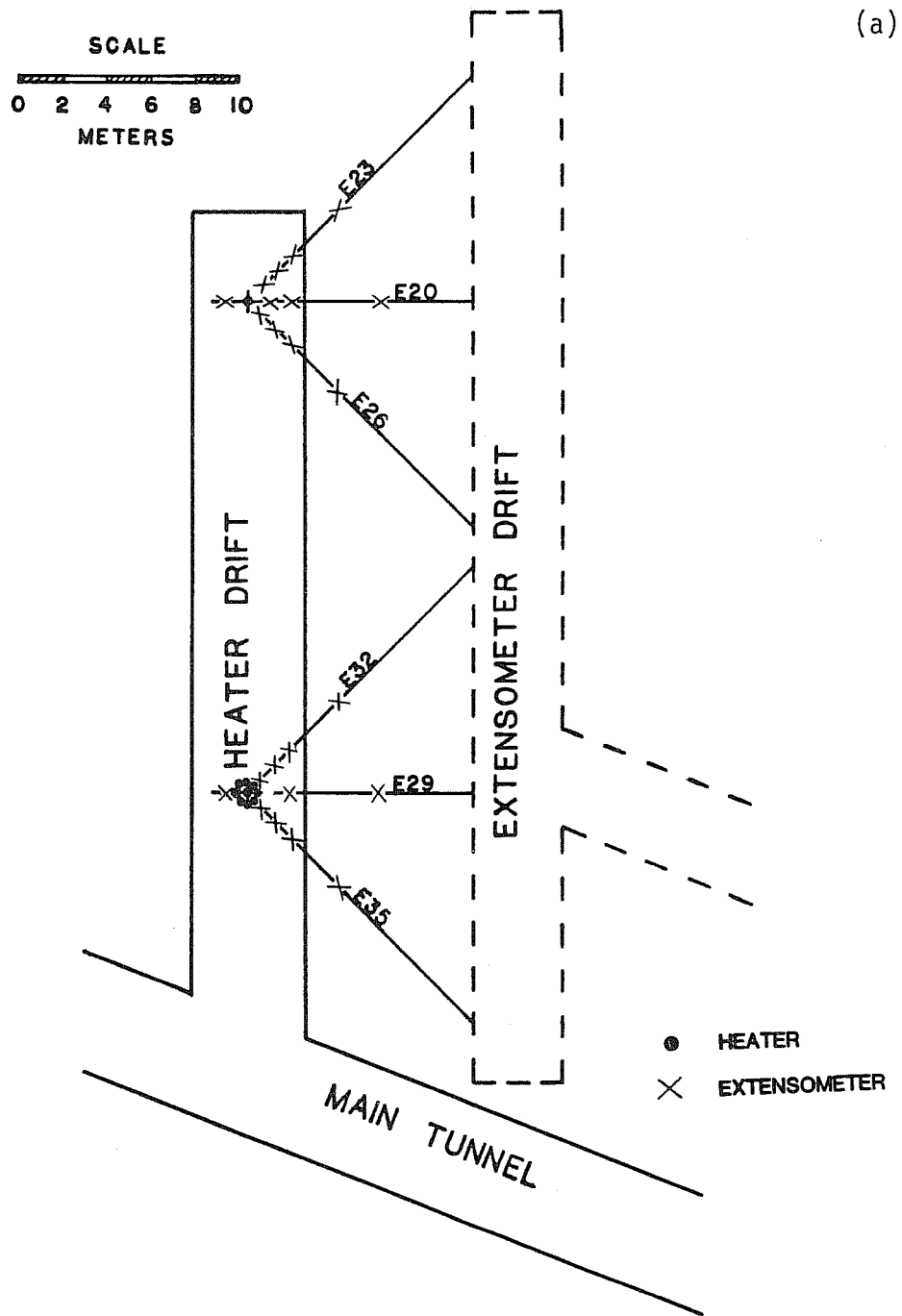
Fig. 2. 3-D view of Experiments 1 and 2 (full-scale experiments) showing heater layout and some instrument holes.



XBL 785-969

Fig. 3. 3-D view of Experiment 3 (time-scaled experiment) showing heater layout.

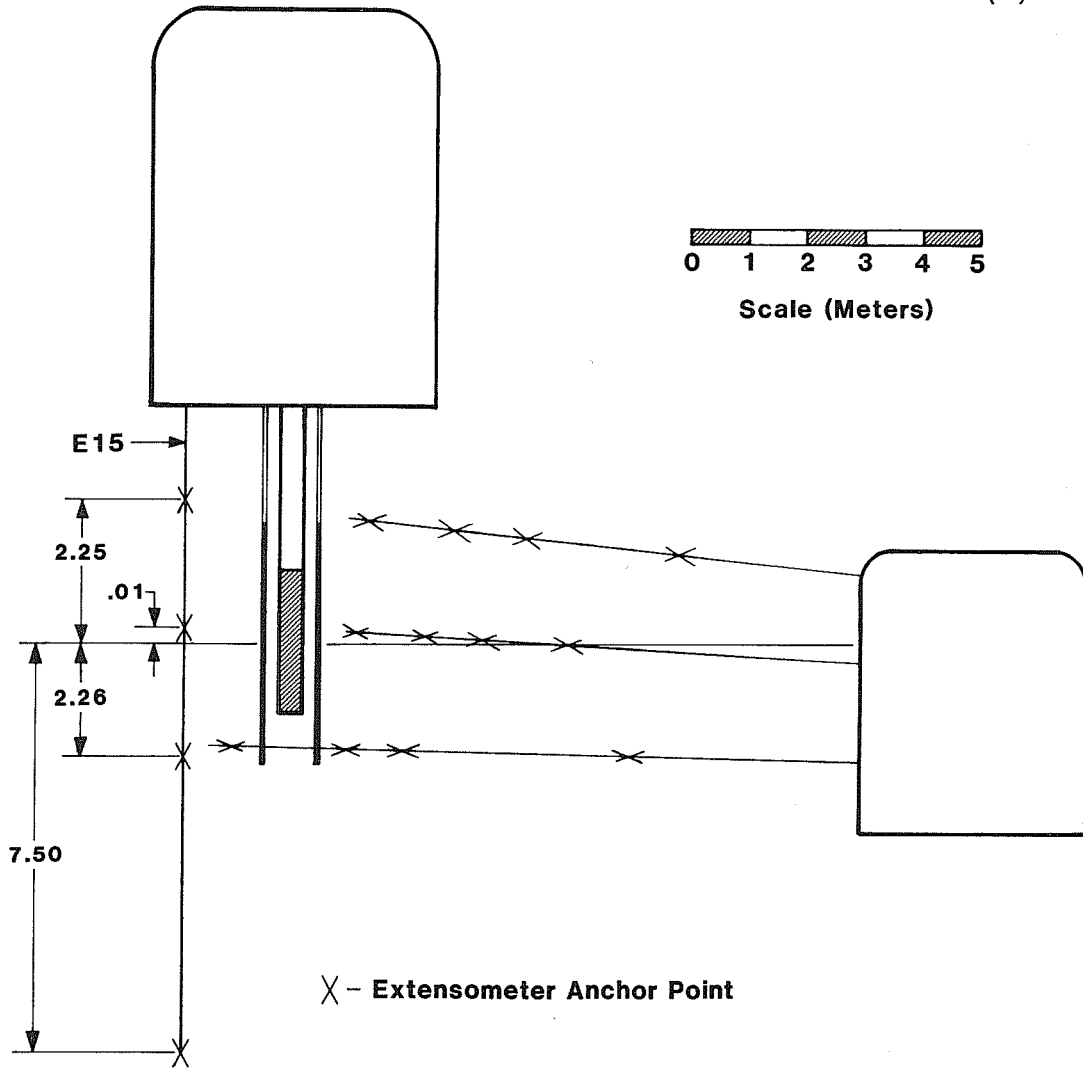
FULL SCALE HEATER EXPT.



XBL 8010-12357

Fig. 4. Plan (a) and elevation (b) views of Experiments 1 and 2 illustrating heater and extensometer locations.

(b)



XBL 8010-12358

Fig. 4 (continued).

Experiment 2 comprised a 5 kW main heater ringed by eight peripheral heaters that were operated at a nominal power of 1 kW each during their first 40 days of operation, then reduced to 0.85 kW each. These peripheral heaters were energized 204 days later than the 5 kW heater to further raise the ambient rock temperature by approximately 100°C. Dimensions of the heaters and heater layout are summarized in Table 1. Nominal power histories for Experiments 1 and 2 are shown in Fig. 5. Detailed plots and tables of the measured heater powers, which were all within 1% of the planned values, are given in Appendix A.

1.1.2 Experiment 3

Experiment 3, the time-scaled experiment, reduced all linear dimensions of the experiment by a factor of 3.2. This compressed time by a factor of 10.2 due to the quadratic relationship between time and distance in linear heat conduction. Eight canisters, with two heater elements each, were emplaced in an array 10 m below the floor of a drift. Spacing between canisters in this array (see Fig. 6) was 3 m by 7 m, representing an equivalent 10 m by 22 m full-scale array spacing. The power to these heaters was scaled linearly with canister size. At the start of the experiment, the power output of each of these time-scaled heaters was 1.125 kW, which represented 3.6 kW in the full-scale. This power was reduced during the experiment to represent the decay of reprocessed PWR (pressurized water reactor) high-level waste (Kisner et al., 1977) over this time period. The power history of such high-level waste was scaled to obtain the power history of one time-scaled heater (Fig. 7). During the experiment, actual reduction of heater power was delayed for two weeks because of some operational problems. Detailed plots and tables are given in Appendix A.

Table 1. Dimensions of the heaters and heater layout

a. Experiments 1 and 2 (full-scale experiments)

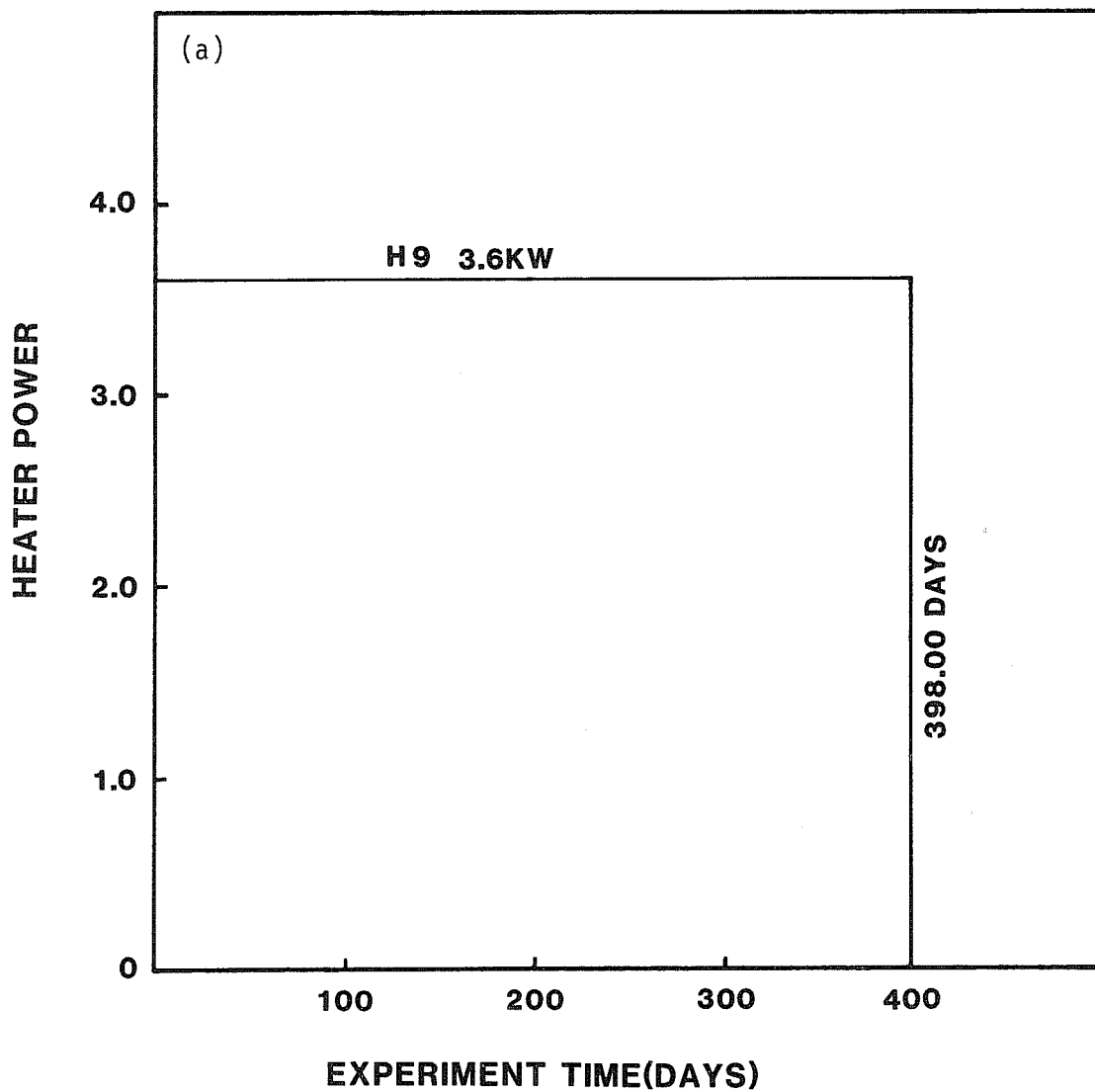
Length of hot section of heater element	2.44 m	(8.00 ft)
Approximate heated length* of heater canister	2.61 m	(8.55 ft)
Diameter of central heater canister	0.324 m	(12.75 in)
Diameter of central heater hole	0.406 m	(16.0 in)
Length of peripheral heater	4.27 m	(14.0 ft)
Diameter of peripheral heater	0.027 m	(1.05 in)
Diameter of peripheral heater hole	0.038 m	(1.50 in)
Radius of the ring of peripheral heaters	0.9 m	(35.4 in)
Nominal depth of the midplane of the heater array below the floor of the drift	4.25 m	(13.9 ft)
Center-to-center separation between the two experiments	22 m	(72.2 ft)

b. Experiment 3 (time-scaled experiment)

Length of hot section of heater element	0.762 m	(2.05 ft)
Approximate heated length of heater canister	0.787 m	(2.58 ft)
Diameter of heater hole	0.127 m	(5.00 in)
Center-to-center spacing of heaters along heater drift axis	7 m	(23.0 ft)
Center-to-center spacing of heaters perpendicular to heater drift axis	3 m	(9.84 ft)
Nominal depth of the midplane of the heater array below the floor of the drift	10 m	(32.8 ft)

*The effective heated length of a heater is a matter of interpretation and the reader should refer to Burleigh et al. (1979) for detailed construction of the heaters.

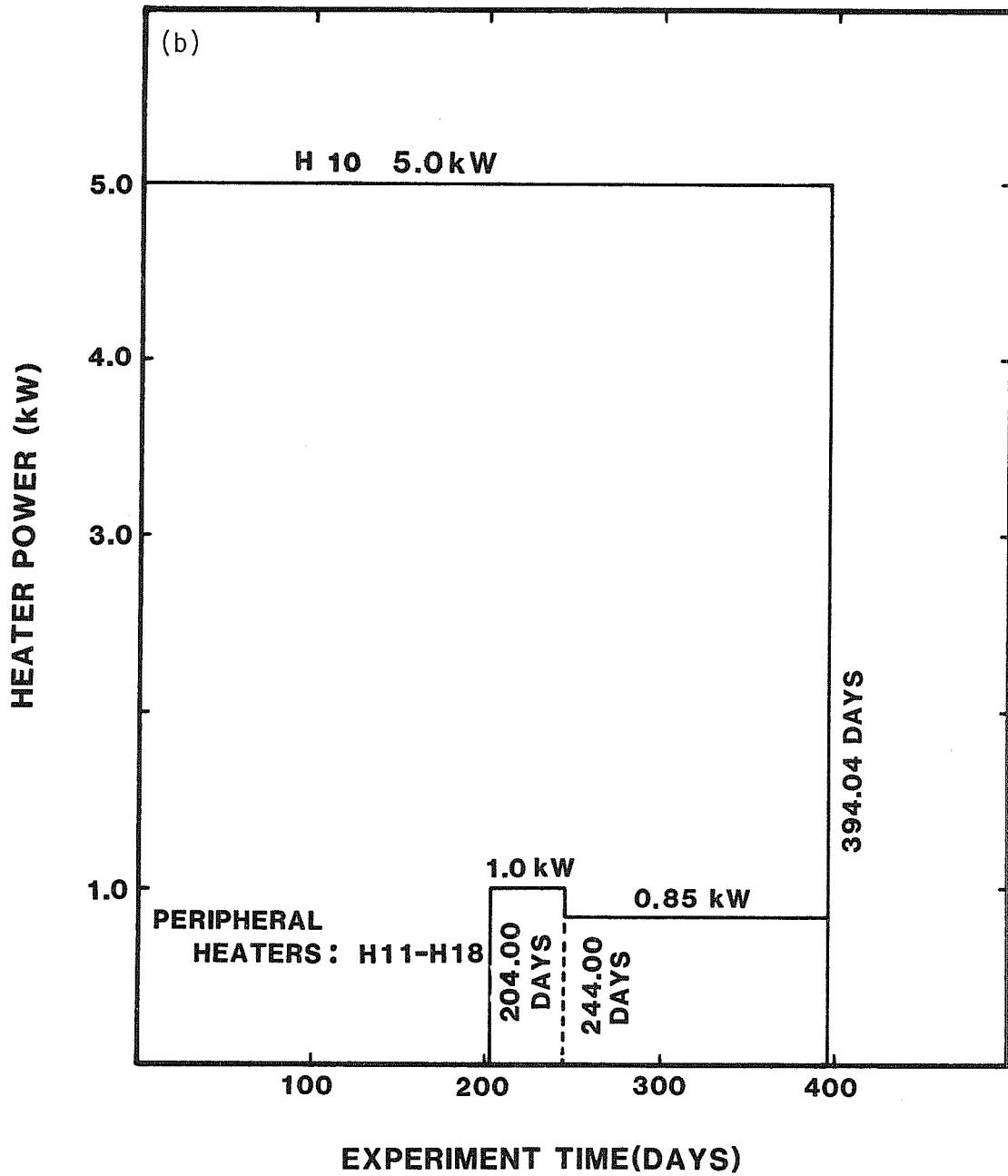
EXPERIMENT 1



XBL 8010-12356

Fig. 5. Nominal power histories of the full-scale heater experiments: (a) Experiment 1, (b) Experiment 2.

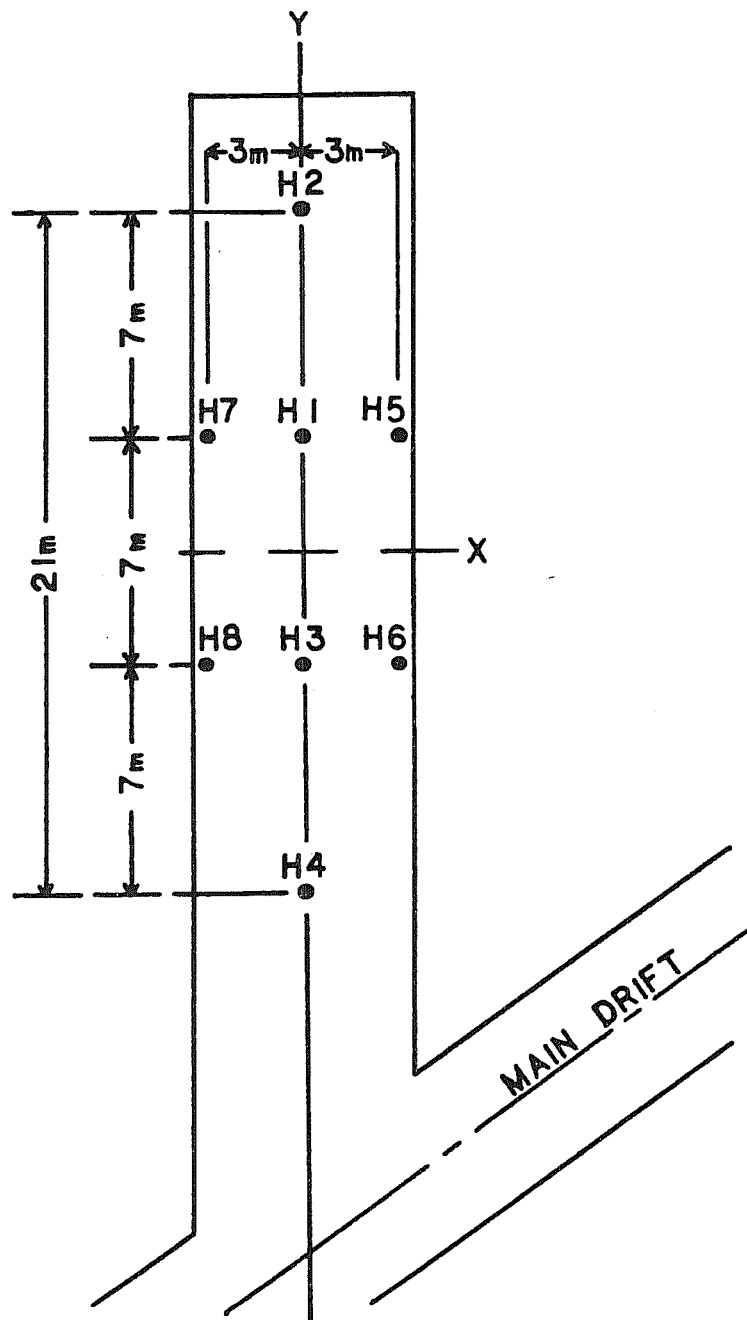
EXPERIMENT 2



XBL 8010-12355

Fig. 5 (continued).

TIME-SCALED DRIFT

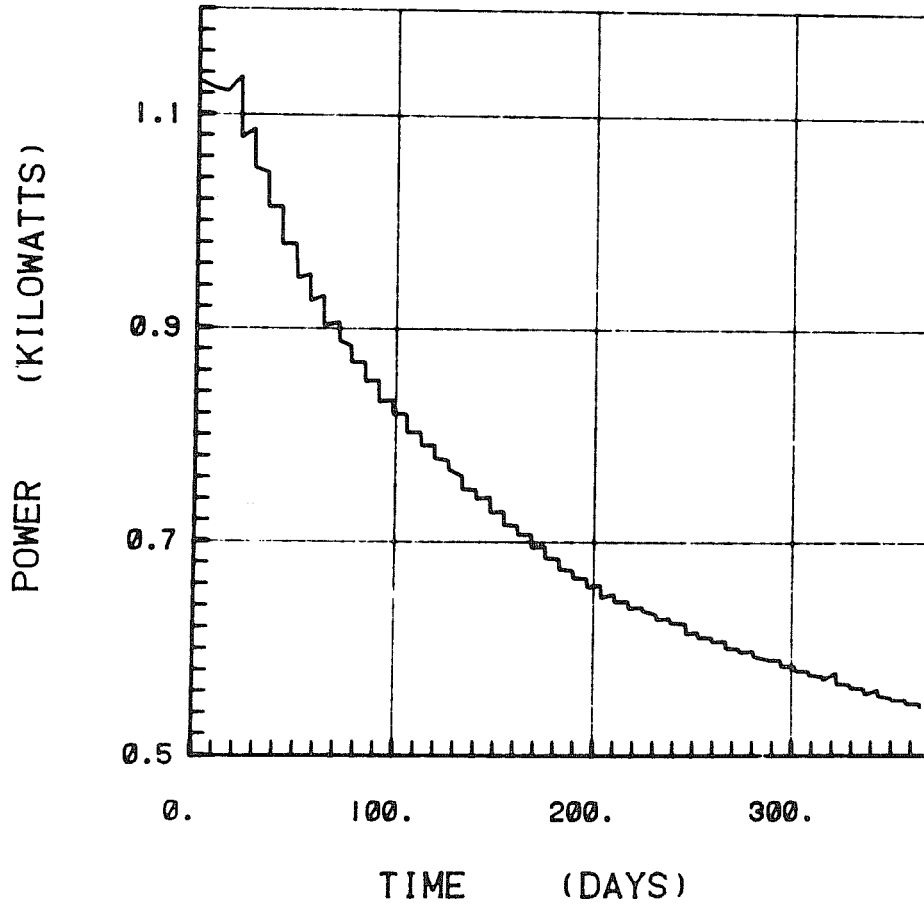


XBL 8010-12354

Fig. 6. Plan view of heater layout in Experiment 3 (time-scaled experiment).

HEATER H1

TOTAL POWER



XBL 8010-12353

Fig. 7. Typical power history of one of the heaters (H1) in Experiment 3.

The initial power in this experiment represents an equivalent areal power density of

$$\frac{3600 \text{ W}}{10 \times 22 \text{ m}^2} = 16.36 \text{ W/m}^2 = 66.21 \text{ kW/acre.}$$

Important milestones for the three experiments are summarized in Fig. 8.

1.2 General Description of Instrumentation and Quantities Measured

For easy reference a brief description is given below of the instrumentation and the quantities measured in each experiment. Table 2 lists the number of heater and instrument boreholes. Details of instrument evaluation, calibration, and installation have been documented in a previous SAC report by Schrauf et al. (1979).

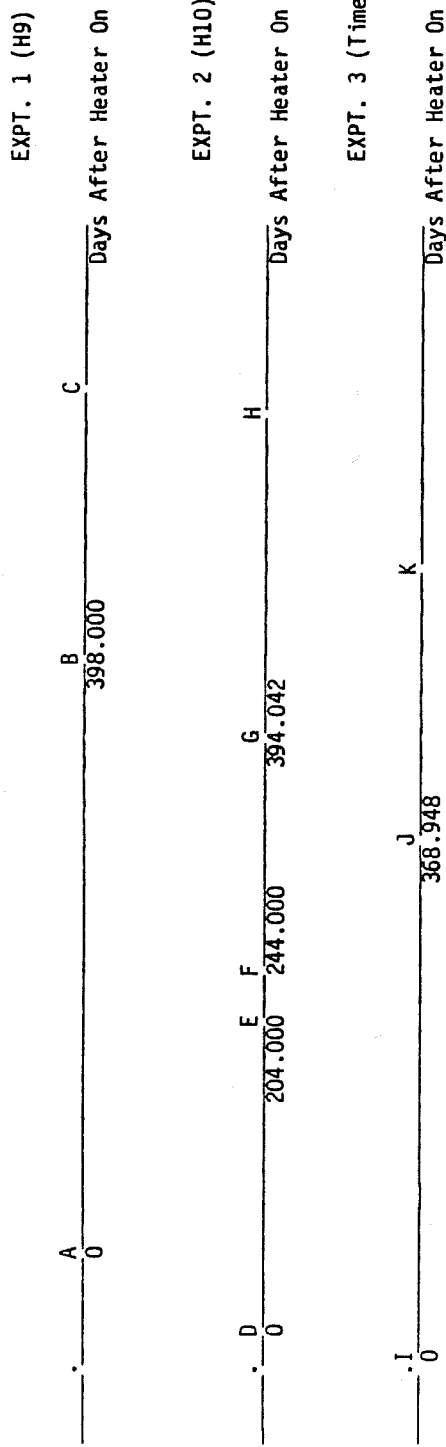
1.2.1 Instruments for Experiments 1 and 2

In full-scale experiments 1 and 2, five different types of thermal and thermomechanical data were collected using:

- a. heater monitors (voltage, current and power of each heater element);
- b. thermocouples (temperatures);
- c. multiple-anchor rod extensometers (vertical and horizontal displacements);
- d. IRAD (CREARE) vibrating-wire gauges (fundamental vibrational periods of gauge wires, from which stress changes were derived¹); and
- e. USBM borehole deformation gauges (diametral displacements of boreholes, from which stress changes were derived¹).

¹ Although data from IRAD and USBM gauges were initially converted to stress changes using the programs implemented on the computer at Stripa, subsequent work has indicated that the calibration parameters, rock properties, and mathematical equations assumed in the original conversion are all questionable. See Sections 4 and 6.

IMPORTANT MILESTONES FOR STRIPA EXPERIMENTS (Drawn to Scale)



- A - 3.6 kW Heater on; 8/24/78; 14:00
- B - Heater off; 9/26/79; 14:00
- C - H9 Expt. Off; March, 1980
- D - 5 kW Heater on; 7/3/78; 9:00
- E - 1 kW Peripheral Heaters On; 1/23/79; 9:00
- F - Peripheral Heater power reduced to 0.85 kW; 3/4/79; 9:00
- G - Heaters Off; 8/1/79; 10:00
- H - H10 Expt. Off; February, 1980
- I - Heater On; 6/1/78; 12:00
- J - Heater Off; 6/5/79; 10:45
- K - T.S. Expt. Off; December, 1979

Fig. 8. Important milestones for the Stripa heater experiments.

Table 2. Number of heater and instrument holes in each experiment

	Heater	Thermo- couple	Exten- someter		IRAD		USBM	
			V*	H	V	H	V	H
Experiment 1	1	6	6	9	2	5	10	5
Experiment 2	9	6	6	9	3	3	10	5
Experiment 3	8	12	5	0	0	0	0	0

*V = vertical hole; H = horizontal hole

Temperatures were measured on the heater canisters, in the rock, and on other instruments. Only the thermocouple boreholes were designed to measure rock temperatures.

1.2.2 Instruments for Experiment 3

Experiment 3, the time-scaled experiment, was instrumented to measure:

- a. heater powers, voltages, and currents;
- b. temperatures; and
- c. vertical displacements.

Selected location figures and a complete table of sensor coordinates are provided in Appendix A. Most figures are essentially the same as those given in Kurfurst et al. (1978) or Schrauf et al. (1979), except that in this report instrument boreholes are labeled in the figures according to the gauges actually installed, rather than the original borehole names. This affects only three USBM gauges and three pairs of IRAD gauges. The primary purpose for providing a complete table of sensor coordinates is to show the exact order in which the data appear in the public-domain tapes.

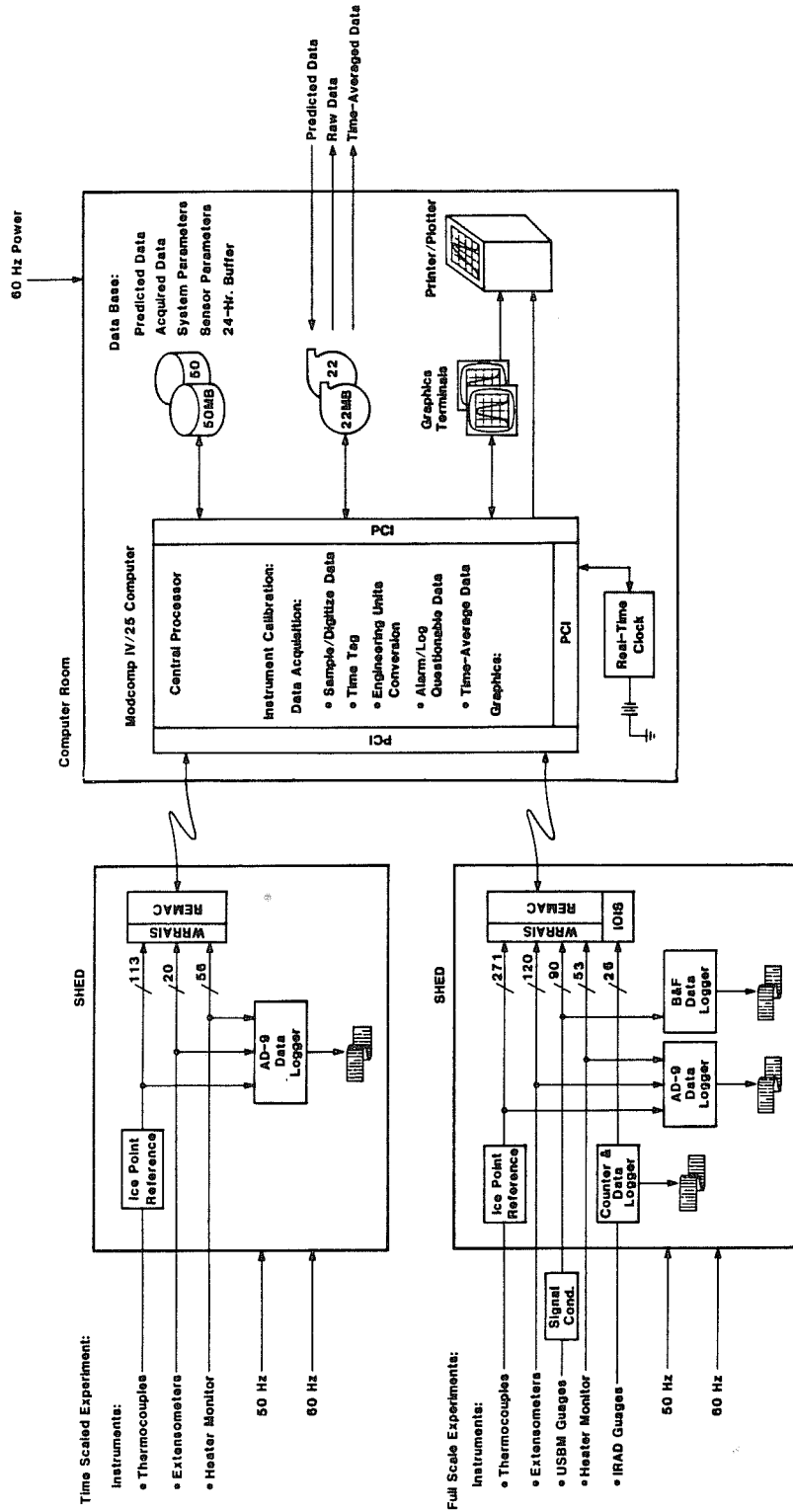
2. DATA ACQUISITION AND TRANSFER PROCEDURES

2.1 Acquisition System

Instrumentation at Stripa included 271 thermocouples, 120 extensometer channels, 90 USBM channels, 26 IRAD channels, and 53 heater monitor channels for the full-scale experiments; and 113 thermocouples, 20 extensometer channels, and 56 heater monitor channels for the time-scaled experiment. Most instruments were individually calibrated using a computer. Resulting calibration constants and other parameters such as sensor type, sensor number, associated experiment, sensor location, data channel numbers, time of last change, and time of last access were maintained on the computer's disc for each signal source. A computer-based data acquisition system was necessary to manage the vast amount of data. However, hardware problems in this system introduced errors into the data (see Appendix B). Instrumentation parameters are listed in Appendix C.

Once the heaters were turned on, data was acquired from the instruments using a computer-based data acquisition system. An independent system consisting of three data loggers provided back-up data as shown in Fig. 9. Precision voltage-source inputs to the data loggers provided a reference that facilitated detection and isolation of changes in the computer's scaling of its analog measurements. A MODCOMP-IV computer provided the basis of the computer system.

Analog data from thermocouples, USBM gauges, extensometers, and heater monitors were digitized using MODCOMP's Wide-Range Relay Analog-Input Subsystems (WRRAISs), which were located in sheds adjacent to the instruments. Each WRRAIS encoded its digitized output as a sign bit, four gain-code bits,



XBL 8010-12352

Fig. 9. Block diagram of the Stripa data acquisition system.

and an 11-bit magnitude or mantissa.

The IRAD data logger used an interval counter to measure the period of oscillation of each IRAD gauge's vibrating wire in units of 10^{-7} seconds. These measurements were encoded as four binary-coded-decimal (BCD) digits of four bits each. The highest-order four bits represented the thousand's place, the next four bits the hundred's place, the next four bits the ten's place, and the least significant four bits the unit's place of the measured period. A MODCOMP-supplied digital Input/Output Interface Subsystem (IOIS) along with some special "hand-shake" circuitry was used to read the IRAD data logger's BCD digits into the computer.

All of these 16-bit measurements were time-division-multiplexed over coaxial cables from remote acquisition subsystems (REMACs) located in both the full-scale and the time-scaled instrument sheds into the MODCOMP central processor, which was located in the computer room.

Data from active sensors were sampled, under software control, at 15-minute intervals for the duration of the experiment. Acquired data were time-tagged from a system clock and converted to engineering units such as temperature, displacement, and stress using previously obtained calibration data and associated curve fits. ASCII-encoded² raw data were recorded on magnetic tape, and data for the previous 24-hours were buffered on disc to prevent data loss whenever the tape unit was off-line. The 16-bit measurements were interpreted as if they were two's-complement decimal integers and were recorded in formatted ASCII-coded blocks of 1200 words (one per allocated channel). Each block was subdivided into two sub-blocks, each consisting of

²ASCII = American Standard Code for Information Interchange

a header line specifying the time and date that the data were acquired, followed by 600 sensor measurements in 50 lines of 12 values each. A value of minus one was recorded for those channels where no data were acquired.

The arithmetic means of data, in engineering units, were computed over specified time intervals. These less frequent "long-term" data were used for LBL's preliminary data analysis, and recomputed time-averaged "engineering data" are now available on the "public domain" data tape. The averaging intervals were chosen to compress the large amount of data while retaining sufficient data whenever interesting changes were expected. Exceptional conditions were monitored and software alarm flags were set or reset for zero data, maximum value (all binary ones) data, and data that were outside alarm ranges that exceed specified maximum rates of change. "Data missing" flags were provided for data missed during system outages. In a previous SAC report McEvoy (1979) describes the Stripa data acquisition, handling, and display in more detail.

2.2 Transfer Procedures

Stripa "raw data" tapes were stored in an on-site tape library, and copies of the tapes were airmailed to LBL every fortnight. These tapes contain unprocessed experimental data and associated calibration parameters which permitted later reprocessing with changed calibration data and engineering conversion algorithms.

"Long-term" data, in engineering units, reduced the quantity of data stored for on-line display and analysis. These data were also ASCII-encoded, recorded on magnetic tapes, and the tapes airmailed to LBL every fortnight.

Once magnetic data tapes were received at LBL, they were translated from ASCII to the CDC display code character set using LBL's CODE9 utility program. These data were divided into sets containing about one month of data each. These data sets were recorded on 6250 bpi (bits per inch) magnetic tapes using LBL's GSS storage and retrieval system. The tapes can be automatically retrieved and mounted in LBL's Automatic Tape Library. Data on these tapes can be accessed interactively via LBL's CDC-6400 and 6600 computers, staged to disc, and accessed by LBL's CDC-7600 in batch mode, or accessed remotely via the Defense Department's ARPA computer network.

Another MODCOMP-IV computer in Berkeley also permits users to access and display data interactively at LBL, using the same capabilities that were available in the mine in Sweden.

Paper tapes from data loggers were shipped to LBL upon request and after the conclusion of the experiments.

3. DATA STORAGE AND REORGANIZATION AT LBL

During the Stripa heater experiments, long-term data that were converted to engineering units and time-averaged in real time provided the basis for preliminary experiment analysis both in Stripa and at LBL. However, malfunctions in the computer portion of the data acquisition system introduced unacceptable biases into the computer-acquired data. A detailed description and analysis of these problems is presented in Appendix B. Removal of these data biases, as well as other uncertainties in the data processing at Stripa, required that the "raw" data be reprocessed. This section describes the associated data handling and reorganization, and Section 6 describes the associated voltage correction and engineering unit conversion algorithms.

3.1 Decoding the Data

The 1200-word integer-coded data records were read from the unprocessed "raw" data tapes. Data not in time order or with non-matching sub-block headers were not processed. Duplicate data blocks were discarded and missing data blocks were ignored. Sensor-off "minus one" flags were replaced by the value -12345. A bad data flag, "-99999," replaced values that had invalid gain codes or IRAD data that had BCD digits other than 0-9. Legal values for analog data were converted to their original voltage by:

$$V = \text{sign} \frac{0.005}{2048} \times 2^G \times \text{mantissa (volts)}$$

where: G = gain code (0-11),
 mantissa = data magnitude (0-2047), and
 sign = "-" if the sign bit is a one.

Values for IRAD "period" data were assembled from their four BCD digits. All data were represented as floating point values which were recorded in 1200-word unformatted binary records on an intermediate magnetic tape.

These stage-one data files consist of 1200 data values for each of 96 time intervals per day (i.e. one per 15 minutes) for approximately one-month periods.

3.2 Reorganization

The data tapes discussed so far had the data values for all three experiments lumped together for each acquisition time. This avoided duplication of time values but proved cumbersome since data history was usually accessed either by individual sensor or by borehole. As a result, records were read from the intermediate tape described above and the data were separated by gauge and hole into separate files. Each file has a one-line header that contains the hole/gauge name and the sensor number for that borehole. The output files contain records that include the integer time, the alphanumeric time and date, and the data value. These separated data files are also stored on 6250 bpi GSS tapes.

Biases in the computer-acquired raw voltages on these separated data files were then removed using the algorithms described in Section 6.1. Appendix B provides additional justification for these adjustments. These corrected voltages were converted to engineering units using the algorithms described in Section 6.2. To fit these data onto 800 bpi public domain tapes, they were recompactd by time-averaging and by re-aggregating data for each time to eliminate redundant times.

3.3 Storage

The structure and format of the public-domain tapes are provided in Section 8. Procedures for acquiring and accessing both the public-domain tapes and other available data are described in Section 9.

4. TYPES OF DATA AVAILABLE

Data are available as 1) raw data, 2) data-logger data, 3) long-term data, and 4) engineering data. This section briefly describes each type of data, the physical media on which they have been recorded, and the quantities available. Section 8 describes the detailed data structures and formats. Section 9 describes how potential users can acquire and access the data.

4.1 Raw Data

Unprocessed "raw" data were recorded on magnetic tapes on-site before conversion to engineering units. The formats of the 16-bit raw data words are as determined by the acquisition hardware described in Section 2. Raw data decoding and reorganization were described in the preceding section and the data are available on fourteen 6250 bpi magnetic tapes accessible via the GSS system on LBL's CDC computers.

Raw data from thermocouples, extensometers, and USBM gauges consist of measured voltages (in volts). Raw heater monitor data were recorded as normalized 0- to 10-volt DC analog representations of power, current, and voltage, as provided by signal conditioners (Burleigh et al., 1979). Raw data for the IRAD vibrating-wire stressmeters, provided by the IRAD MA-2 data logger, are the fundamental vibrational periods (in units of 10^{-7} seconds) of the gauge's stressed steel wires. These periods were measured by electromagnetic resonance (Hawkes and Bailey, 1973; IRAD Gage, Inc., 1977).

There was one 16-bit measurement per sensor every 15 minutes, resulting in a total of approximately 10^8 bytes of raw data. Microfiches containing all the raw data have been cataloged and are available for viewing at LBL's Earth Sciences Division.

4.2 Logger Data

Acurex Autodata-Nine (AD-9), B&F, and IRAD data loggers printed their results on paper tapes (see Section 2 above). Variable sampling rates were set by operators on-site, in accordance with expected rates of change in the measured quantities as the experiments progressed. There were approximately 2×10^4 measurements per sensor, giving a total of 1.5×10^7 data logger measurements.

AD-9 data loggers monitored the heaters and printed their power, current, and voltage.

AD-9 data loggers also printed temperatures in degrees Celsius. A microprocessor, built into the AD-9 data logger, converted measured thermocouple voltages into temperatures, using piecewise linear interpolation based on the NBS calibration table.

The full-scale AD-9 data logger measured extensometer voltages, converted voltage to displacement in millimeters, and printed the results on paper tape, except for a few data points at the beginning of the experiments when measured extensometer voltages were recorded directly in millivolts. The built-in microprocessor converted volts to millimeters according to the equation:

$$u = 2.15254 V + 12.7$$

where u = displacement in mm, and

V = extensometer (DCDT) voltages in volts.

Potential users of the extensometer data recorded on the data loggers should beware that (1) the extensometers were set to initial voltage readings corresponding to about 10 mm and (2) unlike the computer data, no compensation

was made for the thermal expansion of the (superinvar) extensometer rods or variations in calibration coefficients among extensometers.

The B&F data logger, for USBM gauges, and the IRAD data logger printed raw voltages and vibrational periods, respectively. Note that the reliability of the B&F data logger's voltage data from the USBM gauges is questionable, as discussed in Appendix B.

Selected logger data were transcribed into computer files, and subsection 9.2.2 describes how the data can be accessed.

4.3 Long-Term Data

"Long-term" data were obtained by converting "raw" data into engineering units and time-averaging them, using conversion programs implemented in the MODCOMP computer at the experimental site. These programs were documented by Teknekron, Inc. (1978). The conversion algorithms were also given in Schrauf et al. (1979). Long-term data tapes are available on GSS tapes on LBL's CDC computer system (see subsection 9.2.3 below). Certain editing has been done to remove data discontinuities introduced by malfunctions and circuit board interchanges in the Wide-Range Relay Analog-Input Subsystem, as explained in Appendix B.

A set of computer-generated plots of long-term data are available in LBL's Earth Sciences Division for the heating period of the experiments. These plots aided in the initial interpretation of the response of the rock to heating and in identification of problems in the data acquisition system and the original data conversion programs.

The long-term data are of limited use at present because of imperfections in the original data conversion programs and the use of now out-dated sensor parameters. They have now been supplanted by the engineering data described in the next subsection.

Heater power, current, voltage, and temperature data are the most useful "long-term" data. The long-term heater monitor data are practically the same as those in the engineering data, but the temperatures differ somewhat since slightly different thermocouple calibration parameters were used in the conversion and errors in the raw voltages were corrected. The long-term temperature data do provide a reasonably accurate basis for verification of the engineering data conversion for the thermocouples (see subsection 7.2.2 below).

4.4 Engineering Data

"Engineering data" refers to data that have been converted at LBL to engineering units, according to the algorithms presented in Section 6. Engineering data are available both in before time-averaging and in after time-averaging forms. Time-averaging was done selectively to compress the 10^8 bytes of slowly changing data to make them more manageable. The amount of data before averaging is enormous; it would take 100 sizable volumes of 1000 pages each to print them and twenty-five 800-bpi magnetic tapes to store them, even if all information on measurement time was omitted.

Engineering data recorded on the public-domain tapes are the averaged data. The complete set of engineering data before averaging is available on 14 GSS tapes which may be accessed as described in subsection 9.2.4.

Table 3 lists the quantity and unit given in the engineering data for each type of sensor. Note that raw data are given for the IRAD gauges because post-experiment calibration (R. Lingle, Terratek, Inc, personal communication) has indicated that the calibration parameters vary with time, calibration configuration, and the preset stress of the gauge's vibrating wire.

Appendix D--available by request--consists of microfiches containing plots and listings of the engineering data.

4.5 Sign Convention

Sign convention is of concern only for displacement and stress data. The engineering data employs the rock mechanics convention, where contraction is positive, for both the displacement measured by extensometers and borehole diametral displacements measured by USBM gauges. Data logger and long-term data also employ the rock mechanics sign convention for USBM data; however, the opposite convention, i.e., that expansion is positive, has been inadvertently used for extensometer data.

Table 3. Units used in the engineering data

Sensor type	Quantity Measured	Unit
heater power monitor	power	watt
heater current monitor	current	amp
heater voltage monitor	voltage	volt
thermocouple	temperature	°C
extensometer	displacement	mm
IRAD	vibrational period of wire	10^{-7} second
USBM	diametral displacement of 38 mm borehole	mm

5. DATA VERIFICATION

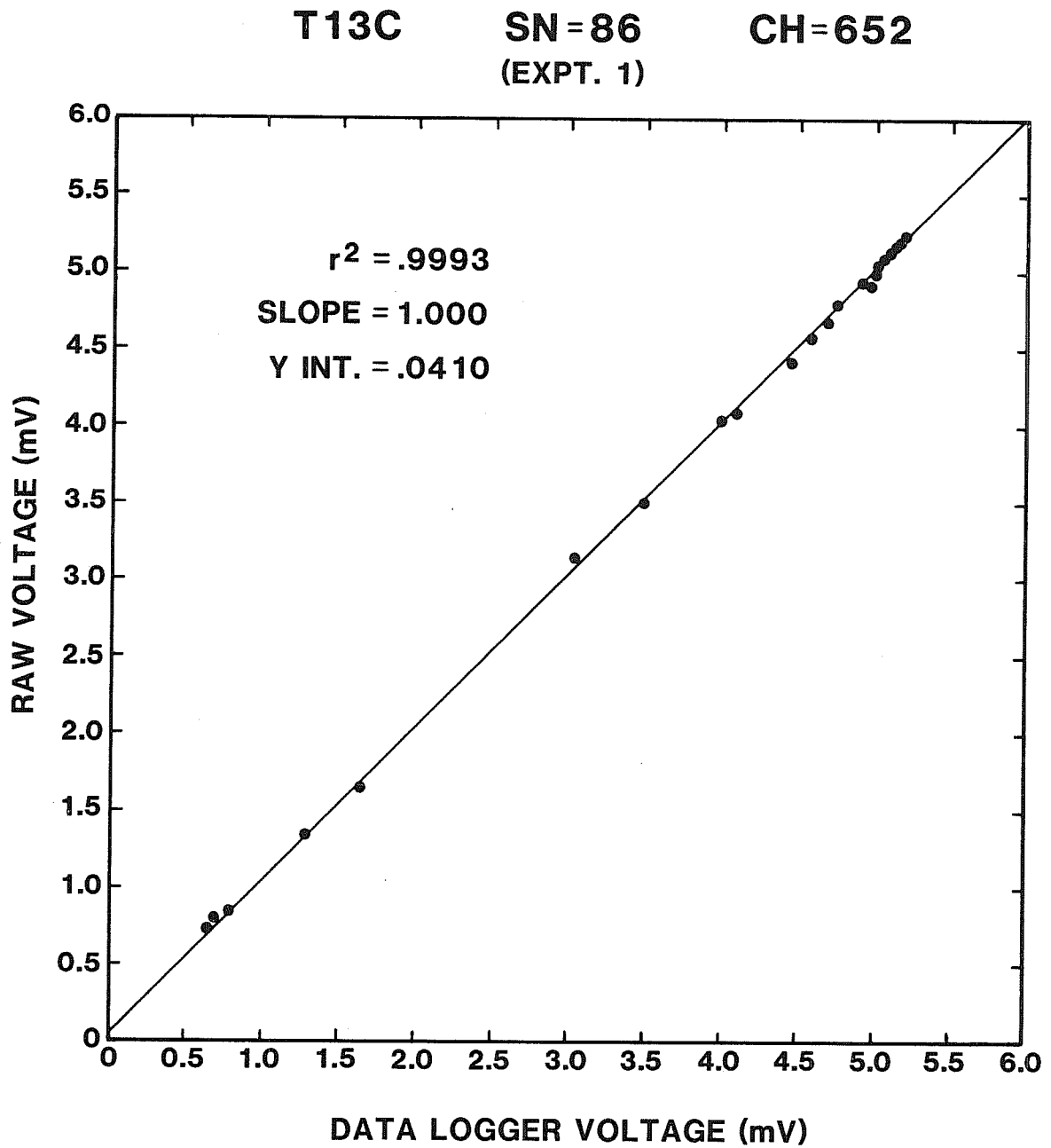
The raw data³ have gone through some encoding-decoding, copying, and reorganization processes, as explained in Sections 2 and 3 above. To ensure that no gross error, such as misidentification of sensor or time, has been inadvertently introduced, the raw data were verified by comparison with logger data⁴, using the procedure described below. Minor differences between these two types of data are treated in Section 6.

A number of sensors were selected to cover the different types of instrumentation and the three different experiments. Data recorded on paper tapes by the data loggers were transcribed into computerized files for approximately 60 randomly selected values of time. In addition, logger data for all the sensors were transcribed for two or three selected times. These sampled logger data were converted back to voltages and compared with the raw data by means of scatter plots. A few examples of these scatter plots are presented in Figs. 10-13. Linear least-squares regression lines are also shown on the same figures. It is evident that, for these four cases, the two types of data are almost perfectly correlated so that the linear regression line for each case illustrated has a slope nearly equal to 1 and a very small intercept. This good correlation is typical of the majority of sensors examined, as indicated by the values of the cross-correlation coefficients listed in Table 4.

Good correlation was also obtained when raw data for all sensors at two values of time were compared to the corresponding logger data. This is

³See Glossary and Subsection 4.1 for definition and description of raw data.

⁴See Glossary and Subsection 4.2 for definition and description of logger data.



XBL 8010-12351

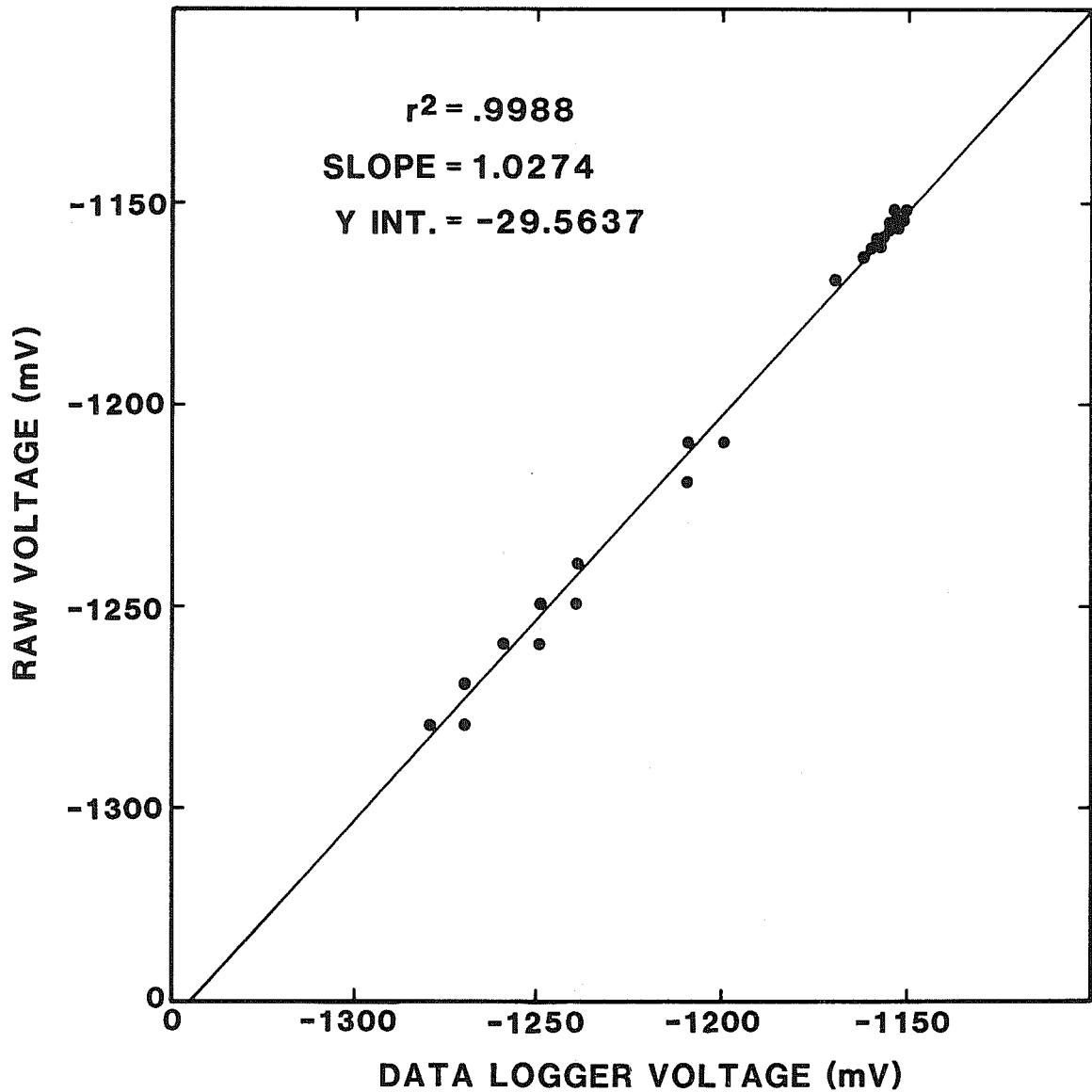
Fig. 10. Scatter plot of raw data versus AD-9 logger data for a thermocouple.

E2B

CH=5

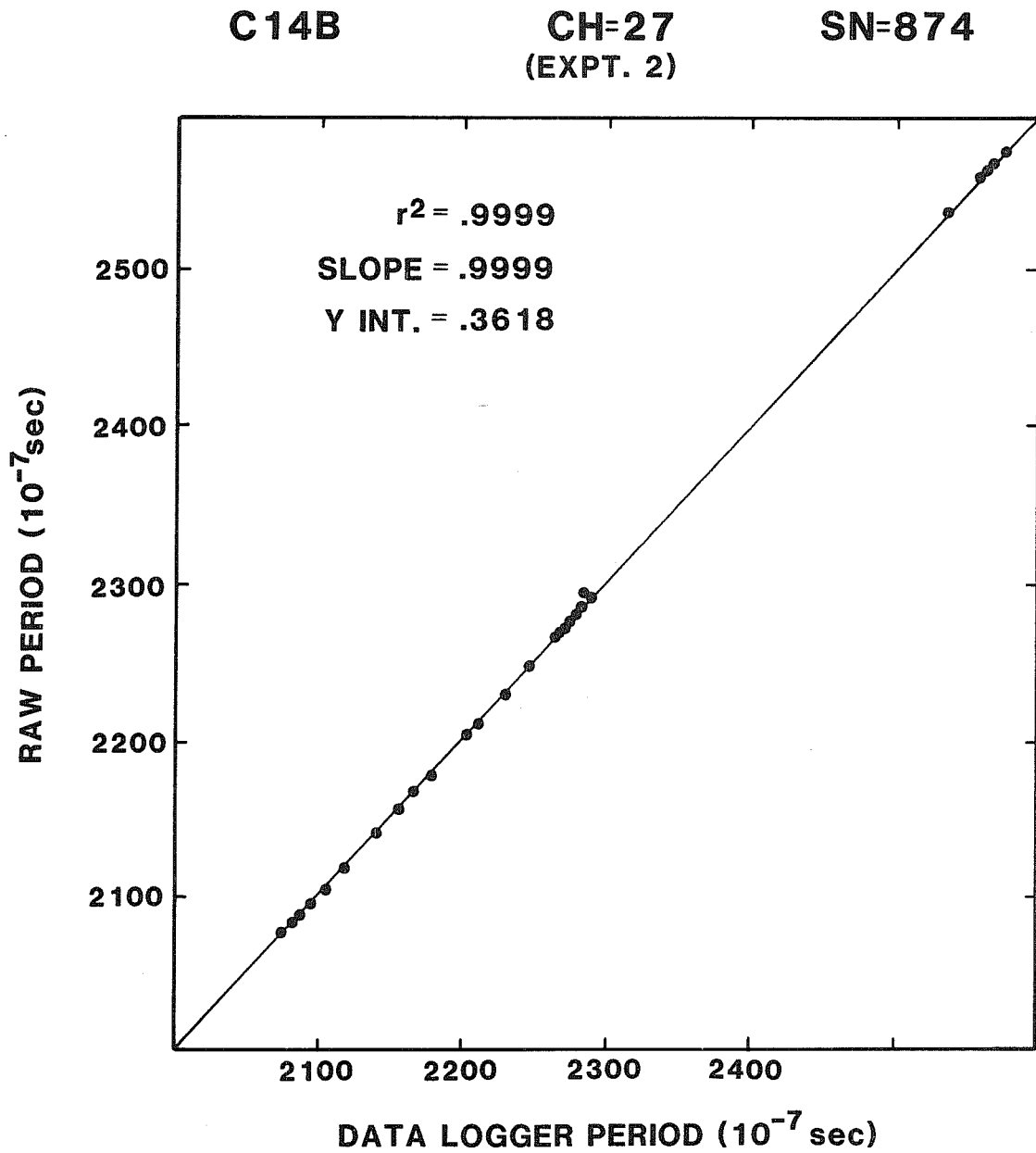
SN=1086

(EXPT. 3)



XBL 8010-12350

Fig. 11. Scatter plot of raw data versus AD-9 logger data for an extensometer anchor point.



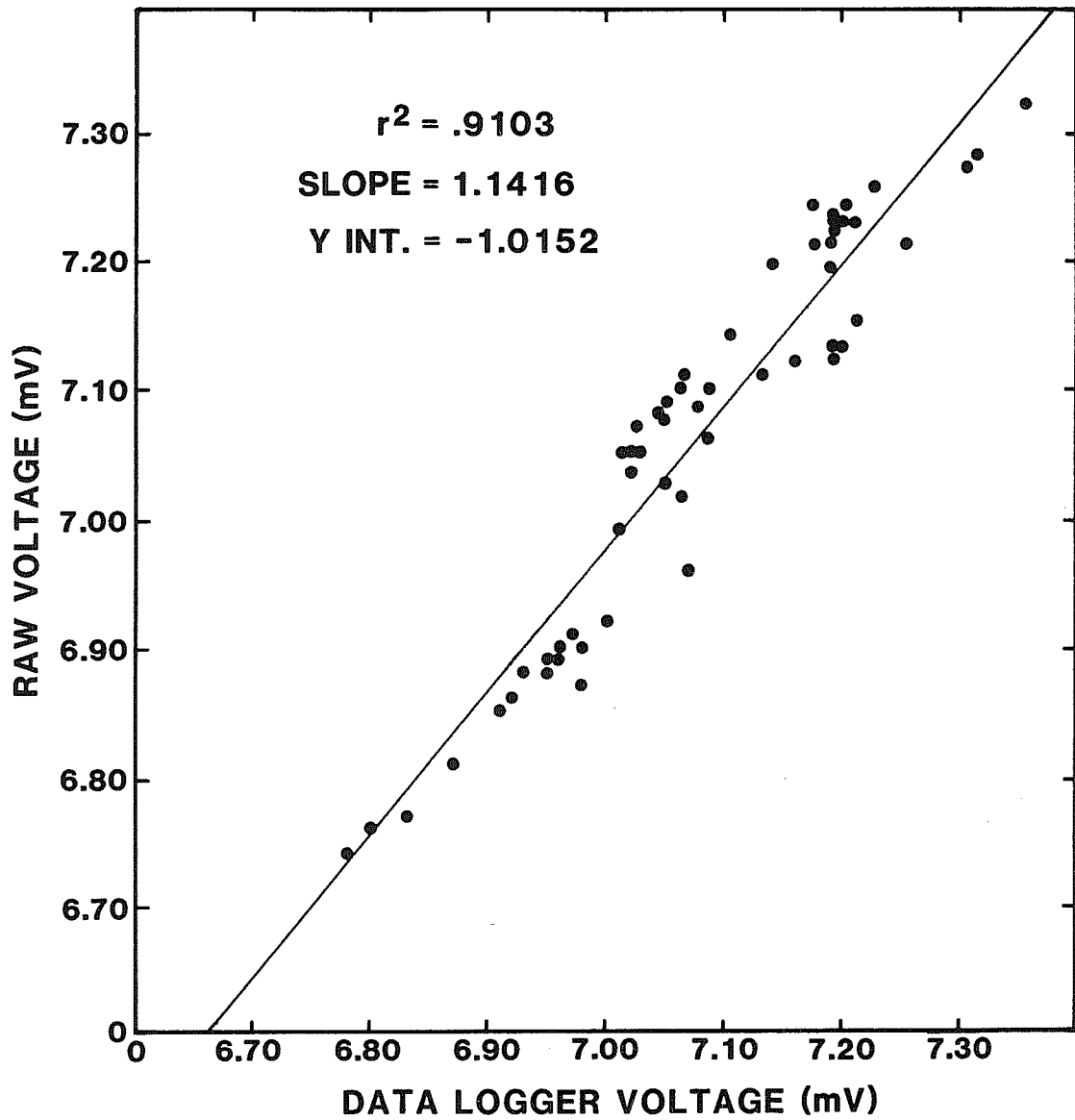
XBL 8010-12349

Fig. 12. Scatter plot of raw data versus IRAD logger data for an IRAD stressmeter.

U24A

CH-69
(EXPT. 2)

SN = 744



XBL 8010-12348

Fig. 13. Scatter plot of raw data versus B&F logger data for USBM gauge.

Table 4. Cross correlation coefficient (r) between raw data and data logger data for some sensors in the Stripa heater experiments

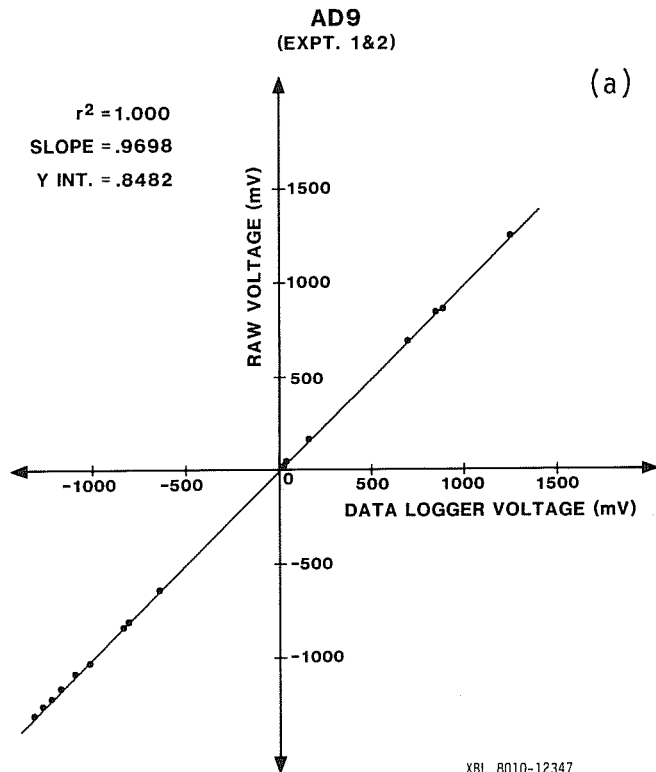
Experiment 1 (Full scale, H9)			Experiment 2 (Full scale, H10)			Experiment 3 (Time Scaled)		
Label	Sensor Number	r	Label	Sensor Number	r	Label	Sensor Number	r
E9A	303	0.990	E16A	817	1.000	E2A	1085	0.985
E9B	304	0.999	E16B	818	1.000	E2B	1086	0.999
E9C	305	1.000	E16C	819	1.000	E2C	1087	1.000
E9D	306	1.000	E16D	820	1.000	E2D	1088	1.000
TE9A	29	0.993	TE12E	140	0.969	TE2E	989	0.882
TE9B	30	0.998	TE16A	458	1.000	TE2A	906	0.990
TE9C	31	0.997	TE16B	459	1.000	TE2B	907	0.996
TE9D	32	0.996	TE16C	460	1.000	TE2C	908	0.996
TE7E	133	0.802	TE16D	461	0.999	TE2D	909	0.997
TE7D	160	0.975	TE15D	162	0.981	E3A	1089	0.995
T13C	86	1.000	E29D	833	0.999	E3B	1090	0.999
			E29C	834	1.000	E3C	1091	1.000
			E29B	835	1.000	E3D	1092	1.000
			E29A	836	1.000	TE3E	993	0.858
			TE31E	153	0.675	TE3F	1016	-0.232
			TE29D	474	0.994	TE3G	1017	-0.170
			TE29C	475	0.999	TE3A	910	0.996
			TE29B	476	0.998	TE3B	911	0.988
			TE29A	477	0.998	TE3C	912	0.988
			U24A	744	0.955	TE3D	913	0.994
			U24B	745	0.957	T4C	939	0.996
			U24C	746	0.969			
			TU24	438	0.997			
			C5A	865	0.288			
			C5B	866	0.359			
			T19C	512	1.000			

illustrated in Fig. 14, which shows scatter plots for the four data loggers: (a) AD-9 logger for full-scale experiments (Experiments 1 and 2), (b) AD-9 logger for time-scaled experiment (Experiment 3), (c) B&F logger for USBM gauges, and (d) IRAD logger for IRAD gauges. Each point on any of these figures represents the raw data and logger data for a certain sensor at one of the two time values. Different points correspond to either different sensors or different times. The number of points plotted in each frame appears to be far fewer than the number of sensors because many of the data values are indistinguishable on this scale. The regression lines, however were computed from all the data points.

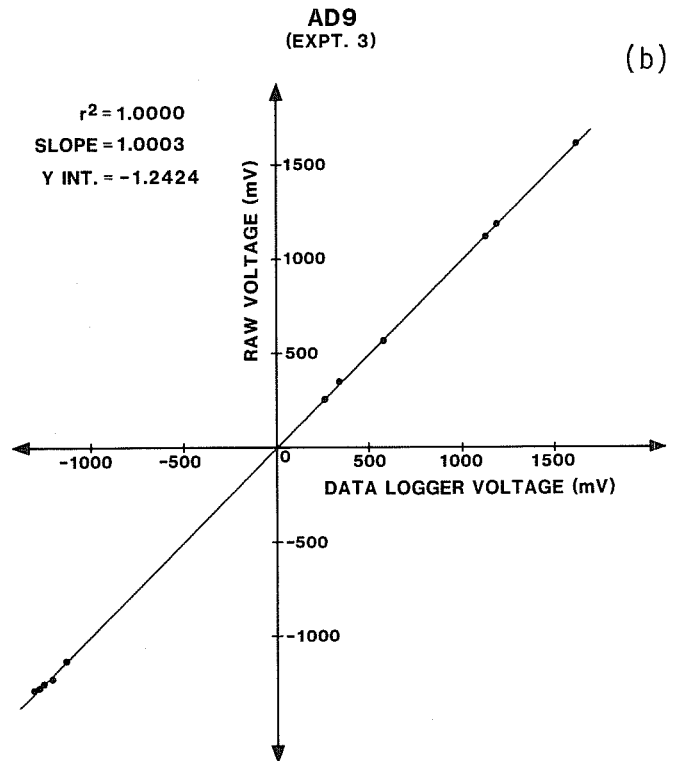
There are a few cases where the cross-correlation coefficient is significantly less than 1. An example is given in Fig. 15 for sensor TE3F (sensor number 1016), a thermocouple in hole E3 in Experiment 3 (the time-scaled experiment). To identify the cause for poor correlation between raw data and logger data for sensors such as TE3F--whose cross-correlation coefficient, r , has a value of -0.232--the time histories for both types of data were plotted. Figures 16 (a) and (b) respectively illustrate the time histories of the raw and logger data for this thermocouple. These figures reveal that noisy signals are responsible for the poor correlation. The noises in the two types of data are not correlated because the data loggers exhibited better common-mode noise rejection, and sampling times were not synchronized with the computer-based data acquisition system. The analog-to-digital converters in both the computer and the data loggers integrated over an integral number of cycles of their power line frequencies; however, the computer used 60 Hz power and the data loggers used 50 Hz power. Thus, 50 Hz common-mode noise would degrade the computer's data much more than the

data logger's. Raw data were collected at 15-minute intervals; this period yields a maximum discrepancy of 7.5 minutes between the time of the logger data and raw data paired for the scatter plot and cross-correlation coefficient. The change in the measured quantity in 7.5 minutes is negligible for a well-behaved sensor providing smooth data but not for rapidly fluctuating noise. When the noisy portions of the data are removed from the comparison, the correlation is substantially improved, as evidenced by the scatter plot shown in Fig. 17 and a cross-correlation coefficient, r , of 0.942.⁵

⁵Since $r^2 = 0.8869$, $r = 0.9418$.



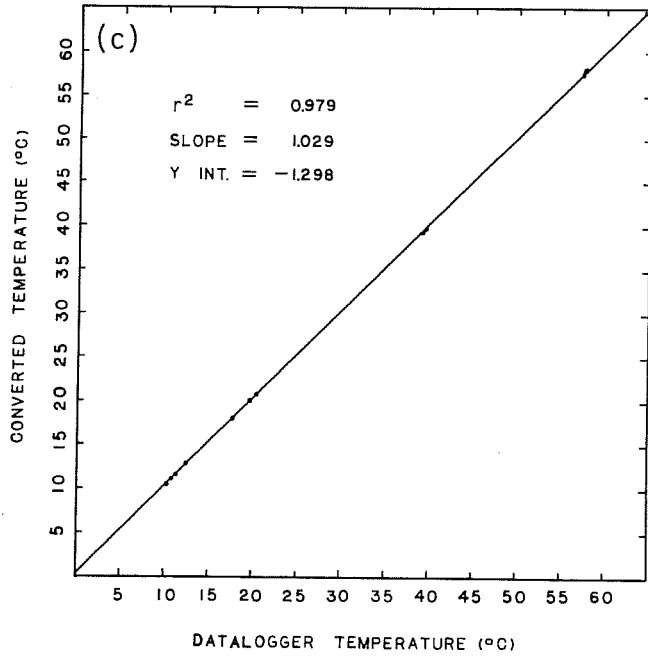
XBL 8010-12347



XBL 8010-12346

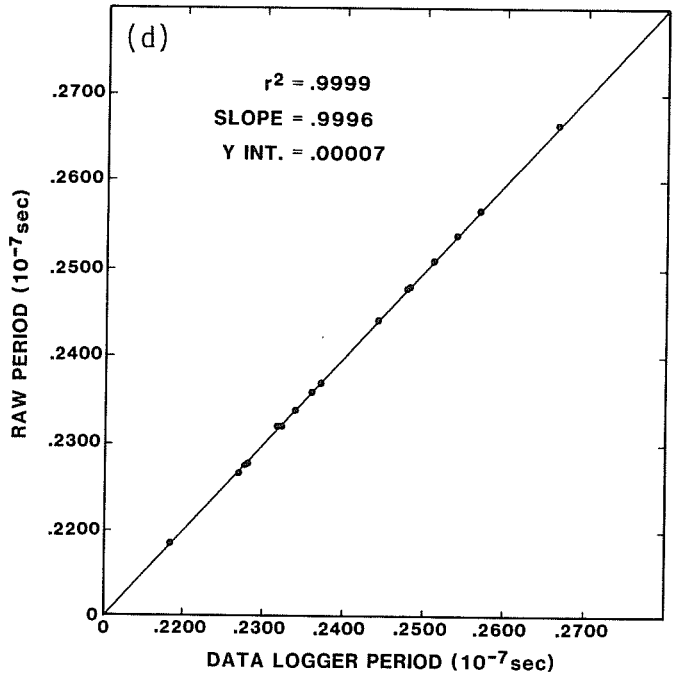
Fig. 14. Scatter plot of raw data versus logger data at two values of time for all sensors: (a) AD-9 logger data for Experiments 1 and 2 (full-scale experiments), (b) AD-9 logger data for Experiment 3 (time-scaled experiment), (c) B&F logger data, and (d) IRAD logger data.

EXPT. 2



XBL 8010-12335

IRAD
(EXPT. 1&2)



XBL 8010-12344

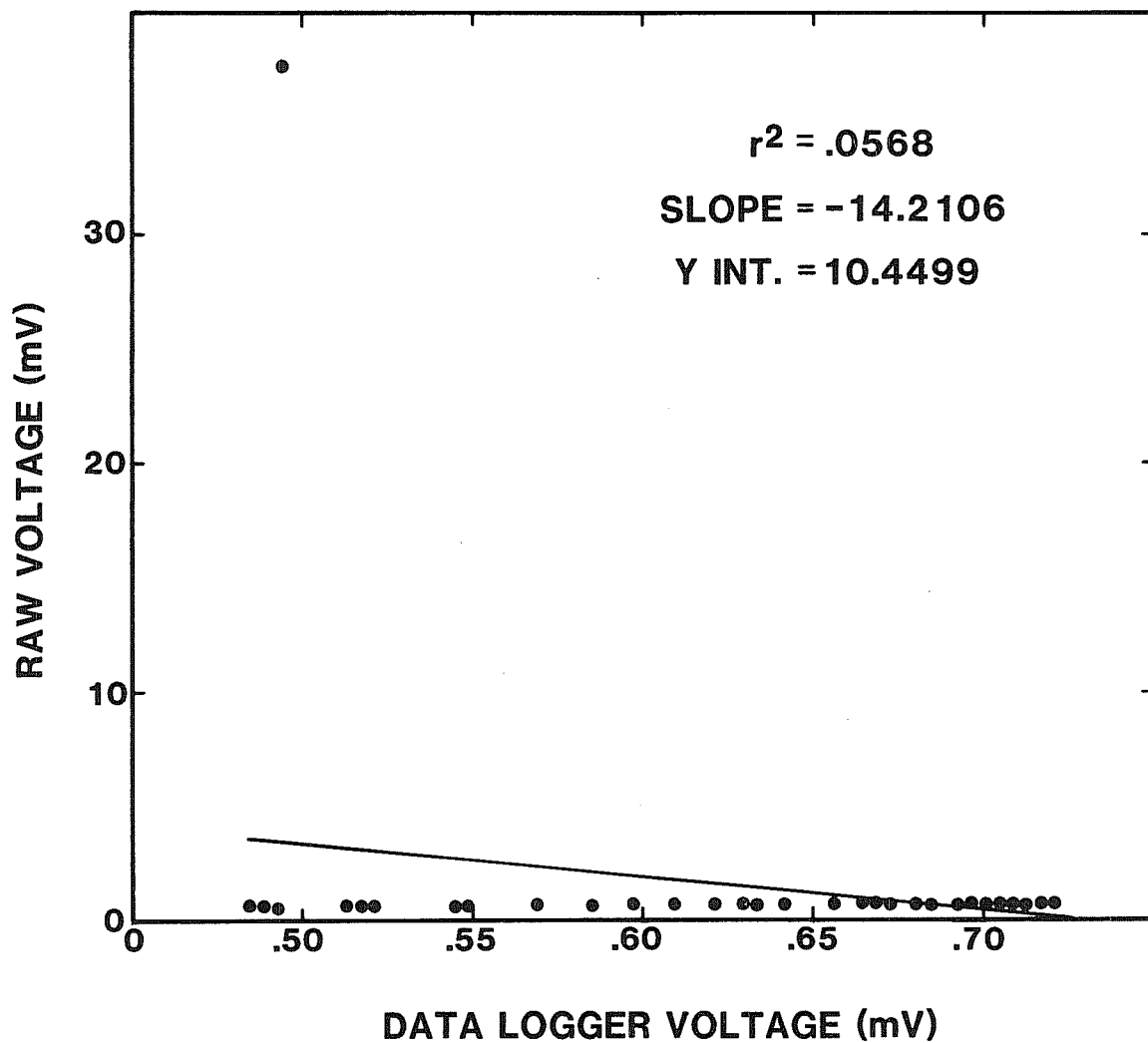
Fig. 14 (continued).

TE3F

CH=72

SN = 1016

(EXPT. 3)

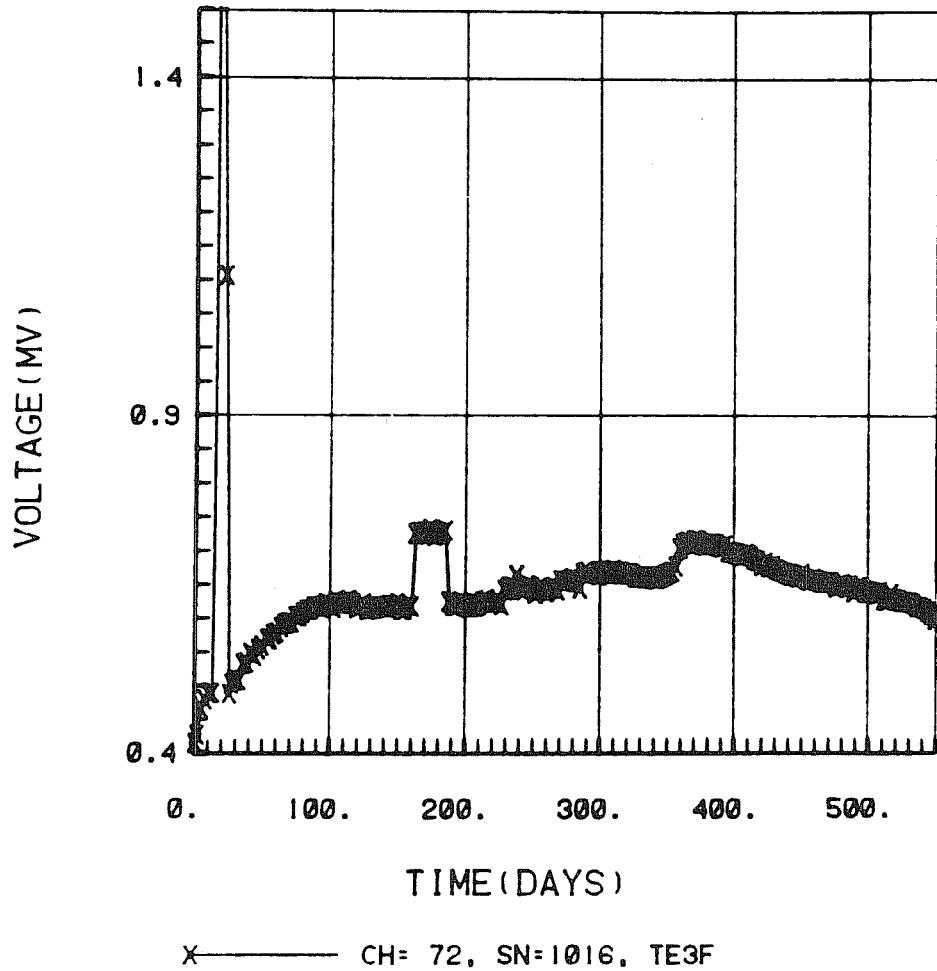


XBL 8010-12343

Fig. 15. Scatter plot of raw data versus AD-9 logger data for a thermocouple, showing poor correlation.

STRIPA TIME SCALE
RAW DATA VERSUS TIME

(a)

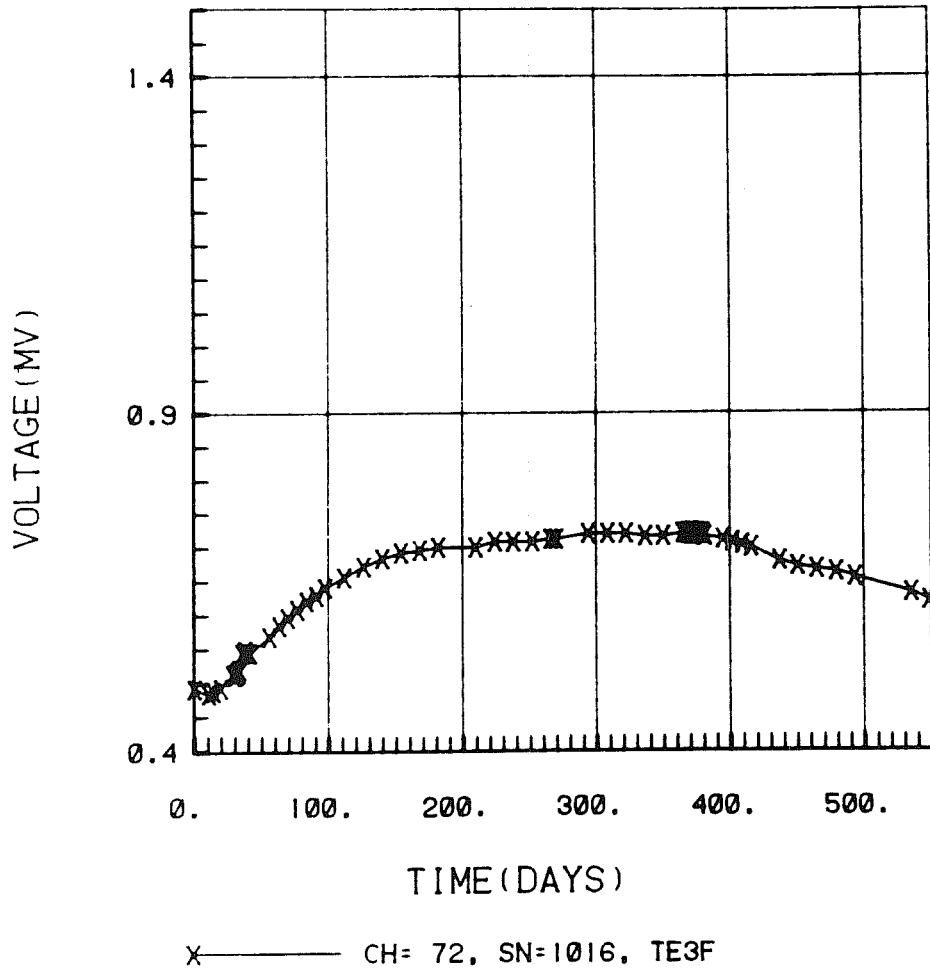


XBL 8010-12342

Fig. 16. Time history for voltage data for the thermocouple in Fig. 15: (a) raw data, (b) AD-9 logger data.

(b)

STRIPA TIME SCALE
LOGGER DATA VERSUS TIME



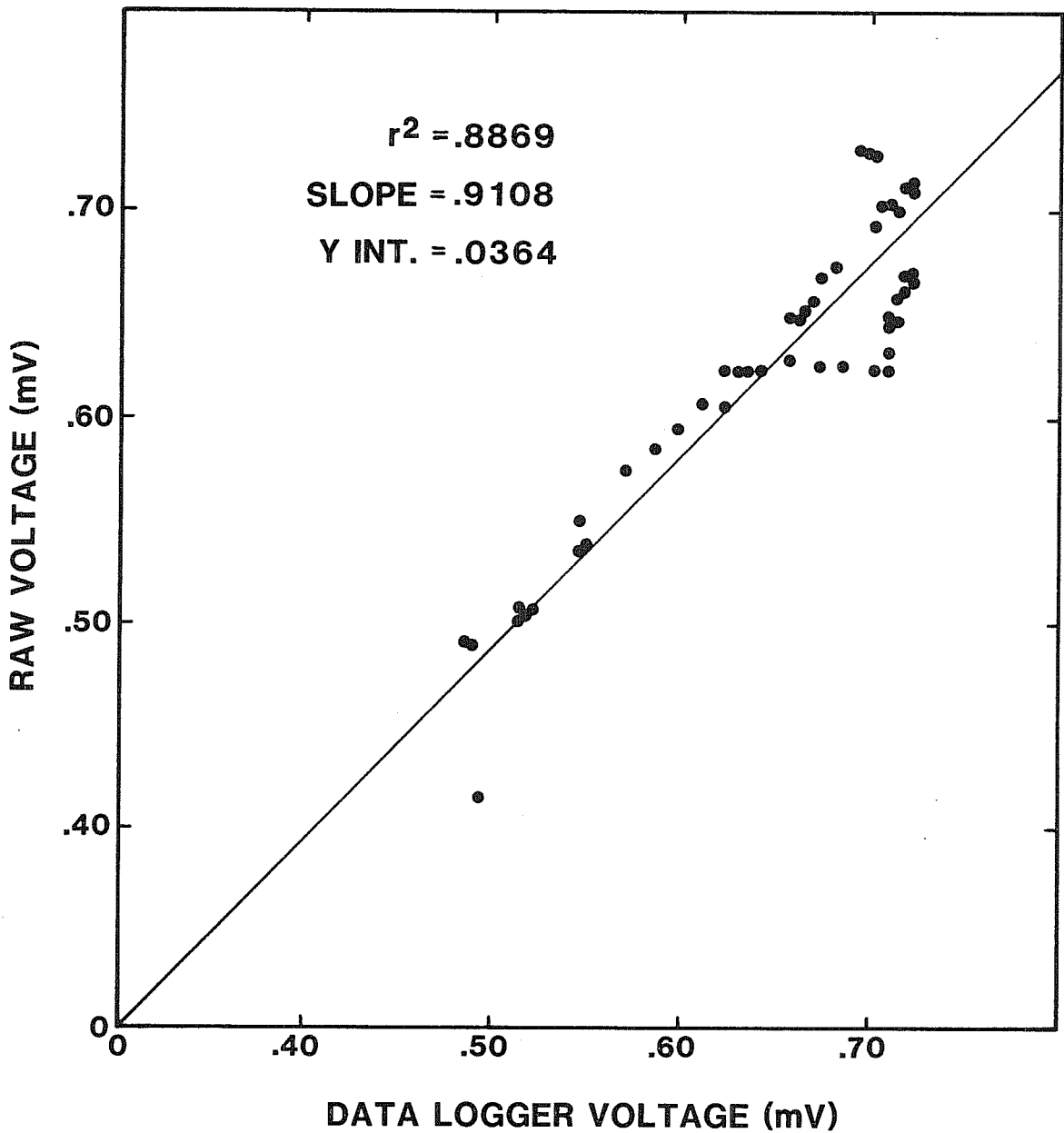
XBL 8010-12341

Fig. 16 (continued).

TE3F

CH-72
(EXPT. 3)

SN=1016



XBL 8010-12340

Fig. 17. Scatter plot of raw data versus AD-9 logger data for the thermocouple in Fig. 15, showing improved correlation after bad data points were removed.

6. DATA PROCESSING PROCEDURES

6.1 Correction for Voltage Errors

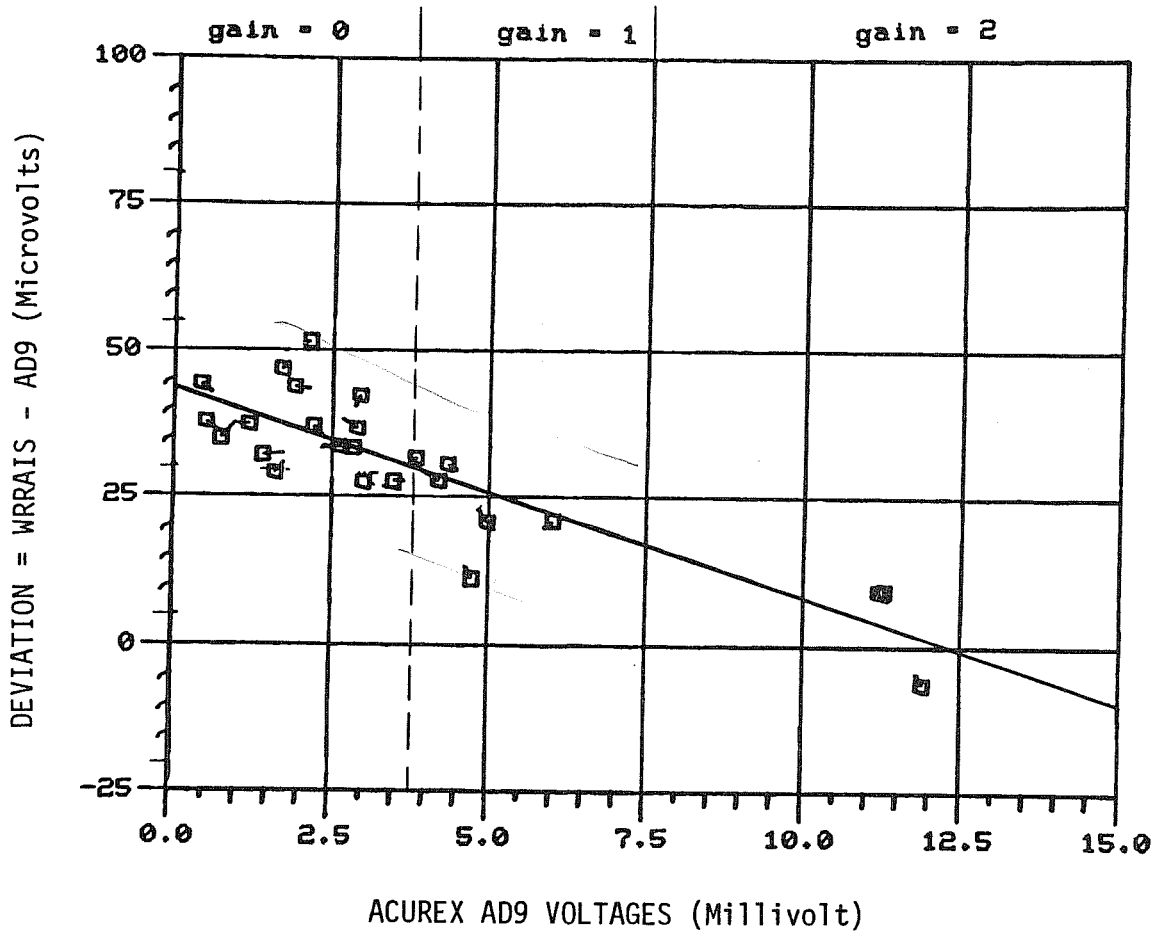
As detailed in Appendix B, errors were introduced into the computer-acquired raw voltage data due to malfunctions in the computer's "Wide-Range Relay Analog-Input Subsystem." These error sources affected measurements from all instrumentation except the IRAD gauges but were negligible for extensometer and heater data. Fortunately, the back-up AD-9 data loggers performed superbly throughout the heater experiments, as demonstrated by calibration with known reference voltages (see Appendix B). Consequently, the AD-9 logger data were utilized as a standard to identify and correct the voltage errors in the computer's raw data.

The following method was used to correct the voltage errors:

Step 1 One sensor from a full-scale experiment and another from the time-scaled experiment were chosen. Plots of raw voltages for these sensors against time were examined to locate the time at which discontinuities occurred.

Step 2 A number of sensors were chosen that spanned the range of voltages experienced by sensors during the experiments. A linear relationship between the computer's raw data and the AD-9 logger data was assumed to exist for time intervals between any two consecutive discontinuities. Least-squares regression was then used to establish the slope and intercept of this relationship. A sample scatter plot of raw (WRR AIS) voltage minus (-) AD9 data logger voltage plotted versus AD-9 logger voltage, along with the least-squares fitted straight line, is given in Fig. 18. Note that although the least squares fit was not carried out directly between the two voltages, it

COMPARISON BETWEEN MODCOMP AND ACUREX DATA FOR FULL SCALE
 JULIAN DAY 305, 11/1/78 11:30



XBL 8010-12339

Fig. 18. Scatter plot of the deviation (raw WRAIS voltage minus AD-9 logger voltage) versus AD-9 logger voltage.

was equivalent to a direct fit because of the linear assumption.

Step 3 Linear regression plots were generated for times before and after the times that voltage discontinuities occurred. The best-fit slopes and intercepts were used in a piecewise linear algorithm to correct for voltage errors. Most slopes and intercepts were treated as constants throughout their respective time slots. When the slope and intercept changed significantly between the beginning and end of a particular time slot, the correction algorithm linearly interpolated between the end-point values.

Steps 1 and 2 above are discussed in detail in Appendix B. Step 3 will be restated below in the form of equations actually coded into the computer program that corrected the errors. The algorithm in Appendix B had to be modified to take account of two conditions, namely (1) NBS calibration coefficients were used for conversion of all thermocouple data and (2) some USBM gauges were removed, reworked, and recalibrated just before reinstallation.

Although all raw voltage data, except IRAD data, were affected by the hardware problem, only thermocouples and USBM gauges operated in voltage ranges such that the discontinuities were significant. All voltage correction slopes and intercepts are listed in Tables B-18 and B-19 (Appendix B). They were all derived from thermocouple data because the reliability of the USBM gauge data recorded by the B&F data logger was questionable.

It must be noted that this method for voltage correction is valid, in a statistical sense, only if the linear relationship is a good assumption.

Even then its correctness still depends on the goodness of fit of the linear regression, which is sometimes only marginal (see Appendix B). Section 7.1 shows that the procedure does lead to reasonable improvement in most cases.

6.1.1 Thermocouples

NBS calibration parameters, rather than the calibration coefficients obtained on-line for each thermocouple, were used to convert thermocouple voltages to temperatures (see subsection 6.2.2 below) because the NBS parameters are independent of the computer's data acquisition system. The unbiased Acurex AD-9 data logger raw voltages could have been used, but they are not computer-compatible. Therefore, the correct voltages had to be recovered from the computer's raw voltages.

Two possible cases exist.

Case (a) If the correction slopes and intercepts were identical at the beginning and end of the i th time slot, then the equation is⁶

$$V_a = (V_r - V_i)/G_i , \quad (1)$$

where V_r = raw voltage,

V_a = raw voltage reading recorded by an AD-9 data logger

and G_i, V_i = slope and intercept, respectively, of the linear

regression line between V_a and V_r for the i th time slot.

Case (b) If the correction slopes and intercepts were different at the beginning and end of the i th time slot, then the equation is

$$V = \left[(1 - \epsilon) (V_r - V_i^1)/G_i^1 \right] + \epsilon (V_r - V_i^2)/G_i^2 , \quad (2)$$

⁶From Fig. 18, $V_r - V_a = V_i + (G_i - 1)V_a$. Transposition gives Eq. (1).

where G_i^1, V_i^1 = slope and intercept of the linear regression line between V_a and V_r at the beginning of the i th time slot,

G_i^2, V_i^2 = slope and intercept of the linear regression line between V_a and V_r at the end of the i th time slot, and

$$\xi = \frac{t - t_i^1}{t_i^2 - t_i^1} \quad . \quad (3)$$

In Eq. (3), t = the time at which V_r was taken, and

t_i^1, t_i^2 = beginning and end of the i th time slot.

6.1.2 USBM Gauges

For USBM gauges the voltage correction algorithm has to account for two additional factors: (i) calibration parameters were obtained using the computer-based data acquisition system and, therefore, have incorporated voltage errors caused by hardware problems; (ii) some of the gauges were removed, reworked, and reinstalled during the experiments. The corrected voltages should be identical to what the computer-based data acquisition system would have recorded if the system had remained unchanged since the time of the latest gauge calibration or recalibration.

Consider a raw voltage reading V taken at time t from the i th time slot. Assume that the most recent calibration (or recalibration) prior to time t occurred at time t' which is in the j th time slot. Four distinct cases can arise depending on whether the correction parameters (G_i, V_i) and (G_j, V_j) have changed between the beginning and end of the respective time slots.

Case (a) Parameters (G_i, V_i) and (G_j, V_j) remained unchanged between the beginning and end of their corresponding time slots.

The correct voltage, V_c , is given by

$$\begin{aligned} V_c &= V_j + G_j V_a \\ &= V_j + G_j (V_r - V_i)/G_i \end{aligned} \quad (4)$$

where the symbols have the same meaning as given previously.

Case (b) Parameters G_i and V_i remained unchanged between the beginning and end of the i th time slot while parameters G_j and V_j changed within the j th time slot.

The correct voltage is given by

$$\begin{aligned} V_c &= V_j + G_j V_a \\ &= (1-\xi')V_j^1 + \xi'V_j^2 + [(1-\xi')G_j^1 + \xi' G_j^2]V_a \\ &= (1-\xi')V_j^1 + \xi'V_j^2 + [(1-\xi')G_j^1 + \xi' G_j^2](V_r - V_i)/G_i \end{aligned} \quad (5)$$

$$\text{where } \xi' = \frac{t' - t_j^1}{t_j^2 - t_j^1}, \quad (6)$$

$G_j^1, V_j^1; G_j^2, V_j^2$ = values of the parameters at the beginning and end of the j th time slot.

Case (c) Parameters G_i and V_i varied between the beginning and end of the i th time slot while the parameters G_j and V_j remained unchanged during the j th time slot.

The correct voltage is given by

$$\begin{aligned} V_c &= V_j + G_j V_a \\ &= V_j + G_j(1-\xi)(V_r - V_i^1)/G_i^1 + G_j \xi (V_r - V_i^2)/G_i^2 \end{aligned} \quad (7)$$

where all the symbols have been previously defined.

Case (d) Both sets of parameters changed within the corresponding time slot.

The correct voltage is given by

$$\begin{aligned}
 V_c &= V_j + G_j V_a \\
 &= (1-\xi')V_j^1 + \xi' V_j^2 + [(1-\xi')G_j^1 + \xi G_j^2]V_a \\
 &= (1-\xi')V_j^1 + \xi' V_j^2 + [(1-\xi')G_j^1 + \xi'G_j^2][(1-\xi)(V_r - V_i^1)/G_i^1 + \xi(V_r - V_i^2)/G_i^2]
 \end{aligned}
 \tag{8}$$

6.2 Conversion to Engineering Units

This section describes how the computer's data was converted to engineering units once the raw voltage biases were removed.

6.2.1 Heater Monitors

The measured quantities, in correct engineering units, were obtained by multiplying the raw data by powers of 10. Thus

$$\text{heater current} = \text{raw data} \times 10 \text{ (amp)}$$

$$\text{heater voltage} = \text{raw data} \times 100 \text{ (volt)}$$

$$\text{heater power} = \text{raw data} \times 1000 \text{ (W)}$$

6.2.2 Thermocouples

All thermocouples were calibrated individually at the test site.

However, it was recently discovered that errors occurred due to a self-heating problem (Binnall and Du Bois, to be published) within the RTD (resistance temperature device) used as a calibration standard. It was, therefore, decided that the NBS (National Bureau of Standard) thermocouple calibration data would be utilized to convert thermocouple voltages to temperature.

Thermocouples were divided into groups: (a) those with peak temperatures over 300°C during the experiment, (b) those with peak temperatures between 200°C and 300°C and (c) those with peak temperatures below 200°C. Least squares fits of those segments of the NBS calibration tables yielded the coefficients A, B, C, D, and E of the 4th order polynomial;

$$T = A + BV + CV^2 + DV^3 + EV^4, \quad (9)$$

where the voltage V is in mV, and the temperature T is in °C. Equation (9) was used to convert the corrected raw voltage to temperature.

This grouping of thermocouples and their polynomial coefficients for each group are tabulated in Tables C-1 and C-2 in Appendix C.

These three separate polynomials fit the NBS table data within 0.3°C for almost all temperatures and to within 0.05°C for thermocouples that did not exceed 200°C. Binnall and DuBois (to be published) verified this by evaluating Eq. (9) for the voltages in the NBS table, and comparing the results with the corresponding NBS calibration temperatures.

6.2.3 Extensometers

Each extensometer borehole had four anchor points. Rock movement at each anchor point was transmitted by a superinvar rod to a DCDT transducer mounted to the collar of the borehole. A detailed description of these extensometers is given in Schrauf et al. (1979). Thus, if the length of the extensometer rod is constant, the displacement detected by the DCDT represents the relative axial displacement between the anchor point and the borehole collar. During the heater experiments, however, the temperature distribution, and therefore the length, of the rod varied with time.

Consequently, the effect of the thermal expansion (or contraction) of the rod must be removed from the displacement detected by the DCDT in order to obtain the true relative displacement in the rock.

The algorithm for converting the raw voltage output by the DCDT to relative rock displacement consists of two separate steps.

Step 1 The apparent relative displacement between the anchor point and the borehole collar in the rock is given by

$$u_a = -C_1(V_r - V_s) \quad (10)$$

where u_a = apparent relative displacement (mm) using rock mechanics sign convention,

V_r = raw extensometer DCDT voltage (mV),

V_s = initial (starting) DCDT voltage before the heaters were turned on (mV),

C_1 = absolute value of calibration slope (mm/mV).

The two parameters, C_1 , and V_s , were determined by in-situ calibration for each anchor-rod-DCDT unit in each extensometer. Calibration was performed before (Schrauf et al., 1979) and after (Binnall and DuBois, to be published) the heating experiments. These two sets of calibration parameters were found to agree within about 1%. Hence, the mean values, listed in Table C-3 (courtesy of DuBois), were used for the conversion.

Step 2 The thermally induced change in the length of the superinvar extensometer rod, which causes a DCDT voltage reading opposite in direction to that caused by relative rock displacement, is added to the observed apparent relative displacement. Thus the true relative

note: ΔL is negative when rod expands

displacement in the rock is given by

$$u = u_a + \Delta L \quad (11)$$

where ΔL = change in length (mm) of extensometer rod due to thermal expansion of superinvar, with contraction taken as positive.

All terms in Eq.(11) are regarded as algebraic quantities, i.e., they are signed numbers.

The change in rod length is calculated by integrating the thermal strains along the entire length of the extensometer rod; thus

$$\Delta L = \int_0^L \left\{ \epsilon_{th} [T(\ell)] - \epsilon_{th} [T_s(\ell)] \right\} d\ell \quad (12)$$

where L = length of extensometer rod

ϵ_{th} = free thermal strain in extensometer rod (mm/mm) with reference to 20°C

$$= -\int_{20}^T \alpha (T) dT, \text{ where } \alpha = \text{coefficient of linear expansion of superinvar}$$

$T(\ell)$ = temperature distribution along the length of the extensometer rod at the time of measurement (°C)

$T_s(\ell)$ = initial temperature distribution along the length of the extensometer rod.

Temperature, T , was measured only at several discrete points along the extensometer rod and the free thermal strain, ϵ_{th} , was measured for superinvar at a discrete number of temperatures (Table 5). Therefore, it was necessary to interpolate for both T and ϵ_{th} in order to numerically evaluate the integral in Eq. (12). Thus the numerical procedure for calculating the change in length of the extensometer rods comprises the following steps:

(i) interpolate the measured discrete temperatures to obtain the

Table 5. Free thermal strain data for superinvar rod. ϵ_{th} = Integrated thermal expansion per unit length as measured from a base value at 20°C

T (°C)	ϵ_{th} (mm/mm) $\times 10^{-6}$
20	0
30	2
40	5
50	12
60	18
70	26
80	35
90	48
100	62
110	79
120	97
130	118
140	141
150	167
160	197
170	233
180	276
190	329
200	380

- temperature distribution, $T(\ell)$, as a function of the length variable, ℓ ;
- (ii) knowing the temperature, T , at a point, ℓ , interpolate Table 5 to obtain the free thermal strain at the corresponding temperature;
 - (iii) numerically integrate the right-hand side of Eq. (12).

Interpolation for temperature profile

For the Stripa experiments, from 4 to 7 thermocouples were attached to the longest extensometer rod, usually near an anchor point, in each extensometer borehole. This sparse distribution of temperature measurements presented some difficulty in interpolation.

The interpolation method adopted here is similar to that implemented on the MODCOMP computer at the Stripa test site (Teknekron, 1978; Schrauf et al., 1979), with a few improvements. A cubic spline was fitted through the measured temperatures and the fitted coefficients were subsequently used to generate the temperature profile. The spline function is a C^1 -function; that is, it is continuous and has continuous derivatives. The values of the first derivative were specified at the end points for the particular spline function used in the conversion algorithm. At the top (i.e. collar), the slope was obtained by fitting an exponential function, $P_{\text{exp}}(Q\ell)$, through the closest three thermocouple temperatures. Slope at a depth of 30 m in the rock was set equal to zero. For the Stripa experiments, very few extensometers had a thermocouple close to the collar of the hole. It was, therefore, necessary to assume that the temperatures in the drifts were uniform such that measurements at the collar of one extensometer hole could be used for other holes. Furthermore, to avoid oscillation in the fitted curve,

the temperature in the rock at a point 20 m deeper than the deepest thermocouple was assumed to be 9°C, based on ambient rock temperature information prior to heating. Some extensometer rods extended across the heater centerline (see Fig. A-8, Appendix A). In some of these cases no valid temperature measurement existed on one side of the centerline, due to either the absence of thermocouples or a failure of installed thermocouples. A temperature profile symmetric about the centerline was assumed for such cases. Temperatures of real thermocouples were reflected across the centerline to create virtual thermocouple readings for the purpose of interpolation.

Interpolation for free thermal strain

Thermal expansion of a superinvar rod was determined in laboratory tests at a sufficient number of temperatures (see Table 5) that piecewise linear interpolation was considered sufficiently accurate.

Numerical evaluation of the integral in Eq. (12)

A crude method of numerical integration was used since the temperature profile along an extensometer rod was a simple smooth curve with no sharp peaks. The distance between any pair of adjacent thermocouples (real or virtual) was divided into 20 equal segments. The integration in Eq. (12) was approximated by direct summation of the thermal expansion of all segments comprising the extensometer rod. The validity of this approximation will be verified in Section 7.2.3. In practice, the second term in the integral in Eq. (12), was omitted in the calculation since the initial rock temperature was less than 20°C anywhere in the experiments and the thermal expansion of superinvar from 0 - 20°C is negligible (Smithells, 1976).

Thermal corrections were not applied whenever all the thermocouple temperatures in an extensometer hole were less than 20°C.

6.2.4 USBM Gauges

The USBM (United States Bureau of Mines) borehole deformation gauges (Hooker et al., 1974) measures the change in diameter of a borehole at three orientations 60° apart. The (two-dimensional) stress tensor can be deduced from these three diametral displacements, provided that either plane-stress or plane-strain condition prevails and the rock mass is isotropic and linearly elastic with known uniform elastic constants over a distance of several borehole diameters.

The diametral displacements of the borehole were detected by three pairs of buttons; each button is attached to a cantilever. Strain gauges mounted on diametrically opposing cantilevers form a bridge circuit, the output voltage of which constitutes the raw gauge readings. Thus, each USBM gauge must be calibrated so that these raw voltages can be converted back to diametral displacements.

In the Stripa heating experiments the USBM gauges were installed to measure the diametral displacements (and hence stress) induced by heating of the rock. Conversion of raw voltages to diametral displacements was complicated by elevated temperatures which varied with time. An extensive program was undertaken to evaluate and calibrate these gauges (Schrauf et al, 1979). Results that influence the conversion algorithm are summarized as follows:

- (a) the diametral displacement of each component of a gauge, at constant temperature, is directly proportional to the raw voltage;

- (b) the constant of proportionality, hereafter referred to as the calibration slope, varies approximately linearly with temperature and varies from gauge to gauge;
- (c) even with no displacement, i.e. with the gauge's buttons removed, the strain-gauge bridge still outputs a non-zero voltage that varies approximately linearly with gauge temperature;
- (d) when the gauge is heated with gauge buttons held at fixed displacement, the uncompensated voltage of the strain-gauge bridge varies approximately linearly with temperature.

In addition to taking into account the factors (a) - (d) above, the conversion algorithm should also correct for (e) the free thermal expansion of the gauge's body with the gauge's buttons held at fixed displacements, and (f) the increase in borehole diameter due to the free thermal expansion of the rock. Considering the rather limited and, therefore, statistically uncertain amount of thermal expansion coefficient data currently available for Stripa granite, the correction factor (f) has been temporarily omitted from the conversion algorithm utilized to generate the present release (Release 1) of the engineering data.

In previous reports (Teknekron, Inc. 1978 and Schrauf et al. 1979) certain simplifying assumptions were made in the conversion algorithm. The validity of these assumptions are questionable, especially after a USBM gauge has been removed from a borehole, reworked, and reinstalled during the heating experiments. The present algorithm, given below, has included the correction factors (a) - (e) above without any further approximation. This algorithm has been derived using both algebraic and geometrical methods that

produce identical results. The geometrical derivation, which is easier to visualize, is illustrated schematically in Fig. 19. The meanings of the symbols in that figure are:

- T_0 = lower reference temperature for zero-displacement voltage = 11°C for the Stripa experiments,
- T_1 = upper reference temperature for zero-displacement voltage = 200°C for the Stripa experiments,
- T_C = temperature at which on-site calibration was performed to obtain the calibration slope
= 14°C for the Stripa experiments,
- T_i = temperature at which raw voltage was recorded, °C
- T_S = starting temperature, i.e. temperature of gauge after installation (just before heating) or reinstallation, °C (word 6 of sensor parameter record),
- C_C = slope of gauge calibration curve at temperature T_C , mm/mV (word 18 of sensor parameter record),
- C_0 = slope of gauge calibration curve at temperature T_0 , mm/mV,
- C_1 = slope of gauge calibration curve at temperature T_1 , mm/mV,
- C_i = slope of gauge calibration curve at temperature T_i , mm/mV,
- C_S = slope of gauge calibration curve at temperature T_S , mm/mV,
- V_{SS} = starting voltage at time of gauge installation or reinstallation, mV (word 16 of sensor parameter record),
- V_{00} = zero-displacement voltage (with gauge's buttons removed) at temperature T_0 , mV,
- V_{01} = zero-displacement voltage (with gauge's buttons removed) at temperature T_1 , mV,
- V_{0i} = zero-displacement voltage (with gauge's buttons removed) at temperature T_i , mV,

V_{oc} = zero-displacement voltage (with gauge's buttons removed) at temperature T_c , mV,

V_{os} = zero-displacement voltage (with gauge's buttons removed) at temperature T_s , mV,

V_i = raw voltage (at temperature T_i), mV,

U_i = borehole diametral displacement corresponding to V_i , mm,

U_s = starting borehole diametral displacement corresponding to V_s , mm.

The difference $V_{01}-V_{00}$ is given as USBM temperature constant in word 24 of the sensor parameter file record.

The calibration results (b) - (d) summarized above can be expressed in the following equations:

$$C_o = C_c / \left(1 + \frac{C_1 - C_o}{C_o} \frac{T_c - T_o}{T_1 - T_o} \right), \quad (13)$$

$$C_i = C_o \left(1 + \frac{C_1 - C_o}{C_o} \frac{T_i - T_o}{T_1 - T_o} \right), \quad (14)$$

$$C_s = C_o \left(1 + \frac{C_1 - C_o}{C_o} \frac{T_s - T_o}{T_1 - T_o} \right), \quad (15)$$

$$V_{oi} = V_{oo} \left[1 + (V_{01} - V_{00}) \frac{T_i - T_o}{T_1 - T_o} \right], \quad (16)$$

$$V_{os} = V_{oo} \left[1 + (V_{01} - V_{00}) \frac{T_s - T_o}{T_1 - T_o} \right]. \quad (17)$$

Calibration results indicate that

$$\frac{C_1 - C_o}{C_o} \sim 0.06,$$

so the terms on the right-hand-sides of equations (13) to (17) are known.

From Fig. 19, the change in borehole diametral displacement since installation or reinstallation of the USBM gauge is given by

$$\begin{aligned}
 \Delta U_i &= U_i - U_s \\
 &= AD \\
 &= AB - DB \\
 &= AB - HE .
 \end{aligned}$$

Now, from triangle ABC

$$\begin{aligned}
 AB &= \frac{AB}{BC} \times BC \\
 &= C_i \times BC \\
 &= C_i (V_i - V_{oi}) .
 \end{aligned}$$

Similarly, from triangle HEF

$$\begin{aligned}
 HE &= \frac{HE}{EF} \times EF \\
 &= C_s \times EF \\
 &= C_s (V_{ss} - V_{os}) .
 \end{aligned}$$

Therefore,

$$\Delta U_i = C_i (V_i - V_{oi}) - C_s (V_{ss} - V_{os}) . \quad (18)$$

This ΔU_i is the apparent change in diametral displacement, without correcting for the free thermal expansion of the gauge's body or the thermal expansion of the rock. When the gauge's body is heated, its free thermal expansion will produce a spurious displacement equivalent to pushing in the gauge's buttons. This spurious displacement must be removed so that the corrected change in diametral displacement is

$$\begin{aligned}
 \Delta U &= \Delta U_i - \alpha_g d (T_i - T_s) \\
 &= C_i (V_i - V_{oi}) - C_s (V_{ss} - V_{os}) - \alpha_g d (T_i - T_s), \quad (19)
 \end{aligned}$$

where

α_g = coefficient of linear thermal expansion of the gauge's body
(word 19 of sensor parameter record)

= $13.75 \times 10^{-6}/^{\circ}\text{C}$ from calibration results;

d = borehole diameter (word 7 of sensor parameter record)

= 38 mm.

Equations (13) to (19) were coded into a computer program that converts raw voltage data from the USBM gauges to changes of borehole diameters. These changes of borehole diameters will be further corrected for the free thermal expansion of the boreholes when more comprehensive data become available on the thermal expansion coefficient of Stripa granite. Another point to note is that in interpreting the diametral displacements in terms of thermal stresses, the usual plane-strain or plane-stress approximations may not be adequate due to the three-dimensional nature of thermal stress. Chan and Cook (1979) have presented an analysis of this problem, with an illustrative example.

The mathematics involved in the algebraic derivation, omitted here for brevity, parallels that encountered in thermodynamics, the triplet (U,V,T) being the mathematical analog of the state variables specifying a thermodynamic state.

7. VERIFICATION OF DATA PROCESSING PROCEDURES

7.1 Verification of Voltage Corrections

7.1.1 Thermocouples

Thermocouple voltages recorded on raw data (magnetic) tapes were compared to those recorded by the AD-9 data loggers before and after the correction described in subsection 6.1.1 were applied. It was observed that the "voltage correction" procedure generally reduced the difference between the computer's raw voltages and the corresponding voltages recorded by the AD-9 data loggers. This is demonstrated in Table 6, which lists deviations between the computer's raw voltage and the AD-9 data logger's voltage for thermocouple TE7D (sensor number 160) in Experiment 1 before and after correction for voltage errors.

The root-mean-square (rms) deviation between raw voltages and data logger voltages before and after correction were calculated from tables similar to Table 6 for several sensors. Table 7 summarizes this information. Evidently, there was significant improvement for thermocouple data in the full-scale experiments (Experiments 1 and 2). For Experiment 3 (time-scaled experiment), the rms deviation was reduced for some thermocouples but not for others. When raw voltages for the latter group were plotted against time, it was found that these thermocouples were all characterized by noisy signals similar to that depicted in Fig. 16(a).

The corrected raw thermocouple voltages differ from those recorded by the AD-9 data logger by less than $20\mu\text{V}$, which corresponds to approximately 0.5°C . This is considered satisfactory.

Table 6. Deviation of raw voltage from AD-9 data logger voltage for thermo-couple TE7D (sensor no. 160) before and after voltage correction.

Time	Date	AD-9 Logger Voltage (μV)	Raw Voltage (μV)	Corrected Raw Voltage (μV)	Deviation (μV)	
					Before Correction	After Correction
11.30	08/23/1978	382.000	390.625	374.368	8.625	-7.632
01.15	08/24/1978	379.000	397.949	381.768	10.949	2.768
07.00	08/25/1978	382.000	402.832	386.770	20.832	4.770
02.45	08/26/1978	382.000	400.391	384.384	18.391	2.384
00.45	08/28/1978	382.999	395.508	379.633	13.508	-2.367
11.15	08/30/1978	382.000	395.508	379.827	13.508	-2.173
13.15	09/06/1978	382.000	397.949	382.842	15.949	.842
21.45	09/13/1978	382.000	400.391	385.881	18.391	3.881
13.30	09/20/1978	386.000	405.273	391.317	19.273	5.317
18.00	09/27/1978	394.000	439.453	397.286	45.453	3.286
08.00	10/04/1978	398.000	446.777	404.513	48.777	6.513
17.30	10/18/1978	411.000	458.984	416.471	47.984	5.471
07.30	10/01/1978	427.000	473.633	430.878	46.633	3.878
22.15	11/15/1978	444.000	437.012	444.016	-6.988	.016
01.30	11/29/1978	456.000	456.543	463.737	.543	7.737
10.15	12/13/1978	464.000	554.199	477.734	90.199	13.734
22.15	12/27/1978	477.000	563.965	487.573	86.965	10.573
17.45	01/10/1979	489.000	573.730	497.411	84.730	8.411
22.15	01/22/1979	497.000	593.262	503.317	96.262	6.317
22.15	01/23/1979	497.000	595.703	505.830	98.703	8.830
22.15	01/24/1979	501.000	593.262	503.431	92.262	2.431
04.15	01/25/1979	501.000	595.703	505.901	94.703	4.901
13.30	01/26/1979	501.000	588.379	498.611	87.379	-2.389
08.15	01/28/1979	501.000	595.703	506.081	94.703	5.081
08.15	01/30/1979	501.000	593.262	503.739	92.262	2.739
12.15	02/01/1979	505.000	598.145	508.775	93.145	3.775
21.45	02/03/1979	505.000	600.586	511.366	95.586	6.366
11.00	02/07/1979	509.000	600.586	511.568	91.586	2.568
01.30	02/14/1979	513.000	607.910	519.310	94.910	6.310
22.30	02/21/1979	513.000	612.793	524.667	99.793	11.667
03.00	02/28/1979	517.000	615.234	527.472	98.234	10.472
21.00	03/07/1979	521.000	617.676	530.366	96.676	9.366
01.00	03/14/1979	525.000	622.559	535.625	97.559	10.625
15.15	03/27/1979	525.000	612.793	526.576	97.793	1.576
14.15	03/28/1979	529.000	625.000	538.901	96.000	9.901
18.30	04/04/1979	533.000	632.324	546.667	99.324	13.667
02.30	04/18/1979	537.000	632.324	547.419	95.324	10.419
15.30	05/02/1979	541.000	632.324	548.239	91.324	7.239
04.45	05/16/1979	546.000	639.648	556.360	93.648	10.360
04.45	05/30/1979	550.000	644.531	562.052	94.531	12.052
08.45	06/13/1979	554.000	651.855	570.203	97.855	16.203
08.45	06/27/1979	558.000	651.855	570.989	93.855	12.989
15.15	07/11/1979	562.000	649.414	570.083	87.414	8.083
10.30	07/25/1979	566.000	649.414	573.136	83.414	7.156
08.30	08/10/1979	570.000	649.414	576.700	79.414	6.700
10.30	08/11/1979	570.000	651.855	579.392	81.855	9.392
04.30	08/12/1979	570.000	654.297	582.010	84.297	12.010
16.30	08/13/1979	570.000	656.738	584.794	86.738	14.794
04.30	08/14/1979	570.000	651.855	580.004	81.855	10.004
20.45	08/16/1979	570.000	646.973	575.699	76.973	5.699
11.45	08/18/1979	574.000	649.414	578.511	75.414	4.511
02.45	08/20/1979	574.000	649.414	578.873	75.414	4.873
23.15	08/22/1979	574.000	654.297	584.410	80.297	10.410
19.30	08/29/1979	578.000	654.297	585.934	76.297	7.934
04.15	09/05/1979	578.000	654.297	587.351	76.297	9.351
15.45	09/12/1979	582.000	654.297	589.017	72.297	7.017
17.30	09/26/1979	582.000	661.621	599.502	79.621	17.502
05.30	09/27/1979	586.000	666.504	604.515	80.504	18.515
00.15	10/10/1979	586.000	683.594	605.927	97.594	19.927
08.45	11/07/1979	582.000	678.711	601.017	96.711	19.017
14.30	11/21/1979	574.000	666.504	588.742	92.504	14.742
08.30	12/05/1979	566.000	359.180	581.378	93.180	15.378

Table 7. Root-mean-square (rms) deviation between raw voltage and AD-9 logger voltage for a number of thermocouples before and after voltage correction

Experiment	Sensor Label	Sensor Number	rms Deviation (μV)	
			Before	After
1 (H9)	TE9A	29	77.727	12.015
	TE9B	30	73.868	14.705
	TE9C	31	129.957	11.656
	TE9D	32	82.968	19.315
	TE7E	133	68.769	11.323
	TE7D	160	78.914	13.649
	T13C	86	50.569	15.042
2 (H10)	TE29D	474	62.971	9.759
	TE29C	475	57.307	10.307
	TE29B	476	68.004	18.355
	TE29A	477	65.293	20.166
	TE31E	153	60.092	10.625
	T19C	512	37.966	16.333
3 (T.S.)	TE2A	906	13.249	10.782
	TE2B	907	14.246	8.534
	TE2C	908	14.875	6.210
	TE2D	909	13.645	8.080
	TE2E	989	15.278	7.484
	TE3A	910	13.598	10.062
	TE3B	911	35.677	34.627
	TE3C	912	101.456	105.177
	TE3D	913	82.172	86.886
	TE3E	993	14.777	7.683
	TE3F	1016	34.320	35.225
	TE3G	1017	39.804	45.059
	T4C	939	14.866	5.014

7.1.2 USBM Gauges

It was not possible to verify the procedure for correcting the USBM raw voltages since the B&F data logger, which recorded the back-up voltage data from USBM gauges, was not very stable during the experiments.

7.2 Verification of Conversion to Engineering Units

7.2.1 Heater Monitors

Raw data for the heater monitors were converted to heater current, voltage or power simply by multiplying them by powers of 10. Thus, visual inspection of power history plots and comparison of numerical values of converted power data at a few time values to those recorded by the AD-9 data logger were considered sufficient.

7.2.2 Thermocouples

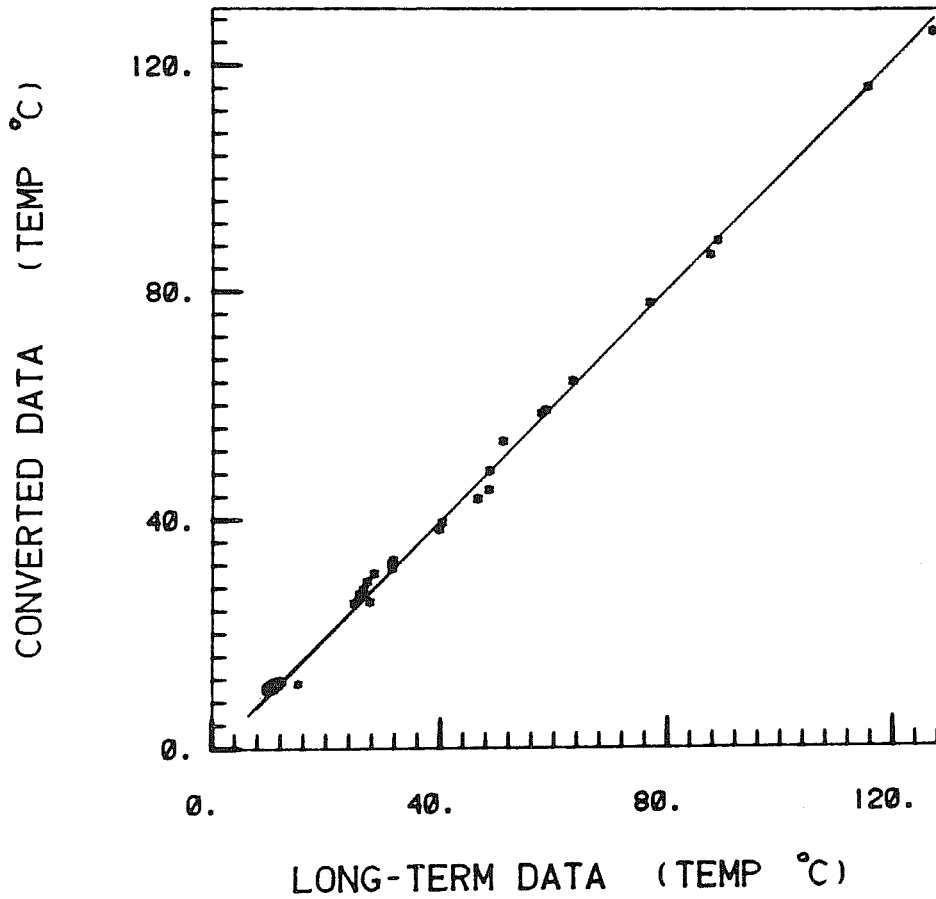
Converted temperature data were compared with temperature data on "long-term" tapes and on the AD-9 logger tapes in scatter plots shown in Figs. 20-21 for sampled thermocouples in the three heater experiments. Excellent correlation was obtained in all cases. The minor differences between temperatures in the engineering data and the long-term data resulted from the different methods for removing errors caused by hardware problems and from the different values of calibration parameters used in the conversion.

7.2.3 Extensometers

A separate computer program, Program 2, was written to verify the procedure for converting the raw extensometer voltage data to displacements. The basic algorithm was the same as that presented in subsection 6.2.3. There were, however, several minor differences between Program 2 and Program 1

LONG-TERM DATA VERSUS CONVERTED DATA

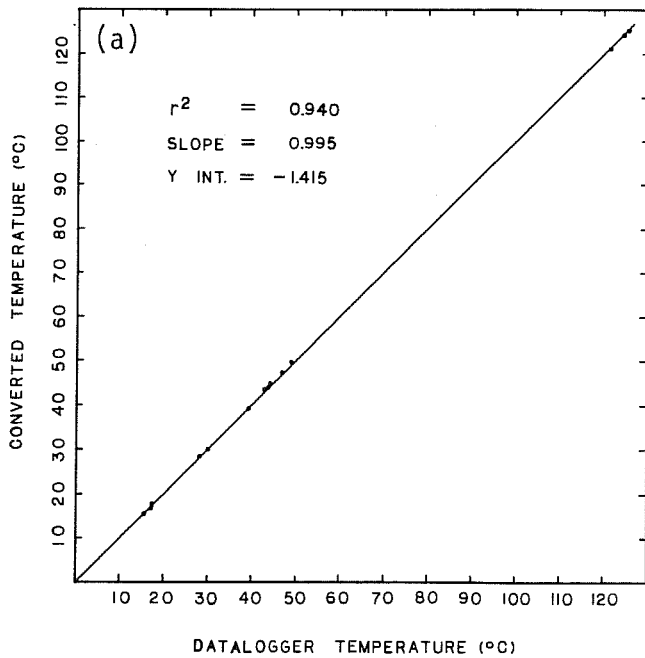
$$Y = 0.9930X + 0.1688$$



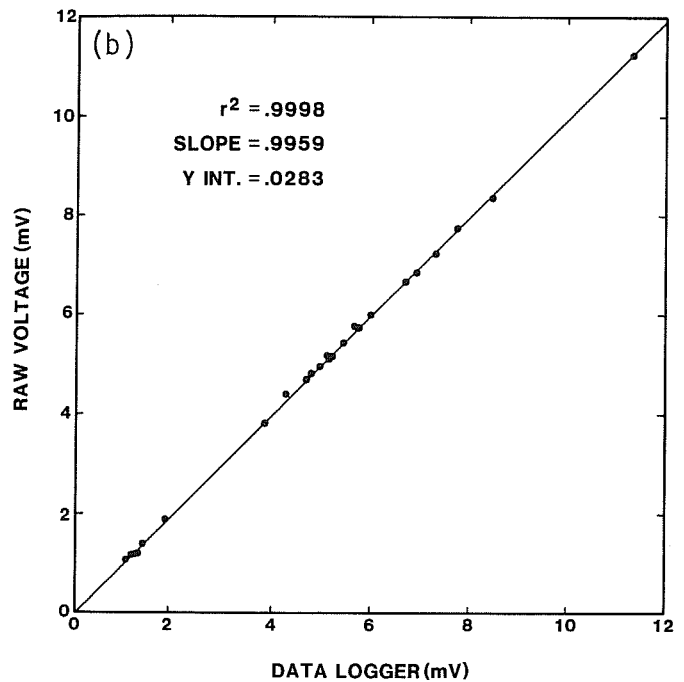
XBL 8010-12337

Fig. 20. Scatter plot of converted temperatures (engineering data) versus long-term temperatures for all thermocouples installed in USBM holes.

EXPT. I



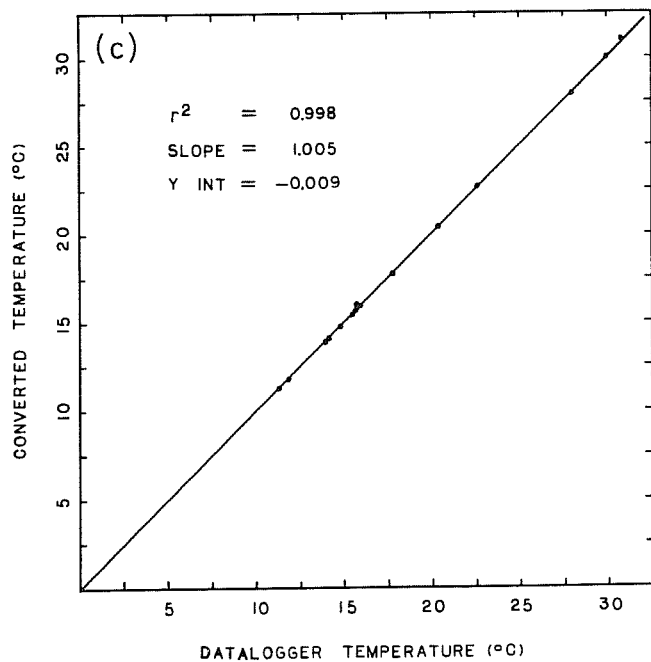
XBL 8010-12336

B&F
(EXPT. 1&2)

XBL 8010-12345

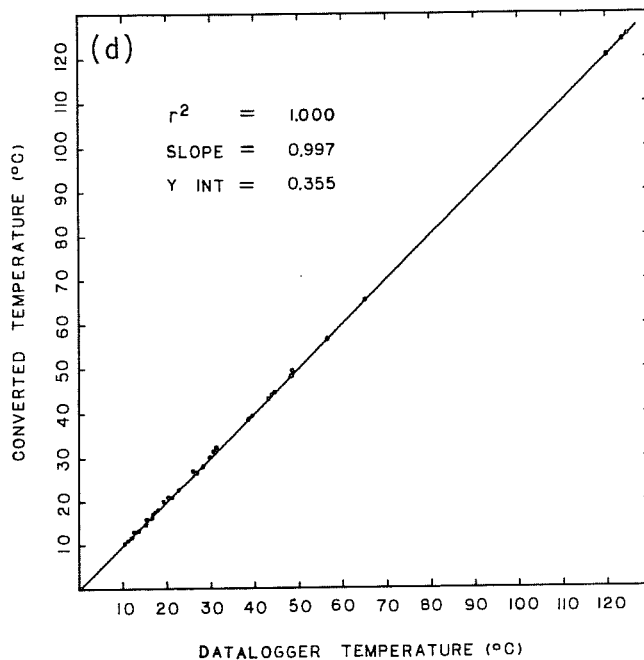
Fig. 21. Scatter plot of converted temperatures (engineering data) versus AD-9 logger temperatures for sampled thermocouples from (a) Experiment 1, (b) Experiment 2, (c) Experiment 3, and (d) all three experiments.

EXPT. 3



XBL 8010-12334

ALL EXPERIMENTS



XBL 8010-12333

Fig. 21 (continued).

which actually converted all the raw voltage data for the extensometers to displacements. These differences were:

- (a) in Program 2, Lagrange interpolation (Carnahan et al., 1969) was used to obtain a continuous temperature profile along an extensometer rod from temperatures measured by thermocouples attached to the rod;
- (b) in Program 2, the integral in Eq. (12), section 6.2.3, was evaluated using the Romberg quadrature (Carnahan et al., 1969) routine, which included automatic convergence criteria;
- (c) in using Program 2, both the raw voltage data and the calibration parameters for extensometers were manually read from microfiches, checked against data recorded by the AD-9 data loggers, and manually input into the program, whereas in Program 1, these quantities were all input by computer file manipulations.

The relative displacements calculated by the two different programs are compared in Table 8 for sampled extensometer data from all three experiments. The two programs are in excellent agreement, considering the very modest number of thermocouples on any extensometer.

7.2.4 USBM Gauges

Again a second computer program, Program 2, was written to confirm the conversion of the raw voltage data for USBM gauges into diametral displacements of boreholes. This time, however, Program 2 employed exactly the same algorithm as Program 1, which was actually used to convert all the raw data to engineering units. The only differences were that (a) raw data and calibration parameters were manually input into Program 2 and (b) Program 2 was executed on an HP-9845B computer.

Table 8. Comparison of engineering data obtained for some extensometers using two different conversion programs
 (a) EXTENSOMETER E6 (Experiment 1, H9)

Experi- ment Time (Days)	Sensor Number	Sensor Label	Uncor- rected Displace- ment, u (mm)	Correction (mm)		$\frac{\Delta u}{u}$ (%)		Corrected Value (mm)		Percentage Difference $\frac{u_{1c} - u_{2c}}{u_{1c}}$ (%)	Max Temp (°C)
				Prog 1 (Δu_1)	Prog 2 (Δu_2)	Prog 1	Prog 2	Prog 1 (u_{1c})	Prog 2 (u_{2c})		
42.47	291	E6A	-.0496	-.0011	-.0014	2.2	2.8	-.0507	-.0510	-0.6	59.4
	292	E6B	-.2793	-.0273	-.0313	9.8	11.2	-.3066	-.3106	-1.3	
	293	E6C	-.4695	-.0475	-.0507	10.1	10.8	-.5170	-.5202	-0.6	
	294	E6D	-.2508	-.0479	-.0514	19.1	20.5	-.2987	-.3022	-1.2	
237.72	291	E6A	-.0524	-.0016	-.0020	3.1	3.8	-.0540	-.0544	-0.7	66.8
	292	E6B	-.3633	-.0369	-.0412	10.2	11.3	-.4002	-.4045	-1.1	
	293	E6C	-.6801	-.0676	-.0708	9.9	10.4	-.7477	-.7509	-0.4	
	294	E6D	-.5068	-.0696	-.0739	13.7	14.6	-.5764	-.5807	-0.8	
328.72	291	E6A	-.0965	-.0019	-.0025	2.0	2.6	-.0984	-.0990	-0.6	67.9
	292	E6B	-.4148	-.0388	-.0435	9.4	10.5	-.4536	-.4583	-1.0	
	293	E6C	-.7445	-.0710	-.0746	9.5	10.0	-.8155	-.8191	-0.4	
	294	E6D	-.5775	-.0735	-.0782	13.2	14.0	-.6510	-.6557	-0.7	

(b) EXTENSOMETER E16 (Experiment 2, H10)

Experi- ment Time (Days)	Sensor Number	Sensor Label	Uncor- rected Displace- ment, u (mm)	Correction (mm)		$\frac{\Delta u}{u}$ (%)		Corrected Value (mm)		Percentage Difference $\frac{u_{1c} - u_{2c}}{u_{1c}}$ (%)	Max Temp (°C)
				Prog 1 (Δu_1)	Prog 2 (Δu_2)	Prog 1	Prog 2	Prog 1 (u_{1c})	Prog 2 (u_{2c})		
94.68	817	E16A	-.1596	-.0025	-.0019	1.6	1.2	-.1621	-.1615	0.4	59.5
	818	E16B	-.5276	-.0327	-.0277	6.2	5.3	-.5603	-.5553	0.9	
	819	E16C	-.8162	-.0573	-.0518	7.0	6.4	-.8735	-.8680	0.6	
	820	E16D	-.5772	-.0589	-.0534	10.2	9.6	-.6361	-.6306	0.9	
298.93	817	E16A	-.5262	-.0370	-.0391	7.0	7.4	-.5632	-.5653	-0.4	105.1
	818	E16B	-.15309	-.2198	-.1873	14.4	12.2	-.17507	-.17182	1.9	
	819	E16C	-.25388	-.3544	-.3204	14.0	12.6	-.28932	-.28592	1.2	
	820	E16D	-.22176	-.3864	-.3591	17.4	16.2	-.26040	-.25767	1.1	
407.23	817	E16A	-.4507	-.0062	-.0053	1.4	1.2	-.4569	-.4560	0.2	67.1
	818	E16B	-.9542	-.0509	-.0434	5.3	4.6	-.10051	-.9976	0.8	
	819	E16C	-.15154	-.0982	-.0904	6.5	6.0	-.16136	-.16058	0.5	
	820	E16D	-.16497	-.1302	-.1252	7.9	7.6	-.17799	-.17749	0.3	

Table 8 (continued)
(c) EXTENSOMETER E3 (Experiment 3, TS)

Experi- ment Time (Days)	Sensor Number	Sensor Label	Uncor- rected Displace- ment, u (mm)	Correction (mm)		$\frac{\Delta u}{u}$ (%)		Corrected Value (mm)		Percentage Difference $\frac{u_{1c} - u_{2c}}{u_{1c}}$ (%)	Max Temp (°C)
				Prog 1 (Δu_1)	Prog 2 (Δu_2)	Prog 1	Prog 2	Prog 1 (u_{1c})	Prog 2 (u_{2c})		
65.88	1089	E3A	-.0265	0	0	0	0	-.0265	-.0265	0	34.7
	1090	E3B	-.0238	0	0	0	0	-.0238	-.0238	0	
	1091	E3C	-.1117	-.0042	-.0044	3.8	3.9	-.1159	-.1161	-0.2	
	1092	E3D	-.1099	-.0085	-.0085	7.7	7.7	-.1184	-.1184	0	
253.03	1089	E3A	-.0796	0	0	0	0	-.0796	-.0796	0	32.1
	1090	E3B	-.1610	-.0007	-.0007	0.4	0.4	-.1617	-.1617	0	
	1091	E3C	-.2845	-.0049	-.0051	1.7	1.8	-.2894	-.2896	-0.1	
	1092	E3D	-.3315	-.0092	-.0092	3.0	3.0	-.3207	-.3207	0	
382.14	1089	E3A	-.1061	0	0	0	0	-.1061	-.1061	0	23.4
	1090	E3B	-.1927	-.0005	-.0006	0.3	0.3	-.1932	-.1933	-0.1	
	1091	E3C	-.3988	-.0020	-.0022	0.5	0.6	-.4008	-.4010	-0.1	
	1092	E3D	-.4555	-.0036	-.0037	0.8	0.8	-.4591	-.4592	-0.02	

Table 9 illustrates the excellent agreement between values calculated by these two programs. The discrepancies in the diametral displacements given by these programs were far less than the probable measurement errors estimated by Schrauf et al. (1979). The programs did not produce identical numerical values because the two different computers retain different numbers of significant figures.

Table 9. Comparison of engineering data obtained for two USBM gauges using two different conversion programs

Sensor Label	Sensor No.	Expt. Time (Days)	Diametral Displacement Program 1	Displacement (mm) Program 2	Difference (1 - 2) (mm)
U2A	204	56.43	-.316787E-02	-.313130E-02	-3.657x10 ⁻⁵
		244.79	-.108102E-01	-.108103E-01	-1.0x10 ⁻⁷
		372.02	-.118564E-01	-.118564E-01	0
		453.43	.332944E-02	.332944E-02	0
		544.85	.260374E-02	.260374E-02	0
U2B	205	56.43	.380719E-02	.384421E-02	3.7x10 ⁻⁵
		244.79	.134930E-01	.134928E-01	2.0x10 ⁻⁷
		372.02	.153576E-01	.153576E-01	0
		453.43	-.253053E-02	-.253053E-02	0
		544.85	-.420620E-02	-.420620E-02	0
U2C	206	56.43	.520767E-02	.523935E-02	-3.2x10 ⁻⁵
		244.79	-.143476E-01	-.143478E-01	+2.0x10 ⁻⁷
		372.02	BAD DATA		
		453.43	-.377763E-02	-.377763E-02	0
		544.85	-.372248E-02	-.372248E-02	0
U14A	720	65.61	.120053E-02	.119993E-02	6.0x10 ⁻⁷
		109.64	-.316598E-03	-.284490E-03	-2.0x10 ⁻⁵
		213.74	-.735532E-02	-.735535E-02	+3.0x10 ⁻⁹
		330.36	.210590E-03	.210590E-03	0
		371.64	.822434E-02	.822434E-02	0
U14B	721	65.61	.193524E-02	.193422E-02	1.02x10 ⁻⁶
		109.64	.123906E-02	.126705E-02	-2.8x10 ⁻⁵
		213.74	.746824E-02	.746814E-02	1.0x10 ⁻⁷
		330.36	-.463410E-03	-.463410E-03	0
		371.64	-.144091E-01	-.144091E-01	0
U14C	722	65.61	.895333E-03	.894710E-03	6.23x10 ⁻⁷
		109.64	-.668303E-02	-.665100E-02	+3.2x10 ⁻⁵
		213.74	.676451E-02	.676448E-02	-3.0x10 ⁻⁸
		330.36	-.114331E-02	-.114331E-02	0
		371.64	-.163030E-01	-.163030E-01	0

8. STRUCTURE AND FORMAT OF THE ENGINEERING DATA ON THE PUBLIC DOMAIN TAPES

8.1 Overall Structure

The public-domain tapes (PDT) consist of two 9-track, 800 bits per inch (bpi), 2400 ft. magnetic tapes written using the NRZI (IBM's own version of non-return on zero) method. The tapes contain character data written in ASCII in 8 bit-fields with the higher order bit equal to zero. Each logical record (or card image) is written in fixed field length with 80 characters per record. Physical records are blocked in groups of 24 (i.e. a blocking factor of 24 logical records per block), giving 1920 characters per block. The last physical record of each file may have fewer than 24 logical records. Both tapes are terminated with a blank file (viz. 2 end-of-file (eof) marks) followed by an end-of-information (eoi) mark. The tapes contain a total of 129 non-blank files; 49 on the first tape (Tape 1) and 80 non-blank files on the second (Tape 2). Figure 22 depicts the overall structure of the PDT.

General Stripa experimental information are stored on files 1 through 3 of Tape 1. The remaining files on Tape 1 contain full-scale (H9, Experiment 1) experimental data. Tape 2 contains both full-scale (H10, Experiment 2) and time-scaled (T.S., Experiment 3) experimental data stored in a format similar to that for Experiment 1.

The master header of the PDT, stored in file 1 of Tape 1, contains the description: "These two tapes contain the time averaged engineering data (Release 1)⁷ for the Stripa heater experiments for the period from June 1978 to June 1980."

⁷A second release of the data is envisaged when sufficient information on rock properties and instrument calibration becomes available to warrant an update of USBM and IRAD data.

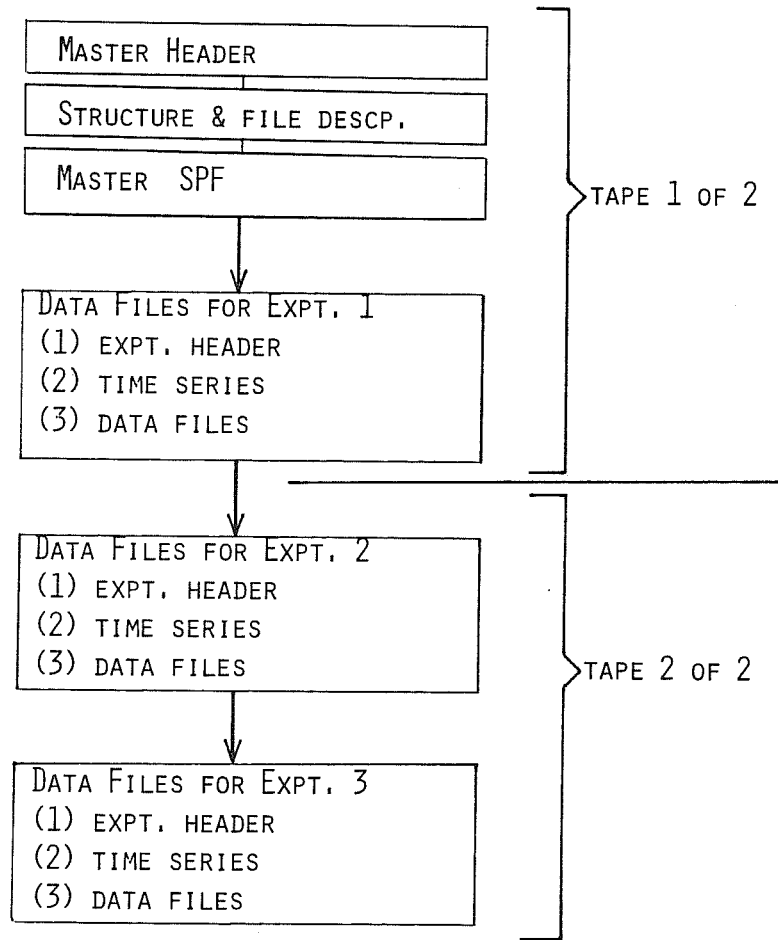
OVERVIEW OF PUBLIC DOMAIN TAPE

Fig. 22. Overall data structure on public-domain tapes.

The PDT's file structure and tape creation methods are stored on file 2 of Tape 1. Content of this file is similar to that described in the first paragraph of Section 8.1 above.

The master sensor-parameter-file (SPF) occupies file 3 of Tape 1. The SPF contains all of the calibration parameters that were used to convert the Stripa raw data to engineering units. Tables 10 and 11 provide detailed field descriptions for the SPF. Parameters for a sample sensor are shown in Fig. 23.

8.2 Structure and Format of Data for Experiments 1 and 2 (Full-Scale Experiments)

Data for both full-scale experiments (header, time series, and engineering data) are stored under identical formats, except that Experiment 1 (H9) data are stored in Tape 1 from file 4 through 49 while Experiment 2 (H10) data are stored in Tape 2 from file 1 through 53 (see Fig. 24).

Header

The full scale Experiment 1 (H9) 3.6 kW header information resides in file 4 on tape 1. The first logical record (or card image) contains the total number of time points (ITOTPT) and experiment number (IEXPT). The format used is:

```
READ(1,9000)ITOTPT,IEXPT
```

```
9000 FORMAT(22X,I5,5X,I1)
```

The next record up to the end of file (eof) contains the total number of holes (NHOLES) and its individual names (IHID) using the format:

```
READ(1,9001)NHOLES,(IHID(I),I=1,NHOLES)
```

```
9001 FORMAT(I3,/, (10(1X,A3)))
```

Table 10. Master sensor parameter file record structure

Total length = 191 words

<u>Word #</u>	<u>Contents</u>
1	Record/Sensor # (1-1200)
2-31	Initial values for parameters 1-30
32	Record Version # (increment by 1 with each update)
33	Date of last update
	Change-records: (m = 0, 1, . . .)
35+m	The number of parameters being changed (N)
36+m	Integer Time that the changes go into effect
37+m	Date that these changes were entered (alpha numeric)
38+m	Name/initials of person entering changes
	Parameter-changes: i = 0 . . . (N-1)
39+m+2i	ID of parameter to be changed
40+m+2i	New value for changed parameter
.	
.	Zero-filled after last change-record
.	
191	Last word in file

Table 11. Master Parameter file description

	Type	Thermocouple	Extensometer	IRAD	USBM	Heater	Corresponding # for SAC-25	Description
1	A	X	X	X	X	X	3	10 character sensor type -- one of "THERMCOUP," "USBM," "EXTENSOMET," "IRAD," "HEATER POW," "HEATER VOL," "HEATER CUR" or "NULL"
2	R	X	X				14	Gauge's Rho coordinate (m)
3	R						15	Gauge's Theta coordinate (degrees)
4	R		X				16	Gauge's Z coordinate (m)
5	R	X	X				17	Gauge's depth in hole (m)
6	R		X	X	X		22	Temperature at time zero (°C)
7	R				X		24	Hole diameter (mm)
8	I		X	X	X		28	Sensor number of gauge's associated thermocouple #1
9-13	I		X				29-33	Sensor numbers for associated thermocouples #2-16
14	I		X				44	Extensometer flag; vertical (0) or horizontal (1)
15	I					X	53	Units flag; Amps (1), Volts (2), or Watts (3)
16	R		X	X	X		54	Zero-offset. Indicates starting voltage for USBM and Extensometer. Indicates zero reading for IRAD gages.
17	R		X		X		55	Re-zero offset. USBM gauge voltage with buttons removed. Extensometer re-zero voltage
18	R		X		X		57	Slope of gauge's calibration curve
19	R	X		X	X		58	The constant A coefficient for thermocouples, $C_1(23)$ for IRAD, and α_{gauge} for USBMs.
20	R	X		X	X		59	The linear B coefficient thermocouples, $C_2(23)$ for IRADS, and α_{rock} for USBM gauges.

Table 11. (continued)

W	T	Th	Ex	I	U	H	C#	Description
21	R	X						C Coefficient of V^2
22	R	X						D Coefficient of V^3
23	R	X						E Coefficient of V^4
24	R				X		86	Voltage offset between ambient and 200°C
25	I	X	X	X	X	X	none	Bad data flag. If non-zero, all data for this gauge are replaced by -99999.
26	R	X					none	Substitute thermocouple temperature for calculating thermal corrections for extensometer, USBM and IRAD gauges. When the thermocouple reading is bad (-99999) or missing (-12345)
27								Sensor label
28-30							none	spare

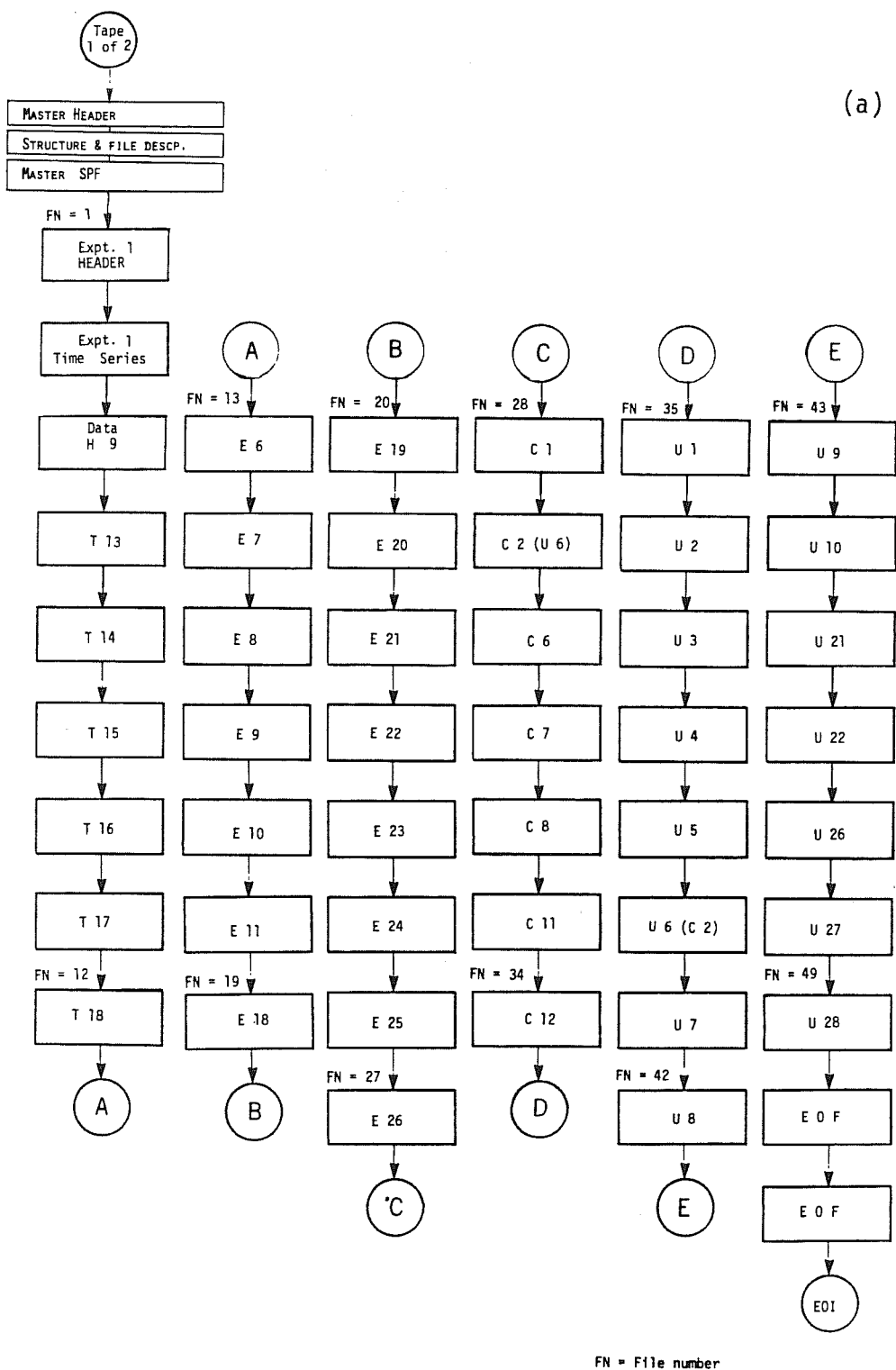
R = real number

I = interger

$C_1(23)$ = calibration coefficient C_1 at 23°C. See Schrauf et al. (1979) for details.

***** SENSOR NUMBER 755 *****		
----- VERSION NUMBER 1 LAST MODIFIED ON 08/22/80 BY -----		
PARAM. NUMBER	DESCRIPTION	INITIAL VALUES
(1)	SENSOR TYPE	USBM
(2)	GAGE RHO COORDINATE	2.26000
(3)	GAGE THETA COCRD.	112.400
(4)	GAGE Z COORDINATE	-.830000
(5)	GAGE DEPTH IN HOLE	8.18000
(6)	TEMP. AT TIME ZERO	10.6360
(7)	HOLE DIAMETER	38.0000
(8)	ASSOC THERMOCOUPLE 1	441
(9)	ASSOC THERMOCOUPLE 2	0
(10)	ASSOC THERMOCOUPLE 3	0
(11)	ASSOC THERMOCOUPLE 4	0
(12)	ASSOC THERMOCOUPLE 5	0
(13)	ASSOC THERMOCOUPLE 6	0
(14)	HORIZ. / VERT. FLAG	0
(15)	HEATER DATA TYPE	0
(16)	ZERO OFFSET	8.91800
(17)	RE-ZERO OFFSET	-.347000
(18)	CALIB. CURVE SLOPE	.687000E-01
(19)	COEFFICIENT A	.137500E-04
(20)	COEFFICIENT B	.111000E-04
(21)	COEFFICIENT C	0.
(22)	COEFFICIENT D	0.
(23)	COEFFICIENT E	0.
(24)	USBM TEMP. CONST.	.219000
(25)	BAD DATA FLAG	0.
(26)	SUBSTITUTE TEMP.	C.
(27)	SENSOR LABEL	U30C
(28)	SPARE	0
(29)	SPARE	0
(30)	SPARE	0

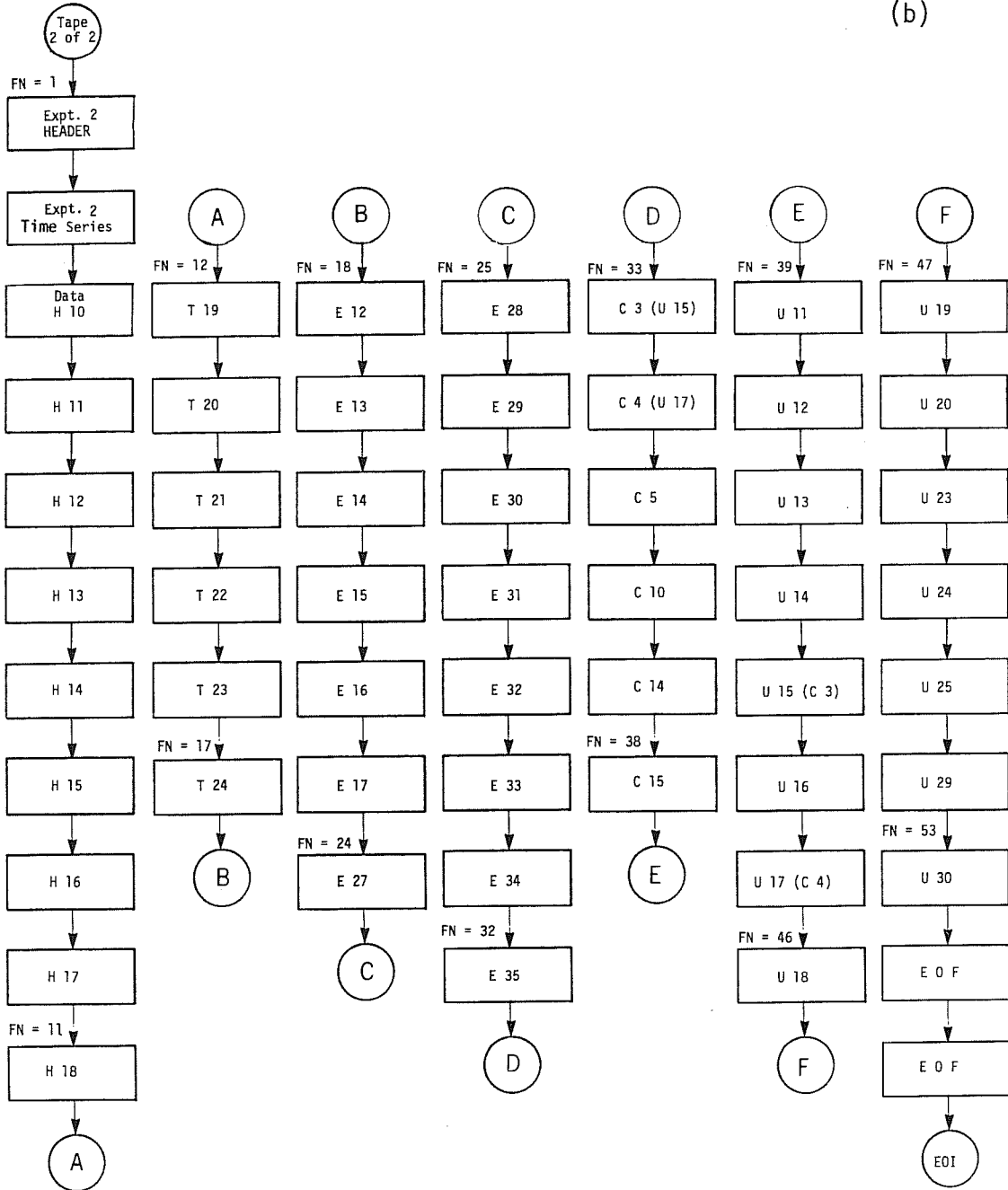
Fig. 23. Sample sensor parameter record.



XBL 8010-12330

Fig. 24. Detailed file arrangement for public-domain tape; (a) tape 1 of 2, (b) tape 2 of 2.

(b)

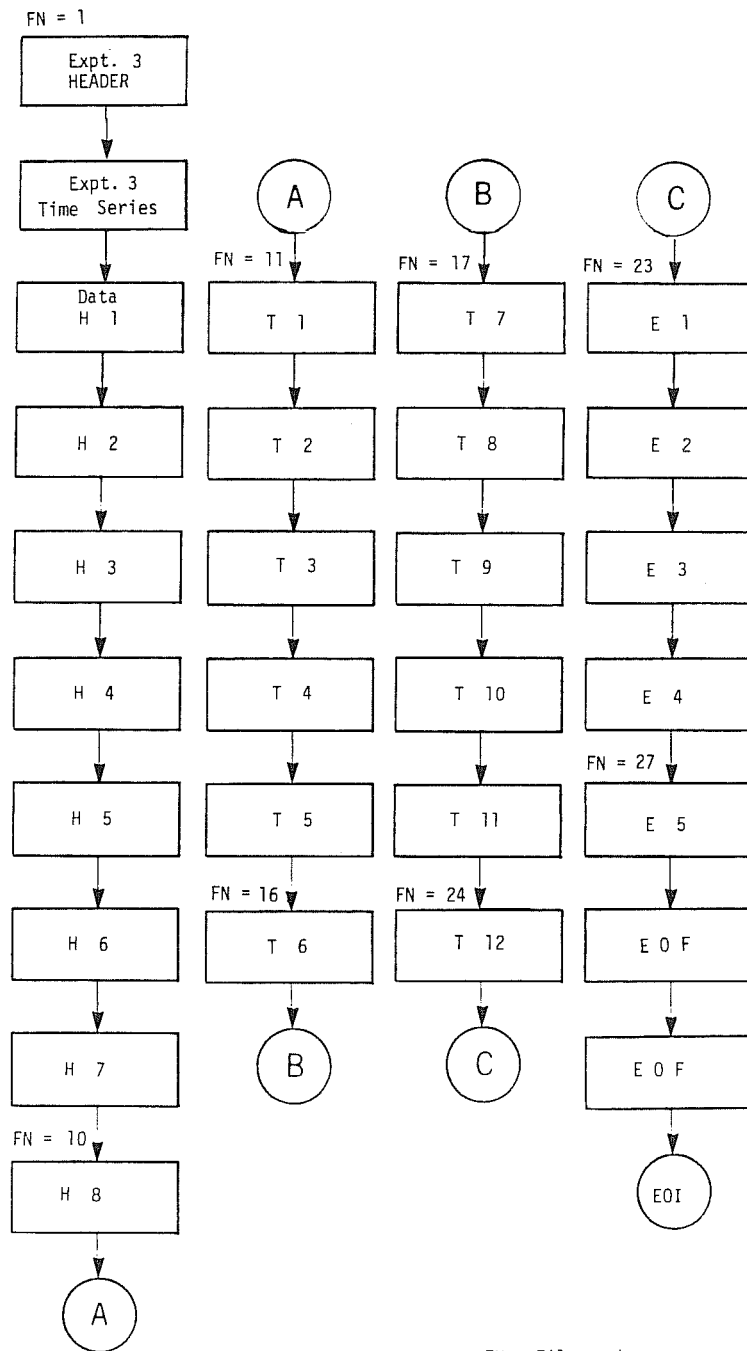


FN = File number

XBL 8010-12331

Fig. 24 (continued).

(b) continued



FN = File number

XBL 8010-12332

Fig. 24 (continued).

Table A-3 specifies the sensors that correspond to each borehole.

Time Series

As indicated in the header, File 5 contains the 1386 values of time points (TIME) in days from Experiment 1 turn-on. The format used is:

```
READ(1,9002)(TIME(I),I=1,ITOTPT)
9002 FORMAT(6F12.3)
```

Engineering Data

Data are stored in order of causality, viz. H-holes, T-holes, E-holes, C-holes and U-holes. Each hole's data occupies a separate file. Sensors within each hole are arranged in the order shown in Table A-3. Each sensor's engineering data set was preceded by a sensor header taking up an 80 character logical record (card image). The format used is:

```
READ(1,9003)ISENUM,LABEL,C1,C2,C3,IUNIT,IOR
9003 FORMAT(5X,I5,5X,A5,3F10.3,5X,A10,2X,A1)
```

where ISENUM is sensor number;

LABEL is sensor label or name;

C1,C2,C3 are the sensor's local cylindrical coordinates (ρ, θ, Z) for full-scale experiments and local rectangular coordinates (X, Y, Z) for the time-scaled experiment;

IUNIT is the quantity and engineering units, viz:

<u>Contents</u>	<u>Meaning</u>
CURR,AMP	heater current in amperes
VLTGE,VOLT	heater voltage in volts
POWER,WATT	heater power in watts
TEMP,DEG.C	thermocouple temperature in degrees Celsius
DISPLAC,MM	extensometer displacement in millimeters
PRD,X10 ⁻⁷ S	IRAD gauge period in 10 ⁻⁷ seconds
DIA.DSP,MM	USBM gauge diametric displacement in millimeters

IOR is orientation of the hole; V for vertical or H for horizontal.

A total of 1386 values of engineering data immediately follow the sensor header for Experiment 1 with six values per record (card image) using the format:

```
READ(1,9004)(AVGDAT(I),I=1,ITOTPT)
```

```
9004 FORMAT(6(1PE12.4))
```

where AVGDAT is the time-averaged engineering data for the sensor;

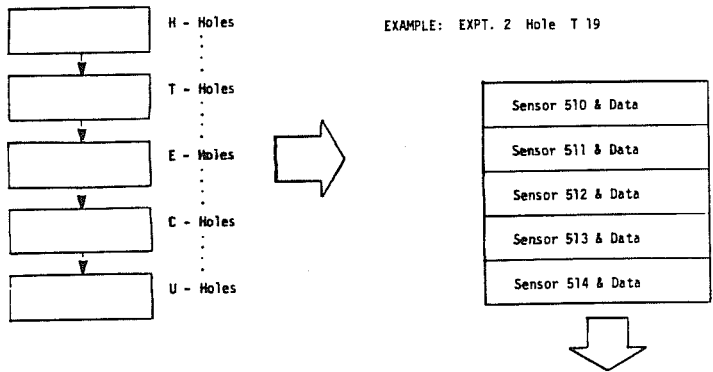
ITOTPT is the total number of data points recorded for that sensor.

After all the sensor headers and their engineering data were written for a hole, an eof is written to mark the termination of data for that hole. The next hole's data are stored in a similar fashion. Figure 25 illustrates the data structure and format within a hole.

Experiment 2 (H10) engineering data are coded on Tape 2. The header begins in file 1 of Tape 2. The time series (total of 2652 time points) in days is written in file 2. Engineering data is stored in files 3 through 53. The detailed structure and format is described in paragraphs 1 to 4 in Section 8.2.

8.3 Structure and Format of Data for Time-Scaled Experiment

Data for the time-scaled experiment (Experiment 3) were formatted as were the full-scale experiments except that there were fewer files since there were no IRAD or USBM gauges (see Fig. 24(b)). The experiment's header information begins in file 54 on Tape 2 of the PDT, followed by a time series (total of 2196 entries) in days from Experiment 3 turn-on time. Engineering data for all Experiment 3 holes and related sensors are stored in files 56 through 80. Sensor headers provide rectangular coordinates (X,Y,Z) for sensor locations where cylindrical coordinates (ρ,θ,Z) were used in the full-scale experiments. Formats were unchanged. Refer to paragraphs 1 to 4 in Section 8.2 for further details.



EXAMPLE : Sensors 510 and 511

card 1 -	510	T19A	.400	0.	3.000	TEMP,DEG.C	V
card 2 -	1.2943E+01	1.2955E+01	1.3095E+01	1.3215E+01	1.3303E+01	1.3379E+01	1.3379E+01
card 3 -	1.3426E+01	1.3481E+01	1.3549E+01	1.3589E+01	1.3713E+01	1.3638E+01	1.3638E+01
card 4 -	1.3666E+01	1.3734E+01	1.3762E+01	1.3799E+01	1.3857E+01	1.3864E+01	1.3864E+01
card 5 -	1.3987E+01	1.4045E+01	1.4137E+01	1.4171E+01	1.4244E+01	1.4335E+01	1.4335E+01
	1.4444E+01	1.4499E+01	1.4584E+01	1.4615E+01	1.4683E+01	1.4744E+01	1.4744E+01
	1.4812E+01	1.4899E+01	1.4935E+01	1.5017E+01	1.5078E+01	1.5107E+01	1.5107E+01
	1.5255E+01	1.5296E+01	1.5355E+01	1.5472E+01	1.5535E+01	1.5657E+01	1.5657E+01
	1.5969E+01	1.5753E+01	1.4418E+01	1.5984E+01	1.6120E+01	1.6215E+01	1.6215E+01
	1.6331E+01	1.6385E+01	1.6501E+01	1.6575E+01	1.6643E+01	1.6752E+01	1.6752E+01
	1.6827E+01	1.6909E+01	1.7004E+01	1.7099E+01	1.7170E+01	1.7241E+01	1.7241E+01
	1.7343E+01	1.7411E+01	1.7486E+01	1.7595E+01	1.7659E+01	1.7764E+01	1.7764E+01
	1.7832E+01	1.7914E+01	1.8002E+01	1.8083E+01	1.8151E+01	1.8240E+01	1.8240E+01
	1.8294E+01	1.8402E+01	1.8639E+01	1.8765E+01	1.8891E+01	1.8986E+01	1.8986E+01
	1.8647E+01	1.8715E+01	1.8769E+01	1.8844E+01	1.8973E+01	1.9000E+01	1.9000E+01
	1.9527E+01	1.9264E+01	1.9278E+01	1.9487E+01	1.9582E+01	1.9643E+01	1.9643E+01
	1.3289E+01	1.2771E+01	1.2589E+01	1.2627E+01	1.2531E+01	1.2483E+01	1.2483E+01
	1.2466E+01	1.2566E+01	1.2598E+01	1.2755E+01	1.2617E+01	1.2654E+01	1.2654E+01
	1.2667E+01	1.2827E+01	1.2881E+01	1.2924E+01	1.2786E+01	1.2750E+01	1.2750E+01
	1.2733E+01	1.2753E+01	1.3015E+01	1.2840E+01	1.3120E+01	1.2992E+01	1.2992E+01
	2.7151E+01	5.3548E+01	6.0310E+01	1.2730E+01	1.9234E+02	5.0279E+01	5.0279E+01
	3.4848E+01	3.4827E+01	3.4825E+01	3.4859E+01	3.5160E+01	8.9658E+01	8.9658E+01
card 441 -	1.1097E+02	1.2617E+02	1.4394E+01	1.2931E+01	1.2911E+01	1.2903E+01	1.2903E+01
card 442 -	1.3228E+01	1.3608E+01	-1.2345E+04	-1.2345E+04	-1.2345E+04	-1.2345E+04	-1.2345E+04
card 443 -	-1.2345E+04						
card 1 -	511	T19B	.400	0.	1.500	TEMP,DEG.C	V
card 2 -	1.1987E+01	1.2792E+01	1.4718E+01	1.6603E+01	1.8591E+01	2.0389E+01	2.0389E+01
card 3 -	2.1980E+01	2.3468E+01	2.4846E+01	2.6362E+01	2.7850E+01	2.8533E+01	2.8533E+01
card 4 -	2.9549E+01	3.0538E+01	3.1433E+01	3.2313E+01	3.3173E+01	3.3992E+01	3.3992E+01
	3.4804E+01	3.5513E+01	3.7296E+01	3.7251E+01	3.7615E+01	3.8356E+01	3.8356E+01
	4.0050E+01	3.9918E+01	4.0449E+01	4.0978E+01	4.1514E+01	4.2037E+01	4.2037E+01
	4.2547E+01	4.4682E+01	4.3871E+01	4.4240E+01	4.4683E+01	4.5126E+01	4.5126E+01
	4.5568E+01	4.5951E+01	4.6407E+01	4.6862E+01	4.7259E+01	4.8570E+01	4.8570E+01
	4.9678E+01	4.9283E+01	5.2633E+01	4.9330E+01	5.0415E+01	5.0371E+01	5.0371E+01
	-1.2345E+04						
	-1.2345E+04						
	-1.2345E+04						
	-1.2345E+04						
	-1.2345E+04						
	-1.2345E+04						
	-1.2345E+04						
card 442 -	-1.2345E+04						
card 443 -	-1.2345E+04						
card 1 -	512	T19C	.400	0.	-0.	TEMP,DEG.C	V

card 1 : Format (5X,15,5X,A5,3F10,3,5X,A10,2X,A1)
 cards 2 - 443 : Format (6(1PE12.4))

Fig. 25. Detailed structure and format of sensor data within a borehole.

9. PROCEDURES FOR ACQUIRING AND ACCESSING DATA

9.1 Acquiring Public-Domain Tapes

The public-domain tapes, two 800 bpi, 2400 ft., 9-track magnetic tapes containing the time-averaged engineering data, can be acquired by writing:

Stripa Data
c/o Dr. Tin Chan
Earth Sciences Division
Building B90A
Lawrence Berkeley Laboratory
University of California
Berkeley, CA 94720
U.S.A.

Note that the words "Stripa Data" must appear in any correspondence concerning these data to ensure prompt response. Users of computers with 36-bit word length must so specify. Also, no telephone orders or inquiries can be accepted. There will be a nominal charge (yet to be determined) to cover the cost of duplicating the tapes.

9.2 Accessing other Available Data

9.2.1 Raw Data

The raw data are stored in various GSS tapes. (For explanation of GSS, refer to GSS writeups by the LBL computer center.) The data are grouped by experiment and all raw data associated with the same borehole are stored together. Also, within a particular experiment, data for the same type of measurements reside in the same tape. There are five GSS tapes for Experiment 1, six tapes for Experiment 2, and three tapes for Experiment 3. Table 12 gives the location of all the available raw data.

There are 24 files for each borehole, and each file contains approximately one month's data. The time period and the access ID (part of the GSS

Table 12. Location of raw data and engineering data before averaging on magnetic tapes

	TAPE NUMBER		DATA FILES	BOREHOLE LABELS*
	Raw Data	Engi- neering Data		
EXP 1	20625	13282	Files for sensors in H and T holes	H9, T13, T14, T15, T16 T17, T18
	20622	13259	Files for sensors in vertical E holes	E6, E7, E8, E9, E10, E11
	20623	13263	Files for sensors in horizontal E holes	E18, E19, E20, E21, E22, E23, E24, E25, E26
	20621	13250	Files for sensors in C holes	C1, U6(C2), C6, C7, C8, C11, C12
	20628	13310	Files for sensors in U holes	U1, U2, U3, U4, U5, C2(U6), U7, U8, U9, U10, U21, U22, U26, U27, U28
EXP 2	20996	15462	Files for sensors in H holes	H10, H11, H12, H13, H14, H15, H17, H17, H18
	20997	15829	Files for sensors in T holes	T19, T20, T21, T22, T23, T24
	20921	15347	Files for sensors in vertical E holes	E12, E13, E14, E15, E16, E17
	21215	15392	Files for sensors in horizontal E holes	E27, E28, E29, E30, E31, E32, E33, E34, E35
	20893	15101	Files for sensors in C holes	U15(C3), U17(C4), C5, C10, C14, C15
	20999	15832	Files for sensors in U holes	U11, U12, U13, U14, C3(U15), U16, C4(U17), U18, U19, U20, U23, U24, U25, U29, U30
EXP 3	21068	15975	Files for sensors in H holes	H1, H2, H3, H4, H5, H6, H7, H8
	21187	15983	Files for sensors in T holes	T1, T2, T3, T4, T5, T6, T7, T8, T9, T10, T11, T12

*Instrument labels appear in parenthesis following borehole labels where they differ.

pathname) for each file are given in Table 13.

The control command

```
GETTAPE,local file=STRIPA/exp/RAWDATA/hole/start/end,tapeno.
```

can be used to access raw data from LBL's CDC computer where:

exp = EXP1H9, EXP2H10, or EXP3TSCL for Experiment 1, 2, or 3
respectively;

hole = HOLE+(hole label) for 2-character hole labels or HOL+(hole
label) for 3-character hole labels. Hole labels are given
in Table 12; and

start/end = an access ID from Table 13.

The following examples illustrate the control commands for accessing
specific subsets of data for the three experiments:

Raw data for the Full Scale Experiment 1 hole T14 from 2 June 78
to 4 July 78 can be accessed using:

```
GETTAPE,local file=STRIPA/EXP1H9/RAWDATA/HOLT14/S780602/F780704,20625.
```

Raw data for the Full Scale Experiment 2 hole U17 from 17 Sep 79 to 18 Oct 79
can be accessed using:

```
GETTAPE,local file=STRIPA/EXP2H10/RAWDATA/HOLU17/S790917/F791018,20893.
```

Raw data for Experiment 3 (the time scale experiment) hole E1 from 16 May 80
to 13 June 80 can be accessed using:

```
GETTAPE,local file=STRIPA/EXP3TSCL/RAWDATA/HOLEE1/S800516/F800613,21007.
```

Raw data for the Full Scale Experiment 1 hole T14 from 2 Jun 78 to 4 Jul 78
can be accessed using:

```
GETTAPE,local file=STRIPA/EXP1H9/RAWDATA/HOLT14/S780602/F780704,20625.
```

Table 13. Time period and access ID for raw data files

	<u>TIME PERIOD</u>	<u>ACCESS ID</u>
1	2 Jun 78 to 4 Jul 78	S780602/F780704
2	4 Jul 78 to 6 Aug 78	S780704/F780806
3	6 Aug 78 to 5 Sep 78	S780806/F780905
4	5 Sep 78 to 6 Oct 78	S780905/F781006
5	6 Oct 78 to 5 Nov 78	S781006/F781105
6	5 Nov 78 to 5 Dec 78	S781105/F781205
7	5 Dec 78 to 10 Jan 79	S781205/F790110
8	10 Jan 79 to 9 Feb 79	S790110/F790209
9	9 Feb 79 to 11 Mar 79	S790209/F790311
10	11 Mar 79 to 19 Apr 79	S790311/F790419
11	19 Apr 79 to 19 May 79	S790419/F790519
12	19 May 79 to 18 Jun 79	S790519/F790618
13	18 Jun 79 to 19 Jul 79	S790618/F790719
14	19 Jul 79 to 18 Aug 79	S790719/F790818
15	18 Aug 79 to 17 Sep 79	S790818/F790917
16	17 Sep 79 to 18 Oct 79	S790917/F791018
17	18 Oct 79 to 18 Nov 79	S791018/F791118
18	18 Nov 79 to 17 Dec 79	S791118/F791217
19	17 Dec 79 to 17 Jan 80	S791217/F800117
20	17 Jan 80 to 17 Feb 80	S800117/F800217
21	17 Feb 80 to 20 Mar 80	S800217/F800320
22	20 Mar 80 to 17 Apr 80	S800320/F800417
23	17 Apr 80 to 16 May 80	S800417/F800516
24	16 May 80 to 13 Jun 80	S800516/F800613

Other raw data can be accessed in a similar way.

All raw data for any experiment and any hole can be accessed using:

GETTAPE,localfile=STRIPA/exp/RAWDATA/hole/*,OR=A,tapeno.

The data format for each raw data file is shown in Table 14.

9.2.2 Logger Data

All logger data were printed on paper tape and cannot in general be accessed in computer readable form. However, a small subset was entered into the CDC computer system at LBL. They were converted to the same units as the raw data, and are stored in subsets in PSS library WSTRIP. (For explanation of PSS, one can refer to the PSS writeups from LBL's computer center).

Available subsets are:

- a) TSDATA: Time-scaled data logger values in mV for 21 channels and 60 time points.
- b) ADDATA: Full scale AD-9 data logger values in mV for 31 channels and 73 time points.
- c) BFDATA: B&F data logger values in mV for 5 channels and 65 time points.
- d) IRDATA: Vibrational periods, in units of 10^{-7} sec, from the IRAD data logger for 12 channels and 60 time points.

The format of the above files is given in Table 15.

The time-scaled logger data can be accessed from LBL's CDC computer system using:

FETCHPS,WSTRIP,localfile,TSDATA.

Other logger data can be accessed similarly.

Table 14. Format for a raw data file

Variables	Definitions	Format	Comments
1) HOLE NSENSOR	HOLE = hole label NSENSOR = total number of sensors in file	(A20, I5)	
2) SENSOR	The sensor numbers of all sensors in the file	(1X, 10I12)	
3) TIME, (VALUE(I) I=1,NSENSOR)	TIME = system time in minutes starting from 1 Jan 77. VALUE = Raw data values for the sensors listed in 2 above at the time specified here. The sequential order of the data corresponds to that in the sensor list in 2	(I20) (1X, E12.5)	If there is any mis- sing datum, the value field is set to -12345. If the value is out of range, the value field is set to -99999. The unit of all the values are in volts, except the values in the C holes and the H holes. In the C holes, data for the sensors are vibra- tional period in units of 10^{-7} sec. In the H holes, the unit of the values depends on the type of sensor. It is in 10 amps, if the sensor is used to measure current. It is in 100 volts, if the sensor is used to measure voltage. It is in kilowatt, if the sensor is used to measure power.

Format 3 repeats until terminated by an end-of-file

Table 15. Format for data logger files

Variables	Definitions	Format	Comments
1) NTIME	total number of time points in the file	(I5)	
2) NCHANNEL	total number of channels in the file	(I5)	
3) YEAR, DAY, HOUR, MIN, SEC (CHANNEL(I), ERROR(I), VALUE(I), I=1, NCHANNEL)	time when the value was taken channel number, error code, and value for the channel	(I2, 1X, I3, 1X, 3I2)	The fields for both the channel number and the value are set to zero whenever data was missed. An "*" following the channel number implies that channel's data is bad.

Format "3" above is repeated "NTIME" times.

9.2.3 Long-Term Data

The long-term data is stored on GSS tape 22257 at LBL. (See the LBL computer center's GSS writeups for instructions on using these tapes.)

A writeup describing the format of the data is stored on this same tape under pathname

STRIPA/LONGTERM/DATA/FORMAT.

This writeup also gives the pathnames necessary to retrieve the data.

9.2.4 Engineering Data

Engineering data, prior to averaging, are organized as described for the raw data. Table 12 gives the location of all available engineering data. The accessing methods are as described for the raw data, except that CONDATA should be substituted for RAWDATA in the pathname.

For example, the engineering data for Full Scale Experiment 2 hole U17 from 17 Sep 79 to 18 Oct 79 can be accessed using:

GETTAPE,localfile=STRIPA/EXP2H10/CONDATA/HOLU17/S790917/F791018,15101.

The engineering data, after averaging, are stored in GSS tape 26318 on LBL's CDC computer system. The file organization and data structure of this tape are as described for the public domain tapes.

To access the above data for Experiment 1, use:

GETTAPE,localfile=STRIPA/EXP1H9/ALL/AVGDATA/26318.

Time-averaged engineering data for the other experiments can be accessed similarly.

ACKNOWLEDGMENTS

N.G.W. Cook and P.A. Witherspoon provided guidance for the writing of this report. A. DuBois, and R. Lingle made their unpublished instrumentation calibration parameters available for data reduction. N. Littlestone provided support in computer programming. T. Strong offered valuable advice on computer data transfer. L. Andersson, C. Coad, P. Strisower, and W. Wong assisted in the preparation of figures and tables. B. Stromdahl arranged for all necessary help to assure prompt completion of the work. Finally, L. Egenberger's extra effort in typing was crucial to the timely production of this report.

The authors gratefully acknowledge the assistance of the above individuals.

REFERENCES

- Binnall, E.P. and DuBois, A.O. (to be published)
- Burleigh, R.H., Binnall, E.P., DuBois, A.O., Norgren, D.O., and Ortiz, A.R. 1979. Electrical heaters for thermo-mechanical tests at the Stripa mine. LBL-7063, SAC-13. Lawrence Berkeley Laboratory, University of California, Berkeley, California.
- Carnahan, B., Luther, H.A., and Wilkes, J.O. 1969. Applied numerical methods. John Wiley and Sons, Inc., New York.
- Chan, T. and Cook, N.G.W. 1979. Calculated thermally induced displacements and stress for heater experiments at Stripa. LBL-7061, SAC-22. Lawrence Berkeley Laboratory, University of California, Berkeley, California.
- Hawkes, I. and Bailey, W.V. 1973. Design, develop, fabricate, test and demonstrate permissible low cost cylindrical stress gauges and associated components capable of measuring change of stress as a function of time in underground coal mines. U.S. Bureau of Mines, Contract Report (H02200550). Washington, D.C.
- Hooker, V., Aggson, J., and Bickel, D. 1974. Improvements in the three-component borehole deformation gauge and overcoring technique. U.S. Bureau of Mines report of Investigation #7894. Washington, D.C.
- IRAD Gage, Inc. 1977. Vibrating wire stress meter instruction manual. Lebanon, New Hampshire.
- Kisner, R.A., Marshall, J.R., Turner, D.W., and Vath, J.E. April 1977. Nuclear waste projections and source term data for FY 1977. Y/OWI/TM-34. Office of Waste Isolation, Oak Ridge, Tennessee.
- Kurfurst, P.J., Hugo-Persson, T. and Rudolph, G. 1978. Borehole drilling and related activities at the Stripa mine. LBL-7080, SAC-05. Lawrence Berkeley Laboratory, University of California, Berkeley, California.
- McEvoy, M.B. 1979. Data acquisition, handling, and display for the heater experiments at Stripa. LBL-7062, SAC-14. Lawrence Berkeley Laboratory, University of California, Berkeley, California.
- Schrauf, T.A., Pratt, H., Simonson, E., Hustrulid, W., Nelson, P., DuBois, A., Binnall, E., Haught, R. 1979. Instrumentation evaluation, calibration and installation for the heater experiments at Stripa. LBL-8313, SAC-25. Lawrence Berkeley Laboratory, University of California, Berkeley, California.
- Smithells, C.J., editor. 1976. Metals reference book, 5th ed. London & Boston: Butterworths.
- Teknekron, Inc. 1978. Geotechnical graphical and data acquisition system user's manual.

U.S. Department of Energy. April, 1979. Management of commercially generated radioactive waste. Draft Environmental Impact Statement.

Witherspoon, P.A. and Degerman, O. 1978. Swedish-American cooperative program on radioactive waste storage in mined caverns -- program summary. LBL-7049, SAC-01. Lawrence Berkeley Laboratory, University of California, Berkeley, California.

Witherspoon, P.A., Cook, N.G.W., and Gale, J.E. 1980. Geological storage of radioactive waste--results from field investigations at Stripa, Sweden. Proc. of Waste Management, 80, Univ. of Arizona.

APPENDIX A: USEFUL INFORMATION ON THE STRIPA HEATER EXPERIMENTS (Figures and Tables)

This appendix contains a number of figures and tables providing information on the power histories of the heaters and the configurations of the heater arrays and instrumentation. Most of these figures and tables are self-explanatory.

Table A-1 gives the correspondence between calendar dates and experiment days for the Stripa heater experiments. Heater power data presented in Fig. A-1 - A-3 and Table A-2 are those recorded by the AD-9 data loggers. These are considered more reliable than the computer acquired data that was recorded on magnetic tapes. The differences, however, are very small, less than 1%. For any heater with more than one heating element, the last sensor listed in Table A-3 measured total heater power.

Note that the local cylindrical coordinates in Table A-3 constitute a left-hand coordinate system. The Z axis is vertical with $Z = 0$ corresponding to the midplane of the heaters and positive Z is above the midplane. See Schrauf et al. (1979) for the relationships between the different coordinate systems.

The hole labels given in Table A-3 are the original borehole names used by the designer for instrumentation layout. During installation the positions of the following 3 USBM gauges and 3 pairs of IRAD stressmeters were interchanged:

C2	U6
C3	U15
C4	U17

In Table A-3 every active sensor is uniquely identified by a label (column 4), which has three fields representing (1) instrument type, (2) the

borehole identifier, and (3) the component identifier for instruments that have more than one component. If the instrument type is the same as that used to identify the borehole, Field (1) is omitted.

For USBM gauges, component A corresponds to component 1, the θ component, while B and C correspond to components 2 and 3 at angles of 60° and 120° , respectively. For IRAD gauges, A again corresponds to component 1, in the θ direction, and B corresponds to component 2, which is at right angles to component 1. Selected plan and (vertical) section views of the full-scale drifts are given in Figs. A-4 - A-7. Designation of extensometer anchor points is illustrated in Fig. A-8. Designation of thermocouples in the E (extensometer) holes corresponds to that for the extensometer anchor points. Some extensometer holes have seven thermocouples. These extra thermocouples are labeled E (for the collar), F, and G.

Table A-1. Correspondence between calendar dates and experiment days for the Stripa experiments.

1978 CALENDAR FOR STRIPA EXPERIMENT

1978 JUNE						1978 AUGUST					
	JULIAN	H9	H10	TS		JULIAN	H9	H10	TS		
TH 6/ 1/78	152	0	0	0	TU 8/ 1/78	213	0	29	61		
FR 6/ 2/78	153	0	0	1	WE 8/ 2/78	214	0	30	62		
SA 6/ 3/78	154	0	0	2	TH 8/ 3/78	215	0	31	63		
SU 6/ 4/78	155	0	0	3	FR 8/ 4/78	216	0	32	64		
MO 6/ 5/78	156	0	0	4	SA 8/ 5/78	217	0	33	65		
TU 6/ 6/78	157	0	0	5	SU 8/ 6/78	218	0	34	66		
WE 6/ 7/78	158	0	0	6	MO 8/ 7/78	219	0	35	67		
TH 6/ 8/78	159	0	0	7	TU 8/ 8/78	220	0	36	68		
FR 6/ 9/78	160	0	0	8	WE 8/ 9/78	221	0	37	69		
SA 6/10/78	161	0	0	9	TH 8/10/78	222	0	38	70		
SU 6/11/78	162	0	0	10	FR 8/11/78	223	0	39	71		
MO 6/12/78	163	0	0	11	SA 8/12/78	224	0	40	72		
TU 6/13/78	164	0	0	12	SU 8/13/78	225	0	41	73		
WE 6/14/78	165	0	0	13	MO 8/14/78	226	0	42	74		
TH 6/15/78	166	0	0	14	TU 8/15/78	227	0	43	75		
FR 6/16/78	167	0	0	15	WE 8/16/78	228	0	44	76		
SA 6/17/78	168	0	0	16	TH 8/17/78	229	0	45	77		
SU 6/18/78	169	0	0	17	FR 8/18/78	230	0	46	78		
MO 6/19/78	170	0	0	18	SA 8/19/78	231	0	47	79		
TU 6/20/78	171	0	0	19	SU 8/20/78	232	0	48	80		
WE 6/21/78	172	0	0	20	MO 8/21/78	233	0	49	81		
TH 6/22/78	173	0	0	21	TU 8/22/78	234	0	50	82		
FR 6/23/78	174	0	0	22	WE 8/23/78	235	0	51	83		
SA 6/24/78	175	0	0	23	TH 8/24/78	236	0	52	84		
SU 6/25/78	176	0	0	24	FR 8/25/78	237	1	53	85		
MO 6/26/78	177	0	0	25	SA 8/26/78	238	2	54	86		
TU 6/27/78	178	0	0	26	SU 8/27/78	239	3	55	87		
WE 6/28/78	179	0	0	27	MO 8/28/78	240	4	56	88		
TH 6/29/78	180	0	0	28	TU 8/29/78	241	5	57	89		
FR 6/30/78	181	0	0	29	WE 8/30/78	242	6	58	90		
					TH 8/31/78	243	7	59	91		

1978 JULY						1978 SEPTEMBER					
	JULIAN	H9	H10	TS		JULIAN	H9	H10	TS		
SA 7/ 1/78	182	0	0	30	FR 9/ 1/78	244	8	60	92		
SU 7/ 2/78	183	0	0	31	SA 9/ 2/78	245	9	61	93		
MO 7/ 3/78	184	0	0	32	SU 9/ 3/78	246	10	62	94		
TU 7/ 4/78	185	0	1	33	MO 9/ 4/78	247	11	63	95		
WE 7/ 5/78	186	0	2	34	TU 9/ 5/78	248	12	64	96		
TH 7/ 6/78	187	0	3	35	WE 9/ 6/78	249	13	65	97		
FR 7/ 7/78	188	0	4	36	TH 9/ 7/78	250	14	66	98		
SA 7/ 8/78	189	0	5	37	FR 9/ 8/78	251	15	67	99		
SU 7/ 9/78	190	0	6	38	SA 9/ 9/78	252	16	68	100		
MO 7/10/78	191	0	7	39	SU 9/10/78	253	17	69	101		
TU 7/11/78	192	0	8	40	MO 9/11/78	254	18	70	102		
WE 7/12/78	193	0	9	41	TU 9/12/78	255	19	71	103		
TH 7/13/78	194	0	10	42	WE 9/13/78	256	20	72	104		
FR 7/14/78	195	0	11	43	TH 9/14/78	257	21	73	105		
SA 7/15/78	196	0	12	44	FR 9/15/78	258	22	74	106		
SU 7/16/78	197	0	13	45	SA 9/16/78	259	23	75	107		
MO 7/17/78	198	0	14	46	SU 9/17/78	260	24	76	108		
TU 7/18/78	199	0	15	47	MO 9/18/78	261	25	77	109		
WE 7/19/78	200	0	16	48	TU 9/19/78	262	26	78	110		
TH 7/20/78	201	0	17	49	WE 9/20/78	263	27	79	111		
FR 7/21/78	202	0	18	50	TH 9/21/78	264	28	80	112		
SA 7/22/78	203	0	19	51	FR 9/22/78	265	29	81	113		
SU 7/23/78	204	0	20	52	SA 9/23/78	266	30	82	114		
MO 7/24/78	205	0	21	53	SU 9/24/78	267	31	83	115		
TU 7/25/78	206	0	22	54	MO 9/25/78	268	32	84	116		
WE 7/26/78	207	0	23	55	TU 9/26/78	269	33	85	117		
TH 7/27/78	208	0	24	56	WE 9/27/78	270	34	86	118		
FR 7/28/78	209	0	25	57	TH 9/28/78	271	35	87	119		
SA 7/29/78	210	0	26	58	FR 9/29/78	272	36	88	120		
SU 7/30/78	211	0	27	59	SA 9/30/78	273	37	89	121		
MO 7/31/78	212	0	28	60							

Table A-1 (continued)

1978 OCTOBER					1978 DECEMBER				
	JULIAN	H9	H10	TS	JULIAN	H9	H10	TS	
SU 10/ 1/78	274	38	90	122	FR 12/ 1/78	335	99	151	183
MO 10/ 2/78	275	39	91	123	SA 12/ 2/78	336	100	152	184
TU 10/ 3/78	276	40	92	124	SU 12/ 3/78	337	101	153	185
WE 10/ 4/78	277	41	93	125	MO 12/ 4/78	338	102	154	186
TH 10/ 5/78	278	42	94	126	TU 12/ 5/78	339	103	155	187
FR 10/ 6/78	279	43	95	127	WE 12/ 6/78	340	104	156	188
SA 10/ 7/78	280	44	96	128	TH 12/ 7/78	341	105	157	189
SU 10/ 8/78	281	45	97	129	FR 12/ 8/78	342	106	158	190
MO 10/ 9/78	282	46	98	130	SA 12/ 9/78	343	107	159	191
TU 10/10/78	283	47	99	131	SU 12/10/78	344	108	160	192
WE 10/11/78	284	48	100	132	MO 12/11/78	345	109	161	193
TH 10/12/78	285	49	101	133	TU 12/12/78	346	110	162	194
FR 10/13/78	286	50	102	134	WE 12/13/78	347	111	163	195
SA 10/14/78	287	51	103	135	TH 12/14/78	348	112	164	196
SU 10/15/78	288	52	104	136	FR 12/15/78	349	113	165	197
MO 10/16/78	289	53	105	137	SA 12/16/78	350	114	166	198
TU 10/17/78	290	54	106	138	SU 12/17/78	351	115	167	199
WE 10/18/78	291	55	107	139	MO 12/18/78	352	116	168	200
TH 10/19/78	292	56	108	140	TU 12/19/78	353	117	169	201
FR 10/20/78	293	57	109	141	WE 12/20/78	354	118	170	202
SA 10/21/78	294	58	110	142	TH 12/21/78	355	119	171	203
SU 10/22/78	295	59	111	143	FR 12/22/78	356	120	172	204
MO 10/23/78	296	60	112	144	SA 12/23/78	357	121	173	205
TU 10/24/78	297	61	113	145	SU 12/24/78	358	122	174	206
WE 10/25/78	298	62	114	146	MO 12/25/78	359	123	175	207
TH 10/26/78	299	63	115	147	TU 12/26/78	360	124	176	208
FR 10/27/78	300	64	116	148	WE 12/27/78	361	125	177	209
SA 10/28/78	301	65	117	149	TH 12/28/78	362	126	178	210
SU 10/29/78	302	66	118	150	FR 12/29/78	363	127	179	211
MO 10/30/78	303	67	119	151	SA 12/30/78	364	128	180	212
TU 10/31/78	304	68	120	152	SU 12/31/78	365	129	181	213
1978 NOVEMBER									
	JULIAN	H9	H10	TS					
WE 11/ 1/78	305	69	121	153					
TH 11/ 2/78	306	70	122	154					
FR 11/ 3/78	307	71	123	155					
SA 11/ 4/78	308	72	124	156					
SU 11/ 5/78	309	73	125	157					
MO 11/ 6/78	310	74	126	158					
TU 11/ 7/78	311	75	127	159					
WE 11/ 8/78	312	76	128	160					
TH 11/ 9/78	313	77	129	161					
FR 11/10/78	314	78	130	162					
SA 11/11/78	315	79	131	163					
SU 11/12/78	316	80	132	164					
MO 11/13/78	317	81	133	165					
TU 11/14/78	318	82	134	166					
WE 11/15/78	319	83	135	167					
TH 11/16/78	320	84	136	168					
FR 11/17/78	321	85	137	169					
SA 11/18/78	322	86	138	170					
SU 11/19/78	323	87	139	171					
MO 11/20/78	324	88	140	172					
TU 11/21/78	325	89	141	173					
WE 11/22/78	326	90	142	174					
TH 11/23/78	327	91	143	175					
FR 11/24/78	328	92	144	176					
SA 11/25/78	329	93	145	177					
SU 11/26/78	330	94	146	178					
MO 11/27/78	331	95	147	179					
TU 11/28/78	332	96	148	180					
WE 11/29/78	333	97	149	181					
TH 11/30/78	334	98	150	182					

Table A-1 (continued)

1979 CALENDAR FOR STRIPA EXPERIMENT

1979 JANUARY					
	JULIAN	H9	H10	TS	
MO	1/ 1/79	1	130	182	214
TU	1/ 2/79	2	131	183	215
WE	1/ 3/79	3	132	184	216
TH	1/ 4/79	4	133	185	217
FR	1/ 5/79	5	134	186	218
SA	1/ 6/79	6	135	187	219
SU	1/ 7/79	7	136	188	220
MO	1/ 8/79	8	137	189	221
TU	1/ 9/79	9	138	190	222
WE	1/10/79	10	139	191	223
TH	1/11/79	11	140	192	224
FR	1/12/79	12	141	193	225
SA	1/13/79	13	142	194	226
SU	1/14/79	14	143	195	227
MO	1/15/79	15	144	196	228
TU	1/16/79	16	145	197	229
WE	1/17/79	17	146	198	230
TH	1/18/79	18	147	199	231
FR	1/19/79	19	148	200	232
SA	1/20/79	20	149	201	233
SU	1/21/79	21	150	202	234
MO	1/22/79	22	151	203	235
TU	1/23/79	23	152	204	236
WE	1/24/79	24	153	205	237
TH	1/25/79	25	154	206	238
FR	1/26/79	26	155	207	239
SA	1/27/79	27	156	208	240
SU	1/28/79	28	157	209	241
MO	1/29/79	29	158	210	242
TU	1/30/79	30	159	211	243
WE	1/31/79	31	160	212	244

1979 MARCH					
	JULIAN	H9	H10	TS	
TH	3/ 1/79	60	189	241	273
FR	3/ 2/79	61	190	242	274
SA	3/ 3/79	62	191	243	275
SU	3/ 4/79	63	192	244	276
MO	3/ 5/79	64	193	245	277
TU	3/ 6/79	65	194	246	278
WE	3/ 7/79	66	195	247	279
TH	3/ 8/79	67	196	248	280
FR	3/ 9/79	68	197	249	281
SA	3/10/79	69	198	250	282
SU	3/11/79	70	199	251	283
MO	3/12/79	71	200	252	284
TU	3/13/79	72	201	253	285
WE	3/14/79	73	202	254	286
TH	3/15/79	74	203	255	287
FR	3/16/79	75	204	256	288
SA	3/17/79	76	205	257	289
SU	3/18/79	77	206	258	290
MO	3/19/79	78	207	259	291
TU	3/20/79	79	208	260	292
WE	3/21/79	80	209	261	293
TH	3/22/79	81	210	262	294
FR	3/23/79	82	211	263	295
SA	3/24/79	83	212	264	296
SU	3/25/79	84	213	265	297
MO	3/26/79	85	214	266	298
TU	3/27/79	86	215	267	299
WE	3/28/79	87	216	268	300
TH	3/29/79	88	217	269	301
FR	3/30/79	89	218	270	302
SA	3/31/79	90	219	271	303

1979 FEBRUARY					
	JULIAN	H9	H10	TS	
TH	2/ 1/79	32	161	213	245
FR	2/ 2/79	33	162	214	246
SA	2/ 3/79	34	163	215	247
SU	2/ 4/79	35	164	216	248
MO	2/ 5/79	36	165	217	249
TU	2/ 6/79	37	166	218	250
WE	2/ 7/79	38	167	219	251
TH	2/ 8/79	39	168	220	252
FR	2/ 9/79	40	169	221	253
SA	2/10/79	41	170	222	254
SU	2/11/79	42	171	223	255
MO	2/12/79	43	172	224	256
TU	2/13/79	44	173	225	257
WE	2/14/79	45	174	226	258
TH	2/15/79	46	175	227	259
FR	2/16/79	47	176	228	260
SA	2/17/79	48	177	229	261
SU	2/18/79	49	178	230	262
MO	2/19/79	50	179	231	263
TU	2/20/79	51	180	232	264
WE	2/21/79	52	181	233	265
TH	2/22/79	53	182	234	266
FR	2/23/79	54	183	235	267
SA	2/24/79	55	184	236	268
SU	2/25/79	56	185	237	269
MO	2/26/79	57	186	238	270
TU	2/27/79	58	187	239	271
WE	2/28/79	59	188	240	272

1979 APRIL					
	JULIAN	H9	H10	TS	
SU	4/ 1/79	91	220	272	304
MO	4/ 2/79	92	221	273	305
TU	4/ 3/79	93	222	274	306
WE	4/ 4/79	94	223	275	307
TH	4/ 5/79	95	224	276	308
FR	4/ 6/79	96	225	277	309
SA	4/ 7/79	97	226	278	310
SU	4/ 8/79	98	227	279	311
MO	4/ 9/79	99	228	280	312
TU	4/10/79	100	229	281	313
WE	4/11/79	101	230	282	314
TH	4/12/79	102	231	283	315
FR	4/13/79	103	232	284	316
SA	4/14/79	104	233	285	317
SU	4/15/79	105	234	286	318
MO	4/16/79	106	235	287	319
TU	4/17/79	107	236	288	320
WE	4/18/79	108	237	289	321
TH	4/19/79	109	238	290	322
FR	4/20/79	110	239	291	323
SA	4/21/79	111	240	292	324
SU	4/22/79	112	241	293	325
MO	4/23/79	113	242	294	326
TU	4/24/79	114	243	295	327
WE	4/25/79	115	244	296	328
TH	4/26/79	116	245	297	329
FR	4/27/79	117	246	298	330
SA	4/28/79	118	247	299	331
SU	4/29/79	119	248	300	332
MO	4/30/79	120	249	301	333

Table A-1 (continued)

1979 MAY					1979 JULY						
	JULIAN	H9	H10	TS		JULIAN	H9	H10	TS		
TU	5/ 1/79	121	250	302	334	SU	7/ 1/79	182	311	363	395
WE	5/ 2/79	122	251	303	335	MO	7/ 2/79	183	312	364	396
TH	5/ 3/79	123	252	304	336	TU	7/ 3/79	184	313	365	397
FR	5/ 4/79	124	253	305	337	WE	7/ 4/79	185	314	366	398
SA	5/ 5/79	125	254	306	338	TH	7/ 5/79	186	315	367	399
SU	5/ 6/79	126	255	307	339	FR	7/ 6/79	187	316	368	400
MO	5/ 7/79	127	256	308	340	SA	7/ 7/79	188	317	369	401
TU	5/ 8/79	128	257	309	341	SU	7/ 8/79	189	318	370	402
WE	5/ 9/79	129	258	310	342	MO	7/ 9/79	190	319	371	403
TH	5/10/79	130	259	311	343	TU	7/10/79	191	320	372	404
FR	5/11/79	131	260	312	344	WE	7/11/79	192	321	373	405
SA	5/12/79	132	261	313	345	TH	7/12/79	193	322	374	406
SU	5/13/79	133	262	314	346	FR	7/13/79	194	323	375	407
MO	5/14/79	134	263	315	347	SA	7/14/79	195	324	376	408
TU	5/15/79	135	264	316	348	SU	7/15/79	196	325	377	409
WE	5/16/79	136	265	317	349	MO	7/16/79	197	326	378	410
TH	5/17/79	137	266	318	350	TU	7/17/79	198	327	379	411
FR	5/18/79	138	267	319	351	WE	7/18/79	199	328	380	412
SA	5/19/79	139	268	320	352	TH	7/19/79	200	329	381	413
SU	5/20/79	140	269	321	353	FR	7/20/79	201	330	382	414
MO	5/21/79	141	270	322	354	SA	7/21/79	202	331	383	415
TU	5/22/79	142	271	323	355	SU	7/22/79	203	332	384	416
WE	5/23/79	143	272	324	356	MO	7/23/79	204	333	385	417
TH	5/24/79	144	273	325	357	TU	7/24/79	205	334	386	418
FR	5/25/79	145	274	326	358	WE	7/25/79	206	335	387	419
SA	5/26/79	146	275	327	359	TH	7/26/79	207	336	388	420
SU	5/27/79	147	276	328	360	FR	7/27/79	208	337	389	421
MO	5/28/79	148	277	329	361	SA	7/28/79	209	338	390	422
TU	5/29/79	149	278	330	362	SU	7/29/79	210	339	391	423
WE	5/30/79	150	279	331	363	MO	7/30/79	211	340	392	424
TH	5/31/79	151	280	332	364	TU	7/31/79	212	341	393	425

1979 JUNE					1979 AUGUST						
	JULIAN	H9	H10	TS		JULIAN	H9	H10	TS		
FR	6/ 1/79	152	281	333	365	WE	8/ 1/79	213	342	394	426
SA	6/ 2/79	153	282	334	366	TH	8/ 2/79	214	343	395	427
SU	6/ 3/79	154	283	335	367	FR	8/ 3/79	215	344	396	428
MO	6/ 4/79	155	284	336	368	SA	8/ 4/79	216	345	397	429
TU	6/ 5/79	156	285	337	369	SU	8/ 5/79	217	346	398	430
WE	6/ 6/79	157	286	338	370	MO	8/ 6/79	218	347	399	431
TH	6/ 7/79	158	287	339	371	TU	8/ 7/79	219	348	400	432
FR	6/ 8/79	159	288	340	372	WE	8/ 8/79	220	349	401	433
SA	6/ 9/79	160	289	341	373	TH	8/ 9/79	221	350	402	434
SU	6/10/79	161	290	342	374	FR	8/10/79	222	351	403	435
MO	6/11/79	162	291	343	375	SA	8/11/79	223	352	404	436
TU	6/12/79	163	292	344	376	SU	8/12/79	224	353	405	437
WE	6/13/79	164	293	345	377	MO	8/13/79	225	354	406	438
TH	6/14/79	165	294	346	378	TU	8/14/79	226	355	407	439
FR	6/15/79	166	295	347	379	WE	8/15/79	227	356	408	440
SA	6/16/79	167	296	348	380	TH	8/16/79	228	357	409	441
SU	6/17/79	168	297	349	381	FR	8/17/79	229	358	410	442
MO	6/18/79	169	298	350	382	SA	8/18/79	230	359	411	443
TU	6/19/79	170	299	351	383	SU	8/19/79	231	360	412	444
WE	6/20/79	171	300	352	384	MO	8/20/79	232	361	413	445
TH	6/21/79	172	301	353	385	TU	8/21/79	233	362	414	446
FR	6/22/79	173	302	354	386	WE	8/22/79	234	363	415	447
SA	6/23/79	174	303	355	387	TH	8/23/79	235	364	416	448
SU	6/24/79	175	304	356	388	FR	8/24/79	236	365	417	449
MO	6/25/79	176	305	357	389	SA	8/25/79	237	366	418	450
TU	6/26/79	177	306	358	390	SU	8/26/79	238	367	419	451
WE	6/27/79	178	307	359	391	MO	8/27/79	239	368	420	452
TH	6/28/79	179	308	360	392	TU	8/28/79	240	369	421	453
FR	6/29/79	180	309	361	393	WE	8/29/79	241	370	422	454
SA	6/30/79	181	310	362	394	TH	8/30/79	242	371	423	455
						FR	8/31/79	243	372	424	456

Table A-1 (continued)

1979 SEPTEMBER					1979 NOVEMBER						
	JULIAN	H9	H10	TS		JULIAN	H9	H10	TS		
SA	9/ 1/79	244	373	425	457	TH	11/ 1/79	305	434	486	518
SU	9/ 2/79	245	374	426	458	FR	11/ 2/79	306	435	487	519
MO	9/ 3/79	246	375	427	459	SA	11/ 3/79	307	436	488	520
TU	9/ 4/79	247	376	428	460	SU	11/ 4/79	308	437	489	521
WE	9/ 5/79	248	377	429	461	MO	11/ 5/79	309	438	490	522
TH	9/ 6/79	249	378	430	462	TU	11/ 6/79	310	439	491	523
FR	9/ 7/79	250	379	431	463	WE	11/ 7/79	311	440	492	524
SA	9/ 8/79	251	380	432	464	TH	11/ 8/79	312	441	493	525
SU	9/ 9/79	252	381	433	465	FR	11/ 9/79	313	442	494	526
MO	9/10/79	253	382	434	466	SA	11/10/79	314	443	495	527
TU	9/11/79	254	383	435	467	SU	11/11/79	315	444	496	528
WE	9/12/79	255	384	436	468	MO	11/12/79	316	445	497	529
TH	9/13/79	256	385	437	469	TU	11/13/79	317	446	498	530
FR	9/14/79	257	386	438	470	WE	11/14/79	318	447	499	531
SA	9/15/79	258	387	439	471	TH	11/15/79	319	448	500	532
SU	9/16/79	259	388	440	472	FR	11/16/79	320	449	501	533
MO	9/17/79	260	389	441	473	SA	11/17/79	321	450	502	534
TU	9/18/79	261	390	442	474	SU	11/18/79	322	451	503	535
WE	9/19/79	262	391	443	475	MO	11/19/79	323	452	504	536
TH	9/20/79	263	392	444	476	TU	11/20/79	324	453	505	537
FR	9/21/79	264	393	445	477	WE	11/21/79	325	454	506	538
SA	9/22/79	265	394	446	478	TH	11/22/79	326	455	507	539
SU	9/23/79	266	395	447	479	FR	11/23/79	327	456	508	540
MO	9/24/79	267	396	448	480	SA	11/24/79	328	457	509	541
TU	9/25/79	268	397	449	481	SU	11/25/79	329	458	510	542
WE	9/26/79	269	398	450	482	MO	11/26/79	330	459	511	543
TH	9/27/79	270	399	451	483	TU	11/27/79	331	460	512	544
FR	9/28/79	271	400	452	484	WE	11/28/79	332	461	513	545
SA	9/29/79	272	401	453	485	TH	11/29/79	333	462	514	546
SU	9/30/79	273	402	454	486	FR	11/30/79	334	463	515	547
1979 OCTOBER					1979 DECEMBER						
	JULIAN	H9	H10	TS		JULIAN	H9	H10	TS		
MO	10/ 1/79	274	403	455	487	SA	12/ 1/79	335	464	516	548
TU	10/ 2/79	275	404	456	488	SU	12/ 2/79	336	465	517	549
WE	10/ 3/79	276	405	457	489	MO	12/ 3/79	337	466	518	550
TH	10/ 4/79	277	406	458	490	TU	12/ 4/79	338	467	519	551
FR	10/ 5/79	278	407	459	491	WE	12/ 5/79	339	468	520	552
SA	10/ 6/79	279	408	460	492	TH	12/ 6/79	340	469	521	553
SU	10/ 7/79	280	409	461	493	FR	12/ 7/79	341	470	522	554
MO	10/ 8/79	281	410	462	494	SA	12/ 8/79	342	471	523	555
TU	10/ 9/79	282	411	463	495	SU	12/ 9/79	343	472	524	556
WE	10/10/79	283	412	464	496	MO	12/10/79	344	473	525	557
TH	10/11/79	284	413	465	497	TU	12/11/79	345	474	526	558
FR	10/12/79	285	414	466	498	WE	12/12/79	346	475	527	559
SA	10/13/79	286	415	467	499	TH	12/13/79	347	476	528	560
SU	10/14/79	287	416	468	500	FR	12/14/79	348	477	529	561
MO	10/15/79	288	417	469	501	SA	12/15/79	349	478	530	562
TU	10/16/79	289	418	470	502	SU	12/16/79	350	479	531	563
WE	10/17/79	290	419	471	503	MO	12/17/79	351	480	532	564
TH	10/18/79	291	420	472	504	TU	12/18/79	352	481	533	565
FR	10/19/79	292	421	473	505	WE	12/19/79	353	482	534	566
SA	10/20/79	293	422	474	506	TH	12/20/79	354	483	535	567
SU	10/21/79	294	423	475	507	FR	12/21/79	355	484	536	568
MO	10/22/79	295	424	476	508	SA	12/22/79	356	485	537	569
TU	10/23/79	296	425	477	509	SU	12/23/79	357	486	538	570
WE	10/24/79	297	426	478	510	MO	12/24/79	358	487	539	571
TH	10/25/79	298	427	479	511	TU	12/25/79	359	488	540	572
FR	10/26/79	299	428	480	512	WE	12/26/79	360	489	541	573
SA	10/27/79	300	429	481	513	TH	12/27/79	361	490	542	574
SU	10/28/79	301	430	482	514	FR	12/28/79	362	491	543	575
MO	10/29/79	302	431	483	515	SA	12/29/79	363	492	544	576
TU	10/30/79	303	432	484	516	SU	12/30/79	364	493	545	577
WE	10/31/79	304	433	485	517	MO	12/31/79	365	494	546	578

Table A-1 (continued)

1980 MAY		JULIAN	H9	H10	TS
TH	5/ 1/80	122	616	668	700
FR	5/ 2/80	123	617	669	701
SA	5/ 3/80	124	618	670	702
SU	5/ 4/80	125	619	671	703
MO	5/ 5/80	126	620	672	704
TU	5/ 6/80	127	621	673	705
WE	5/ 7/80	128	622	674	706
TH	5/ 8/80	129	623	675	707
FR	5/ 9/80	130	624	676	708
SA	5/10/80	131	625	677	709
SU	5/11/80	132	626	678	710
MO	5/12/80	133	627	679	711
TU	5/13/80	134	628	680	712
WE	5/14/80	135	629	681	713
TH	5/15/80	136	630	682	714
FR	5/16/80	137	631	683	715
SA	5/17/80	138	632	684	716
SU	5/18/80	139	633	685	717
MO	5/19/80	140	634	686	718
TU	5/20/80	141	635	687	719
WE	5/21/80	142	636	688	720
TH	5/22/80	143	637	689	721
FR	5/23/80	144	638	690	722
SA	5/24/80	145	639	691	723
SU	5/25/80	146	640	692	724
MO	5/26/80	147	641	693	725
TU	5/27/80	148	642	694	726
WE	5/28/80	149	643	695	727
TH	5/29/80	150	644	696	728
FR	5/30/80	151	645	697	729
SA	5/31/80	152	646	698	730

1980 JUNE		JULIAN	H9	H10	TS
SU	6/ 1/80	153	647	699	731
MO	6/ 2/80	154	648	700	732
TU	6/ 3/80	155	649	701	733
WE	6/ 4/80	156	650	702	734
TH	6/ 5/80	157	651	703	735
FR	6/ 6/80	158	652	704	736
SA	6/ 7/80	159	653	705	737
SU	6/ 8/80	160	654	706	738
MO	6/ 9/80	161	655	707	739
TU	6/10/80	162	656	708	740
WE	6/11/80	163	657	709	741
TH	6/12/80	164	658	710	742
FR	6/13/80	165	659	711	743
SA	6/14/80	166	660	712	744
SU	6/15/80	167	661	713	745
MO	6/16/80	168	662	714	746
TU	6/17/80	169	663	715	747
WE	6/18/80	170	664	716	748
TH	6/19/80	171	665	717	749
FR	6/20/80	172	666	718	750
SA	6/21/80	173	667	719	751
SU	6/22/80	174	668	720	752
MO	6/23/80	175	669	721	753
TU	6/24/80	176	670	722	754
WE	6/25/80	177	671	723	755
TH	6/26/80	178	672	724	756
FR	6/27/80	179	673	725	757
SA	6/28/80	180	674	726	758
SU	6/29/80	181	675	727	759
MO	6/30/80	182	676	728	760

Table A-2. Power histories for the Stripa heater experiments.

FULL SCALE EXPERIMENT 1

Heater H9

Time (Exp. Days)	Power (kW)	Time (Exp. Days)	Power (kW)	Time (Exp. Days)	Power (kW)
8	3.5896	138	3.6039	258	3.5917
18	3.6218	152	3.6146	268	3.5961
28	3.6182	158	3.5765	278	3.6053
38	3.6071	168	3.5945	288	3.6074
48	3.6083	178	3.6032	298	3.5862
68	3.6026	192	3.5962	308	3.6019
78	3.5993	198	3.5965	318	3.6092
88	3.5993	208	3.6024	328	3.6046
98	3.6159	218	3.5981	338	3.6044
108	3.5902	228	3.6116	348	3.6030
118	3.5969	238	3.5977	358	3.6096
128	3.5968	248	3.5977	379	3.6075

FULL SCALE EXPERIMENT 2

Heater H10

Time (Exp. Days)	Power (kW)	Time (Exp. Days)	Power (kW)	Time (Exp. Days)	Power (kW)
10	4.9954	150	5.0239	270	5.0079
20	5.0071	160	4.9924	280	5.0034
30	5.0016	170	5.0095	290	5.0051
50	4.9993	180	5.0098	300	4.9995
60	5.0510	190	5.0088	310	5.0018
70	5.1501	204	5.0090	320	5.0255
80	5.0317	210	5.0135	330	5.0009
90	5.0253	220	5.0012	340	5.0015
100	5.0145	230	5.0111	350	4.9992
120	5.0183	244	5.0178	360	5.0038
130	5.0093	250	5.0009		
140	5.0082	260	4.9966		

FULL SCALE EXPERIMENT 2

Peripheral Heaters

Time (Exp. Days)	Power (kW)							
	H11	H12	H13	H14	H15	H16	H17	H18
10	0	0	0	0	0	0	0	0
243 203	0	0	0	0	0	0	0	0
204	1.0062	.9936	1.0024	.9956	.9962	.9957	1.0123	.9972
210	.9936	.9984	.9993	.9785	1.0032	.9839	1.0031	1.0110
220	.9918	1.0014	1.0028	.9984	1.0045	.9994	1.0046	1.0153
230	.9868	1.0046	1.0007	.9974	1.0038	.9967	.9927	1.0156
244	.9982	.9992	1.0022	.9982	1.0053	.9995	1.0099	1.0135
244.1	.8499	.8471	.8530	.8547	.8519	.8498	.8643	.8662
250	.8511	.8449	.8506	.8506	.8533	.8485	.8578	.8617
260	.8482	.8450	.8485	.8471	.8496	.8458	.8552	.8595
270	.8479	.8436	.8506	.8470	.8483	.8487	.8593	.8594
280	.8507	.8456	.8495	.8472	.8490	.8486	.8590	.8582
290	.8531	.8461	.8500	.8444	.8517	.8477	.8597	.8583
300	.8500	.8442	.8484	.8470	.8494	.8439	.8573	.8583
310	.8549	.8458	.8483	.8455	.8485	.8456	.8569	.8551
320	.8452	.8458	.8478	.8434	.8470	.8463	.8505	.8586
330	.8463	.8441	.8479	.8422	.8483	.8483	.8536	.8559
340	.8446	.8430	.8450	.8433	.8499	.8427	.8530	.8553
350	.8431	.8448	.8463	.8437	.8471	.8446	.8567	.8559
360	.8462	.8456	.8455	.8435	.8495	.8431	.8528	.8561

Table A-2 (continued)

TIME SCALE EXPERIMENT 3
HEATER POWER VS TIME

TIME EXP. DAYS	POWER (KILOWATTS)							
	H1	H2	H3	H4	H5	H6	H7	H8
1.1	1.1234	1.1248	1.1254	1.1188	1.1226	1.1236	1.1239	1.1227
8.0	1.1247	1.1248	1.1238	1.1245	1.1263	1.1250	1.1270	1.1244
14.63	1.1218	1.1255	1.1220	1.1231	1.1244	1.1250	1.1215	1.1226
21.58	1.1359	1.1454	1.1304	1.1328	1.1323	1.1318	1.1346	1.1318
21.69	1.0781	1.0792	1.0821	1.0830	1.0845	1.0805	1.0818	1.0811
28.46	1.0861	1.0904	1.0859	1.0830	1.0855	1.0833	1.0836	1.0860
28.50	1.0503	1.0465	1.0438	1.0492	1.0510	1.0493	1.0500	1.0499
35.42	1.0454	1.0494	1.0464	1.0456	1.0474	1.0478	1.0485	1.0508
35.50	1.0138	1.0104	1.0106	1.0142	1.0070	1.0108	1.0122	1.0124
42.42	1.0137	1.0139	1.0153	1.0133	1.0142	1.0141	1.0127	1.0135
42.50	.9793	.9808	.9793	.9797	.9945	1.0206	1.0122	1.0133
42.63	.9787	.9784	.9783	.9782	.9778	.9785	.9795	.9782
49.50	.9792	.9818	.9814	.9816	.9816	.9790	.9783	.9801
50.25	.9472	.9466	.9473	.9465	.9477	.9480	.9473	.9469
56.58	.9503	.9511	.9509	.9516	.9511	.9487	.9509	.9516
56.67	.9258	.9259	.9242	.9253	.9267	.9263	.9262	.9261
63.50	.9311	.9304	.9291	.9261	.9271	.9237	.9281	.9276
63.67	.9031	.9027	.9046	.9060	.9061	.9042	.9023	.9050
71.29	.9059	.9044	.9053	.9038	.9031	.9066	.9061	.9045
71.54	.8885	.8854	.8875	.8816	.8888	.8859	.8835	.8831
77.42	.8836	.8872	.8901	.8779	.8899	.8893	.8825	.8792
77.50	.8686	.8664	.8697	.8717	.8662	.8674	.8690	.8695
84.46	.8685	.8703	.87224	.8681	.8699	.8637	.8680	.8668
84.54	.8508	.8556	.8574	.8535	.8540	.8457	.8565	.8450
91.33	.8520	.8494	.8514	.8545	.8467	.8512	.8556	.8516
91.52	.8322	.8345	.8354	.8343	.8358	.8373	.8376	.8368
98.33	.8332	.8343	.8360	.8345	.8369	.8390	.8383	.8340
98.50	.8205	.8181	.8179	.8150	.8189	.8185	.8192	.8187
105.38	.8199	.8150	.8177	.8180	.8167	.8188	.8186	.8176
105.54	.8031	.8047	.8040	.8057	.8052	.8053	.8071	.8056
112.38	.8030	.8035	.8070	.8038	.8058	.8047	.8064	.8049
113.00	.7908	.7937	.7907	.7919	.7914	.7868	.7914	.7938
119.42	.7910	.7933	.7892	.7909	.7896	.7894	.7930	.7904
119.63	.7786	.7773	.7770	.7772	.7795	.7768	.7793	.7775
126.33	.7767	.7773	.7765	.7790	.7775	.7780	.7778	.7742
126.65	.7681	.7700	.7662	.7614	.7622	.7663	.7636	.7630
133.40	.7625	.7632	.7639	.7619	.7634	.7602	.7641	.7636
133.56	.7499	.7522	.7513	.7528	.7516	.7518	.7488	.7520
140.50	.7492	.7481	.7509	.7515	.7511	.7505	.7517	.7502
140.67	.7409	.7389	.7398	.7392	.7374	.7389	.7406	.7385
147.46	.7423	.7425	.7393	.7400	.7412	.7400	.7395	.7376
147.63	.7280	.7253	.7269	.7178	.7261	.7266	.7282	.7283
154.44	.7285	.7254	.7288	.7285	.7276	.7261	.7276	.7288
154.58	.7164	.7147	.7149	.7153	.7136	.7138	.7164	.7151
161.46	.7157	.7168	.7168	.7166	.7187	.7166	.7151	.7144
161.63	.7071	.7055	.7069	.7063	.7050	.7037	.7039	.7033
168.42	.7073	.7060	.7066	.7082	.7077	.7064	.7050	.7036
168.54	.6950	.6938	.6933	.6944	.6958	.6945	.6954	.6951
175.38	.6959	.6976	.6954	.6967	.6935	.6950	.6947	.6960
175.54	.6847	.6855	.6859	.6879	.6831	.6855	.6845	.6867
182.44	.6842	.6884	.6885	.6885	.6849	.6865	.6867	.6867
182.60	.6746	.6760	.6749	.6741	.6730	.6727	.6737	.6729
189.33	.6731	.6757	.6724	.6783	.6732	.6744	.6767	.6758
189.50	.6663	.6658	.6642	.6649	.6626	.6642	.6659	.6648
196.38	.6656	.6655	.6656	.6662	.6640	.6674	.6675	.6651
196.54	.6579	.6607	.6585	.6590	.6580	.6590	.6598	.6590
203.42	.6595	.6599	.6577	.6568	.6565	.6577	.6561	.6574

Table A-2 (continued)

TIME SCALE EXPERIMENT 3
HEATER POWER VS TIME

TIME EXP. DAYS	POWER (KILOWATTS)							
	H1	H2	H3	H4	H5	H6	H7	H8
203.58	.6483	.6519	.6514	.6511	.6514	.6511	.6537	.6504
210.42	.6512	.6554	.6503	.6527	.6528	.6532	.6540	.6525
210.58	.6440	.6453	.6452	.6426	.6440	.6406	.6437	.6434
217.38	.6443	.6553	.6441	.6442	.6446	.6429	.6456	.6457
217.50	.6384	.6423	.6388	.6385	.6367	.6403	.6379	.6401
224.46	.6389	.6401	.6389	.6390	.6394	.6385	.6399	.6401
224.58	.6359	.6350	.6339	.6335	.6329	.6337	.6329	.6317
231.42	.6322	.6315	.6351	.6320	.6302	.6324	.6315	.6315
231.58	.6276	.6269	.6291	.6269	.6283	.6289	.6291	.6291
238.42	.6288	.6284	.6300	.6296	.6260	.6269	.6305	.6277
238.58	.6243	.6229	.6232	.6241	.6245	.6220	.6246	.6226
246.25	.6237	.6220	.6229	.6238	.6249	.6227	.6262	.6230
246.42	.6142	.6134	.6154	.6168	.6165	.6146	.6171	.6160
252.38	.6156	.6138	.6141	.6158	.6156	.6140	.6176	.6126
252.54	.6110	.6122	.6126	.6115	.6113	.6132	.6135	.6116
259.46	.6105	.6129	.6114	.6100	.6126	.6114	.6127	.6111
259.63	.6070	.6083	.6085	.6074	.6077	.6081	.6078	.6086
266.46	.6075	.6108	.6069	.6071	.6018	.6092	.6064	.6060
266.63	.6010	.6010	.6024	.6026	.6032	.6030	.6016	.6017
273.46	.6002	.6005	.6027	.6031	.6030	.6018	.6041	.5989
273.63	.5971	.5954	.5976	.5975	.5962	.5955	.5978	.5965
280.50	.5984	.5966	.5970	.5970	.5976	.5962	.5981	.5947
280.67	.5930	.5934	.5931	.5924	.5919	.5924	.5922	.5915
287.63	.5905	.5888	.5844	.5916	.5886	.5917	.5904	.5883
287.79	.5899	.5876	.5874	.5887	.5881	.5892	.5877	.5879
294.17	.5901	.5898	.5884	.5912	.5905	.5884	.5886	.5893
294.50	.5842	.5868	.5833	.5835	.5824	.5857	.5835	.5833
301.38	.5844	.5828	.5822	.5824	.5847	.5860	.5850	.5807
301.71	.5796	.5796	.5770	.5781	.5778	.5801	.5786	.5784
308.50	.5795	.5803	.5791	.5767	.5793	.5793	.5802	.5781
308.67	.5756	.5751	.5733	.5745	.5738	.5749	.5749	.5759
315.46	.5743	.5747	.5736	.5739	.5742	.5732	.5760	.5742
315.63	.5713	.5709	.5719	.5719	.5716	.5715	.5716	.5728
322.33	.5778	.5713	.5707	.5712	.5707	.5711	.5723	.5710
322.50	.5673	.5674	.5666	.5682	.5664	.5702	.5684	.5663
329.33	.5669	.5668	.5648	.5668	.5645	.5677	.5675	.5651
329.50	.5634	.5635	.5612	.5611	.5609	.5628	.5622	.5607
336.46	.5627	.5631	.5605	.5629	.5611	.5621	.5635	.5603
336.79	.5572	.5572	.5591	.5590	.5592	.5590	.5586	.5587
343.33	.5617	.5591	.5597	.5589	.5600	.5579	.5587	.5580
343.50	.5558	.5561	.5558	.5563	.5541	.5533	.5562	.5560
350.33	.5540	.5539	.5573	.5562	.5560	.5534	.5544	.5544
350.50	.5517	.5485	.5521	.5510	.5517	.5508	.5523	.5528
357.46	.5521	.5497	.5504	.5510	.5509	.5499	.5505	.5495
357.63	.5487	.5467	.5474	.5492	.5475	.5468	.5473	.5472
364.46	.5486	.5465	.5494	.5492	.5477	.5472	.5499	.5489
364.79	.5445	.5439	.5432	.5433	.5452	.5427	.5452	.5436

Table A-3. Sensor locations in the Stripa heater experiments.

SENSOR LOCATIONS FOR EXPERIMENT 1, FULL SCALE HEATER H9														
HOLE ID	SENSOR TYPE	SENSOR NUMBER	SENSOR LABEL	RHO	THETA	Z	LOCAL X	RECTANGULAR Y	RECTANGULAR Z	MINE X	RECTANGULAR Y	RECTANGULAR Z	DEPTH	HOLE LENGTH
H9	HEATER CURRENT	351	IH9A	.00	0.	-0.51	.00	-0.00	-0.51	323.41	1007.25	343.51	4.73	5.60
H9	HEATER VOLTAGE	352	VH9A	.00	0.	-0.51	.00	-0.00	-0.51	323.41	1007.25	343.51	4.73	5.60
H9	HEATER POWER	353	PH9A	0.	0.	.10	0.	0.	.10	323.41	1007.25	342.90	4.12	5.60
H9	HEATER CURRENT	354	IH9B	0.	0.	.10	0.	0.	.10	323.41	1007.25	342.90	4.12	5.60
H9	HEATER VOLTAGE	355	VH9B	.00	0.	.71	.00	.00	.71	323.41	1007.25	342.29	3.51	5.60
H9	HEATER POWER	356	PH9B	.00	0.	.71	.00	.00	.71	323.41	1007.25	342.29	3.51	5.60
H9	HEATER CURRENT	357	IH9C	.00	0.	2.44	.00	.00	2.44	323.42	1007.25	340.56	1.78	5.60
H9	HEATER VOLTAGE	358	VH9C	.00	0.	2.44	.00	.00	2.44	323.42	1007.25	340.56	1.78	5.60
H9	HEATER POWER	359	PH9C	.40	357.9	3.00	.01	.40	3.00	323.62	1007.59	340.01	1.27	7.64
H9	HEATER CURRENT	360	IH9D	.40	357.8	3.00	.01	.40	3.00	323.62	1007.59	340.01	1.27	7.64
H9	HEATER VOLTAGE	361	VH9D	.40	357.6	-0.1	.02	.40	-0.1	323.62	1007.59	343.01	4.27	7.64
H9	HEATER POWER	362	PH9D	.40	357.4	-1.51	.02	.40	-1.51	323.62	1007.59	344.51	5.77	7.64
H9	HEATER CURRENT	363	PH9E	.40	357.2	-3.01	.02	.40	-3.01	323.62	1007.59	346.01	7.27	7.64
H9	HEATER VOLTAGE	364	PH9F	.90	0.	3.00	.01	.90	3.00	323.86	1008.03	340.00	1.30	7.70
H9	HEATER POWER	365	PH9G	.89	0.	3.00	.01	.89	3.00	323.86	1008.03	340.00	1.30	7.70
H9	HEATER CURRENT	366	PH9H	.89	0.	1.50	.00	.89	1.50	323.85	1008.02	341.50	2.80	7.70
H9	HEATER VOLTAGE	367	PH9I	.89	0.	1.50	.00	.89	1.50	323.85	1008.02	343.00	4.30	7.70
H9	HEATER POWER	368	PH9J	.89	0.	-1.50	.01	.88	-1.50	323.85	1008.02	344.50	5.80	7.70
H9	HEATER CURRENT	369	PH9K	.88	0.	-3.00	.01	.88	-3.00	323.85	1008.02	346.00	7.30	7.70
H9	HEATER VOLTAGE	370	PH9L	.69	44.2	3.00	.48	.49	3.00	323.23	1007.92	340.01	1.25	7.64
H9	HEATER POWER	371	PH9M	.69	44.1	3.00	.48	.49	3.00	323.23	1007.92	340.01	1.25	7.64
H9	HEATER CURRENT	372	PH9N	.68	44.1	-0.1	.47	.49	-0.1	323.24	1007.91	341.51	2.75	7.64
H9	HEATER VOLTAGE	373	PH9O	.68	44.0	-1.51	.47	.49	-1.51	323.24	1007.91	343.01	4.25	7.64
H9	HEATER POWER	374	PH9P	.67	43.9	-3.01	.47	.49	-3.01	323.24	1007.91	344.51	5.75	7.64
H9	HEATER CURRENT	375	PH9Q	.50	182.8	3.00	.02	.50	3.00	323.19	1006.81	340.00	1.15	7.57
H9	HEATER VOLTAGE	376	PH9R	.50	184.3	1.50	.04	.49	1.50	323.20	1006.80	341.50	2.65	7.57
H9	HEATER POWER	377	PH9S	.50	186.0	.00	.05	.49	.00	323.22	1006.79	343.00	4.15	7.57
H9	HEATER CURRENT	378	PH9T	.50	187.6	-1.50	.07	.49	-1.50	323.23	1006.79	344.50	5.65	7.57
H9	HEATER VOLTAGE	379	PH9U	.81	189.1	-3.00	.08	.49	-3.00	323.24	1006.78	346.00	7.15	7.57
H9	HEATER POWER	380	PH9V	.81	225.7	3.00	.58	.56	3.00	323.64	1006.48	340.00	1.23	7.64
H9	HEATER CURRENT	381	PH9W	.81	226.0	1.50	.58	.56	1.50	323.65	1006.48	341.50	2.73	7.64
H9	HEATER VOLTAGE	382	PH9X	.81	226.2	.00	.58	.56	.00	323.65	1006.48	343.00	4.23	7.64
H9	HEATER POWER	383	PH9Y	.81	226.4	-1.50	.59	.56	-1.50	323.65	1006.48	344.50	5.73	7.64
H9	HEATER CURRENT	384	PH9Z	.81	226.7	-3.00	.59	.56	-3.00	323.66	1006.48	346.00	7.23	7.64
H9	HEATER VOLTAGE	385	PH9AA	.61	314.5	3.00	.44	.44	3.00	324.00	1007.41	340.00	1.32	7.72
H9	HEATER POWER	386	PH9AB	.62	314.6	1.50	.44	.44	1.50	324.01	1007.42	341.50	2.82	7.72
H9	HEATER CURRENT	387	PH9AC	.62	314.7	.00	.44	.44	.00	324.01	1007.42	343.00	4.32	7.72
H9	HEATER VOLTAGE	388	PH9AD	.62	314.8	-1.50	.44	.44	-1.50	324.01	1007.42	344.50	5.82	7.72
H9	HEATER POWER	389	PH9AE	.63	314.8	-3.00	.44	.44	-3.00	324.02	1007.42	346.00	7.32	7.72
H9	HEATER CURRENT	390	PH9AF	1.00	189.8	2.23	.01	-1.00	2.23	322.94	1006.37	340.77	1.97	12.95
H9	HEATER VOLTAGE	391	PH9AG	1.00	189.9	-0.2	.02	-1.00	-0.2	322.94	1006.37	340.77	1.97	12.95
H9	HEATER POWER	392	PH9AH	1.00	189.9	-2.27	.02	-1.00	-2.27	322.94	1006.37	345.27	6.47	12.95
H9	HEATER CURRENT	393	PH9AI	1.00	189.9	-2.27	.02	-1.00	-2.27	322.94	1006.37	345.27	6.47	12.95

Table A-3 (continued)
SENSOR LOCATIONS FOR EXPERIMENT 1, FULL SCALE HEATER H9

HOLE ID	SENSOR TYPE	SENSOR NUMBER	SENSOR LABEL	CYLINDRICAL COORDINATES	LOCAL	RECTANGULAR	MFNE	RECTANGULAR	DEPTH	HOLE LENGTH	
				RHO THETA Z	X Y Z	X Y Z	X X X	Y Y Y	Z Z Z		
E6	EXTENSOMETER	294	E6D	1.00 181.1	-7.32	-1.00	322.94	1006.37	350.33	11.53	12.95
E6	THERMOCOUPLE	17	TE6A	1.00 180.8	2.43	-1.00	322.94	1006.37	340.58	1.78	12.95
E6	THERMOCOUPLE	18	TE6B	1.00 180.9	-0.82	-1.00	322.94	1006.37	343.83	5.03	12.95
E6	THERMOCOUPLE	19	TE6C	1.00 180.9	-2.07	-1.00	322.94	1006.37	345.08	6.28	12.95
E6	THERMOCOUPLE	20	TE6D	1.00 181.1	-7.32	-1.00	322.94	1006.37	350.33	11.53	12.95
E6	THERMOCOUPLE	130	RF128	1.00 180.8	4.20	-1.00	322.94	1006.37	338.80	0.	12.95
E6	THERMOCOUPLE	122	TE6F	1.00 180.9	1.18	-1.00	322.94	1006.37	342.83	4.03	12.95
E6	THERMOCOUPLE	123	TE6G	1.00 181.0	-4.70	-1.00	322.94	1006.37	347.71	8.91	12.95
E7	EXTENSOMETER	295	E7A	2.00 180.4	2.22	-2.00	322.45	1005.50	340.78	2.11	12.69
E7	EXTENSOMETER	296	E7B	2.00 180.4	-0.03	-2.00	322.45	1005.50	343.03	4.36	12.69
E7	EXTENSOMETER	297	E7C	2.00 180.4	-2.28	-2.00	322.45	1005.49	345.28	6.61	12.69
E7	EXTENSOMETER	298	E7D	2.01 180.3	-7.50	-2.01	322.44	1005.49	350.50	11.83	12.69
E7	THERMOCOUPLE	21	TE7A	2.00 180.4	-1.02	-2.00	322.45	1005.50	344.02	5.35	12.69
E7	THERMOCOUPLE	22	TE7B	2.00 180.4	-2.25	-2.00	322.45	1005.49	345.25	6.58	12.69
E7	THERMOCOUPLE	23	TE7C	2.01 180.4	-4.88	-2.01	322.45	1005.49	347.88	9.21	12.69
E7	THERMOCOUPLE	24	TE7D	2.01 180.3	-7.50	-2.01	322.44	1005.49	350.50	11.83	12.69
E7	THERMOCOUPLE	128	TE7E	2.00 180.4	4.33	-2.00	322.45	1005.50	338.67	0.	12.69
E7	THERMOCOUPLE	124	TE7F	2.00 180.4	2.26	-2.00	322.45	1005.50	340.75	2.08	12.69
E7	THERMOCOUPLE	125	TE7G	2.00 180.4	0.01	-2.00	322.45	1005.50	343.00	4.33	12.69
E8	EXTENSOMETER	299	E8A	2.99 180.2	2.25	-2.99	321.97	1004.63	340.75	2.07	12.67
E8	EXTENSOMETER	300	E8B	2.99 180.3	0.00	-2.99	321.97	1004.63	343.00	4.32	12.67
E8	EXTENSOMETER	301	E8C	2.99 180.3	-2.26	-2.99	321.97	1004.63	345.26	6.58	12.67
E8	EXTENSOMETER	302	E8D	2.98 180.3	-7.48	-2.98	321.98	1004.64	350.48	11.80	12.67
E8	THERMOCOUPLE	25	TE8A	2.99 180.2	2.27	-2.99	321.97	1004.63	340.73	2.05	12.67
E8	THERMOCOUPLE	26	TE8B	2.99 180.3	0.02	-2.99	321.97	1004.63	342.98	4.30	12.67
E8	THERMOCOUPLE	27	TE8C	2.99 180.3	-2.23	-2.99	321.97	1004.63	345.23	6.55	12.67
E8	THERMOCOUPLE	28	TE8D	2.98 180.3	-7.48	-2.98	321.98	1004.64	350.48	11.80	12.67
E8	THERMOCOUPLE	132	RF128	3.00 180.2	4.32	-3.00	321.96	1004.63	338.68	0.	12.67
E9	EXTENSOMETER	303	E9A	1.51 225.3	2.23	-1.07	323.83	1005.80	340.77	2.01	12.58
E9	EXTENSOMETER	304	E9B	1.50 225.2	-0.02	-1.06	323.83	1005.81	343.02	4.26	12.58
E9	EXTENSOMETER	305	E9C	1.50 225.2	-2.27	-1.06	323.83	1005.81	345.27	6.51	12.58
E9	EXTENSOMETER	306	E9D	1.50 225.0	-7.42	-1.06	323.82	1005.81	350.42	11.66	12.58
E9	THERMOCOUPLE	29	TE9A	1.51 225.3	2.39	-1.07	323.83	1005.80	340.61	1.85	12.58
E9	THERMOCOUPLE	30	TE9B	1.50 225.2	1.14	-1.07	323.83	1005.81	342.86	4.10	12.58
E9	THERMOCOUPLE	31	TE9C	1.50 225.2	-0.86	-1.07	323.83	1005.81	343.86	5.10	12.58
E9	THERMOCOUPLE	32	TE9D	1.50 225.4	-2.11	-1.06	323.83	1005.80	345.11	6.35	12.58
E9	THERMOCOUPLE	133	RF128	1.51 225.4	4.24	-1.06	323.83	1005.80	338.76	0.	12.58
E9	THERMOCOUPLE	160	RF 24	1.50 225.0	-7.42	-1.06	323.82	1005.81	350.42	11.66	12.58
E10	EXTENSOMETER	307	E10A	2.51 225.1	2.23	-1.77	324.10	1004.84	340.77	2.03	12.63
E10	EXTENSOMETER	308	E10B	2.51 225.0	-0.02	-1.77	324.10	1004.84	343.02	4.28	12.63
E10	EXTENSOMETER	309	E10C	2.51 225.0	-2.21	-1.78	324.10	1004.83	345.21	6.47	12.63
E10	EXTENSOMETER	310	E10D	2.52 224.9	-7.49	-1.78	324.10	1004.83	350.49	11.75	12.63
E10	THERMOCOUPLE	33	TE10A	2.51 225.1	2.26	-1.77	324.10	1004.84	340.74	2.00	12.63
E10	THERMOCOUPLE	34	TE10B	2.51 225.0	0.01	-1.77	324.10	1004.84	342.99	4.25	12.63
E10	THERMOCOUPLE	35	TE10C	2.51 225.0	-0.99	-1.77	324.10	1004.84	343.99	5.25	12.63
E10	THERMOCOUPLE	36	TE10D	2.51 225.0	-2.24	-1.78	324.10	1004.83	345.24	6.50	12.63
E10	THERMOCOUPLE	134	RF128	2.51 225.1	4.26	-1.77	324.10	1004.84	338.74	0.	12.63
E10	THERMOCOUPLE	161	RF 24	2.52 224.9	-7.49	-1.78	324.10	1004.83	350.49	11.75	12.63
E11	EXTENSOMETER	311	E11A	2.01 270.1	2.23	-2.01	325.17	1006.27	340.77	2.00	12.54
E11	EXTENSOMETER	312	E11B	2.01 270.1	-0.03	-2.01	325.17	1006.28	343.03	4.26	12.54
E11	EXTENSOMETER	313	E11C	2.01 270.1	-2.28	-2.01	325.17	1006.28	345.28	6.51	12.54
E11	EXTENSOMETER	314	E11D	2.00 270.1	-7.44	-2.00	325.17	1006.28	350.44	11.67	12.54
E11	THERMOCOUPLE	37	TE11A	2.01 270.1	2.31	-2.01	325.17	1006.27	340.69	1.92	12.54
E11	THERMOCOUPLE	38	TE11B	2.01 270.1	0.06	-2.01	325.17	1006.28	342.94	4.17	12.54

Table A-3 (continued)
 SENSOR LOCATIONS FOR EXPERIMENT 1, FULL SCALE HEATER H9

HOLE ID	SENSOR TYPE	SENSOR NUMBER	SENSOR LABEL	CYLINDRICAL COORDINATES	LOCAL	RECTANGULAR	MINE	RECTANGULAR	DEPTH	HOLE LENGTH
				RHO THETA Z	X	Y Z	X Y Z	Y Z		
E11	THERMOCOUPLE	39	TE11C	2.01 270.1 -2.19	-2.01	.00 -2.19	325.17 1006.28 345.19	1006.28 345.19	6.42	12.54
E11	THERMOCOUPLE	40	TE11D	2.00 270.1 -7.44	-2.00	.00 -7.44	325.17 1006.28 350.44	1006.28 350.44	11.67	12.54
E11	THERMOCOUPLE	135	RF128	2.01 270.1 4.23	-2.01	.00 4.23	325.17 1006.27 338.77	1006.27 338.77	0.	12.54
E18	EXTENSOMETER	316	E18A	1.63 89.7 1.96	1.63	.01 1.96	321.99 1008.05 341.04	1008.05 341.04	8.46	9.03
E18	EXTENSOMETER	317	E18B	3.05 89.9 1.81	3.05	.01 1.81	320.75 1008.74 341.19	1008.74 341.19	7.03	9.03
E18	EXTENSOMETER	318	E18C	4.30 89.9 1.68	4.30	.01 1.68	319.66 1009.35 341.32	1009.35 341.32	5.77	9.03
E18	EXTENSOMETER	315	E18D	7.06 90.0 1.40	7.06	.00 1.40	317.25 1010.69 341.60	1010.69 341.60	3.00	9.03
E18	THERMOCOUPLE	44	TE18A	1.63 89.7 1.96	1.63	.01 1.96	321.99 1008.05 341.04	1008.05 341.04	8.46	9.03
E18	THERMOCOUPLE	43	TE18B	3.12 89.9 1.80	3.12	.01 1.80	320.69 1008.78 341.20	1008.78 341.20	6.96	9.03
E18	THERMOCOUPLE	42	TE18C	4.36 89.9 1.68	4.36	.00 1.68	319.60 1009.38 341.32	1009.38 341.32	5.71	9.03
E18	THERMOCOUPLE	41	TE18D	8.10 92.0 1.30	8.10	.00 1.30	316.34 1011.19 341.70	1011.19 341.70	1.96	9.03
E18	THERMOCOUPLE	142	RF572	10.04 50.0 1.10	10.04	.00 1.10	314.64 1012.14 341.90	1012.14 341.90	0.	9.03
E19	EXTENSOMETER	321	E19A	1.23 89.5 .05	1.23	.01 .05	322.35 1007.86 342.95	1007.86 342.95	8.69	8.90
E19	EXTENSOMETER	320	E19B	2.53 89.8 -.01	2.53	.01 -.01	321.21 1008.49 343.01	1008.49 343.01	7.39	8.90
E19	EXTENSOMETER	319	E19C	3.49 89.9 -.06	3.49	.01 -.06	320.36 1008.96 343.06	1008.96 343.06	6.42	8.90
E19	EXTENSOMETER	322	E19D	-1.14 89.9 -.14	5.01	.01 -.14	319.04 1009.70 343.14	1009.70 343.14	4.90	8.90
E19	THERMOCOUPLE	48	TE19A	1.23 89.5 .05	1.23	.01 .05	322.35 1007.86 342.95	1007.86 342.95	8.69	8.90
E19	THERMOCOUPLE	47	TE19B	2.48 89.8 -.01	2.48	.01 -.01	321.25 1008.46 343.01	1008.46 343.01	7.44	8.90
E19	THERMOCOUPLE	46	TE19C	3.47 89.9 -.06	3.47	.01 -.06	320.38 1008.95 343.06	1008.95 343.06	6.44	8.90
E19	THERMOCOUPLE	45	TE19D	4.97 89.9 -.14	4.97	.01 -.14	319.07 1009.68 343.14	1009.68 343.14	4.94	8.90
E20	THERMOCOUPLE	143	RF572	9.91 90.0 -.39	9.91	.00 -.39	314.76 1012.07 343.39	1012.07 343.39	0.	8.90
E20	EXTENSOMETER	326	E20A	-1.84 89.7 271.4	-1.84	.02 -1.84	324.27 1006.80 344.84	1006.80 344.84	10.66	11.12
E20	EXTENSOMETER	325	E20B	1.01 88.9 -1.90	1.01	.02 -1.90	322.54 1007.76 344.90	1007.76 344.90	8.68	11.12
E20	EXTENSOMETER	324	E20C	2.01 89.5 -1.93	2.01	.02 -1.93	321.66 1008.25 344.93	1008.25 344.93	7.68	11.12
E20	EXTENSOMETER	323	E20D	-2.04 89.9 -2.04	5.97	.01 -2.04	318.20 1010.17 345.04	1010.17 345.04	3.72	11.12
E20	THERMOCOUPLE	52	TE20A	1.87 88.9 -1.87	1.87	.02 -1.87	323.39 1007.29 344.87	1007.29 344.87	9.66	11.12
E20	THERMOCOUPLE	51	TE20B	1.90 88.9 -1.90	1.03	.02 -1.90	322.52 1007.77 344.90	1007.77 344.90	7.66	11.12
E20	THERMOCOUPLE	50	TE20C	2.03 89.5 -1.93	2.03	.02 -1.93	321.65 1008.25 344.93	1008.25 344.93	8.66	11.12
E20	THERMOCOUPLE	49	TE20D	6.03 89.9 -2.04	6.03	.01 -2.04	318.15 1010.20 345.04	1010.20 345.04	3.66	11.12
E20	THERMOCOUPLE	144	RF572	9.69 90.0 -2.14	9.69	.00 -2.14	314.95 1011.97 345.14	1011.97 345.14	0.	11.12
E21	EXTENSOMETER	330	E21A	1.49 44.3 2.03	1.04	1.07 2.03	323.02 1008.69 340.97	1008.69 340.97	12.77	13.28
E21	EXTENSOMETER	329	E21B	3.00 44.7 1.92	2.11	2.13 1.92	322.61 1010.14 341.08	1010.14 341.08	11.26	13.28
E21	EXTENSOMETER	328	E21C	4.24 44.8 1.83	2.98	3.01 1.83	322.27 1011.33 341.17	1011.33 341.17	10.02	13.28
E21	EXTENSOMETER	327	E21D	6.96 44.9 1.63	4.91	4.93 1.63	321.52 1013.95 341.37	1013.95 341.37	7.29	13.28
E21	THERMOCOUPLE	56	TE21A	1.49 44.3 2.03	1.04	1.07 2.03	323.02 1008.69 340.97	1008.69 340.97	12.77	13.28
E21	THERMOCOUPLE	55	TE21B	2.99 44.7 1.92	2.10	2.13 1.92	322.61 1010.13 341.08	1010.13 341.08	11.27	13.28
E21	THERMOCOUPLE	54	TE21C	4.24 44.8 1.83	2.98	3.01 1.83	322.27 1011.33 341.17	1011.33 341.17	10.02	13.28
E21	THERMOCOUPLE	53	TE21D	7.98 44.9 1.55	5.63	5.65 1.55	321.24 1014.93 341.45	1014.93 341.45	6.27	13.28
E21	THERMOCOUPLE	145	RF572	14.23 45.0 1.09	10.06	10.07 1.09	319.53 1020.94 341.91	1020.94 341.91	0.	13.28
E22	EXTENSOMETER	334	E22A	1.29 44.0 .08	.90	.93 .08	323.08 1008.50 342.92	1008.50 342.92	12.73	13.01
E22	EXTENSOMETER	333	E22B	2.52 44.5 .03	1.77	1.80 .03	322.74 1009.68 342.97	1009.68 342.97	11.50	13.01
E22	EXTENSOMETER	332	E22C	3.51 44.7 -.03	2.47	2.49 -.03	322.47 1010.63 343.00	1010.63 343.00	10.51	13.01
E22	EXTENSOMETER	331	E22D	5.03 44.8 -.06	3.54	3.57 -.06	322.05 1012.09 343.06	1012.09 343.06	8.99	13.01
E22	THERMOCOUPLE	60	TE22A	1.29 44.0 .08	.90	.93 .08	323.08 1008.50 342.92	1008.50 342.92	12.73	13.01
E22	THERMOCOUPLE	59	TE22B	2.54 44.5 .03	1.78	1.81 .03	322.74 1009.70 342.97	1009.70 342.97	11.48	13.01
E22	THERMOCOUPLE	58	TE22C	3.54 44.7 -.00	2.49	2.52 -.00	322.46 1010.66 343.00	1010.66 343.00	10.48	13.01
E22	THERMOCOUPLE	57	TE22D	5.04 44.8 -.06	3.55	3.57 -.06	322.05 1012.10 343.06	1012.10 343.06	8.98	13.01
E22	THERMOCOUPLE	146	RF572	14.01 45.0 -1.40	9.90	9.91 -.40	319.59 1020.73 343.40	1020.73 343.40	0.	13.01
E23	EXTENSOMETER	338	E23A	1.07 44.1 -1.88	.75	.77 -1.88	323.14 1008.29 344.88	1008.29 344.88	12.81	12.85
E23	EXTENSOMETER	337	E23B	2.00 44.5 -1.90	1.40	1.43 -1.90	322.88 1009.18 344.90	1009.18 344.90	11.88	12.85
E23	EXTENSOMETER	336	E23C	3.02 44.7 -1.92	2.13	2.15 -1.92	322.60 1010.16 344.92	1010.16 344.92	10.86	12.85
E23	EXTENSOMETER	335	E23D	6.00 44.9 -1.98	4.23	4.25 -1.98	321.78 1013.03 344.98	1013.03 344.98	7.88	12.85
E23	THERMOCOUPLE	64	TE23A	1.07 44.1 -1.88	.75	.77 -1.88	323.14 1008.29 344.88	1008.29 344.88	12.81	12.85
E23	THERMOCOUPLE	63	TE23B	2.07 44.6 -1.90	1.45	1.48 -1.90	322.86 1009.25 344.90	1009.25 344.90	11.81	12.85

Table A-3 (continued)

SENSOR LOCATIONS FOR EXPERIMENT 1, FULL SCALE HEATER H9

HOLE ID	SENSOR TYPE	SENSOR NUMBER	SENSOR LABEL	CYLINDRICAL COORDINATES RHC	THETA	Z	LOCAL X	RECTANGULAR Y	RECTANGULAR Z	MINE X	RECTANGULAR Y	RECTANGULAR Z	DEPTH	HOLE LENGTH
E23	THERMOCOUPLE	62	TE23C	3.07	44.7	-1.92	2.16	2.18	-1.92	322.59	1010.21	344.92	10.81	12.85
E23	THERMOCOUPLE	61	TE23D	6.07	44.9	-1.98	4.28	4.30	-1.98	321.77	1013.09	344.98	7.81	12.85
E25	THERMOCOUPLE	147	RF572	13.88	45.0	-2.15	9.81	9.82	-2.15	319.63	1020.60	345.15	0.	12.85
E24	EXTENSOMETER	342	E24A	1.48	133.2	2.04	1.98	-1.01	2.04	321.98	1006.89	340.96	12.77	13.25
E24	EXTENSOMETER	339	E24B	2.99	134.2	1.93	2.14	-2.09	1.93	320.52	1006.47	341.07	11.25	13.25
E24	EXTENSOMETER	340	E24C	4.26	134.5	1.83	3.04	-2.99	1.83	319.31	1006.12	341.17	9.98	13.25
E24	EXTENSOMETER	341	E24D	6.59	134.8	1.63	4.96	-4.93	1.63	316.68	1005.36	341.37	7.24	13.25
E24	THERMOCOUPLE	68	TE24A	1.48	133.2	2.04	1.08	-1.01	2.04	321.98	1006.89	340.96	12.77	13.25
E24	THERMOCOUPLE	67	TE24B	2.97	134.2	1.93	2.13	-2.07	1.93	320.54	1006.48	341.07	11.27	13.25
E24	THERMOCOUPLE	66	TE24C	4.22	134.5	1.84	3.01	-2.96	1.84	319.35	1006.13	341.16	10.02	13.25
E24	THERMOCOUPLE	65	TE24D	7.96	134.9	1.56	5.64	-5.61	1.56	315.75	1005.09	341.44	6.27	13.25
E24	THERMOCOUPLE	148	RF572	14.21	135.0	1.09	10.04	-10.05	1.09	309.75	1003.36	341.91	0.	13.25
E25	EXTENSOMETER	346	E25A	1.25	132.6	.10	.92	-.84	.10	322.20	1006.96	342.90	13.14	13.38
E25	EXTENSOMETER	345	E25B	2.48	133.9	.05	1.78	-1.72	.05	321.02	1006.62	342.95	11.91	13.38
E25	EXTENSOMETER	344	E25C	3.47	134.3	.01	2.48	-2.42	.01	320.07	1006.34	342.99	10.92	13.38
E25	EXTENSOMETER	343	E25D	4.96	134.6	-.04	3.54	-3.49	-.04	318.63	1005.93	343.04	9.42	13.38
E25	THERMOCOUPLE	72	TE25A	1.25	132.6	.10	.92	-.84	.10	322.20	1006.96	342.90	13.14	13.38
E25	THERMOCOUPLE	71	TE25B	2.50	133.9	.05	1.80	-1.73	.05	321.00	1006.61	342.95	11.89	13.38
E25	THERMOCOUPLE	70	TE25C	3.50	134.3	.01	2.50	-2.44	.01	320.04	1006.34	342.99	10.89	13.38
E25	THERMOCOUPLE	69	TE25D	4.99	134.6	-.05	3.56	-3.51	-.05	318.60	1005.92	343.05	9.39	13.38
E25	THERMOCOUPLE	149	RF572	14.38	135.0	-.41	10.16	-10.17	-.41	309.59	1007.00	344.87	0.	13.38
E26	EXTENSOMETER	350	E26A	1.09	132.4	-1.87	.80	-.73	-1.87	322.35	1007.00	344.87	13.01	13.08
E26	EXTENSOMETER	349	E26B	2.05	133.7	-1.89	1.48	-1.42	-1.89	321.43	1006.74	344.89	12.05	13.08
E26	EXTENSOMETER	348	E26C	3.04	134.2	-1.91	2.18	-2.12	-1.91	320.48	1006.46	344.91	11.06	13.08
E26	EXTENSOMETER	347	E26D	6.04	134.7	-1.98	4.29	-4.25	-1.98	317.60	1005.63	344.98	8.06	13.08
E26	THERMOCOUPLE	76	TE26A	1.09	132.4	-1.87	.80	-.73	-1.87	322.35	1007.00	344.87	13.01	13.08
E26	THERMOCOUPLE	75	TE26B	2.09	133.8	-1.89	1.51	-1.44	-1.89	321.39	1006.72	344.89	12.01	13.08
E26	THERMOCOUPLE	74	TE26C	3.09	134.2	-1.91	2.21	-2.15	-1.91	320.43	1006.45	344.91	11.01	13.08
E26	THERMOCOUPLE	73	TE26D	6.09	134.7	-1.98	4.32	-4.28	-1.98	317.55	1005.61	344.98	8.01	13.08
E26	THERMOCOUPLE	150	RF572	14.09	135.0	-2.15	9.96	-9.97	-2.15	309.86	1003.39	345.15	0.	13.08
C1	IRAD GAGE	272	C1A	.99	22.1	.85	.37	.92	.85	323.53	1008.24	342.15	3.42	7.12
C1	IRAD GAGE	271	C1B	.99	22.1	.85	.37	.92	.85	323.53	1008.24	342.15	3.42	7.12
C1	THERMOCOUPLE	77	TC1	.99	22.1	.85	.37	.92	.85	323.53	1008.24	342.15	3.42	7.12
U6	IRAD GAGE	273	C2A	1.01	314.8	-.65	-.72	.71	-.65	324.38	1007.52	343.65	4.96	7.42
U6	IRAD GAGE	274	C2B	1.01	314.8	-.65	-.72	.71	-.65	324.38	1007.52	343.65	4.96	7.42
U6	THERMOCOUPLE	78	TC2	1.01	314.8	-.65	-.72	.71	-.65	324.38	1007.52	343.65	4.96	7.42
C6	IRAD GAGE	275	C6A	2.50	47.5	.65	1.84	1.69	.65	322.62	1009.62	342.35	11.64	13.18
C6	IRAD GAGE	276	C6B	2.50	47.5	.65	1.84	1.69	.65	322.62	1009.62	342.35	11.64	13.18
C6	THERMOCOUPLE	79	TC6	2.50	47.5	.65	1.84	1.69	.65	322.62	1009.62	342.35	11.64	13.18
C7	IRAD GAGE	277	C7A	2.00	50.1	.66	2.00	-.00	.66	321.66	1008.22	342.34	8.08	9.09
C7	IRAD GAGE	278	C7B	2.00	50.1	.66	2.00	-.00	.66	321.66	1008.22	342.34	8.08	9.09
C7	THERMOCOUPLE	80	TC7	2.00	50.1	.66	2.00	-.00	.66	321.66	1008.22	342.34	8.08	9.09
C8	IRAD GAGE	279	C8A	3.01	134.8	.70	2.13	-2.12	.70	320.52	1006.44	342.30	11.20	13.16
C8	IRAD GAGE	280	C8B	3.01	134.8	.70	2.13	-2.12	.70	320.52	1006.44	342.30	11.20	13.16
C8	THERMOCOUPLE	81	TC8	3.01	134.8	.70	2.13	-2.12	.70	320.52	1006.44	342.30	11.20	13.16
C11	IRAD GAGE	281	C11A	3.99	67.8	-.85	3.69	1.51	-.85	320.92	1010.37	343.85	6.50	9.49
C11	IRAD GAGE	282	C11B	3.99	67.8	-.85	3.69	1.51	-.85	320.92	1010.37	343.85	6.50	9.49
C11	THERMOCOUPLE	82	TC11	3.99	67.8	-.85	3.69	1.51	-.85	320.92	1010.37	343.85	6.50	9.49
C12	IRAD GAGE	283	C12A	3.48	112.7	-.87	3.21	-1.34	-.87	319.95	1007.64	343.87	7.53	8.02
C12	IRAD GAGE	284	C12B	3.48	112.7	-.87	3.21	-1.34	-.87	319.95	1007.64	343.87	7.53	8.02
C12	THERMOCOUPLE	83	TC12	3.48	112.7	-.87	3.21	-1.34	-.87	319.95	1007.64	343.87	7.53	8.02
U1	JSBM	201	U1A	1.51	0.	.85	-.02	1.51	.85	324.16	1008.56	342.15	3.50	7.45
U1	USBM	202	U1B	1.51	0.	.85	-.02	1.51	.85	324.16	1008.56	342.15	3.50	7.45

Table A-3 (continued)
 SENSOR LOCATIONS FOR EXPERIMENT 1, FULL SCALE HEATER H9

HOLE ID	SENSOR TYPE	SENSOR NUMBER	SENSOR LABEL	RHO	CYLINDRICAL COORDINATES	LOCAL X	LOCAL Y	LOCAL Z	RECTANGULAR X	RECTANGULAR Y	RECTANGULAR Z	MINE X	MINE Y	MINE Z	DEPTH	HOLE LENGTH
U1	USBM	203	U1C	1.51	0.	-0.2	1.51	.85	-0.2	1.51	.85	324.16	1008.56	342.15	3.50	7.45
U1	THERMOCOUPLE	2	TU1	1.51	0.	-0.2	1.51	.85	-0.2	1.51	.85	324.16	1008.56	342.15	3.50	7.45
U2	USBM	204	U2A	2.49	0.	-0.1	2.49	-.65	-0.1	2.49	-.65	324.64	1009.42	343.65	5.03	7.77
U2	USBM	205	U2B	2.49	0.	-0.1	2.49	-.65	-0.1	2.49	-.65	324.64	1009.42	343.65	5.03	7.77
U2	USBM	206	U2C	2.49	0.	-0.1	2.49	-.65	-0.1	2.49	-.65	324.64	1009.42	343.65	5.03	7.77
U2	THERMOCOUPLE	3	TU2	2.49	0.	-0.1	2.49	-.65	-0.1	2.49	-.65	324.64	1009.42	343.65	5.03	7.77
U3	USBM	207	U3A	3.49	0.	-0.1	3.49	.85	-0.1	3.49	.85	325.12	1010.30	342.15	3.54	7.46
U3	USBM	208	U3B	3.49	0.	-0.1	3.49	.85	-0.1	3.49	.85	325.12	1010.30	342.15	3.54	7.46
U3	USBM	209	U3C	3.49	0.	-0.1	3.49	.85	-0.1	3.49	.85	325.12	1010.30	342.15	3.54	7.46
U3	THERMOCOUPLE	4	TU3	3.49	0.	-0.1	3.49	.85	-0.1	3.49	.85	325.12	1010.30	342.15	3.54	7.46
U4	USBM	210	U4A	2.25	202.6	-0.6	-2.08	.85	-0.6	-2.08	.85	323.15	1005.01	342.15	3.32	7.04
U4	USBM	211	U4B	2.25	202.6	-0.6	-2.08	.85	-0.6	-2.08	.85	323.15	1005.01	342.15	3.32	7.04
U4	USBM	212	U4C	2.25	202.6	-0.6	-2.08	.85	-0.6	-2.08	.85	323.15	1005.01	342.15	3.32	7.04
U4	THERMOCOUPLE	5	TU4	2.25	202.6	-0.6	-2.08	.85	-0.6	-2.08	.85	323.15	1005.01	342.15	3.32	7.04
U5	USBM	213	U5A	3.27	202.8	-0.6	-3.01	-.65	-1.26	-3.01	-.65	323.05	1004.00	343.65	4.99	7.22
U5	USBM	214	U5B	3.27	202.8	-0.6	-3.01	-.65	-1.26	-3.01	-.65	323.05	1004.00	343.65	4.99	7.22
U5	USBM	215	U5C	3.27	202.8	-0.6	-3.01	-.65	-1.26	-3.01	-.65	323.05	1004.00	343.65	4.99	7.22
U5	THERMOCOUPLE	6	TU5	3.27	202.8	-0.6	-3.01	-.65	-1.26	-3.01	-.65	323.05	1004.00	343.65	4.99	7.22
C2	USBM	216	U6A	1.48	157.6	.57	-1.37	-.65	-1.42	1.40	-.65	325.34	1007.78	343.65	4.90	7.34
C2	USBM	217	U6B	1.48	157.6	.57	-1.37	-.65	-1.42	1.40	-.65	325.34	1007.78	343.65	4.90	7.34
C2	USBM	218	U6C	1.48	157.6	.57	-1.37	-.65	-1.42	1.40	-.65	325.34	1007.78	343.65	4.90	7.34
C2	THERMOCOUPLE	7	TU6	1.48	157.6	.57	-1.37	-.65	-1.42	1.40	-.65	325.34	1007.78	343.65	4.90	7.34
U7	USBM	219	U7A	2.00	314.6	-0.6	-1.42	-.65	-2.14	2.12	-.65	326.32	1008.06	343.65	4.90	7.14
U7	USBM	220	U7B	2.00	314.6	-0.6	-1.42	-.65	-2.14	2.12	-.65	326.32	1008.06	343.65	4.90	7.14
U7	USBM	221	U7C	2.00	314.6	-0.6	-1.42	-.65	-2.14	2.12	-.65	326.32	1008.06	343.65	4.90	7.14
U7	THERMOCOUPLE	8	TU7	2.00	314.6	-0.6	-1.42	-.65	-2.14	2.12	-.65	326.32	1008.06	343.65	4.90	7.14
U8	USBM	222	U8A	3.01	314.7	-0.6	-2.14	-.65	-2.14	2.12	-.65	326.32	1008.06	343.65	4.90	7.14
U8	USBM	223	U8B	3.01	314.7	-0.6	-2.14	-.65	-2.14	2.12	-.65	326.32	1008.06	343.65	4.90	7.14
U8	USBM	224	U8C	3.01	314.7	-0.6	-2.14	-.65	-2.14	2.12	-.65	326.32	1008.06	343.65	4.90	7.14
U8	THERMOCOUPLE	9	TU8	3.01	314.7	-0.6	-2.14	-.65	-2.14	2.12	-.65	326.32	1008.06	343.65	4.90	7.14
U9	USBM	225	U9A	2.28	337.1	.85	-0.89	.85	-0.89	2.10	.85	325.21	1008.66	342.15	3.41	7.14
U9	USBM	226	U9B	2.28	337.1	.85	-0.89	.85	-0.89	2.10	.85	325.21	1008.66	342.15	3.41	7.14
U9	USBM	227	U9C	2.28	337.1	.85	-0.89	.85	-0.89	2.10	.85	325.21	1008.66	342.15	3.41	7.14
U9	THERMOCOUPLE	10	TU9	2.28	337.1	.85	-0.89	.85	-0.89	2.10	.85	325.21	1008.66	342.15	3.41	7.14
U10	USBM	228	U10A	3.25	337.2	.95	-1.26	.95	-1.26	3.00	.95	325.97	1009.26	342.05	3.32	7.19
U10	USBM	229	U10B	3.25	337.2	.95	-1.26	.95	-1.26	3.00	.95	325.97	1009.26	342.05	3.32	7.19
U10	USBM	230	U10C	3.25	337.2	.95	-1.26	.95	-1.26	3.00	.95	325.97	1009.26	342.05	3.32	7.19
U10	THERMOCOUPLE	11	TU10	3.25	337.2	.95	-1.26	.95	-1.26	3.00	.95	325.97	1009.26	342.05	3.32	7.19
U21	USBM	231	U21A	2.49	67.9	.62	2.31	.62	2.31	.94	.62	321.85	1009.19	342.38	8.26	9.75
U21	USBM	232	U21B	2.49	67.9	.62	2.31	.62	2.31	.94	.62	321.85	1009.19	342.38	8.26	9.75
U21	USBM	233	U21C	2.49	67.9	.62	2.31	.62	2.31	.94	.62	321.85	1009.19	342.38	8.26	9.75
U21	THERMOCOUPLE	12	TU21	2.49	67.9	.62	2.31	.62	2.31	.94	.62	321.85	1009.19	342.38	8.26	9.75
U22	USBM	234	U22A	3.49	112.7	.68	3.22	.68	3.22	-1.35	.68	319.94	1007.64	342.32	7.58	8.08
U22	USBM	235	U22B	3.49	112.7	.68	3.22	.68	3.22	-1.35	.68	319.94	1007.64	342.32	7.58	8.08
U22	USBM	236	U22C	3.49	112.7	.68	3.22	.68	3.22	-1.35	.68	319.94	1007.64	342.32	7.58	8.08
U22	THERMOCOUPLE	13	TU22	3.49	112.7	.68	3.22	.68	3.22	-1.35	.68	319.94	1007.64	342.32	7.58	8.08
U26	USBM	237	U26A	2.48	46.2	-.82	1.79	-.82	1.79	1.72	-.82	322.68	1009.63	343.82	11.47	12.91
U26	USBM	238	U26B	2.48	46.2	-.82	1.79	-.82	1.79	1.72	-.82	322.68	1009.63	343.82	11.47	12.91
U26	USBM	239	U26C	2.48	46.2	-.82	1.79	-.82	1.79	1.72	-.82	322.68	1009.63	343.82	11.47	12.91
U26	THERMOCOUPLE	14	TU26	2.48	46.2	-.82	1.79	-.82	1.79	1.72	-.82	322.68	1009.63	343.82	11.47	12.91
U27	USBM	240	U27A	2.93	90.9	-.83	2.00	-.83	2.00	-.03	-.83	321.65	1008.20	343.83	7.85	8.83
U27	USBM	241	U27B	2.00	90.9	-.83	2.00	-.83	2.00	-.03	-.83	321.65	1008.20	343.83	7.85	8.83
U27	USBM	242	U27C	2.00	90.9	-.83	2.00	-.83	2.00	-.03	-.83	321.65	1008.20	343.83	7.85	8.83
U27	THERMOCOUPLE	15	TU27	2.00	90.9	-.83	2.00	-.83	2.00	-.03	-.83	321.65	1008.20	343.83	7.85	8.83
U28	USBM	243	U28A	2.99	135.3	-.84	2.10	-.84	2.10	-2.13	-.84	320.54	1006.42	343.84	11.27	13.24

Table A-3 (continued)
 SENSOR LOCATIONS FOR EXPERIMENT 1, FULL SCALE HEATER H9

HOLE ID	SENSOR TYPE	SENSOR NUMBER	SENSOR LABEL	CYLINDRICAL COORDINATES	LOCAL X	RECTANGULAR Y	RECTANGULAR Z	MINE X	RECTANGULAR Y	RECTANGULAR Z	DEPTH	HOLE LENGTH
U28	JSBM	244	U28B	2.99 135.3 -0.84	2.10	-2.13	-0.84	320.54	1006.42	343.84	11.27	13.24
U28	JSBM	245	U28C	2.99 135.3 -0.84	2.10	-2.13	-0.84	320.54	1006.42	343.84	11.27	13.24
U28	THERMOCOUPLE	16	TU28	2.99 135.3 -0.84	2.10	-2.13	-0.84	320.54	1006.42	343.84	11.27	13.24

Table A-3 (continued)

SENSOR LOCATIONS FOR EXPERIMENT 2, FULL SCALE HEATER H10

HOLE ID	SENSOR TYPE	SENSOR NUMBER	SENSOR LABEL	CYLINDRICAL COORDINATES	LOCAL X	RECTANGULAR Y	RECTANGULAR Z	MINE X	RECTANGULAR Y	RECTANGULAR Z	DEPTH	HOLE LENGTH
				PHO THETA Z	X	Y	Z	X	Y	Z		
H16	THERMOCOUPLE	563	TH16A	.90 247.6 -1.22	-.83	-.34	-1.22	313.27	987.32	344.22	5.13	6.17
H16	THERMOCOUPLE	564	TH16B	.90 247.6 0.61	-.83	-.34	0.61	313.27	987.32	342.39	3.30	6.17
H16	THERMOCOUPLE	565	TH16C	.90 247.6 2.34	-.83	-.34	2.34	313.27	987.32	340.66	1.57	6.17
H17	HEATER CURRENT	618	IH17									
H17	HEATER VOLTAGE	619	VH17									
H17	HEATER POWER	620	PH17									
H17	THERMOCOUPLE	566	TH17A	.90 252.8 -1.22	-.83	.35	-1.22	313.61	987.93	344.22	5.27	6.32
H17	THERMOCOUPLE	567	TH17B	.90 292.8 0.61	-.83	.35	0.61	313.61	987.93	342.39	3.44	6.32
H17	THERMOCOUPLE	568	TH17C	.90 292.8 2.34	-.83	.35	2.34	313.61	987.93	340.67	1.72	6.32
H18	HEATER CURRENT	621	IH18									
H18	HEATER VOLTAGE	622	VH18									
H18	HEATER POWER	623	PH18									
H18	THERMOCOUPLE	569	TH18A	.91 337.6 -1.22	-.34	.84	-1.22	313.42	988.59	344.22	5.31	6.39
H18	THERMOCOUPLE	570	TH18B	.91 337.6 0.61	-.34	.84	0.61	313.42	988.59	342.39	3.48	6.39
H18	THERMOCOUPLE	571	TH18C	.91 337.6 2.34	-.34	.84	2.34	313.42	988.59	340.66	1.75	6.39
H19	THERMOCOUPLE	510	TI19A	.40 0 3.00	.00	.40	3.00	312.91	988.37	340.00	1.10	7.47
H19	THERMOCOUPLE	511	TI19B	.40 0 1.50	.00	.40	1.50	312.91	988.37	341.50	2.60	7.47
H19	THERMOCOUPLE	512	TI19C	.40 0 -0.00	-.00	.40	-0.00	312.91	988.38	343.00	4.10	7.47
H19	THERMOCOUPLE	513	TI19D	.40 0 -1.50	-.00	.40	-1.50	312.91	988.38	344.50	5.60	7.47
H19	THERMOCOUPLE	514	TI19E	.41 0 -3.00	-.00	.41	-3.00	312.91	988.38	346.00	7.10	7.47
T20	THERMOCOUPLE	515	T20A	.91 0 3.00	-.00	.91	3.00	313.16	988.82	340.00	1.22	7.58
T20	THERMOCOUPLE	516	T20B	.91 0 1.50	-.00	.91	1.50	313.16	988.82	341.50	2.72	7.58
T20	THERMOCOUPLE	517	T20C	.91 0 -0.00	-.00	.91	-0.00	313.17	988.82	343.00	4.22	7.58
T20	THERMOCOUPLE	518	T20D	.92 0 -1.50	-.02	.92	-1.50	313.18	988.82	344.50	5.72	7.58
T20	THERMOCOUPLE	519	T20E	.92 358.7 -3.00	-.02	.92	-3.00	313.18	988.82	346.00	7.22	7.58
T21	THERMOCOUPLE	520	T21A	.70 44.7 3.00	.49	.50	3.00	312.53	988.70	340.00	1.21	7.69
T21	THERMOCOUPLE	521	T21B	.70 44.5 1.50	.49	.50	1.50	312.53	988.70	341.50	2.71	7.69
T21	THERMOCOUPLE	522	T21C	.69 44.2 0.00	.48	.50	.00	312.53	988.70	343.00	4.21	7.69
T21	THERMOCOUPLE	523	T21D	.69 44.0 -1.50	.48	.50	-1.50	312.54	988.69	344.50	5.71	7.69
T21	THERMOCOUPLE	524	T21E	.69 43.8 -3.00	.48	.50	-3.00	312.54	988.69	346.00	7.21	7.69
T22	THERMOCOUPLE	525	T22A	.50 179.8 3.00	.00	-.50	3.00	312.47	987.59	340.00	1.03	7.40
T22	THERMOCOUPLE	526	T22B	.50 179.3 1.50	.01	-.50	1.50	312.47	987.60	341.50	2.53	7.40
T22	THERMOCOUPLE	527	T22C	.50 178.7 0.00	.01	-.50	.00	312.46	987.60	343.00	4.03	7.40
T22	THERMOCOUPLE	528	T22D	.49 178.1 -1.50	.02	-.49	-1.50	312.46	987.60	344.50	5.53	7.40
T22	THERMOCOUPLE	529	T22E	.49 177.6 -3.00	.02	-.49	-3.00	312.46	987.61	346.00	7.03	7.40
T23	THERMOCOUPLE	530	T23A	.79 224.8 3.00	-.56	-.56	3.00	312.93	987.26	340.00	1.01	7.38
T23	THERMOCOUPLE	531	T23B	.79 224.5 1.50	-.55	-.56	1.50	312.92	987.27	341.50	2.51	7.38
T23	THERMOCOUPLE	532	T23C	.78 224.3 -0.00	-.55	-.56	-.00	312.92	987.27	343.00	4.01	7.38
T23	THERMOCOUPLE	533	T23D	.78 224.1 -1.50	-.54	-.56	-1.50	312.92	987.27	344.50	5.51	7.38
T23	THERMOCOUPLE	534	T23E	.78 223.9 -3.00	-.54	-.56	-3.00	312.91	987.27	346.00	7.01	7.38
T24	THERMOCOUPLE	535	T24A	.60 315.2 3.00	-.43	.43	3.00	313.30	988.19	340.00	.98	7.38
T24	THERMOCOUPLE	536	T24B	.61 315.4 1.50	-.43	.44	1.50	313.30	988.20	341.50	2.48	7.38
T24	THERMOCOUPLE	537	T24C	.62 315.6 0.00	-.43	.44	.00	313.31	988.20	343.00	3.98	7.38
T24	THERMOCOUPLE	538	T24D	.62 315.7 -1.50	-.44	.45	-1.50	313.31	988.20	344.50	5.48	7.38
T24	THERMOCOUPLE	539	T24E	.63 315.9 -3.00	-.44	.45	-3.00	313.32	988.21	346.00	6.98	7.38
E12	EXTENSOMETER	804	E12A	2.00 0 2.24	.01	2.00	2.24	313.68	989.77	340.76	1.97	12.58
E12	EXTENSOMETER	801	E12B	1.99 0 -0.07	.01	1.99	-.07	313.68	989.77	342.07	4.28	12.58
E12	EXTENSOMETER	802	E12C	1.98 0 -2.24	.01	1.98	-2.24	313.68	989.76	345.24	6.45	12.58
E12	EXTENSOMETER	803	E12D	1.97 0 -7.39	.01	1.97	-7.39	313.67	989.74	350.39	11.60	12.58
E12	THERMOCOUPLE	442	TE12A	2.00 0 2.36	.01	2.00	2.36	313.68	989.77	340.64	1.85	12.58
E12	THERMOCOUPLE	443	TE12B	1.99 0 .11	.01	1.99	.11	313.68	989.77	342.89	4.10	12.58
E12	THERMOCOUPLE	444	TE12C	1.98 0 -.89	.01	1.99	-.89	313.68	989.76	343.89	5.10	12.58
E12	THERMOCOUPLE	445	TE12D	1.98 0 -2.14	.01	1.99	-2.14	313.68	989.76	345.14	6.35	12.58
E12	THERMOCOUPLE	573	TE12E	2.00 0 4.21	.01	2.00	4.21	313.69	989.78	338.79	0.	12.58

Table A-3 (continued)

SENSOR LOCATIONS FOR EXPERIMENT 2, FULL SCALE HEATER H10												
HOLE ID	SENSOR TYPE	SENSOR NUMBER	SENSOR LABEL	CYLINDRICAL COORDINATES	LOCAL X	RECTANGULAR Y	RECTANGULAR Z	MINE X	RECTANGULAR Y	RECTANGULAR Z	DEPTH	HOLE LENGTH
				RHO THETA Z	X	Y	Z	X	Y	Z		
H10	HEATER CURRENT	624	IH10A	0.	0.	0.	-0.05	312.72	988.03	343.50	4.55	5.43
H10	HEATER VOLTAGE	625	VH10A	0.	0.	0.	-0.05	312.72	988.03	343.50	4.55	5.43
H10	HEATER POWER	626	PH10A	.03	.00	.00	.10	312.72	988.03	342.90	3.95	5.43
H10	HEATER CURRENT	627	IH10B	.00	.00	.00	.10	312.72	988.03	342.90	3.95	5.43
H10	HEATER VOLTAGE	628	VH10B	.00	.00	.00	.10	312.72	988.03	342.90	3.95	5.43
H10	HEATER POWER	629	PH10B	.00	.00	.00	.70	312.72	988.03	342.30	3.35	5.43
H10	HEATER CURRENT	630	IH10C	.00	.00	.00	.70	312.72	988.03	342.30	3.35	5.43
H10	HEATER VOLTAGE	631	VH10C	.00	.00	.00	.70	312.72	988.03	342.30	3.35	5.43
H10	HEATER POWER	632	PH10C	.00	.00	.00	.70	312.72	988.03	342.30	3.35	5.43
H10	HEATER CURRENT	633	IH10D	.00	.00	.00	2.44	312.71	988.03	340.56	1.61	5.43
H10	HEATER VOLTAGE	634	VH10D	.00	.00	.00	2.44	312.71	988.03	340.56	1.61	5.43
H10	HEATER POWER	635	PH10D	.00	.00	.00	2.44	312.71	988.03	340.56	1.61	5.43
H10	HEATER CURRENT	636	PH10E	.00	.00	.00	2.44	312.71	988.03	340.56	1.61	5.43
H10	THERMOCOUPLE	540	TH10A	0.	0.	0.	-0.50	312.72	988.03	343.50	4.55	5.43
H10	THERMOCOUPLE	541	TH10B	0.	0.	0.	-0.50	312.72	988.03	343.50	4.55	5.43
H10	THERMOCOUPLE	542	TH10C	.03	.00	.00	.10	312.72	988.03	342.90	3.95	5.43
H10	THERMOCOUPLE	543	TH10D	.00	.00	.00	.10	312.72	988.03	342.90	3.95	5.43
H10	THERMOCOUPLE	544	TH10E	.00	.00	.00	.70	312.72	988.03	342.30	3.35	5.43
H10	THERMOCOUPLE	545	TH10F	.00	.00	.00	.70	312.72	988.03	342.30	3.35	5.43
H10	THERMOCOUPLE	546	TH10G	.00	.00	.00	2.44	312.71	988.03	340.56	1.61	5.43
H10	THERMOCOUPLE	547	TH10H	.00	.00	.00	2.44	312.71	988.03	340.56	1.61	5.43
H11	HEATER CURRENT	600	IH11	0.	0.	0.	0.	312.72	988.03	343.50	4.55	5.43
H11	HEATER VOLTAGE	601	VH11	0.	0.	0.	0.	312.72	988.03	343.50	4.55	5.43
H11	HEATER POWER	602	PH11	.91	22.8	-1.22	-1.22	312.82	588.93	344.22	5.42	6.49
H11	THERMOCOUPLE	548	TH11A	.91	22.8	0.61	0.61	312.82	588.93	342.39	3.59	6.49
H11	THERMOCOUPLE	549	TH11B	.91	22.8	0.61	0.61	312.82	588.93	342.39	3.59	6.49
H11	THERMOCOUPLE	550	TH11C	.91	22.8	2.34	2.34	312.82	588.93	340.66	1.86	6.49
H12	HEATER CURRENT	603	IH12	0.	0.	0.	0.	312.72	988.03	343.50	4.55	5.43
H12	HEATER VOLTAGE	604	VH12	0.	0.	0.	0.	312.72	988.03	343.50	4.55	5.43
H12	HEATER POWER	605	PH12	.91	67.4	-1.22	-1.22	312.15	988.74	344.31	5.55	6.55
H12	THERMOCOUPLE	551	TH12A	.91	67.4	0.61	0.61	312.15	988.74	342.39	3.63	6.55
H12	THERMOCOUPLE	552	TH12B	.91	67.4	0.61	0.61	312.15	988.74	342.39	3.63	6.55
H12	THERMOCOUPLE	553	TH12C	.91	67.4	2.34	2.34	312.15	988.74	340.66	1.90	6.55
H13	HEATER CURRENT	606	IH13	0.	0.	0.	0.	312.72	988.03	343.50	4.55	5.43
H13	HEATER VOLTAGE	607	VH13	0.	0.	0.	0.	312.72	988.03	343.50	4.55	5.43
H13	HEATER POWER	608	PH13	.91	112.0	-1.22	-1.22	311.82	988.14	344.22	5.31	6.37
H13	THERMOCOUPLE	554	TH13A	.91	112.0	0.61	0.61	311.82	988.14	342.40	3.49	6.37
H13	THERMOCOUPLE	555	TH13B	.91	112.0	0.61	0.61	311.82	988.14	342.40	3.49	6.37
H13	THERMOCOUPLE	556	TH13C	.91	112.0	2.34	2.34	311.82	988.14	340.67	1.76	6.37
H14	HEATER CURRENT	609	IH14	0.	0.	0.	0.	312.72	988.03	343.50	4.55	5.43
H14	HEATER VOLTAGE	610	VH14	0.	0.	0.	0.	312.72	988.03	343.50	4.55	5.43
H14	HEATER POWER	611	PH14	.90	157.2	-1.22	-1.22	312.01	987.47	344.22	5.35	6.42
H14	THERMOCOUPLE	557	TH14A	.90	157.2	0.61	0.61	312.01	987.47	342.39	3.52	6.42
H14	THERMOCOUPLE	558	TH14B	.90	157.2	0.61	0.61	312.01	987.47	342.39	3.52	6.42
H14	THERMOCOUPLE	559	TH14C	.90	157.2	2.34	2.34	312.01	987.47	340.66	1.79	6.42
H15	HEATER CURRENT	612	IH15	0.	0.	0.	0.	312.72	988.03	343.50	4.55	5.43
H15	HEATER VOLTAGE	613	VH15	0.	0.	0.	0.	312.72	988.03	343.50	4.55	5.43
H15	HEATER POWER	614	PH15	.89	202.5	-1.22	-1.22	312.61	987.14	344.22	5.34	6.37
H15	THERMOCOUPLE	560	TH15A	.89	202.5	0.61	0.61	312.61	987.14	342.39	3.51	6.37
H15	THERMOCOUPLE	561	TH15B	.89	202.5	0.61	0.61	312.61	987.14	342.39	3.51	6.37
H15	THERMOCOUPLE	562	TH15C	.89	202.5	2.34	2.34	312.61	987.14	340.66	1.78	6.37
H16	HEATER CURRENT	615	IH16	0.	0.	0.	0.	312.72	988.03	343.50	4.55	5.43
H16	HEATER VOLTAGE	616	VH16	0.	0.	0.	0.	312.72	988.03	343.50	4.55	5.43
H16	HEATER POWER	617	PH16	.89	202.5	-1.22	-1.22	312.61	987.14	344.22	5.34	6.37

Table A-3 (continued)
 SENSOCK LOCATIONS FOR EXPERIMENT 2, FULL SCALE HEATER H10

HOLE ID	SENSOR TYPE	SENSOR NUMBER	SENSOR LABEL	CYLINDRICAL COORDINATES	LOCAL	RECTANGULAR	MINE	RECTANGULAR	DEPTH	HOLE LENGTH
				RHO THETA Z	X	Y Z	X	Y Z		
E12	THERMOCOUPLE	163	RF457	1.96 0. -7.39	.00	1.96 -7.39	313.67	989.74 350.39	11.60	12.58
E13	EXTENSOMETER	805	E13A	3.00 J. 2.23	.01	3.00 2.23	314.17	990.65 340.77	1.87	12.30
E13	EXTENSOMETER	806	E13B	3.00 0. -0.2	.01	3.00 -0.2	314.17	990.65 343.02	4.12	12.30
E13	EXTENSOMETER	807	E13C	3.00 0. -2.27	.00	3.00 -2.27	314.17	990.65 345.27	6.37	12.30
E13	EXTENSOMETER	808	E13D	3.00 0. -7.52	.00	3.00 -7.52	314.17	990.65 350.52	11.62	12.30
E13	THERMOCOUPLE	446	TE13A	3.00 0. -1.02	.01	3.00 -1.02	314.17	990.65 344.02	5.12	12.30
E13	THERMOCOUPLE	447	TE13B	3.00 J. -2.27	.00	3.00 -2.27	314.17	990.65 345.27	6.37	12.30
E13	THERMOCOUPLE	448	TE13C	3.00 0. -4.90	.00	3.00 -4.90	314.17	990.65 347.90	9.00	12.30
E13	THERMOCOUPLE	449	TE13D	3.00 0. -7.52	.00	3.00 -7.52	314.17	990.65 350.52	11.62	12.30
E13	THERMOCOUPLE	137	RF573	3.00 0. 4.10	.01	3.00 4.10	314.17	990.65 338.90	0.	12.30
E13	THERMOCOUPLE	126	TE13F	3.00 J. -0.02	.00	3.00 -0.02	314.17	990.65 343.02	4.12	12.30
E13	THERMOCOUPLE	127	TE13G	3.00 J. 2.23	.01	3.00 2.23	314.17	990.65 340.77	1.87	12.30
E14	EXTENSOMETER	809	E14A	2.50 179.8 2.26	.01	-2.50 2.26	311.49	985.85 340.74	1.92	12.57
E14	EXTENSOMETER	810	E14B	2.50 179.8 -0.0	.01	-2.50 -0.0	311.49	985.85 343.00	4.18	12.57
E14	EXTENSOMETER	811	E14C	2.50 179.8 -2.29	.01	-2.50 -2.29	311.49	985.85 345.29	6.47	12.57
E14	EXTENSOMETER	812	E14D	2.50 179.7 -7.47	.01	-2.50 -7.47	311.49	985.85 350.47	11.65	12.57
E14	THERMOCOUPLE	451	TE14A	2.50 179.8 2.28	.01	-2.50 2.28	311.49	985.85 340.72	1.90	12.57
E14	THERMOCOUPLE	452	TE14C	2.50 179.8 -2.22	.01	-2.50 -2.22	311.49	985.85 345.22	6.40	12.57
E14	THERMOCOUPLE	453	TE14D	2.50 179.7 -7.47	.01	-2.50 -7.47	311.49	985.85 350.47	11.65	12.57
E14	THERMOCOUPLE	138	RF573	2.50 179.8 4.18	.01	-2.50 4.18	311.49	985.85 338.82	0.	12.57
E15	EXTENSOMETER	813	E15A	1.99 270.2 2.25	-1.99	.01 2.25	314.46	987.06 340.75	1.77	12.38
E15	EXTENSOMETER	816	E15B	1.99 270.3 .01	-1.99	.01 .01	314.46	987.07 342.99	4.01	12.38
E15	EXTENSOMETER	815	E15C	1.99 270.4 -2.26	-1.99	.01 -2.26	314.46	987.07 345.26	6.28	12.38
E15	EXTENSOMETER	814	E15D	1.99 270.6 -7.50	-1.98	.02 -7.50	314.46	987.08 350.50	11.52	12.38
E15	THERMOCOUPLE	454	TE15A	1.99 270.2 2.25	-1.99	.01 2.25	314.46	987.06 340.75	1.77	12.38
E15	THERMOCOUPLE	455	TE15B	1.99 270.3 0.	-1.99	.01 0.	314.46	987.07 343.00	4.02	12.38
E15	THERMOCOUPLE	456	TE15C	1.99 270.4 -2.25	-1.99	.01 -2.25	314.46	987.07 345.25	6.27	12.38
E15	THERMOCOUPLE	457	TE15D	1.98 270.6 -7.50	-1.98	.02 -7.50	314.46	987.08 350.50	11.52	12.38
E15	THERMOCOUPLE	139	RF573	1.99 270.1 4.02	-1.99	.00 4.02	314.46	987.06 338.98	0.	12.38
E16	EXTENSOMETER	817	E16A	1.50 315.4 2.27	-1.05	1.07 2.27	314.15	988.44 340.73	1.81	12.47
E16	EXTENSOMETER	818	E16B	1.50 315.4 .02	-1.05	1.07 .02	314.15	988.44 342.98	4.06	12.47
E16	EXTENSOMETER	819	E16C	1.50 315.5 -2.23	-1.05	1.07 -2.23	314.16	988.45 345.23	6.31	12.47
E16	EXTENSOMETER	820	E16D	1.51 315.6 -7.46	-1.06	1.08 -7.46	314.16	988.45 350.46	11.54	12.47
E16	THERMOCOUPLE	458	TE16A	1.50 315.4 2.29	-1.05	1.07 2.29	314.15	988.44 340.71	1.79	12.47
E16	THERMOCOUPLE	459	TE16B	1.50 315.4 .04	-1.05	1.07 .04	314.16	988.45 342.96	4.04	12.47
E16	THERMOCOUPLE	460	TE16C	1.50 315.4 -2.13	-1.05	1.07 -2.13	314.16	988.45 345.13	5.04	12.47
E16	THERMOCOUPLE	461	TE16D	1.50 315.5 4.08	-1.05	1.07 4.08	314.16	988.45 350.46	6.21	12.47
E16	THERMOCOUPLE	140	RF573	1.51 315.3 -7.46	-1.05	1.06 -7.46	314.15	988.44 338.92	0.	12.47
E16	THERMOCOUPLE	162	RF457	1.51 315.6 2.22	-1.06	1.08 2.22	314.16	988.45 350.46	11.54	12.47
E17	EXTENSOMETER	821	E17A	2.50 315.2 2.22	-1.76	1.77 2.22	315.11	988.72 340.78	1.93	12.55
E17	EXTENSOMETER	822	E17B	2.50 315.3 .08	-1.76	1.78 .08	315.12	988.72 342.92	4.07	12.55
E17	EXTENSOMETER	823	E17C	2.50 315.5 -2.27	-1.75	1.78 -2.27	315.12	988.73 345.27	6.42	12.55
E17	EXTENSOMETER	824	E17D	2.51 315.8 -7.50	-1.75	1.80 -7.50	315.12	988.74 350.50	11.65	12.55
E17	THERMOCOUPLE	462	TE17A	2.50 315.2 2.25	-1.76	1.77 2.25	315.11	988.72 340.75	1.90	12.55
E17	THERMOCOUPLE	463	TE17B	2.50 315.3 -0.0	-1.76	1.78 -0.0	315.12	988.72 343.00	4.15	12.55
E17	THERMOCOUPLE	464	TE17C	2.50 315.4 -2.25	-1.75	1.78 -2.25	315.12	988.73 345.25	5.15	12.55
E17	THERMOCOUPLE	141	RF573	2.50 315.1 4.15	-1.76	1.77 4.15	315.11	988.71 338.85	0.	12.55
E17	THERMOCOUPLE	164	RF457	2.51 315.7 -7.50	-1.75	1.79 -7.50	315.12	988.74 350.50	11.65	12.55
E27	EXTENSOMETER	828	E27A	1.47 89.4 1.96	1.47	.02 1.96	311.44	988.75 341.04	8.64	9.08
E27	EXTENSOMETER	827	E27B	2.98 89.7 1.81	2.98	.01 1.81	310.12	989.49 341.19	7.12	9.08
E27	EXTENSOMETER	826	E27C	4.23 89.8 1.68	4.23	.01 1.68	309.02	990.10 341.32	5.86	9.08
E27	EXTENSOMETER	825	E27D	6.97 89.9 1.41	6.97	.01 1.41	306.63	991.42 341.59	3.11	9.08

Table A-3 (continued)

SENSOR LOCATIONS FOR EXPERIMENT 2, FULL SCALE HEATER H10

HOLE ID	SENSOR TYPE	SENSOR NUMBER	SENSOR LABEL	RHC	CYLINDRICAL COORDINATES	LOCAL X	RECTANGULAR Y	RECTANGULAR Z	MINE X	RECTANGULAR Y	RECTANGULAR Z	DEPTH	HOLE LENGTH
				THETA	Z	X	Y	Z	X	Y	Z		
E27	THERMOCOUPLE	469	TE27A	1.47	89.4	1.96	1.47	1.96	311.44	588.75	341.04	8.64	9.08
E27	THERMOCOUPLE	468	TE27B	2.96	89.7	1.81	2.96	1.81	310.14	989.48	341.19	7.14	9.08
E27	THERMOCOUPLE	467	TE27C	4.20	89.8	1.69	4.20	1.69	309.05	990.08	341.31	5.89	9.08
E27	THERMOCOUPLE	466	TE27D	7.93	90.0	1.31	7.93	1.31	305.79	951.89	341.69	2.14	9.08
E27	THERMOCOUPLE	151	RF572	10.06	90.0	1.10	10.06	1.10	303.93	952.93	341.90	0.	9.08
E28	EXTENSOMETER	832	E28A	1.22	88.9	.06	1.22	.06	311.66	988.64	342.94	8.44	8.62
E28	EXTENSOMETER	831	E28B	2.46	89.5	-.01	2.46	-.01	310.58	989.24	343.01	7.20	8.62
E28	EXTENSOMETER	830	E28C	3.46	89.7	-.06	3.46	-.06	309.70	989.72	343.06	6.20	8.62
E28	EXTENSOMETER	829	E28D	4.95	89.8	-.14	4.95	-.14	308.40	990.44	343.14	4.71	8.62
E28	THERMOCOUPLE	473	TE28A	1.22	88.9	.06	1.22	.06	311.66	988.64	342.94	8.44	8.62
E28	THERMOCOUPLE	472	TE28B	2.47	89.6	-.01	2.47	-.01	310.57	989.24	343.01	7.19	8.62
E28	THERMOCOUPLE	471	TE28C	3.47	89.7	-.06	3.47	-.06	309.70	989.73	343.06	6.19	8.62
E28	THERMOCOUPLE	470	TE28D	4.96	89.9	-.14	4.96	-.14	308.39	950.45	343.14	4.69	8.62
E28	THERMOCOUPLE	152	RF572	9.65	90.0	-.38	9.65	-.38	304.29	992.72	343.38	0.	8.62
E29	EXTENSOMETER	836	E29A	1.01	271.8	-1.85	-1.01	.03	313.61	987.56	344.85	10.64	11.02
E29	EXTENSOMETER	835	E29B	.99	88.5	-1.91	.99	.03	311.86	988.53	344.91	8.64	11.02
E29	EXTENSOMETER	834	E29C	2.00	89.3	-1.93	2.00	.02	310.98	989.02	344.93	7.63	11.02
E29	EXTENSOMETER	833	E29D	6.03	89.9	-2.04	6.03	.01	307.48	990.96	345.04	3.63	11.02
E29	THERMOCOUPLE	477	TE29A	.03	271.8	-1.88	-.01	.03	312.74	988.04	344.88	9.64	11.02
E29	THERMOCOUPLE	476	TE29B	.99	88.5	-1.91	.99	.03	311.86	988.53	344.91	8.64	11.02
E29	THERMOCOUPLE	475	TE29C	1.99	89.3	-1.93	1.99	.02	310.99	989.01	344.93	7.64	11.02
E29	THERMOCOUPLE	474	TE29D	5.99	87.9	-2.04	5.99	.01	307.49	950.95	345.04	3.64	11.02
E29	THERMOCOUPLE	153	RF572	9.63	89.9	-2.14	9.63	.01	304.31	992.72	345.14	0.	11.02
E30	EXTENSOMETER	840	E30A	1.61	45.7	2.03	1.15	1.12	312.26	989.57	340.97	12.69	13.23
E30	EXTENSOMETER	839	E30B	3.13	45.3	1.92	2.22	2.20	311.84	991.03	341.08	11.17	13.23
E30	EXTENSOMETER	838	E30C	4.35	45.2	1.83	3.09	3.07	311.51	992.21	341.17	9.94	13.23
E30	EXTENSOMETER	837	E30D	7.12	45.1	1.63	5.04	5.02	310.76	994.87	341.38	7.17	13.23
E30	THERMOCOUPLE	481	TE30A	1.61	45.7	2.03	1.15	1.12	312.26	989.57	340.97	12.69	13.23
E30	THERMOCOUPLE	480	TE30B	3.11	45.3	1.92	2.21	2.18	311.85	991.01	341.08	11.19	13.23
E30	THERMOCOUPLE	479	TE30C	4.35	45.2	1.83	3.09	3.07	311.51	992.21	341.17	9.94	13.23
E30	THERMOCOUPLE	478	TE30D	8.09	45.1	1.55	5.73	5.71	310.49	995.81	341.45	6.19	13.23
E30	THERMOCOUPLE	154	RF572	14.27	45.0	1.09	10.08	10.09	308.81	1001.75	341.91	0.	13.23
E31	EXTENSOMETER	843	E31A	1.23	45.4	.11	.87	.86	312.37	989.20	342.89	12.97	13.13
E31	EXTENSOMETER	842	E31B	2.24	45.2	.07	1.59	1.58	312.09	990.18	342.93	11.95	13.13
E31	EXTENSOMETER	844	E31C	3.45	45.1	.02	2.45	2.44	311.76	991.34	342.98	10.74	13.13
E31	EXTENSOMETER	841	E31D	4.98	45.1	-.04	3.53	3.52	311.35	992.82	343.04	9.21	13.13
E31	THERMOCOUPLE	485	TE31A	1.23	45.4	.11	.87	.86	312.37	989.20	342.89	12.97	13.13
E31	THERMOCOUPLE	484	TE31B	2.47	45.2	.06	1.76	1.74	312.03	990.40	342.94	11.72	13.13
E31	THERMOCOUPLE	483	TE31C	3.47	45.1	.02	2.46	2.45	311.76	991.36	342.98	10.72	13.13
E31	THERMOCOUPLE	482	TE31D	4.97	45.1	-.04	3.52	3.51	311.35	992.81	343.04	9.22	13.13
E31	THERMOCOUPLE	572	TE31E	14.18	45.0	-.40	10.03	10.03	308.83	1001.67	343.40	0.	13.13
E32	EXTENSOMETER	848	E32A	1.15	44.3	-1.87	.81	.83	312.41	989.14	344.87	12.96	13.11
E32	EXTENSOMETER	847	E32B	2.04	44.6	-1.89	1.44	1.46	312.17	989.99	344.89	12.07	13.11
E32	EXTENSOMETER	846	E32C	3.02	44.8	-1.91	2.13	2.15	311.90	990.94	344.91	11.09	13.11
E32	EXTENSOMETER	845	E32D	6.00	44.9	-1.97	4.24	4.25	311.08	993.80	344.98	8.11	13.11
E32	THERMOCOUPLE	489	TE32A	1.15	44.3	-1.87	.81	.83	312.41	989.14	344.87	12.96	13.11
E32	THERMOCOUPLE	488	TE32B	2.15	44.7	-1.89	1.51	1.53	312.14	990.10	344.89	11.96	13.11
E32	THERMOCOUPLE	487	TE32C	3.15	44.8	-1.91	2.22	2.24	311.86	991.06	344.91	10.96	13.11
E32	THERMOCOUPLE	486	TE32D	6.15	44.9	-1.98	4.35	4.36	311.04	993.95	344.98	7.96	13.11
E32	THERMOCOUPLE	156	RF572	14.11	45.0	-2.15	9.97	9.98	308.85	1001.60	345.15	0.	13.11
E33	EXTENSOMETER	852	E33A	1.48	131.1	2.04	1.12	-.97	311.27	987.72	340.96	12.90	13.36
E33	EXTENSOMETER	851	E33B	2.99	133.3	1.93	2.17	-2.05	309.82	987.29	341.07	11.39	13.36
E33	EXTENSOMETER	850	E33C	4.24	133.9	1.83	3.06	-2.94	308.61	986.94	341.17	10.13	13.36
E33	EXTENSOMETER	849	E33D	7.03	134.5	1.63	5.02	-4.93	305.93	986.16	341.37	7.33	13.36

Table A-3 (continued)
 SENSOR LOCATIONS FOR EXPERIMENT 2, FULL SCALE HEATER H10

HOLE ID	SENSOR TYPE	SENSOR NUMBER	SENSOR LABEL	CYLINDRICAL COORDINATES	LOCAL X	RECTANGULAR Y	RECTANGULAR Z	MINE X	RECTANGULAR Y	RECTANGULAR Z	DEPTH	HOLE LENGTH
				RHO THETA Z	X	Y	Z	X	Y	Z		
E33	THERMOCOUPLE	493	TE33A	1.48 131.1 2.04	1.12	-0.97	2.04	311.27	987.72	340.96	12.90	13.36
E33	THERMOCOUPLE	492	TE33B	2.98 133.3 1.93	2.17	-2.04	1.93	309.83	987.30	341.07	11.40	13.36
E33	THERMOCOUPLE	491	TE33C	4.22 133.9 1.83	3.04	-2.93	1.83	308.63	986.95	341.17	10.15	13.36
E33	THERMOCOUPLE	157	RF572	7.96 134.6 1.56	5.67	-5.59	1.56	305.04	985.90	341.44	6.40	13.36
E34	EXTENSOMETER	856	E34A	14.34 134.9 1.09	10.16	-10.13	1.09	298.92	984.11	341.91	0.	13.36
E34	EXTENSOMETER	855	E34B	1.23 131.7 1.0	.92	-0.82	1.0	311.51	987.76	342.90	12.83	13.02
E34	EXTENSOMETER	854	E34C	2.49 133.5 0.05	1.81	-1.72	0.05	310.30	987.41	342.95	11.57	13.02
E34	EXTENSOMETER	853	E34D	3.53 134.0 0.01	2.54	-2.45	0.01	309.30	987.12	342.99	10.53	13.02
E34	THERMOCOUPLE	497	TE34A	5.02 134.4 -0.05	3.59	-3.51	-0.05	307.87	986.70	343.05	9.04	13.02
E34	THERMOCOUPLE	496	TE34B	1.23 131.7 1.0	.92	-0.82	1.0	311.51	987.76	342.90	12.83	13.02
E34	THERMOCOUPLE	495	TE34C	2.48 133.5 0.05	1.80	-1.71	0.05	310.31	987.41	342.95	11.58	13.02
E34	THERMOCOUPLE	494	TE34D	3.48 134.0 0.02	2.50	-2.42	0.02	309.35	987.13	342.99	10.58	13.02
E34	THERMOCOUPLE	158	RF572	4.58 134.4 -0.04	3.56	-3.48	-0.04	307.91	986.71	343.04	9.08	13.02
E35	EXTENSOMETER	860	E35A	14.05 134.9 -0.39	9.95	-9.93	-0.39	299.20	984.19	343.39	0.	13.02
E35	EXTENSOMETER	859	E35B	1.10 131.0 1.87	1.83	-1.72	1.87	311.64	987.80	344.87	12.62	12.70
E35	EXTENSOMETER	858	E35C	2.05 133.0 -1.89	1.50	-1.40	-1.89	310.72	987.53	344.89	11.67	12.70
E35	EXTENSOMETER	857	E35D	3.05 133.8 -1.91	2.20	-2.11	-1.91	309.76	987.25	344.91	10.67	12.70
E35	THERMOCOUPLE	501	TE35A	6.02 134.5 -1.97	4.29	-4.22	-1.97	306.91	986.43	344.97	7.70	12.70
E35	THERMOCOUPLE	500	TE35B	1.10 131.0 -1.87	.83	-0.72	-1.87	311.64	987.80	344.87	12.62	12.70
E35	THERMOCOUPLE	499	TE35C	2.10 133.0 -1.89	1.54	-1.43	-1.89	310.68	987.52	344.89	11.62	12.70
E35	THERMOCOUPLE	498	TE35D	3.10 133.8 -1.91	2.24	-2.14	-1.91	309.72	987.24	344.91	10.62	12.70
E35	THERMOCOUPLE	159	RF572	6.10 134.5 -1.97	4.35	-4.28	-1.97	306.84	986.41	344.98	7.62	12.70
U15	IRAD GAGE	861	C3A	13.72 134.9 -2.14	9.71	-9.69	-2.14	299.52	984.28	345.14	0.	12.70
U15	IRAD GAGE	862	C3B	1.71 225.6 -0.65	-1.22	-1.20	-0.65	313.20	986.38	343.65	4.73	6.92
U15	THERMOCOUPLE	502	TC3	1.71 225.6 -0.65	-1.22	-1.20	-0.65	313.20	986.38	343.65	4.73	6.92
U17	IRAD GAGE	863	C4A	2.46 252.7 -0.65	-2.27	-2.20	-0.65	313.20	986.38	343.65	4.73	6.92
U17	THERMOCOUPLE	503	TC4	2.46 252.7 -0.65	-2.27	-2.20	-0.65	313.20	986.38	343.65	4.73	6.92
C5	IRAD GAGE	865	C5A	1.51 247.9 0.85	-1.39	-0.57	0.85	315.16	987.75	343.65	4.89	7.13
C5	IRAD GAGE	866	C5B	1.51 247.9 0.85	-1.39	-0.57	0.85	315.16	987.75	343.65	4.89	7.13
C5	THERMOCOUPLE	504	TC5	1.51 247.9 0.85	-1.39	-0.57	0.85	315.16	987.75	343.65	4.89	7.13
C10	IRAD GAGE	869	C10A	4.02 112.5 0.65	3.72	-1.54	0.65	308.72	988.49	342.35	6.56	9.58
C10	IRAD GAGE	870	C10B	4.02 112.5 0.65	3.72	-1.54	0.65	308.72	988.49	342.35	6.56	9.58
C10	THERMOCOUPLE	506	TC10	4.02 112.5 0.65	3.72	-1.54	0.65	308.72	988.49	342.35	6.56	9.58
C14	IRAD GAGE	873	C14A	1.50 90.9 -0.82	1.50	-0.02	-0.82	311.40	988.73	343.82	8.12	8.59
C14	IRAD GAGE	874	C14B	1.50 90.9 -0.82	1.50	-0.02	-0.82	311.40	988.73	343.82	8.12	8.59
C14	THERMOCOUPLE	508	TC14	1.50 90.9 -0.82	1.50	-0.02	-0.82	311.40	988.73	343.82	8.12	8.59
C15	IRAD GAGE	875	C15A	3.00 135.2 -0.81	2.11	-2.13	-0.81	309.84	987.19	343.81	11.00	12.99
C15	IRAD GAGE	876	C15B	3.00 135.2 -0.81	2.11	-2.13	-0.81	309.84	987.19	343.81	11.00	12.99
C15	THERMOCOUPLE	509	TC15	3.00 135.2 -0.81	2.11	-2.13	-0.81	309.84	987.19	343.81	11.00	12.99
U11	JSBM	711	U11A	1.51 180.1 0.85	-0.00	-1.51	0.85	311.99	986.71	342.15	3.20	6.88
U11	JSBM	712	U11B	1.51 180.1 0.85	-0.00	-1.51	0.85	311.99	986.71	342.15	3.20	6.88
U11	JSBM	713	U11C	1.51 180.1 0.85	-0.00	-1.51	0.85	311.99	986.71	342.15	3.20	6.88
U11	THERMOCOUPLE	427	TU11	1.51 180.1 0.85	-0.00	-1.51	0.85	311.99	986.71	342.15	3.20	6.88
U12	JSBM	714	U12A	3.48 180.2 -0.65	-0.01	-3.48	-0.65	311.03	984.98	343.65	4.71	6.95
U12	JSBM	715	U12B	3.48 180.2 -0.65	-0.01	-3.48	-0.65	311.03	984.98	343.65	4.71	6.95
U12	JSBM	716	U12C	3.48 180.2 -0.65	-0.01	-3.48	-0.65	311.03	984.98	343.65	4.71	6.95
U12	THERMOCOUPLE	428	TU12	3.48 180.2 -0.65	-0.01	-3.48	-0.65	311.03	984.98	343.65	4.71	6.95
U13	JSBM	717	U13A	2.26 202.0 -0.65	-0.85	-2.10	-0.65	312.43	985.78	343.65	4.71	6.95
U13	JSBM	718	U13B	2.26 202.0 -0.65	-0.85	-2.10	-0.65	312.43	985.78	343.65	4.71	6.95
U13	JSBM	719	U13C	2.26 202.0 -0.65	-0.85	-2.10	-0.65	312.43	985.78	343.65	4.71	6.95

Table A-3 (continued)
 SENSOR LOCATIONS FOR EXPERIMENT 2, FULL SCALE HEATER H10

HOLE ID	SENSOR TYPE	SENSOR NUMBER	SENSOR LABEL	CYLINDRICAL COORDINATES	LOCAL X	RECTANGULAR Y	RECTANGULAR Z	MINE X	RECTANGULAR Y	RECTANGULAR Z	DEPTH	HOLE LENGTH
				RHC	THETA	Z						
U13	THERMOCOUPLE	429	TU13	2.26	202.0	-0.65	-2.10	312.43	985.78	343.65	4.71	6.95
U14	USBM	720	U14A	3.22	202.0	-0.65	-2.98	312.32	984.83	343.65	4.87	7.12
U14	JSBM	721	U14B	3.22	202.0	-0.65	-2.98	312.32	984.83	343.65	4.87	7.12
U14	JSBM	722	U14C	3.22	202.0	-0.65	-2.98	312.32	984.83	343.65	4.87	7.12
U14	THERMOCOUPLE	430	TU14	3.22	202.0	-0.65	-2.98	312.32	984.83	343.65	4.87	7.12
C3	USBM	723	U15A	1.59	21.6	-0.53	1.48	312.92	989.60	343.53	4.73	7.09
C3	USBM	724	U15B	1.59	21.6	-0.53	1.48	312.92	989.60	343.53	4.73	7.09
C3	USBM	725	U15C	1.59	21.6	-0.53	1.48	312.92	989.60	343.53	4.73	7.09
C3	THERMOCOUPLE	431	TU15	1.59	21.6	-0.53	1.48	312.92	989.60	343.53	4.73	7.09
U16	USBM	726	U16A	2.77	224.8	-0.85	-1.97	313.46	985.36	342.15	3.26	7.01
U16	JSBM	727	U16B	2.77	224.8	-0.85	-1.97	313.46	985.36	342.15	3.26	7.01
U16	USBM	728	U16C	2.77	224.8	-0.85	-1.97	313.46	985.36	342.15	3.26	7.01
U16	THERMOCOUPLE	432	TU16	2.77	224.8	-0.85	-1.97	313.46	985.36	342.15	3.26	7.01
C4	USBM	729	U17A	2.50	22.6	-0.57	2.31	313.00	990.51	343.57	4.89	7.20
C4	USBM	730	U17B	2.50	22.6	-0.57	2.31	313.00	990.51	343.57	4.89	7.20
C4	USBM	731	U17C	2.50	22.6	-0.57	2.31	313.00	990.51	343.57	4.89	7.20
C4	THERMOCOUPLE	433	TU17	2.50	22.6	-0.57	2.31	313.00	990.51	343.57	4.89	7.20
U18	USBM	732	U18A	1.99	337.9	-0.85	1.85	314.27	989.27	342.15	3.31	7.06
U18	USBM	733	U18B	1.99	337.9	-0.85	1.85	314.27	989.27	342.15	3.31	7.06
U18	USBM	734	U18C	1.99	337.9	-0.85	1.85	314.27	989.27	342.15	3.31	7.06
U18	THERMOCOUPLE	434	TU18	1.99	337.9	-0.85	1.85	314.27	989.27	342.15	3.31	7.06
U19	USBM	735	U19A	3.00	337.8	-0.85	2.78	315.06	989.90	342.15	3.29	7.04
U19	USBM	736	U19B	3.00	337.8	-0.85	2.78	315.06	989.90	342.15	3.29	7.04
U19	USBM	737	U19C	3.00	337.8	-0.85	2.78	315.06	989.90	342.15	3.29	7.04
U19	THERMOCOUPLE	435	TU19	3.00	337.8	-0.85	2.78	315.06	989.90	342.15	3.29	7.04
U20	USBM	738	U20A	4.01	338.2	-0.65	3.73	315.83	990.55	343.65	4.80	7.04
U20	USBM	739	U20B	4.01	338.2	-0.65	3.73	315.83	990.55	343.65	4.80	7.04
U20	USBM	740	U20C	4.01	338.2	-0.65	3.73	315.83	990.55	343.65	4.80	7.04
U20	THERMOCOUPLE	436	TU20	4.01	338.2	-0.65	3.73	315.83	990.55	343.65	4.80	7.04
U23	USBM	741	U23A	2.50	46.6	-0.66	1.72	311.96	990.41	342.34	11.65	13.12
U23	USBM	742	U23B	2.50	46.6	-0.66	1.72	311.96	990.41	342.34	11.65	13.12
U23	USBM	743	U23C	2.50	46.6	-0.66	1.72	311.96	990.41	342.34	11.65	13.12
U23	THERMOCOUPLE	437	TU23	2.50	46.6	-0.66	1.72	311.96	990.41	342.34	11.65	13.12
U24	USBM	744	U24A	2.00	50.4	-0.66	-0.01	310.96	988.99	342.34	8.00	8.93
U24	USBM	745	U24B	2.00	50.4	-0.66	-0.01	310.96	988.99	342.34	8.00	8.93
U24	USBM	746	U24C	2.00	50.4	-0.66	-0.01	310.96	988.99	342.34	8.00	8.93
U24	THERMOCOUPLE	438	TU24	2.00	50.4	-0.66	-0.01	310.96	988.99	342.34	8.00	8.93
U25	USBM	747	U25A	2.99	134.5	-0.62	-2.09	309.83	987.23	342.38	11.31	13.29
U25	USBM	748	U25B	2.99	134.5	-0.62	-2.09	309.83	987.23	342.38	11.31	13.29
U25	USBM	749	U25C	2.99	134.5	-0.62	-2.09	309.83	987.23	342.38	11.31	13.29
U25	THERMOCOUPLE	439	TU25	2.99	134.5	-0.62	-2.09	309.83	987.23	342.38	11.31	13.29
U29	USBM	750	U29A	3.50	67.7	-0.85	1.33	310.53	990.76	343.85	7.36	9.84
U29	USBM	751	U29B	3.50	67.7	-0.85	1.33	310.53	990.76	343.85	7.36	9.84
U29	USBM	752	U29C	3.50	67.7	-0.85	1.33	310.53	990.76	343.85	7.36	9.84
U29	THERMOCOUPLE	440	TU29	3.50	67.7	-0.85	1.33	310.53	990.76	343.85	7.36	9.84
U30	USBM	753	U30A	2.26	112.4	-0.83	-0.86	310.47	988.29	343.83	8.18	9.37
U30	USBM	754	U30B	2.26	112.4	-0.83	-0.86	310.47	988.29	343.83	8.18	9.37
U30	USBM	755	U30C	2.26	112.4	-0.83	-0.86	310.47	988.29	343.83	8.18	9.37
U30	THERMOCOUPLE	441	TU30	2.26	112.4	-0.83	-0.86	310.47	988.29	343.83	8.18	9.37

Table A-3 (continued)
SENSOR LOCATIONS FOR EXPERIMENT 3, TIME SCALE HEATERS

HOLE ID	SENSOR TYPE	SENSOR NUMBER	SENSOR LABEL	CYLINDRICAL COORDINATES	LOCAL X	RECTANGULAR Y	RECTANGULAR Z	MINE X	RECTANGULAR Y	RECTANGULAR Z	DEPTH	HOLE LENGTH
				RHO THETA Z	X	Y	Z	X	Y	Z		
H5	HEATER POWER	1134	PH5B									
H5	HEATER POWER	1135	PH5C									
H5	THERMOCOUPLE	998	TH5A	4.58 41.4 0.	3.03	3.44	0.	339.03	957.54	347.00	9.90	11.07
H5	THERMOCOUPLE	999	TH5B	4.58 41.4 0.	3.03	3.44	0.	339.03	957.54	347.00	9.90	11.07
H5	THERMOCOUPLE	1000	TH5C	4.58 41.4 .91	3.03	3.44	.91	339.03	957.54	346.09	8.99	11.07
H6	HEATER CURRENT	1136	IH6A									
H6	HEATER VOLTAGE	1137	VH6A									
H6	HEATER POWER	1138	PH6A									
H6	HEATER CURRENT	1139	IH6B									
H6	HEATER VOLTAGE	1140	VH6B									
H6	HEATER POWER	1141	PH6B									
H6	HEATER POWER	1142	PH6C									
H6	THERMOCOUPLE	1002	TH6A	4.65 139.5 0.	3.02	-3.54	0.	335.64	963.64	347.00	9.78	10.80
H6	THERMOCOUPLE	1003	TH6B	4.65 139.5 0.	3.02	-3.54	0.	335.64	963.64	347.00	9.78	10.80
H6	THERMOCOUPLE	1004	TH6C	4.65 139.5 .91	3.02	-3.53	.91	335.64	963.63	346.09	8.87	10.80
H7	HEATER CURRENT	1143	IH7A									
H7	HEATER VOLTAGE	1144	VH7A									
H7	HEATER POWER	1145	PH7A									
H7	HEATER CURRENT	1146	IH7B									
H7	HEATER VOLTAGE	1147	VH7B									
H7	HEATER POWER	1148	PH7B									
H7	HEATER POWER	1149	PH7C									
H7	THERMOCOUPLE	1006	TH7A	4.61 319.4 0.	-3.00	3.50	0.	333.78	954.57	347.00	9.97	11.18
H7	THERMOCOUPLE	1007	TH7B	4.61 319.4 0.	-3.00	3.50	0.	333.78	954.57	347.00	9.97	11.18
H7	THERMOCOUPLE	1008	TH7C	4.61 319.4 .91	-3.00	3.50	.91	333.78	954.57	346.09	9.06	11.18
H8	HEATER CURRENT	1150	IH8A									
H8	HEATER VOLTAGE	1151	VH8A									
H8	HEATER POWER	1152	PH8B									
H8	HEATER CURRENT	1153	IH8B									
H8	HEATER VOLTAGE	1154	VH8B									
H8	HEATER POWER	1155	PH8B									
H8	HEATER POWER	1156	PH8C									
H8	THERMOCOUPLE	1010	TH8A	4.65 220.0 0.	-2.99	-3.56	0.	330.37	960.75	347.00	9.83	10.92
H8	THERMOCOUPLE	1011	TH8B	4.65 220.0 0.	-2.99	-3.56	0.	330.37	960.75	347.00	9.83	10.92
H8	THERMOCOUPLE	1012	TH8C	4.65 220.0 .91	-2.99	-3.56	.91	330.37	960.75	346.09	8.92	10.92
T1	THERMOCOUPLE	923	TI1A	.52 180.2 5.00	-0.0	-0.92	5.00	334.27	959.88	342.00	4.86	13.22
T1	THERMOCOUPLE	925	TI1B	.93 180.5 3.00	-0.1	-0.93	3.00	334.26	959.89	344.00	6.86	13.22
T1	THERMOCOUPLE	924	TI1C	.54 180.7 1.00	-0.1	-0.94	1.00	334.25	959.90	346.00	8.86	13.22
T1	THERMOCOUPLE	926	TI1D	.94 180.9 0.00	-0.1	-0.94	0.00	334.25	959.90	347.00	9.86	13.22
T1	THERMOCOUPLE	922	TI1E	.95 181.1 -2.00	-0.2	-0.95	-2.00	334.24	959.91	349.00	11.86	13.22
T2	THERMOCOUPLE	931	TI2A	1.77 180.0 5.00	-0.0	-1.77	5.00	333.86	960.64	342.01	4.75	12.86
T2	THERMOCOUPLE	930	TI2B	1.78 180.0 3.00	-0.0	-1.78	3.00	333.85	960.64	344.01	6.75	12.86
T2	THERMOCOUPLE	929	TI2C	1.78 180.1 .99	-0.0	-1.78	.99	333.85	960.64	346.01	8.75	12.86
T2	THERMOCOUPLE	928	TI2D	1.79 180.1 -0.01	-0.0	-1.79	-0.01	333.85	960.64	347.01	5.75	12.86
T2	THERMOCOUPLE	927	TI2E	1.79 180.1 -2.01	-0.0	-1.79	-2.01	333.85	960.65	349.01	11.75	12.86
T3	THERMOCOUPLE	936	TI3A	2.61 179.1 5.00	.04	-2.61	5.00	333.49	961.39	342.00	4.69	12.79
T3	THERMOCOUPLE	935	TI3B	2.60 178.7 3.00	.06	-2.60	3.00	333.51	961.39	344.00	6.69	12.79
T3	THERMOCOUPLE	934	TI3C	2.59 178.4 1.00	.07	-2.59	1.00	333.52	961.39	346.00	8.69	12.79
T3	THERMOCOUPLE	933	TI3D	2.59 178.2 0.	.08	-2.59	0.	333.53	961.38	347.00	9.69	12.79
T3	THERMOCOUPLE	932	TI3E	2.58 177.9 -2.00	.10	-2.58	-2.00	333.55	961.38	349.00	11.69	12.79
T4	THERMOCOUPLE	941	TI4A	3.64 166.1 5.00	.88	-3.53	5.00	333.77	962.60	342.00	4.69	12.82
T4	THERMOCOUPLE	940	TI4B	3.64 166.0 3.00	.88	-3.54	3.00	333.77	962.60	344.00	6.69	12.82
T4	THERMOCOUPLE	939	TI4C	3.65 166.1 1.00	.88	-3.54	1.00	333.77	962.61	346.00	8.69	12.82
T4	THERMOCOUPLE	938	TI4D	3.66 166.1 0.	.88	-3.55	0.	333.77	962.61	347.00	9.65	12.82

Table A-3 (continued)
 SENSOR LOCATIONS FOR EXPERIMENT 3, TIME SCALE HEATERS

HOLE ID	SENSOR TYPE	SENSOR NUMBER	SENSOR LABEL	CYLINDRICAL COORDINATES	LOCAL X	RECTANGULAR Y	RECTANGULAR Z	MINE X	RECTANGULAR Y	RECTANGULAR Z	DEPTH	HOLE LENGTH
				RHO THETA Z	X	Y	Z	X	Y	Z		
T4	THERMOCOUPLE	937	T4E	3.66 166.1 -2.00	.88	-3.56	-2.00	333.77	962.62	349.00	11.69	12.82
T5	THERMOCOUPLE	946	T5A	2.29 40.9 8.00	1.50	1.73	8.00	336.86	958.29	339.00	1.76	13.99
T5	THERMOCOUPLE	945	T5B	2.28 40.8 6.00	1.49	1.72	6.00	336.85	958.30	341.00	3.76	13.99
T5	THERMOCOUPLE	944	T5C	2.27 40.8 4.00	1.48	1.72	4.00	336.85	958.30	343.00	5.76	13.99
T5	THERMOCOUPLE	943	T5D	2.25 40.8 0.	1.47	1.71	0.	336.83	958.30	347.00	5.76	13.99
T5	THERMOCOUPLE	942	T5E	2.24 40.8 -3.00	1.46	1.70	-3.00	336.82	958.31	350.00	12.76	13.99
T6	THERMOCOUPLE	951	T6A	3.79 23.4 5.00	1.51	3.47	5.00	337.71	956.77	342.00	5.06	13.28
T6	THERMOCOUPLE	950	T6B	3.78 23.4 3.00	1.51	3.47	3.00	337.71	956.77	344.00	7.06	13.28
T6	THERMOCOUPLE	949	T6C	3.78 23.5 1.00	1.51	3.47	1.00	337.71	956.78	346.00	9.06	13.28
T6	THERMOCOUPLE	948	T6D	3.78 23.5 0.	1.51	3.47	0.	337.71	956.78	347.00	10.06	13.28
T6	THERMOCOUPLE	947	T6E	3.78 23.5 -2.00	1.51	3.47	-2.00	337.71	956.78	349.00	12.06	13.28
T7	THERMOCOUPLE	956	T7A	3.84 157.0 5.00	1.50	-3.53	5.00	334.32	962.90	342.00	4.67	12.81
T7	THERMOCOUPLE	955	T7B	3.84 157.1 3.00	1.49	-3.54	3.00	334.31	962.90	344.00	6.67	12.81
T7	THERMOCOUPLE	954	T7C	3.85 157.2 1.00	1.49	-3.55	1.00	334.30	962.91	346.00	8.67	12.81
T7	THERMOCOUPLE	953	T7D	3.86 157.3 0.	1.49	-3.56	0.	334.30	962.92	347.00	9.67	12.81
T7	THERMOCOUPLE	952	T7E	3.86 157.4 -2.00	1.48	-3.57	-2.00	334.29	962.92	349.00	11.67	12.81
T8	THERMOCOUPLE	961	T8A	3.66 194.0 5.00	.88	-3.55	5.00	332.22	961.76	342.00	4.67	12.76
T8	THERMOCOUPLE	960	T8B	3.68 194.0 3.00	.89	-3.57	3.00	332.21	961.77	344.00	6.67	12.76
T8	THERMOCOUPLE	959	T8C	3.69 194.1 1.00	.90	-3.58	1.00	332.20	961.78	346.00	8.67	12.76
T8	THERMOCOUPLE	958	T8D	3.70 194.1 0.	.90	-3.59	0.	332.19	961.79	347.00	9.67	12.76
T8	THERMOCOUPLE	957	T8E	3.72 194.1 -2.00	.91	-3.61	-2.00	332.17	961.80	349.00	11.67	12.76
T9	THERMOCOUPLE	966	T9A	3.80 336.8 5.00	1.50	3.49	5.00	335.09	955.30	342.00	4.92	13.54
T9	THERMOCOUPLE	965	T9B	3.80 336.7 3.00	1.50	3.49	3.00	335.09	955.30	344.00	6.92	13.54
T9	THERMOCOUPLE	964	T9C	3.80 336.7 1.00	1.50	3.49	1.00	335.09	955.30	346.00	8.92	13.54
T9	THERMOCOUPLE	963	T9D	3.80 336.7 0.	1.50	3.49	0.	335.09	955.30	347.00	9.92	13.54
T9	THERMOCOUPLE	962	T9E	3.81 336.7 -2.00	1.50	3.50	-2.00	335.09	955.30	349.00	11.92	13.54
T10	THERMOCOUPLE	971	T10A	2.28 319.3 7.95	1.49	1.73	7.95	334.25	956.85	339.05	2.03	13.10
T10	THERMOCOUPLE	970	T10B	2.27 319.4 5.95	1.48	1.73	5.95	334.26	956.86	341.05	4.03	13.10
T10	THERMOCOUPLE	969	T10C	2.27 319.5 3.95	1.47	1.72	3.95	334.26	956.86	343.05	6.03	13.10
T10	THERMOCOUPLE	968	T10D	2.25 319.6 .05	1.46	1.71	.05	334.27	956.88	346.95	9.93	13.10
T10	THERMOCOUPLE	967	T10E	2.24 319.8 -2.65	1.45	1.71	-2.65	334.28	956.89	349.65	12.63	13.10
T11	THERMOCOUPLE	976	T11A	2.31 220.1 8.00	1.49	-1.77	8.00	332.56	959.92	339.00	1.76	13.98
T11	THERMOCOUPLE	975	T11B	2.30 219.8 6.00	1.47	-1.76	6.00	332.57	959.92	341.00	3.76	13.98
T11	THERMOCOUPLE	974	T11D	2.26 219.0 0.	1.42	-1.76	0.	332.62	959.94	347.00	9.76	13.98
T11	THERMOCOUPLE	973	T11E	2.29 219.5 4.00	1.45	-1.76	4.00	332.59	959.92	343.00	5.76	13.98
T11	THERMOCOUPLE	972	T11E	2.25 218.5 -3.00	1.40	-1.76	-3.00	332.64	959.94	350.00	12.76	13.98
T12	THERMOCOUPLE	981	T12A	3.83 202.8 5.00	1.49	-3.53	5.00	331.71	961.45	342.00	4.77	12.93
T12	THERMOCOUPLE	980	T12B	3.83 202.7 3.00	1.48	-3.53	3.00	331.71	961.46	344.00	6.77	12.93
T12	THERMOCOUPLE	979	T12C	3.84 202.6 1.00	1.48	-3.54	1.00	331.71	961.47	346.00	8.77	12.93
T12	THERMOCOUPLE	978	T12D	3.84 202.6 0.	1.47	-3.54	0.	331.71	961.47	347.00	9.77	12.93
T12	THERMOCOUPLE	977	T12E	3.84 202.5 -2.00	1.47	-3.55	-2.00	331.71	961.48	349.00	11.77	12.93
E1	EXTENSOMETER	1081	E1A	.01 164.3 7.04	.00	-.01	7.04	334.71	959.09	339.96	2.73	13.99
E1	EXTENSOMETER	1082	E1B	.01 186.8 3.04	.00	-.01	3.04	334.71	959.09	343.96	6.73	13.99
E1	EXTENSOMETER	1083	E1C	.01 195.3 .05	.00	-.01	.05	334.71	959.09	346.95	9.72	13.99
E1	EXTENSOMETER	1084	E1D	.02 203.3 -2.90	.01	-.01	-2.90	334.70	959.09	349.90	12.67	13.99
E1	THERMOCOUPLE	902	TE1A	.01 186.8 3.10	.00	-.01	3.10	334.71	959.09	343.90	6.67	13.99
E1	THERMOCOUPLE	903	TE1B	.01 187.9 2.10	.00	-.01	2.10	334.71	959.09	344.90	7.67	13.99
E1	THERMOCOUPLE	904	TE1C	.01 191.6 1.10	.00	-.01	1.10	334.71	959.09	345.90	8.67	13.99
E1	THERMOCOUPLE	905	TE1D	.01 195.3 .10	.00	-.01	.10	334.71	959.09	346.90	9.67	13.99
E1	THERMOCOUPLE	985	TE1E	.01 144.4 9.77	.00	-.01	9.77	334.72	959.09	337.23	0.	13.99
E1	THERMOCOUPLE	1014	TE1F	.01 164.3 7.10	.00	-.01	7.10	334.71	959.09	339.90	2.67	13.99
E1	THERMOCOUPLE	1015	TE1G	.01 173.5 5.35	.00	-.01	5.35	334.71	959.09	341.65	4.42	13.99
E2	EXTENSOMETER	1085	E2A	1.74 0. 7.01	.00	1.74	7.01	335.56	957.56	339.99	2.94	14.17
E2	EXTENSOMETER	1086	E2B	1.74 0. 3.02	.01	1.74	3.02	335.55	957.56	343.98	6.93	14.17

Table A-3 (continued)
 SENSOR LOCATIONS FOR EXPERIMENT 3, TIME SCALE HEATERS

HOLE ID	SENSOR TYPE	SENSOR NUMBER	SENSOR LABEL	CYLINDRICAL COORDINATES	LOCAL X	RECTANGULAR Y	RECTANGULAR Z	MINE X	RECTANGULAR Y	RECTANGULAR Z	DEPTH	HOLE LENGTH
				RHO THETA Z	X	Y	Z	X	Y	Z		
E2	EXTENSOMETER	1087	E2C	1.74 0. 0.	-0.1	1.74	.05	335.55	957.56	346.95	9.90	14.17
E2	EXTENSOMETER	1088	E2D	1.74 0. 0.	-0.1	1.74	-2.93	335.54	957.56	349.93	12.88	14.17
E2	THERMOCOUPLE	906	TE2A	1.74 0. 0.	-0.0	1.74	7.07	335.56	957.56	339.93	2.88	14.17
E2	THERMOCOUPLE	907	TE2B	1.74 0. 0.	-0.1	1.74	3.07	335.55	957.56	343.93	6.88	14.17
E2	THERMOCOUPLE	908	TE2C	1.74 0. 0.	-0.1	1.74	1.07	335.55	957.56	345.93	8.88	14.17
E2	THERMOCOUPLE	909	TE2D	1.74 0. 0.	-0.1	1.74	.07	335.55	957.56	346.93	9.88	14.17
E2	THERMOCOUPLE	989	TE2F	1.74 0. 0.	.00	1.74	9.95	335.56	957.56	337.05	0.	14.17
E3	EXTENSOMETER	1089	E3A	2.61 0. 0.	.01	2.61	7.00	335.98	956.80	340.00	3.07	14.64
E3	EXTENSOMETER	1090	E3B	2.60 0. 0.	.00	2.60	2.98	335.98	956.81	344.02	7.09	14.64
E3	EXTENSOMETER	1091	E3C	2.60 0. 0.	.00	2.60	.01	335.98	956.81	346.99	10.06	14.64
E3	EXTENSOMETER	1092	E3D	2.60 0. 0.	.00	2.60	-2.97	335.97	956.81	349.97	13.04	14.64
E3	THERMOCOUPLE	910	TE3A	2.60 0. 0.	.00	2.60	2.98	335.98	956.81	344.02	7.09	14.64
E3	THERMOCOUPLE	911	TE3B	2.60 0. 0.	.00	2.60	2.01	335.98	956.81	344.99	8.06	14.64
E3	THERMOCOUPLE	912	TE3C	2.60 0. 0.	.00	2.60	1.01	335.98	956.81	345.99	9.06	14.64
E3	THERMOCOUPLE	913	TE3D	2.60 0. 0.	.00	2.60	.01	335.98	956.81	346.99	10.06	14.64
E3	THERMOCOUPLE	993	TE3E	2.61 0. 0.	.01	2.61	10.07	335.98	956.80	336.93	0.	14.64
E3	THERMOCOUPLE	1016	TE3F	2.61 0. 0.	.01	2.61	7.00	335.98	956.80	340.00	3.07	14.64
E3	THERMOCOUPLE	1017	TE3G	2.61 0. 0.	.00	2.61	5.23	335.98	956.80	341.77	4.84	14.64
E4	EXTENSOMETER	1093	E4A	1.50 269.6	-1.50	-0.1	7.01	333.40	958.37	339.99	2.92	14.57
E4	EXTENSOMETER	1094	E4B	1.50 269.8	-1.50	-0.1	3.01	333.40	958.36	343.99	6.92	14.57
E4	EXTENSOMETER	1095	E4C	1.50 270.0	-1.50	-0.0	-0.1	333.40	958.36	347.01	9.94	14.57
E4	EXTENSOMETER	1096	E4D	1.50 270.2	-1.50	.00	-2.93	333.40	958.35	349.93	12.86	14.57
E4	THERMOCOUPLE	914	TE4A	1.50 269.6	-1.50	-0.1	7.07	333.40	958.37	339.93	2.86	14.57
E4	THERMOCOUPLE	915	TE4B	1.50 269.8	-1.50	-0.1	3.07	333.40	958.36	343.93	6.86	14.57
E4	THERMOCOUPLE	916	TE4C	1.50 269.9	-1.50	-0.0	1.07	333.40	958.36	345.93	8.86	14.57
E4	THERMOCOUPLE	917	TE4D	1.50 270.0	-1.50	-0.0	.07	333.40	958.36	346.93	9.86	14.57
E4	THERMOCOUPLE	997	TE4E	1.50 269.4	-1.50	-0.2	9.93	333.40	958.37	337.07	0.	14.57
E5	EXTENSOMETER	1097	E5A	2.31 139.5	1.50	-1.76	6.97	335.18	961.34	340.03	2.81	14.00
E5	EXTENSOMETER	1098	E5B	2.30 139.8	1.49	-1.76	2.96	335.16	961.34	344.04	6.82	14.00
E5	EXTENSOMETER	1099	E5C	2.30 139.9	1.48	-1.76	-0.04	335.16	961.34	347.04	9.82	14.00
E5	EXTENSOMETER	1100	E5D	2.29 140.1	1.47	-1.76	-3.00	335.15	961.33	350.00	12.78	14.00
E5	THERMOCOUPLE	918	TE5A	2.31 139.5	1.50	-1.76	7.00	335.17	961.34	340.00	2.78	14.00
E5	THERMOCOUPLE	919	TE5B	2.30 139.8	1.49	-1.76	3.00	335.17	961.34	344.00	6.78	14.00
E5	THERMOCOUPLE	920	TE5C	2.30 139.9	1.48	-1.76	1.00	335.16	961.34	346.00	8.78	14.00
E5	THERMOCOUPLE	921	TE5D	2.30 139.9	1.48	-1.76	-0.0	335.16	961.34	347.00	9.78	14.00
E5	THERMOCOUPLE	1001	TE5E	2.31 139.4	1.51	-1.76	9.78	335.18	961.35	337.22	0.	14.00

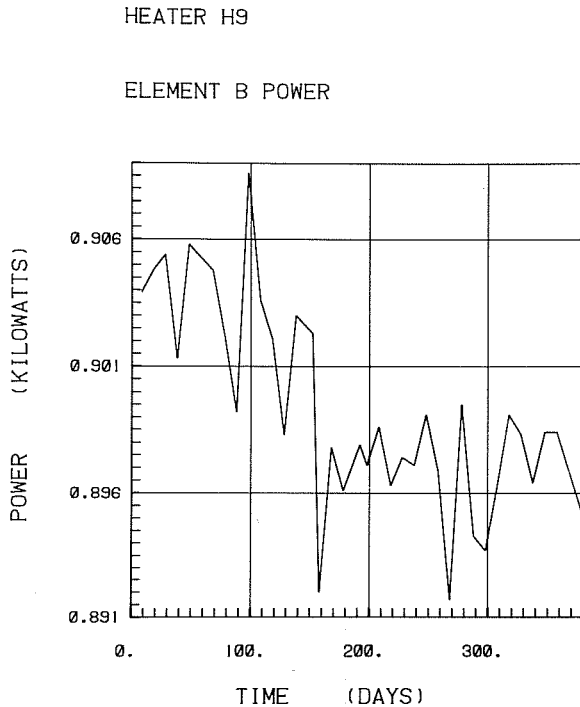
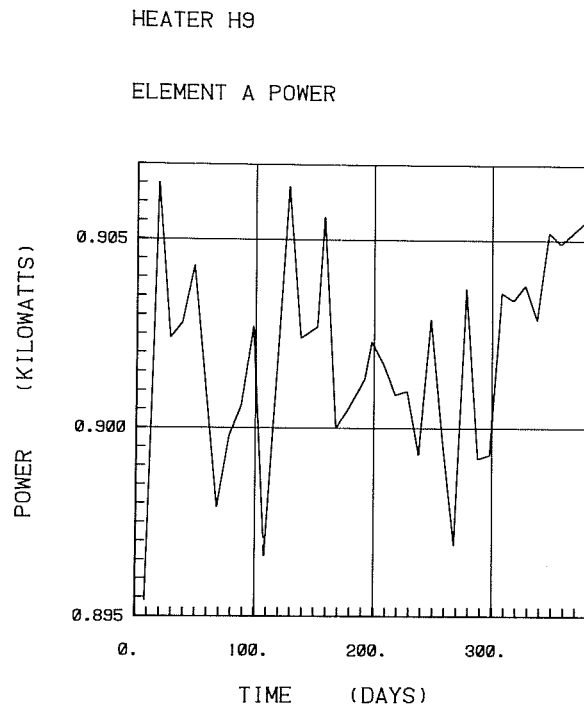
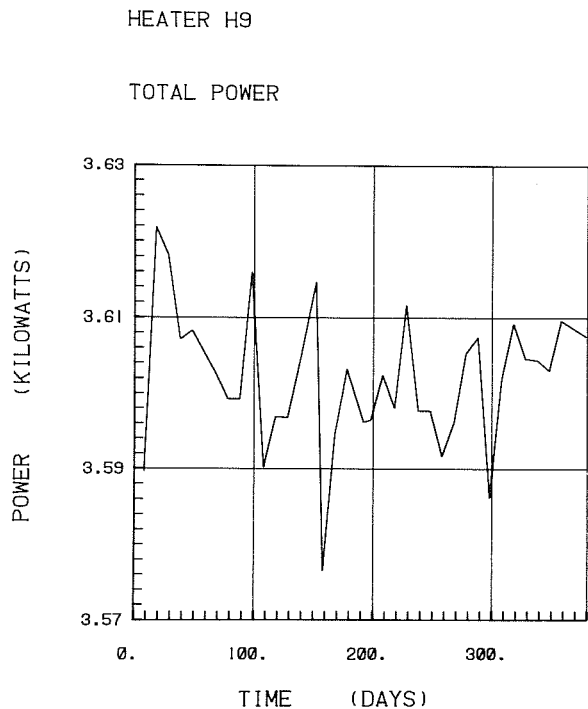


Fig. A-1. Power history for Experiment 1 (H9).

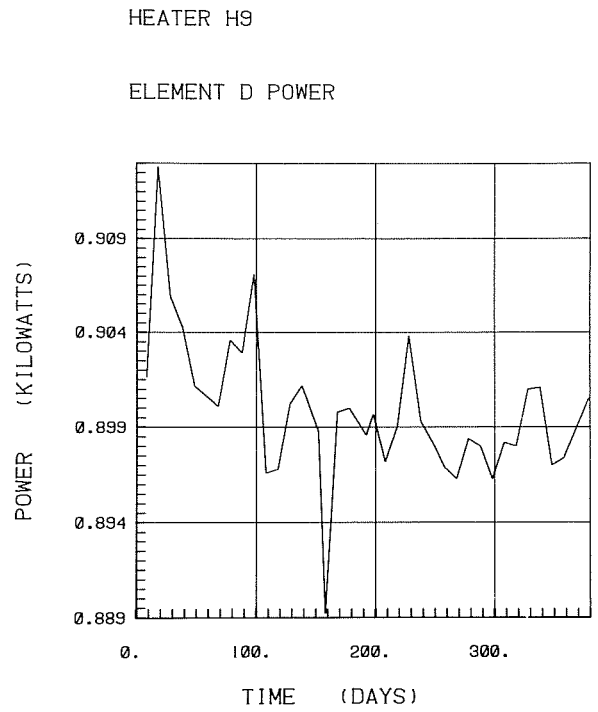
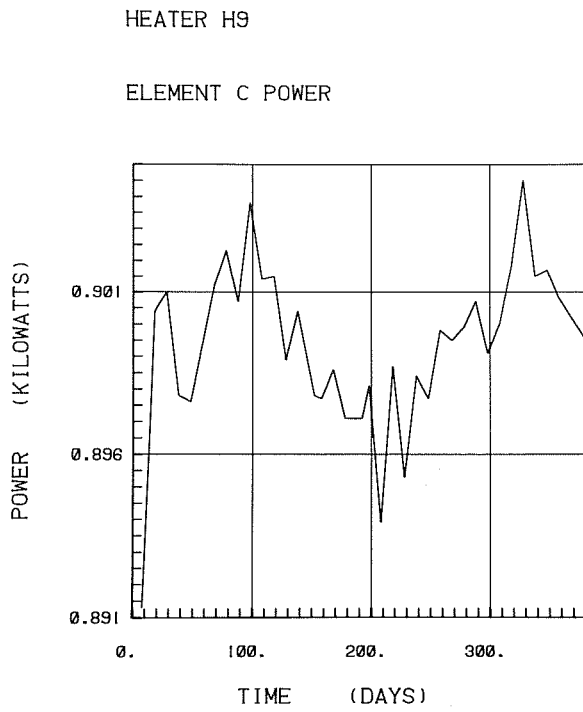


Fig. A-1. (continued).

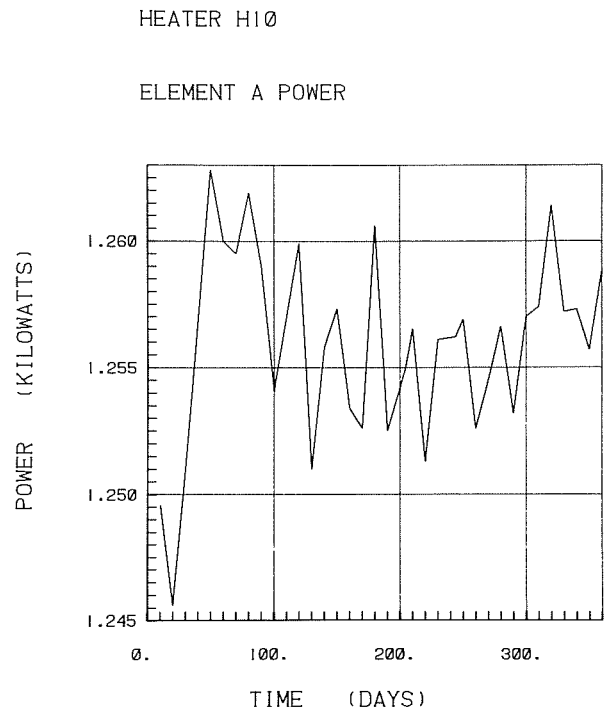
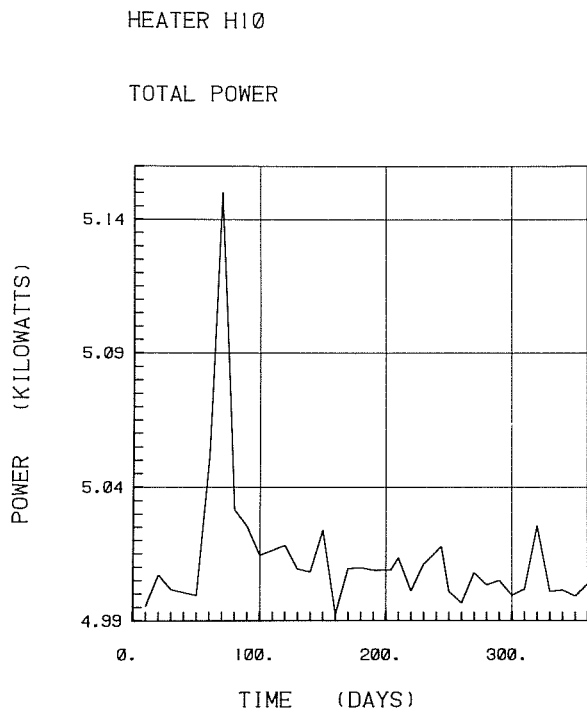
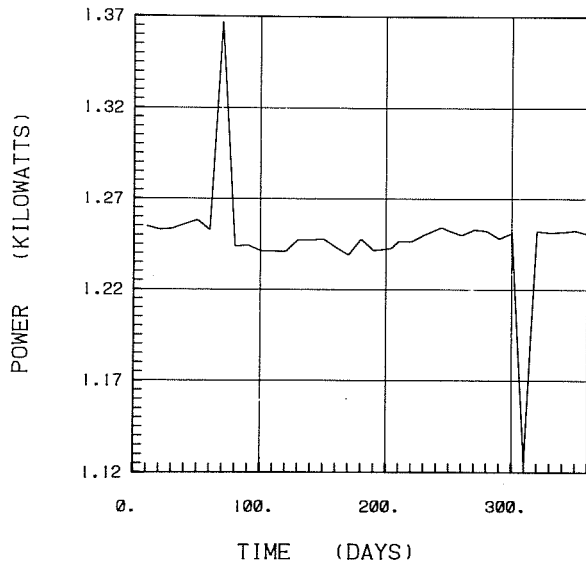


Fig. A-2. Power history for Experiment 2 (H10 - H18).

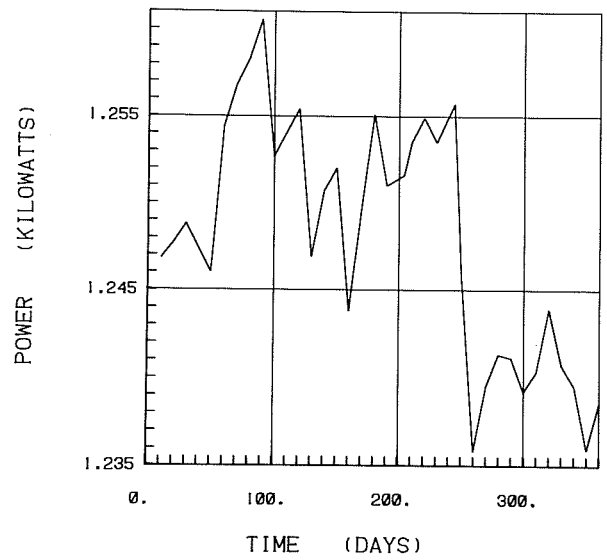
HEATER H10

ELEMENT B POWER



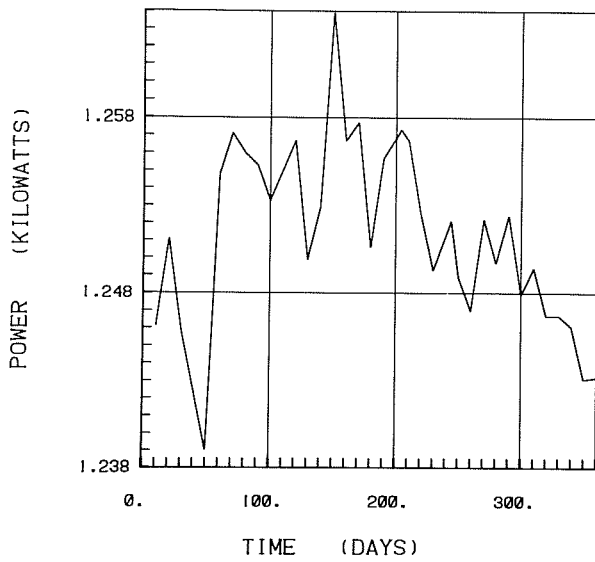
HEATER H10

ELEMENT C POWER



HEATER H10

ELEMENT D POWER



HEATER H11

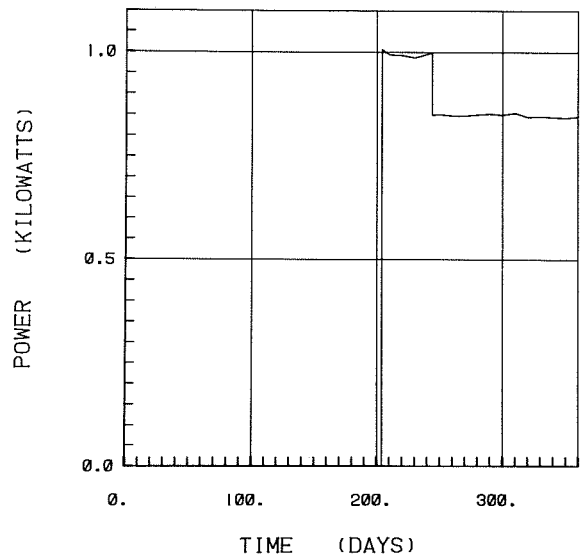
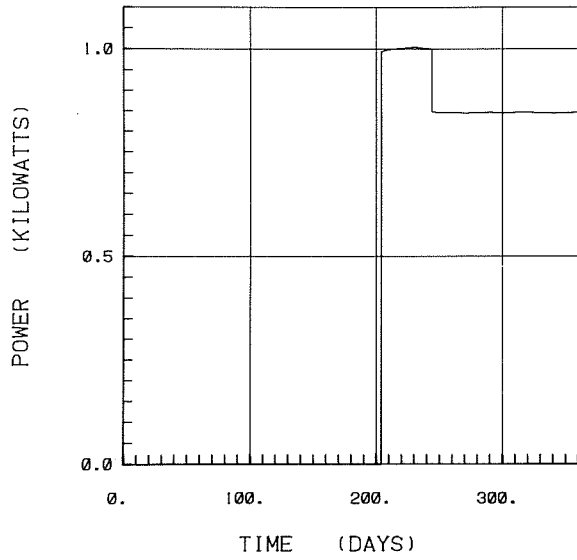
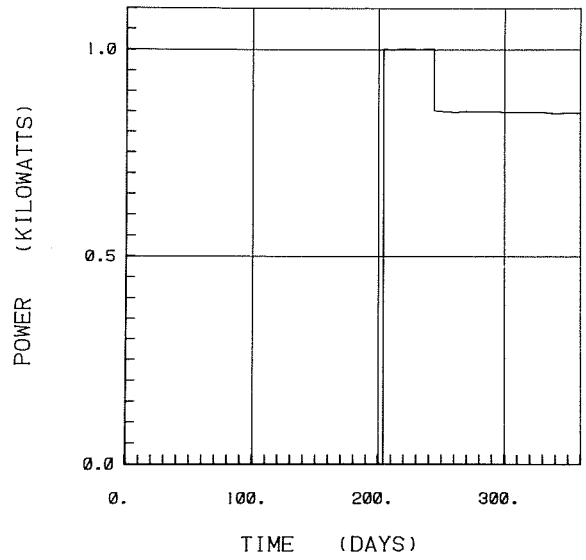


Fig. A-2. (continued).

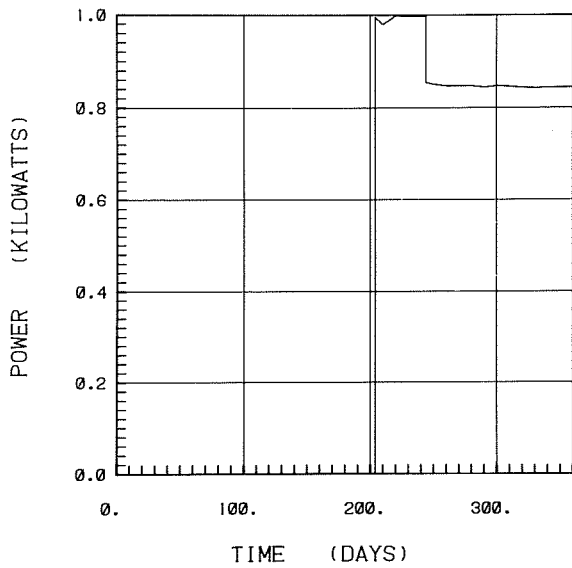
HEATER H12



HEATER H13



HEATER H14



HEATER H15

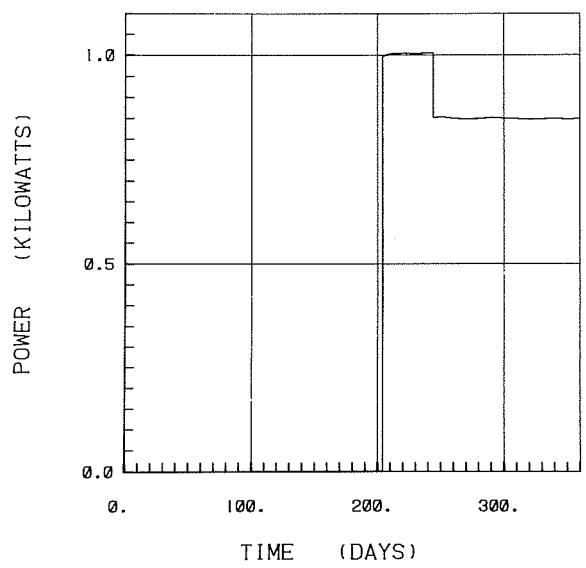
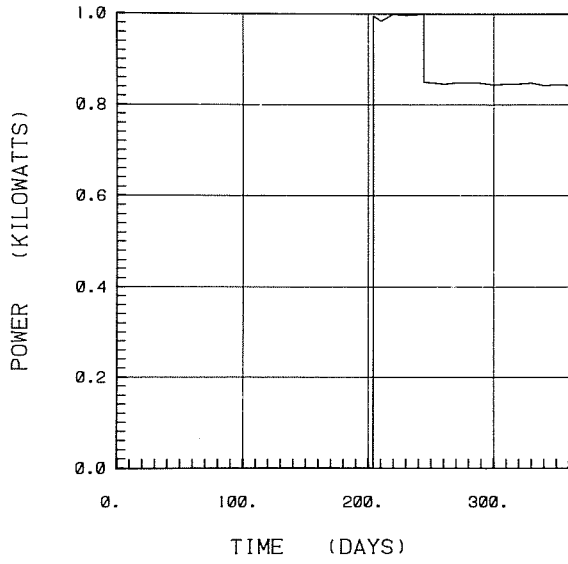
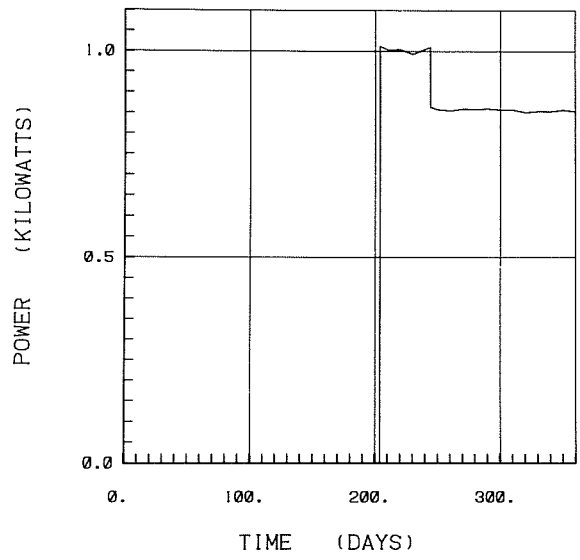


Fig. A-2. (continued).

HEATER H16



HEATER H17



HEATER H18

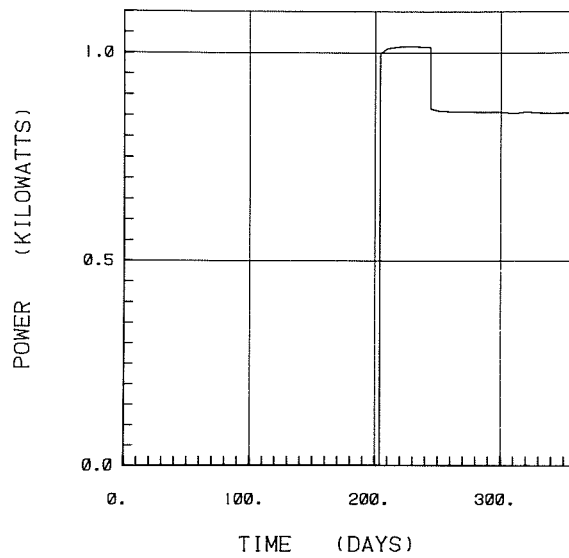


Fig. A-2. (continued).

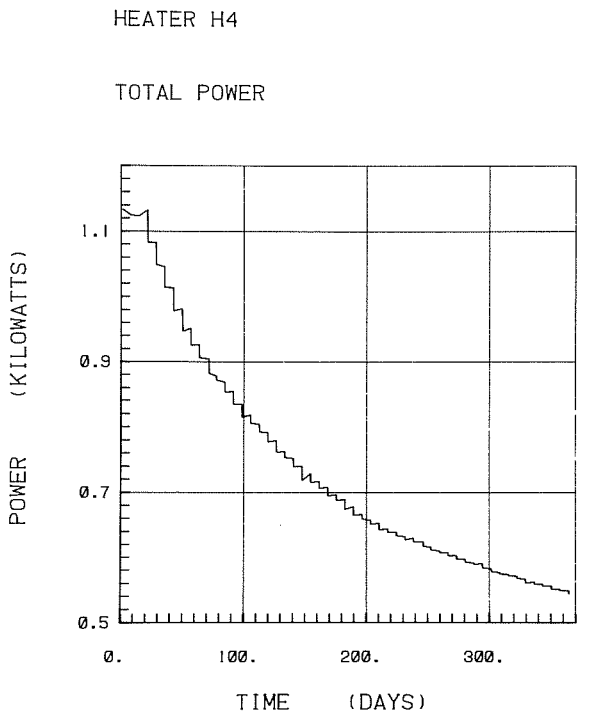
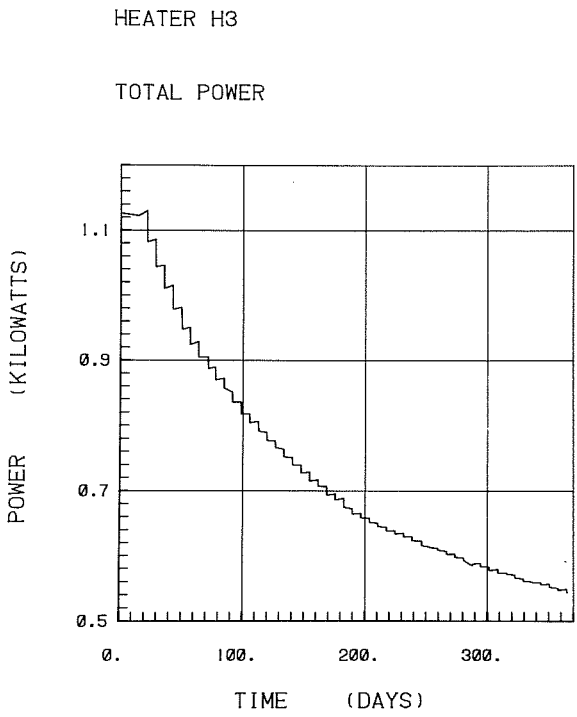
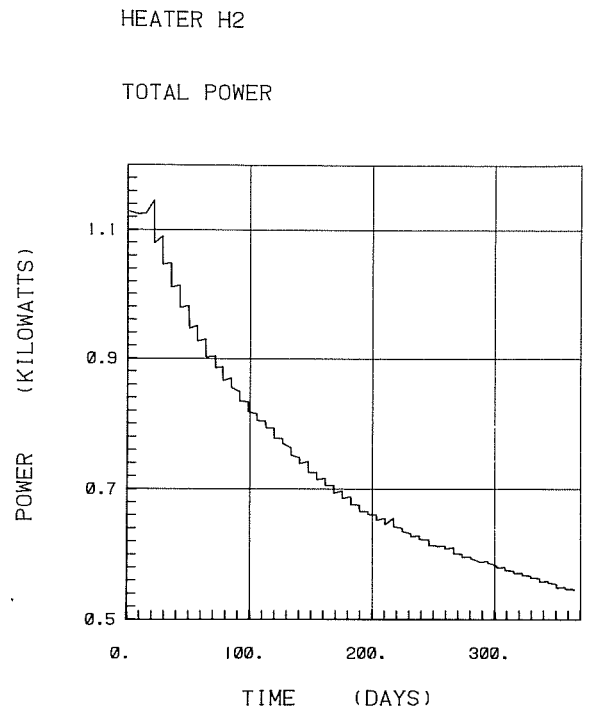
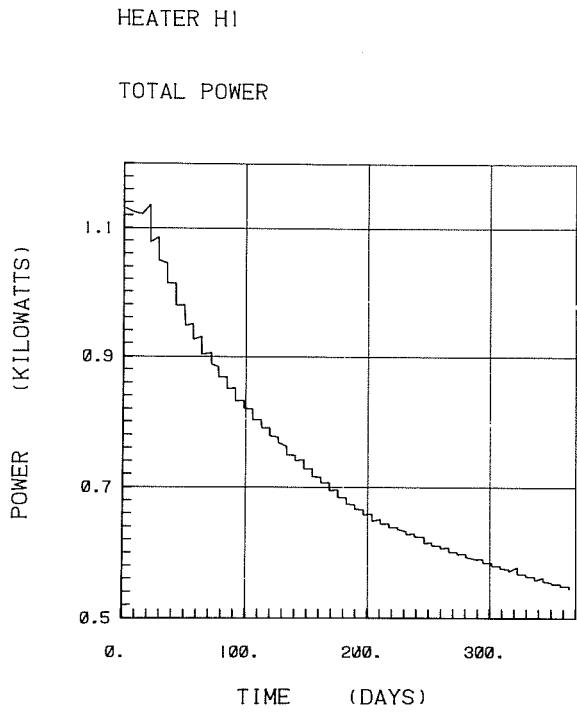
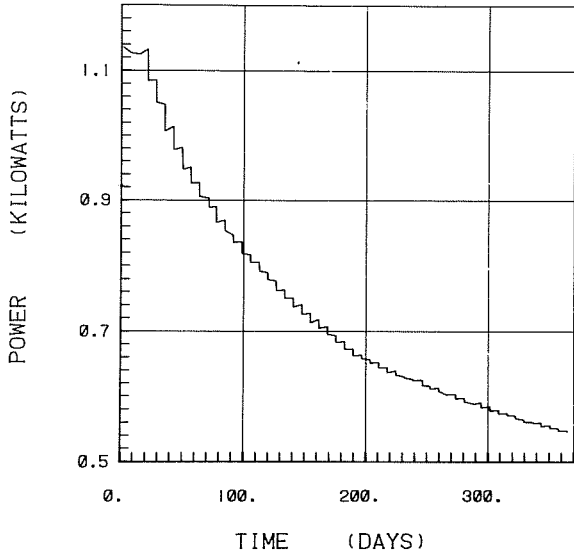


Fig. A-3. Power history for Experiment 3 (H1 - H8).

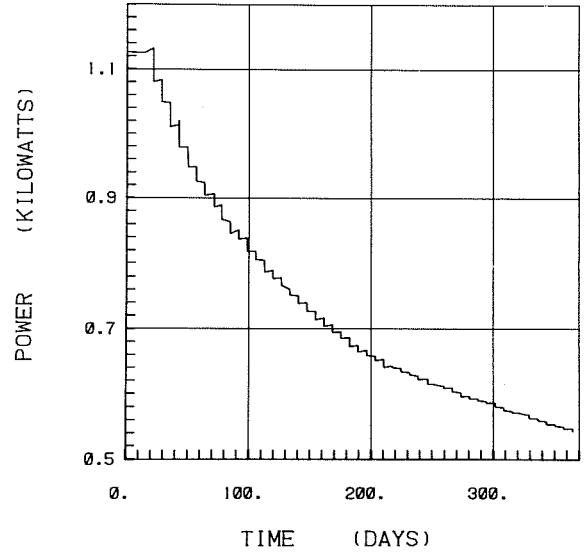
HEATER H5

TOTAL POWER



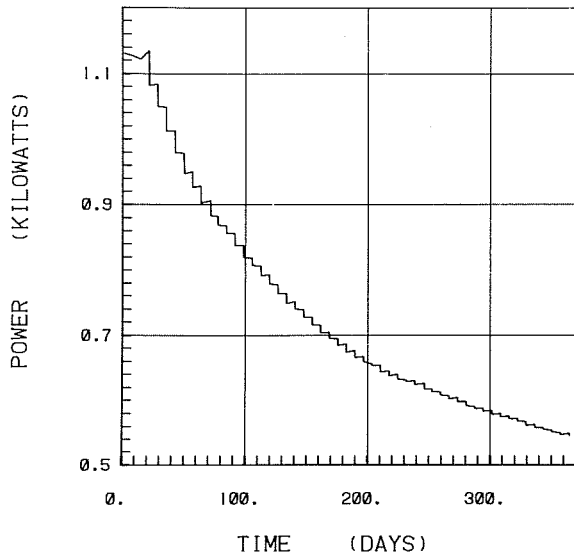
HEATER H6

TOTAL POWER



HEATER H7

TOTAL POWER



HEATER H8

TOTAL POWER

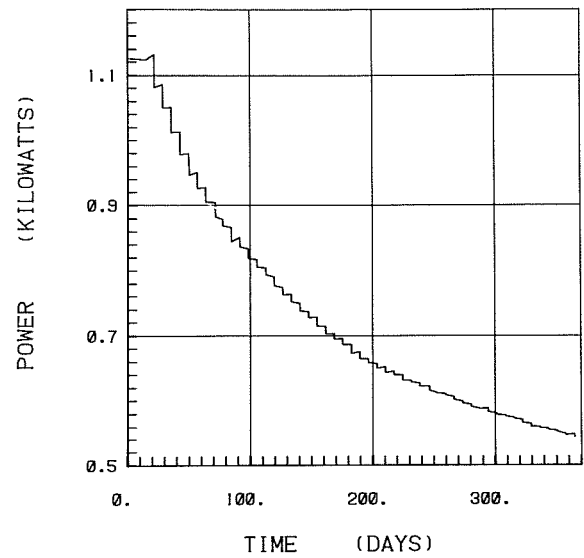
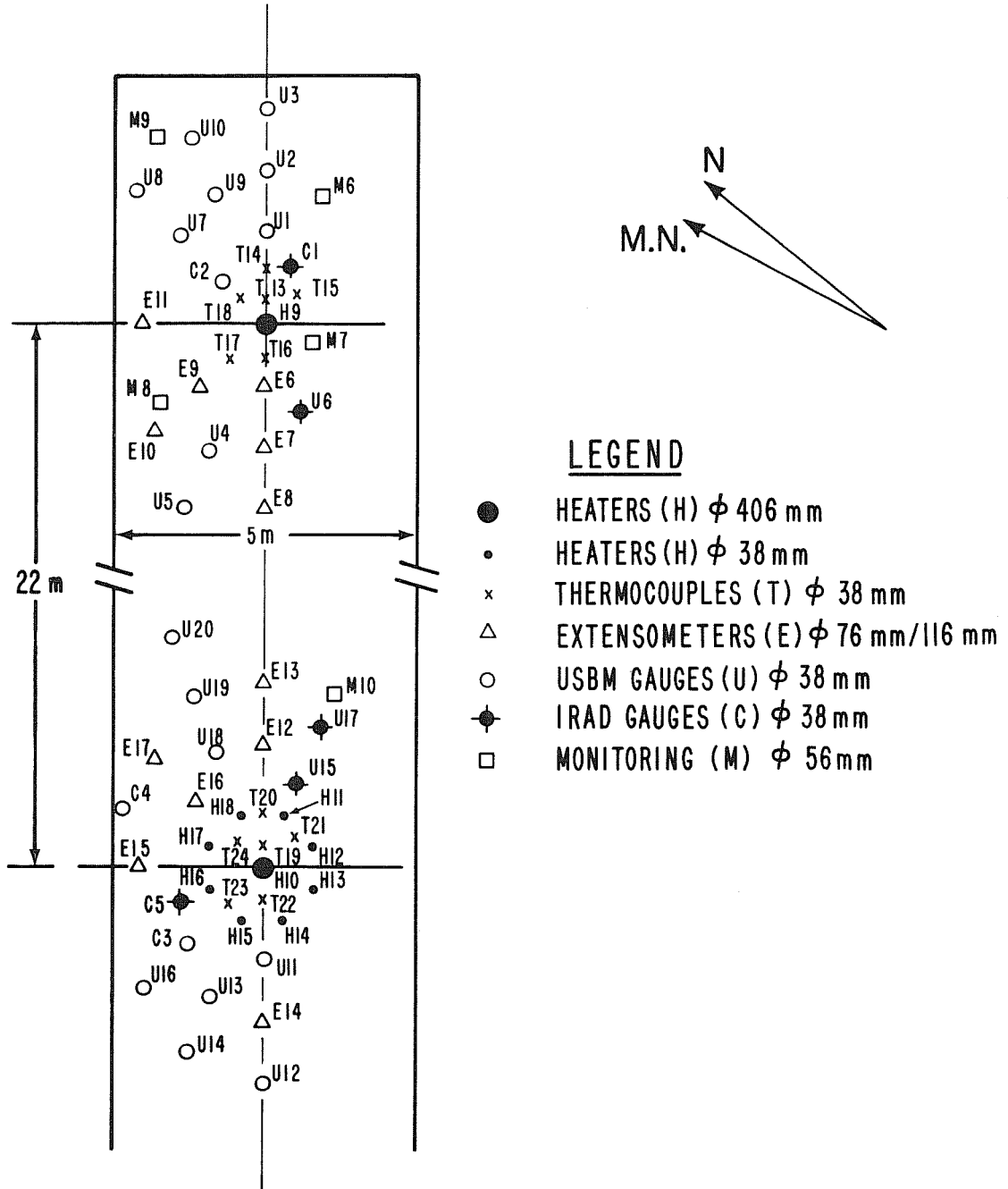


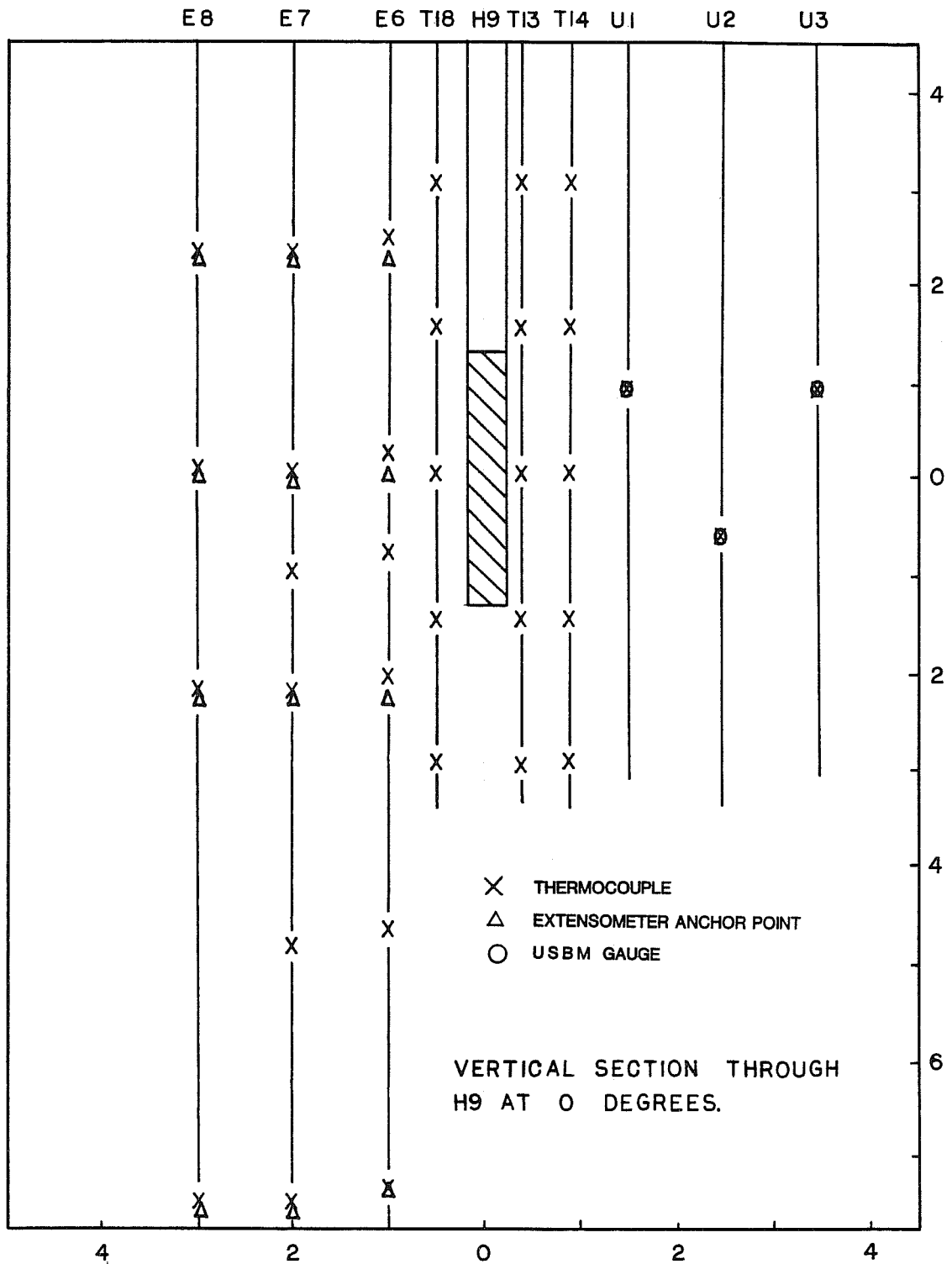
Fig. A-3. (continued).

FULL-SCALE DRIFT



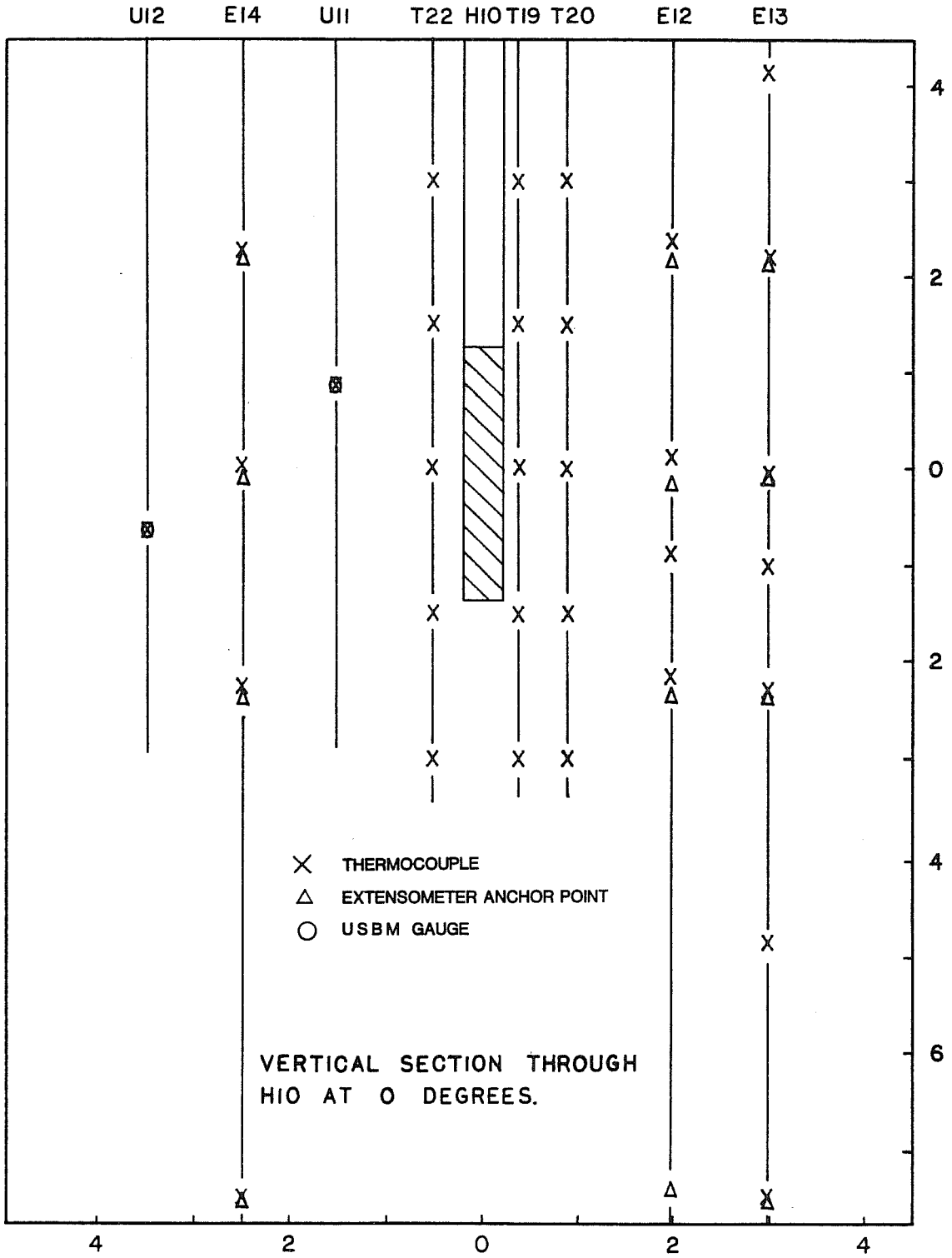
XBL 787-1982A (B)

Fig. A-4. Plan view of full-scale heater drift showing locations of heater and instrument boreholes.



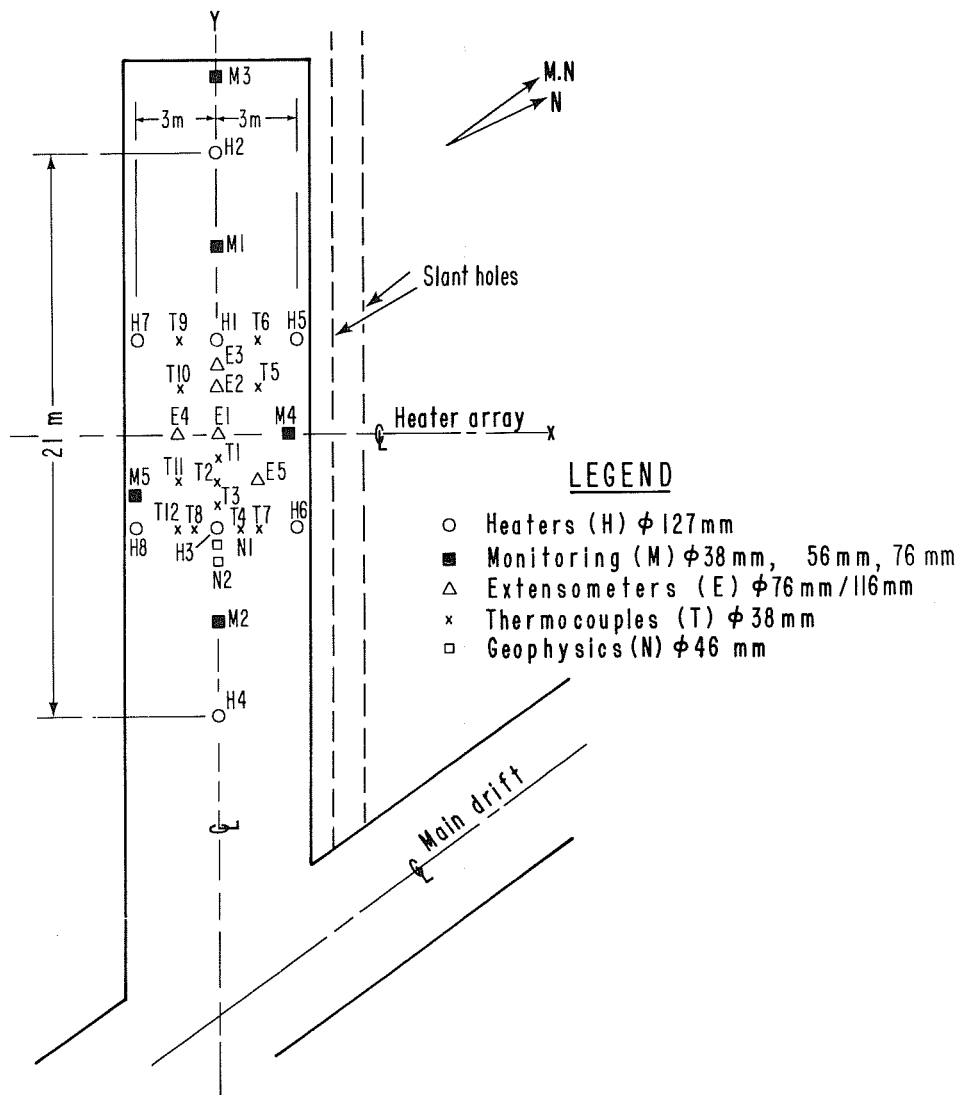
XBL 8011-12726

Fig. A-5. Vertical sections of full-scale heater drift and extensometer drift.



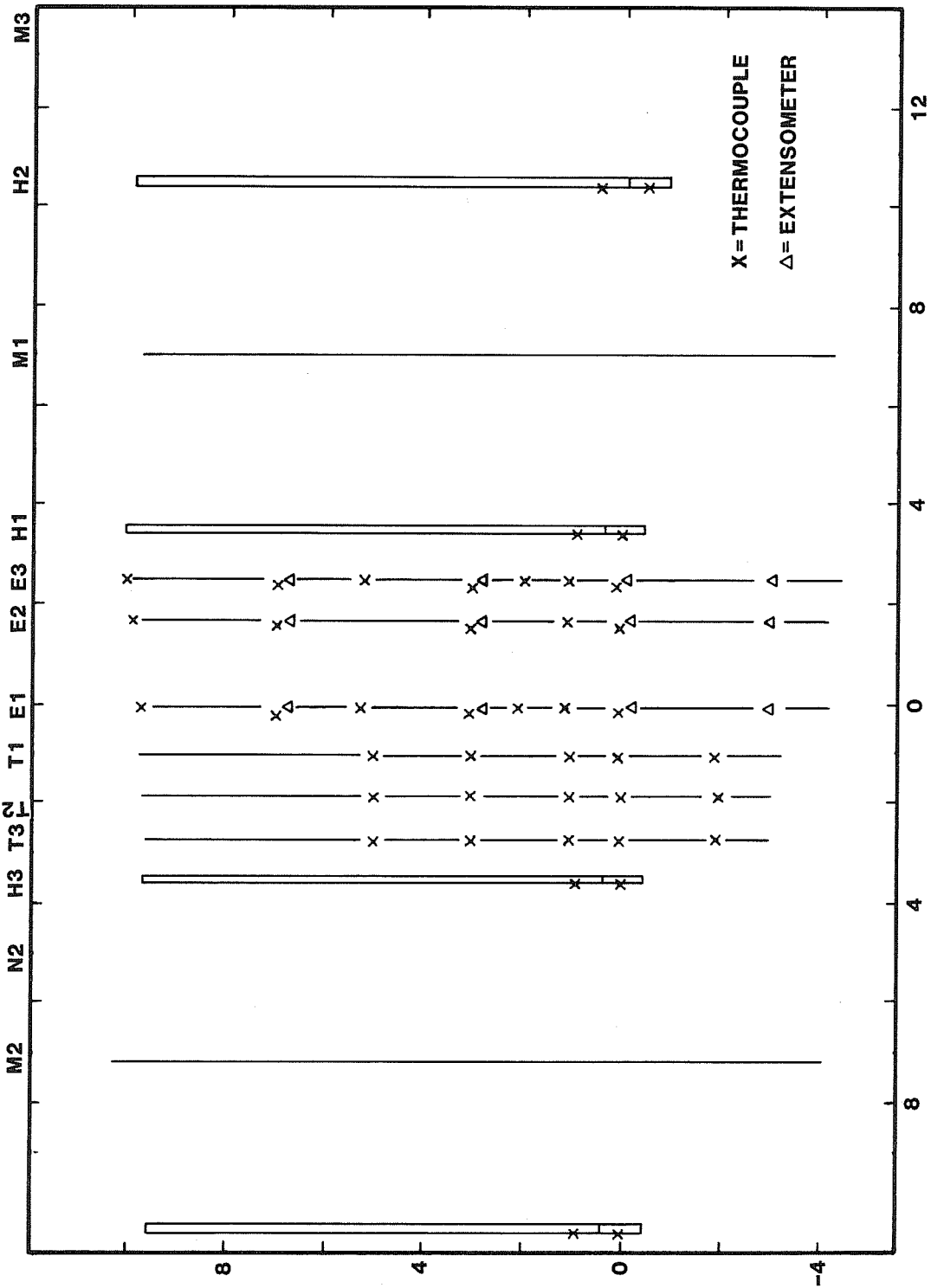
XBL 8011-12728

Fig. A-5. (continued).



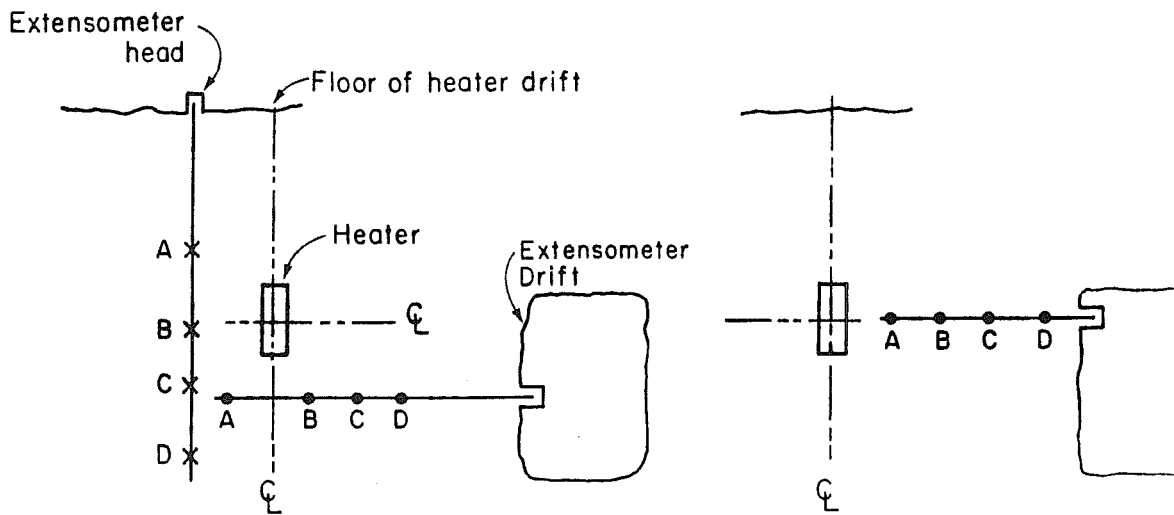
XBL 787-1986A

Fig. A-6. Plan view of time-scaled drift showing locations of heater and instrument boreholes.



XBL 8011-3991

Fig. A-7. Vertical section along axis of time-scaled drift.



Case I

Anchors cross a heater midplane

- Anchor points in horizontal hole
- x Anchor points in vertical hole

Case II

Anchors do not cross a heater midplane

XBL 798-1141

Fig. A-8. Extensometer anchor point designation.

APPENDIX B: PERFORMANCE OF STRIPA DATA ACQUISITION SYSTEM

TABLE OF CONTENTS

	<u>Page</u>
LIST OF ABBREVIATIONS	B-4
B.1 OVERVIEW	B-6
B.2 MAJOR EQUIPMENT PROBLEMS	B-10
B.2.1 Description of the Computer-Controlled DAS	B-10
B.2.2 Measurement Resolution	B-13
B.2.3 The Computer's Voltage Offset Problem	B-16
B.3 CALIBRATION OF DATA ACQUISITION SYSTEM COMPONENTS	B-21
B.3.1 Description of the Calibration Setup	B-21
B.3.2 Manufacturer's Performance Specifications of DAS Components	B-21
Fluke's 343A Voltage Calibrator	B-21
Fluke's 8500A Digital Voltmeter	B-24
Acurex's Autodata-Nine (AD-9) Data Logger	B-24
MODCOMP's Wide-Range Relay Analog-Input Subsystem (WRRAIS)	B-24
B.3.3 Observed Stability of DAS Components	B-29
AD-9 Stability	B-29
WRRAIS Stability	B-33
B&F Data Logger Stability	B-35
B.3.4 Calibration Results and Accuracies	B-35
AD-9 Calibration	B-35
WRRAIS Calibration	B-38
B.4 HISTORY OF THE WRRAIS's GAIN AND VOLTAGE OFFSETS	B-47
B.5 EVENT CHRONOLOGY	B-57
B.5.1 Reliability of the Data Acquisition System	B-57
B.5.2 Data Gaps and Errors	B-59
B.5.3 Instrument Operating History	B-69
REFERENCES	B-74

LIST OF ABBREVIATIONS

AC	Alternating Current
ADC	Analog-to-Digital Converter
AD-9	Autodata-Nine data logger manufactured by the Acurex Corp.
AIS	Analog Input Subsystem
BCD	Binary Coded Decimal
B&F	A data logger used with USBM gauges
CPU	Central Processing Unit of a computer
DAS	Data Acquisition System
DC	Direct Current
DCDT	A special LVDT containing hybrid circuits that provide signal conditioning for direct current input and output. A DC-LVDT, hence, DCDT
DVM	Digital Volt meter
D/A	Digital-to-Analog converter
f.s.	Full scale reading
IOIS	Input/Output Interface Subsystem
IRAD	IRAD Gage, Inc., Lebanon, New Hampshire
I/O	Input and Output
LBL	Lawrence Berkeley Laboratory
LSB	Least Significant Bit
LVDT	Linear Variable Differential Transformer displacement transducer
MODCOMP	Modular Computer Systems, Inc.
MTBF	Mean Time Between Failures
MTTR	Mean Time To Repair
MUX	Multiplexer
PCI	Peripheral Controller Interface
ppm	parts per million

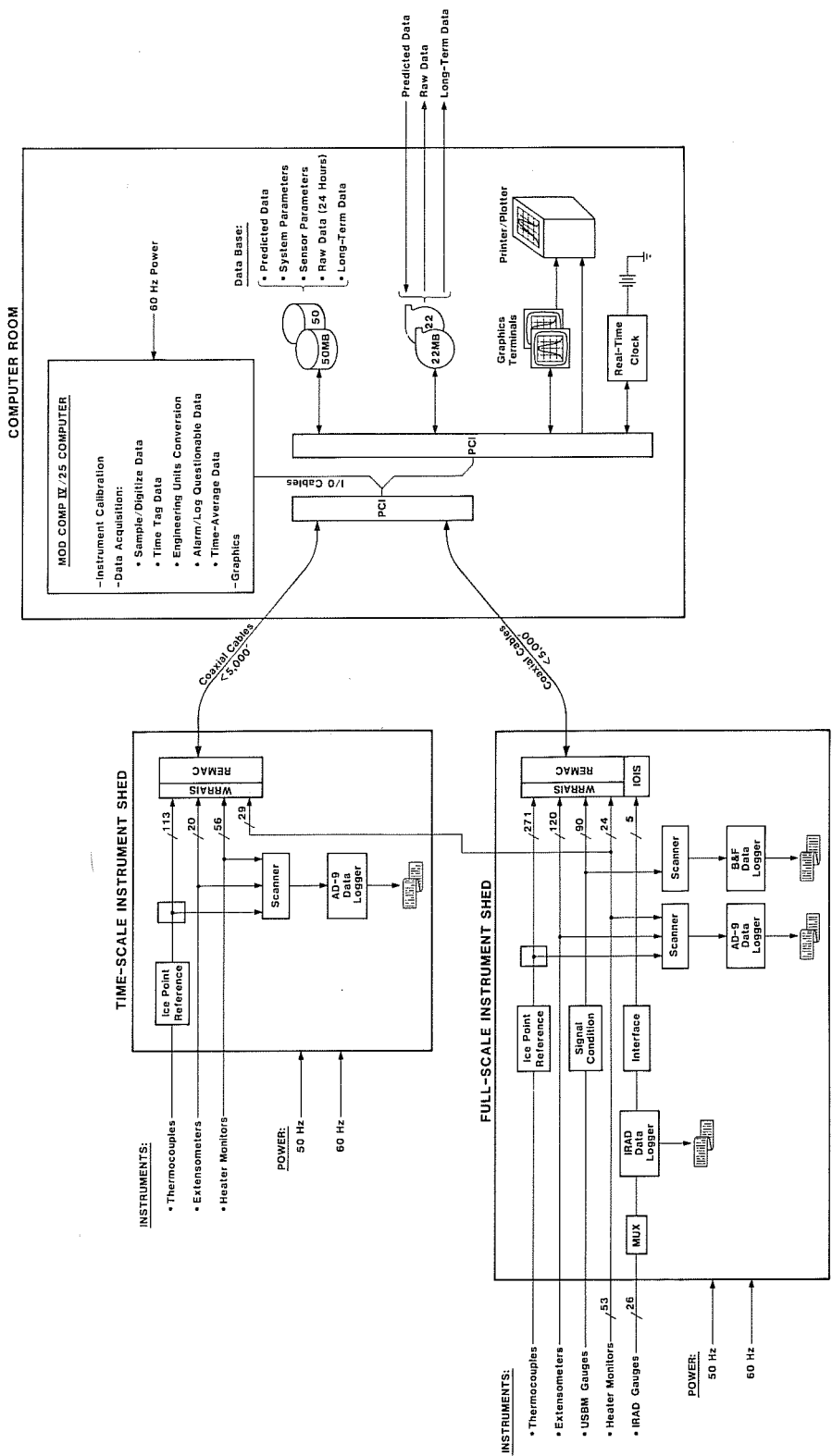
RC Filter	An electronic frequency filter constructed using resistors and capacitors
REMAC	Remote Data Acquisition Subsystem, manufactured by MODCOMP
rms	root-mean-square
RTD	Resistance temperature device-- a temperature-sensing transducer that changes in electrical resistance as a function of temperature
T.S.	Time Scale
USBM	United States Bureau of Mines
WRRAIS	Wide-Range Relay Analog-Input Subsystem, manufactured by MODCOMP

B.1 OVERVIEW

Data were acquired from more than 700 instrumentation channels at Stripa during a two year period using a computer as the primary data acquisition system and four data loggers as backup. The portions of the data acquisition system (DAS) that were physically located in the time-scaled and full-scale experiment drifts, and the software functions, on-line data base and major hardware subsystems are shown in Fig. B-1. McEvoy (1979) describes the data acquisition system in greater detail.

The computer acquired data from each active sensor at 15-minute intervals and logged this "raw" data on magnetic tape. Data were converted to engineering units, using preliminary calibrations, and time-averaged values were written to "long-term" data tapes. When raw data tapes became full, which took approximately two weeks, they were removed and air-mailed to Berkeley. The data loggers acquired data independently but in parallel with the computer and printed it on paper tape, providing a third permanent record. These unprocessed experimental data and associated calibration parameters were air-mailed to Berkeley on the long-term data tapes and reprocessed in Berkeley with changed engineering conversion algorithms after failure-induced changes in scale factors in the DAS were removed.

Voltage measurement errors of 110 μ V accumulated during the two years of operation. Errors were caused by component failures, drift, instability of the analog-to-digital conversion units, and maintenance activities. The data logger stability was better than the computer's analog section; offsets were negligible and gain was stable within 0.1%. As a result it was necessary to use selected data logger records as references to correct for spurious offset voltages and gain variations in order to improve long-term stability of the computer-collected data in the high-gain ranges.



XBL 8011-7433

XBL 8011-7433 A

Fig. B-1. Block diagram of the Stripa data acquisition system.

Before the experiments were started, the computer was used interactively to individually calibrate all USBM gauges, extensometers, and low-temperature (below 200°C) thermocouples. This was done in the mine after these instruments were wired in their final operating configuration. This technique was used to eliminate inaccuracies caused by small voltage offsets and board-to-board variations that occur throughout the data acquisition hardware and thus approach the accuracy of the reference standards used for calibration. Schrauf et al. (1979) provides additional instrument calibration information.

Several occurrences, listed chronologically in Table B-1, significantly affected the accuracy of the data acquired by the computer. On September 27, 1978 a capacitor failed in a power supply in the computer's time-scale Wide-Range Relay Analog-Input Subsystem (WRR AIS). This failure and circuit board changes caused offsets in voltage measurements subsequently acquired by the computer. A second factor that affected the accuracy of thermocouple data was discovered after the conclusion of the experiments. The temperature of the reference resistance temperature device (RTD) reference had an offset due to "self-heating" during the initial thermocouple calibrations. A third difference between the accuracy of the computer and the logger data was that the data logger's common-mode rejection was significantly better than the computer's.

As a result of these problems, the computer data has been adjusted. NBS calibration curves were used for the thermocouples and data logger data were used to establish when voltage offsets occurred and to aid in re-establishing improved WRR AIS scale factors for the time intervals between offsets.

Table B-1. Chronology of important events.

Date	Time	Julian Day	H9 Day	H10 Day	T.S. Day	Event Description
78 Jun 01	12:00	152			0	Eight (1.125 kW) time-scaled heaters turned on
78 Jun 02	11:00	153				First raw data available from the computer.
78 Jul 03	9:00	184		0		H10 (5 kW) full-scale heater turned on
78 Aug 24	14:00	236	0			H9 (3.6 kW) full-scale heater turned on
78 Sep 27						A failed capacitor, in the computer's data acquisition system, caused voltage offsets in acquired data
78 Nov 02						An unexplained voltage offset occurred in the full scale WRR AIS
79 Jan 23		23		204		Eight (1.0 kW) H10 peripheral heaters turned on
79 Mar 04		63		244		H10 peripheral heater power reduced to 0.85 kW/heater
79 Mar 07		63	196	247	280	Started rapping extensometers periodically to release stored displacements
79 Jun 05	10:45	156			369	Time-scaled heaters (0.55 kW) turned off
79 Jul 12	9:00	193		370 (0)		Time reset to zero for H10 experiment
79 Aug 01	10:00	213		394 (20)		H10 (5 kW) and peripheral heaters turned off
79 Sep 26	14:00	269	398			H9 (3.6 kW) heater turned off
79 Dec 03	13:00	337			550	Last raw data acquired for time scale experiment
80 Feb 27	15:15	58	552			End of H9 experiment
80 Feb 28	3:30	59		605 (231)		End of H10 experiment
80 Apr						Instruments recalibrated
80 Jun 13						Computer turned off

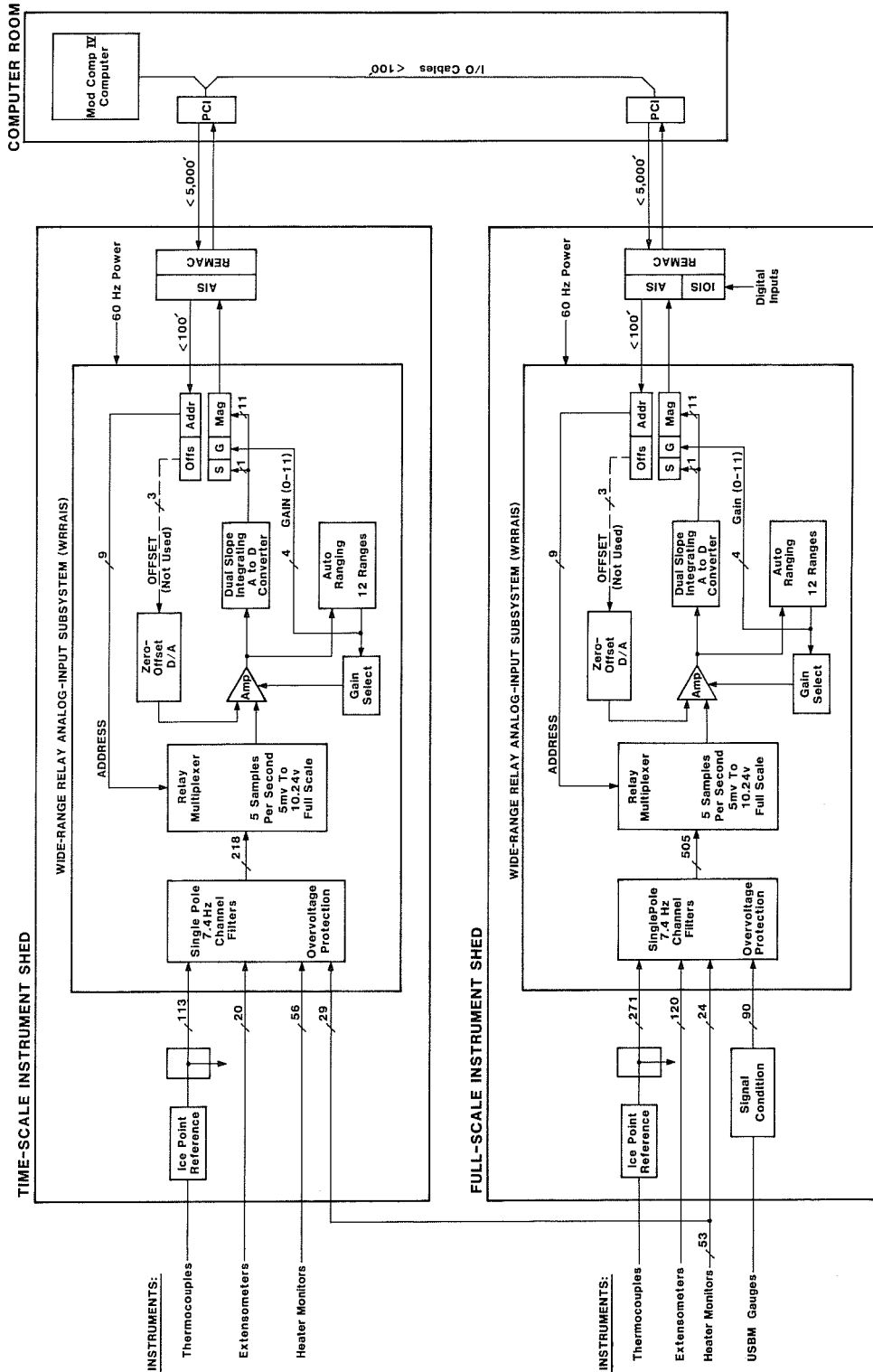
B.2 MAJOR EQUIPMENT PROBLEMS

B.2.1 Description of the Computer-Controlled DAS

Software in a MODCOMP IV/25 computer initiated the multiplexing, sampling, and digitizing of analog instrumentation signals from thermocouples, USBM gauges, extensometers, and heater monitors by using MODCOMP's Wide-Range Relay Analog-Input Subsystems (WRRAISSs). Separate WRRAISSs were located in the time-scale and full-scale instrument sheds, which were remote from the computer. MODCOMP's Remote Acquisition Systems (REMACs) were utilized to connect each remote WRRAISS with the computer. They, in effect, extend the computer's I/O bus to the remote instrument locations. Figure B-2 illustrates this setup.

The WRRAISSs used mercury-wetted relay switches to steer selected analog signals to its amplifier board. Automatic selection of a gain ranging from 1 to 2048, in twelve binary increments, provides increased resolution with a full-scale measurement capability from ± 5 mV to ± 10.24 V. A voltage comparator on the output of the amplifier determined if the output signal level was less than $\pm 3/8$ full scale. If less than this level, a gain counter was stepped to the next highest gain. This process was repeated until the output was greater than $\pm 3/8$ full scale, or until maximum gain was reached. This automatic gain selection results in the "operating range" limits shown in the right two columns of Table B-2.

The resulting amplified analog signal was digitized into an 11-bit magnitude-plus-sign binary value by utilizing a dual-slope integration technique. Integration over one or more full cycles of the 60-Hz power-supply frequency provided common mode rejection of 60-Hz noise. Amplifier



REL 8911-7435

Fig. B-2. Block diagram of the analog input portion of the computer-controlled data acquisition system.

Table B-2. WRRAIS's analog input voltage ranges.

GAIN CODE	FULL RANGE (mv)		OPERATING RANGE (mv)	
	Lower	Upper	Lower	Upper
0	+ 0	+ 5	+ 0	+ 3.75
1	+ 1	+ 10	+ 3.75	+ 7.50
2	+ 1	+ 20	+ 7.50	+ 15.0
3	+ 1	+ 40	+ 15.0	+ 30.0
4	+ 1	+ 80	+ 30.0	+ 60.0
5	+ 1	+ 160	+ 60.0	+ 120.0
6	+ 50	+ 320	+ 120.0	+ 240.0
7	+ 100	+ 640	+ 240.0	+ 480.0
8	+ 100	+ 1280	+ 480.0	+ 960.0
9	+ 300	+ 2560	+ 960.0	+ 1920.0
10	+ 500	+ 5120	+ 1920.0	+ 3840.0
11	+ 1000	+ 10240	+ 2840.0	+ 10240.0

over-ranging was detected and flagged as invalid data in the gain bits. These 12 bits of data, together with the 4 bits of gain information, were transmitted back to the CPU.

Full duplex (8.7 K 16-bit words per second) data transfers, between the CPU and the REMAC terminals, occurred over two coaxial-cable serial-links. A 7-bit character redundancy check was used to detect data transmission errors. System software automatically requested retransmission whenever transmission errors were detected.

B.2.2 Measurement Resolution

The analog-to-digital converter (ADC) of the WRRAISS could digitize both positive and negative voltages, so that functionally there were 24 possible gain ranges, as shown in Table B-3. The vertical bars in Table B-3 also show the voltage ranges spanned by the thermocouples, extensometers, and USBM gauges. Note that thermocouples and USBM gauges require only the three highest gain ranges of positive polarity. Most of the extensometers operated at fairly low gain settings (gain codes -7, -8, -9) during the experiment, but some produced low magnitude positive voltages.

The ADC used eleven bits plus one sign bit to digitally encode analog signals. Encoding resolution was determined by the magnitude of the least significant bit that was a function of gain. Table B-4 gives the voltage magnitude of the least significant bit and its corresponding magnitude when converted to temperature, linear displacement, or borehole displacement. The conversion factors used to convert voltages to engineering parameters are typical of the experiment. Note that the extensometers' resolutions were excellent on all ranges, with a worst case value of only 2.70 μm . Worst case

Table B-3. WRRAIS gain ranges and instrument operating bands.

Gain Code	Voltage Ranges (mV)		INSTRUMENT OPERATING RANGE		
	Lower	Upper	Extensometers	USBMS	Thermocouples
11	3840	10240			
10	1920	3840			
9	960	1920			
8	480	960			
7	240	480			
6	120	240			
5	60	120			
4	30	60			
3	15	30			
2	7.5	15			
1	3.75	7.5			
0	0.0	3.75			
-0	-3.75	0.0			
-1	-7.5	-3.75			
-2	-15	-7.5			
-3	-30	-15			
-4	-60	-30			
-5	-120	-60			
-6	-240	-120			
-7	-480	-240			
-8	-960	-480			
-9	-1920	-960			
-10	-3840	-1920			
-11	-10240	-3840			

initial USBM settings
range from 3 to 11 mV

490°
367°
188°
93°
10°

one extensometer (E11) was set initially in the -10 to -40 mV range

most extensometer settings range from -800 to -1400 mV

most extensometers operated on these ranges during experiment

Table B-4. Measurement resolution of thermocouples, extensometers, and USBM gauges imposed by the WRRAIS's 11-bit ADC.

Gain Code	Upper Voltage Limit(mV)	Least Significant bit LSB (mV)	Magnitude of LSB in engineering units		
			δT Temp ($^{\circ}C$)	δE Extensometer (μm)	δU USBM (μm)
0	5	0.0024	0.061	0.0052	0.16
1	10	0.0049	0.12	0.011	0.32
2	20	0.010	0.25	0.022	0.64
3	40	0.020	0.50	0.043	
4	80	0.039		0.084	
5	160	0.078		0.17	
6	320	0.156		0.34	
7	640	0.313		0.68	
8	1280	0.625		1.35	
9	2560	1.250		2.70	
10	5120	2.50			
11	10240	5.0			

$$\delta T(^{\circ}C) = 25 (^{\circ}C/mV) \times LSB$$

$$\delta E(\mu m) = 2.16 \mu m/mV \times LSB$$

$$\delta U(\mu m) = 64 \mu m/mV \times LSB$$

$$LSB = \text{upper voltage limit}/2^{11}$$

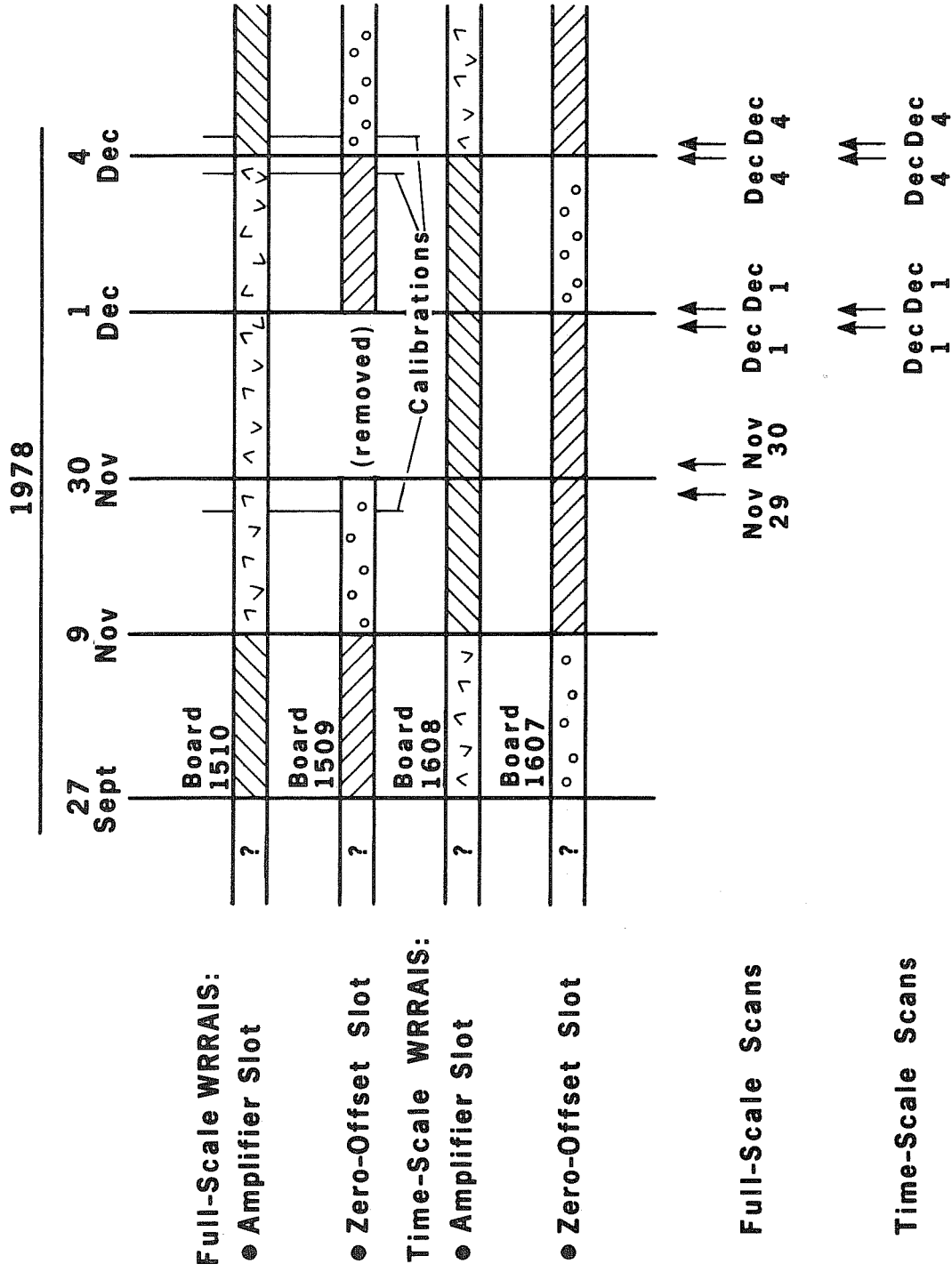
temperature resolution is 0.25°C on gain 2, which occurs only for temperatures greater than 188°C , where less precision can be tolerated. USBM gauge resolution is marginal, however, since most of those gauges operated on gain code 2 during the experiment where the resolution was 0.64 microns. This minimum step might well be discernible on some records.

B.2.3 The Computer's Voltage Offset Problem

On September 27, 1978, a capacitor failed in a power supply in the time-scale WRR AIS. "Amplifier" and "Zero-Offset" circuit boards were interchanged between the time-scale and full-scale WRR AISs to help isolate and identify the problems. An attempt was made to restore all boards to their original locations; however, significant voltage offsets remained in both the time-scaled and full-scale data. Another unexplained increase in the full-scale readings occurred on November 2, 1978.

Figure B-3 summarizes how and when the two amplifier and two zero-offset circuit boards were transposed among the amplifier and zero-offset slots in the time-scale and full-scale WRR AIS. The original board configuration is unknown, but the four symbols indicate the location of the four boards for which serial numbers are given in the first column. Note that time is not linear. All sensors were scanned and the full-scale WRR AIS was calibrated in late November and on December 4 and 6.

A reliable thermocouple, which would experience little temperature change during the experiment, was selected from each drift to establish the time and magnitude of the offsets. Full-scale thermocouple 478, at a radius of 8.1 m in horizontal hole E30 (H10 area), and time-scale thermocouple 910, in hole E3 at an elevation of 3 m above the midplane, were chosen. Tables B-5



XBL 8011-7434

Fig. B-3. History of circuit board changes between the full-scale and time-scale WRR AISs.

and B-6 contain the results of a careful inspection of the voltages from sensors 478 and 910. Whenever an offset occurred, the voltage and the time just before the switch are noted, followed by the first valid voltage and its time after the offset. The difference in offset voltage before and after the break is given in microvolts.

Several of these reported board changes produced no offsets in the data. The shift on November 2 occurred at midnight, on the full-scale system only, and is unexplained by a board shift. Likewise, the 20 μV shifts on both systems on January 16, 1979, were not explained by any known board shifts. An unexplained offset of 13 μV also occurred on September 28, 1979, on the full-scale system only.

Figure B-4 shows a plot of the AD-9 voltage overlaid with a plot of the difference between the WRRAIS's and the AD-9's voltage for full-scale thermocouple 478 and time-scale thermocouple 910. The smoothness of the AD-9 plots demonstrates the stability of the AD-9s and indicates that they can provide a reference against which the voltage stability of the WRRAISs can be compared. Additional justification is presented in Section B.3 of this Appendix.

The times and magnitudes of the offsets shown in Fig. B-4 are the same as those tabulated in Tables B-5 and B-6. Figure B-4 also shows the cumulative drift of the WRRAIS over the entire experiment. The range of offsets is 116 μV for the full-scale WRRAIS with a difference of about 60 μV between the beginning and the end of the experiment. This latter change is important because the instruments were calibrated using the WRRAIS before and after the experiment. The 60 μV offset translates into a temperature shift of approximately 1.5°C, which should show up as a difference in the thermocouple

Table B-5. Significant voltage offsets for full-scale thermocouple 478.

Date	Julian	Hours:Mins	mV	$\Delta V(\mu V)$	Comments
09/27/78	270	12:15 17:45	0.5029 0.5298	+ 27	Delete data from 12:30 to 17:30
11/02/78	306	00:00 00:15	0.5615 0.6079	+ 46	
11/09/78	313	11:15 11:45	0.6218 0.5054	-116	
12/04/78	338	13:15 13:45	0.5371 0.6152	+ 78	At 13:30: 0.6201, delete it
01/16/79	16	11:00 11:30	0.6030 0.6226	+ 20	At 11:15: 0.6104, delete it
09/28/79	271	13:45 14:00	0.776 0.789	+ 13	

Table B-6. Significant voltage offsets for time-scale thermocouple 910.

Date	Julian	Hours:Mins	mV	$\Delta V(\mu V)$	Comments
09/27/78	270	09:15 18:00	0.8789 0.8691	- 10	Delete from 9:30 to 17:45
11/09/78	313	10:45 11:30	0.8936 0.9668	+ 73	Delete from 11:00 to 11:15
12/04/78	338	13:15 14:15	0.9717 0.9033	- 68	
01/16/79	16	10:45 11:15	0.9009 0.9223	+ 21	

Data were deleted where a value differed from the average values before or after it.

calibrations. The results from time-scale are not as severe, with a total offset range of 80 μV , and a before and after shift of about 35 μV . The time-scale WRR AIS does show a monotonic drift during the first few months of the experiment of about 30 μV , which is not as apparent on the full-scale WRR AIS.

B.3 CALIBRATION OF DATA ACQUISITION SYSTEM COMPONENTS

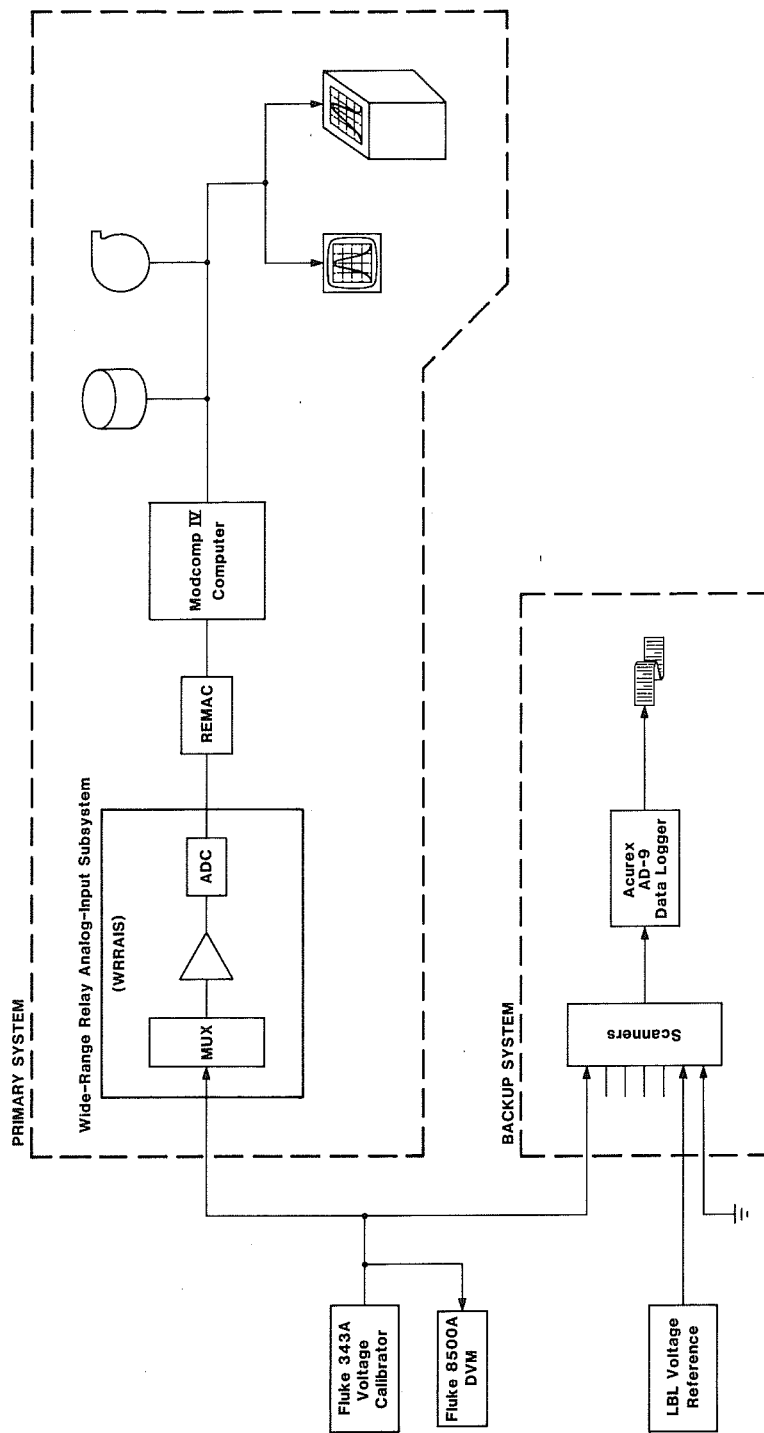
B.3.1 Description of the Calibration Setup

Figure B-5(a) illustrates the general hardware configuration used to calibrate the DAS in July 1979 and in February and June 1980. A more detailed diagram of the June 1980 calibration configuration is shown in Fig. B-5(b). Cabling for the last calibration differs from that for the first two calibrations by the inclusion of an ice point reference "signal splitter" to better simulate the actual operating configuration. This, however, appeared to have negligible affect on the calibration. For all calibrations a Fluke 343A dc voltage calibrator provided a precision voltage source that was applied to both the WRR AIS and AD-9 systems, and a Fluke 8500A digital voltmeter was used to accurately measure the input voltages provided by the 343A. Very close agreement was observed between the voltage settings on the 343A dials and the voltages read by the 8500A.

B.3.2 Manufacturer's Performance Specifications of DAS Components

Fluke's 343A DC Voltage Calibrator. Fluke's model 343A DC Voltage Calibrator provided 7-digit ($1\mu\text{V}$) resolution, output voltage from 0 to 1100 V (DC) with an accuracy of 20 ppm, combined ripple and noise of less than $50\mu\text{V}$ rms, and short-term jitter and other random excursions of less than 1 ppm. Current output limits from 1 to 30 mA could be set via a front panel control.

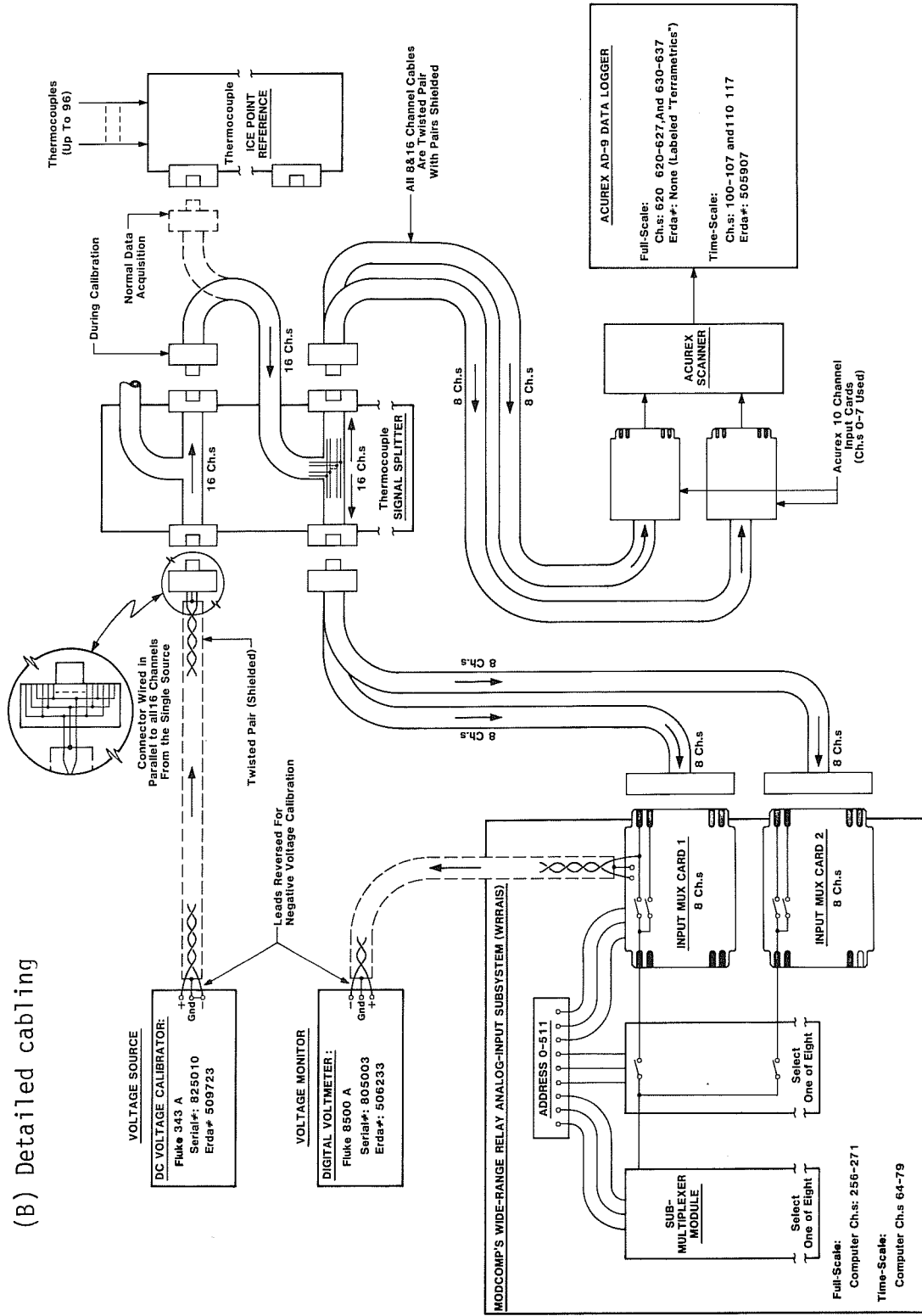
(A) General setup



XBL 8011-7437

Fig. B-5. Diagrams of the calibration setup: (A) General setup and (B) Detailed cabling.

(B) Detailed cabling



XBL 8011-7438

Fig. B-5. (continued).

Table B-7 provides additional specifications. Calibration in Sweden used only the 10-volt range.

Fluke's 8500A Digital Voltmeter. Fluke's 8500A Digital Voltmeter provided common mode rejection of 100 dB at 60 Hz with 1 k Ω imbalance and common mode noise rejection > 120 dB, dc to 60 Hz, with 100 Ω imbalance. Specifications of DC voltage input characteristics are provided in Table B-8 and its accuracy is specified in Table B-9.

Acurex's Autodata-Nine (AD-9) Data Logger. The specifications for the Acurex Autodata-9 data logger are provided in Table B-10.

MODCOMP's Wide-Range Relay Analog-Input System. The following performance specifications for Modcomp's WRR AIS apply to an ambient temperature of 25°C, unless otherwise specified.

The WRR AISs digitized and encoded bipolar analog inputs into 11-bits magnitude plus a sign bit. The resolution of the least significant bit depended on which gain (encoded in 4 bits), or voltage range, was used (see Table B-4). Characteristics of the WRR AIS's guarded differential inputs are specified in Table B-11.

The WRR AIS also provides a zero-offset feature that permits a user to digitally specify a voltage to be treated as zero while centering the WRR AIS's full precision and ± 10.24 V range at the specified voltage. This capability was not used explicitly at Stripa; however, the associated circuit boards were installed and did affect the accuracy and stability of the system. Specifications for these zero-offset circuits are shown in Table B-12. The large ± 5 μ V drift per day, specified for the WRR AIS's ± 5 mV range, may

Table B-7. Specifications for the Fluke 343A DC voltage calibrator.

	Range [Volts]	Fluke 343A
Accuracy for 90 days	10	$\pm 0.002\%$ of setting or $\pm 0.0002\%$ of range*
	100	$\pm 0.002\%$ of setting or $\pm 0.0001\%$ of range*
	1000	$\pm 0.002\%$ of setting or $\pm 0.0001\%$ of range*
Resolution	10	1 μ V
	100	10 μ V
	1000	100 μ V
Stability at 23°C $\pm 1^\circ$ C	10	per hr. $\pm 0.005\%$ of setting or 5 μ V* per mo. $\pm 0.0015\%$ of setting or 15 μ V* per 6 mo. $\pm 0.0025\%$ of setting or 30 μ V*
	100	per hr. $\pm 0.0005\%$ of setting or 10 μ V* per mo. $\pm 0.0015\%$ of setting or 25 μ V* per 6 mo. $\pm 0.0025\%$ of setting or 40 μ V*
	1000	per hr. $\pm 0.0005\%$ of setting or 20 μ V* per mo. $\pm 0.0015\%$ of setting or 50 μ V* per 6 mo. $\pm 0.0025\%$ of setting or 60 μ V*
Temperature Coefficient	10	+15°C to +35°C: (3 ppm of setting + 0.1 ppm of range + 2 μ V)/°C
	100	0°C to 50°C: (5 ppm of setting + 0.1 ppm of range + 2 μ V)/°C
Output Current		0 to 25mA
Settling Time		Within 15 ppm of final output in 5 sec.
Ripple & Noise (All Frequencies)		< 50 μ V rms
Regulation		< 0.0005% of setting + 25 μ V for a 10% line voltage change or a full load change
Isolation		Output may be floated 500V dc from chassis

*Whichever is greater

Table B-8. Input characteristic specifications for the Fluke 8500A DVM.

Range	Full Scale	Normal Resolution	Resistance
100 mV	312 mV	1 μ V	>10,000 M Ω
1V	2.5V	10 μ V	>10,000 M Ω
10V	20V	100 μ V	>10,000 M Ω
100V	160V	1 mV	10 M Ω
1000V	1200V	10 mV	10 M Ω

Table B-9. Accuracy specifications for the Fluke 8500A DVM.

6-1/2 Digit accuracy: \pm (% of input + no. of digits)

Range	24 Hours 23°C \pm 1°C	90 Days 18°C to 28°C	1 Year 18°C to 28°C	Plus Temp Coefficient per °C (2)
100 mV(1)	0.002+4	0.003+5	0.005+8	0.0003+0.5
1V	0.001+6	0.002+8	0.004+9	0.0003+0.1
10V	0.0006 or 6*	0.001+8	0.002+9	0.0002+0.5
100V	0.001+6	0.002+8	0.004+9	0.0003+1
1000V	0.001+6	0.002+8	0.004+9	0.0003+0.5

*Whichever is greater

(1) 5-1/2 digit accuracy on lowest range
(2) 18°C to 0°C and 28°C to 50°C

Table B-10. Specifications for the AD-9 data logger.

Characteristic	Specification
Temp Stability	± 20 ppm of reading ± 0.25 $\mu\text{V}/^\circ\text{C}$
Time Stability	100 ppm of reading/month for 1st six months improving to 50 ppm/month thereafter
Repeatability	± 1 count ± 2 μV in addition (so on 100 mV scale, repeatability is ± 3 μV)
Initial Calibration Accuracy	± 50 ppm of full scale ± 50 ppm of reading at 25°C (includes scanning, $\pm 10\%$ ac power variations, and linearity)

Table B-11. General input specifications for the WRR AIS.

Characteristic	Specification
Maximum Input:	
Common Mode Voltage (CMV)	± 10 V peak operating
Signal Plus CMV	± 12 V peak operating
Over voltage	± 15 V without damage
Differential Input Impedance	10 megohms minimum
Differential Source Impedance	1000 ohms maximum
Common Mode Source Impedance	100 ohms maximum

Table B-12 Specifications for the WRAIS's zero-offset feature.

f.s. INPUT (mV)	GAIN	SETABILITY (±% f.s.)	DRIFT/°C (±% f.s.)	DRIFT/DAY (±% f.s.)
±5	2048	.1	.06	.1
±10	1024	.05	.03	.05
±20	512	.04	.02	.03
±40	256	.03	.01	.02
±80	128	.025	.01	.01
±160	64	.05	.02	.005
±320	32	.04	.01	.005
±640	16	.03	.005	.005
±1280	8	.025	.005	.005
±2560	4	.04	.01	.005
±5120	2	.03	.005	.005
±10240	1	.025	.005	.005

explain much of its instability.

Additional WRR AIS specifications appear in Tables B-13, B-14, and B-15.

B.3.3 Observed Stability of DAS Components

AD-9 Stability. The stability and accuracy of the two AD-9 data loggers are crucial because logger records were used to compensate for errors induced in the computer's data by problems with its WRR AISs. Logger performance was checked twice during the heater experiments. The loggers continuously recorded both a reference voltage from external sources and zero-volt references from shorted input terminals. The AD-9s were also calibrated using an external voltage source and the Fluke DVM. These two checks, with emphasis on the 0 to +15 mV ranges, quantify the AD-9's stability.

The temperature-compensated voltage reference units were built by LBL. Table B-16 lists their output voltages measured before and after the heater experiments. These measurements, made with the Fluke DVM, indicate that the drifts were 1 and 10 μV for the time-scale and full-scale reference sources, respectively.

Figure B-6 shows the reference voltages recorded by the data loggers, which indicate that drift occurred. Full-scale drift amounts to about 40 μV and time-scale drift about 60 μV . The same reference voltages recorded in parallel on other data logger channels agreed to within one or two microvolts. The stability of the calibrator source voltage, shown in Table B-16, indicates that the AD-9 data loggers drifted rather than the source voltage

Table B-13. General output specifications for the WRR AIS.

Characteristics	Specification
Voltage Range	± 10.24 volts
Drive Capability	± 5 mA max.
Capacitive Load	100 pF max.
Output Impedance	0.5 ohm max.
Gain:	
Setability @ f.s.	$\pm .01\%$
Drift/ $^{\circ}$ C	$\pm .002\%$
Drift/Month	$\pm .01\%$
Gain Dispersion:	
Gains 1 through 2048	$\pm .12$
Gains 8 through 2048	$\pm .03$
Drift/ $^{\circ}$ C	$\pm .001\%$
Linearity (Straight line between zero and full scale):	
@25 $^{\circ}$ C	$\pm .01\%$ f.s.
Drift/ $^{\circ}$ C	5 PPM f.s.
Drift/Month	$\pm .005\%$ f.s.
Settling time (including gain switching)	35 μ sec. max. time to settle within $\pm .02\%$ of final value for full scale step input.
Small Signal Bandwidth	100 KHz min.
Overload Recover	Output will settle to within $\pm .05$ f.s. in 50 μ sec for 200% overload, regardless of gain settings.

Table B-14. Peak 3-sigma output noise specification for the WRRAIS.

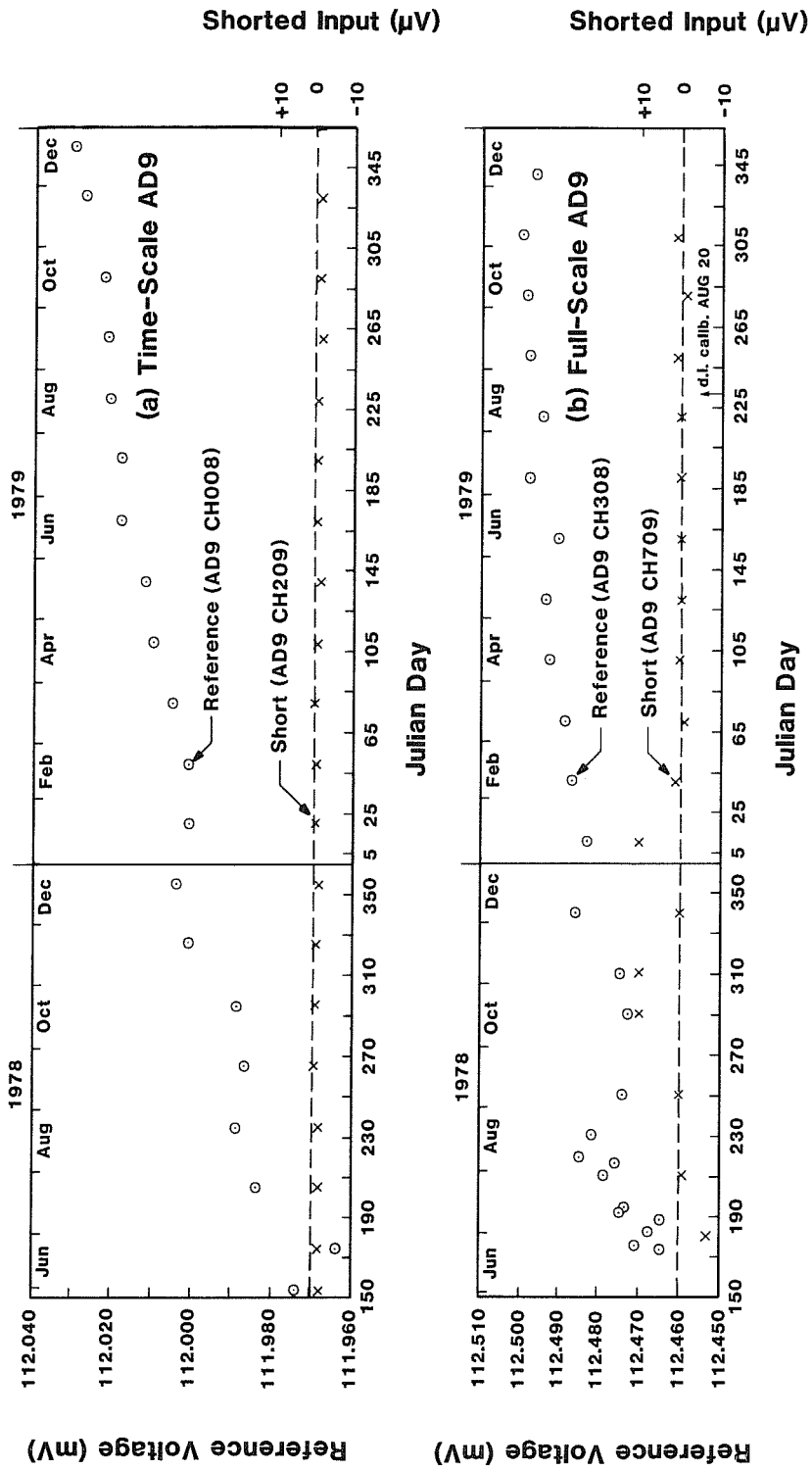
RANGE (MV)	GAIN	PEAK NOISE 1 Hz to 5 KHz (±% f.s.)	PEAK NOISE 1 Hz to 100 KHz (±% f.s.)
±5	2048	.1	.3
±10	1024	.05	.15
±20	512	.03	.10
±40	256	.02	.06
±80	128	.01	.03
±160	64	.03	.10
±320	32	.02	.06
±640	16	.01	.03
±1280	8	.005	.015
±2560	4	.02	.06
±5120	2	.01	.03
±10240	1	.005	.015

Table B-15. Common mode rejection (CMR), from DC to 60 Hz, for the WRRAIS.

RANGE	GAIN	CMR
±5 MV to ±80 MV	128 to 2048	120 db
±160 MV to ±1.28 V	8 to 64	90 db
±2.56 V to ±10.24 V	1 to 4	70 db

Table B-16. Reference output voltages, measured with the Fluke 8500A DVM.

Voltage Reference #	Location	Pre-burn-in 4 Jan 78 at LBL (mV)	Post-burn-in 18 Jan 78 (mV)	Final 24 Apr 80 at Stripa (mV)	Final(-) Initial (µV)	Final(-) Post- burn-in (µV)
-1	time-scale	111.962	111.978	111.979	17	1
-2	full-scale	112.408	112.424	112.414	6	-10
-3	stored in Lulea drift	114.086	114.100	114.100	14	0



XBL 8011-7439

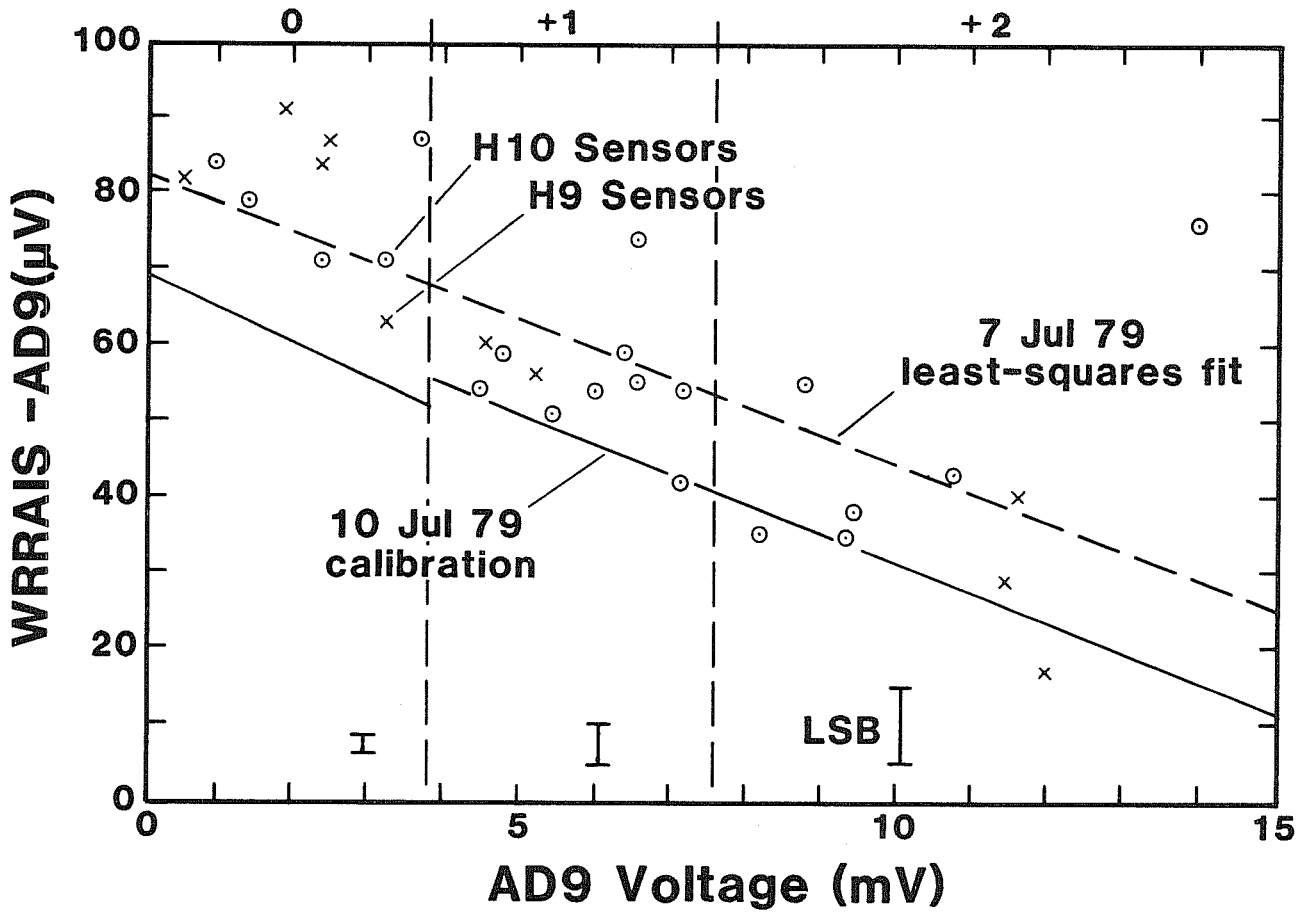
Fig. B-6. Reference voltage and shorted input for: (A) Time-scale AD-9 and (B) Full-scale AD-9.

with the exception of a negative $10\mu\text{V}$ drift in the reference voltage source used with the full-scale AD-9. This brings the total drift in the full scale AD-9 up to $50\mu\text{V}$, nearly equivalent to the $60\mu\text{V}$ drift monitored in the time-scale AD-9. Calibrations discussed in the next section furnish additional evidence that this was the case.

The zero voltage reference is also shown in Fig. B-6, denoted by the symbol x. On the time-scale data logger, all voltages were within $2\mu\text{V}$ of zero. The full-scale data logger recorded a few readings of 10 microvolts, but these occurred when the data logger precision was reduced and thus may be a recording error. Other channels recorded from shorted input terminals showed the same behavior as the ones in Fig. B-6, to within $2\mu\text{V}$.

WRR AIS Stability. Three calibrations were performed on the computer's full-scale and time-scale WRR AISs. Results from one of these calibrations are shown in Fig. B-7 as differences between the full-scale WRR AIS and AD-9 voltage readings as a function of input voltage. The dashed line is a least-squares fit to the differences between full-scale WRR AIS and AD-9 thermocouple data collected during regular experiment data acquisition on July 7, 1979. The slopes (gain factors) are very close and the offsets differ by about $13\mu\text{V}$. It was discovered later (June, 1980) that a peculiarity of the WRR AISs results in a downward offset of about $14\mu\text{V}$ when computer readings are taken in rapid succession as done by the calibration program. Taking this into account effectively moves the calibration line in Fig. B-7 upward so that it overlays the least-squares fit within a few microvolts. This match is sufficiently close to verify the validity of using the AD-9 data to track the WRR AIS deviations. As a result of this comparison,

WRRAIS Gain Code



XBL 8011-7440

Fig. B-7. Difference between WRRAIS and AD-9 voltages from full-scale thermocouples on July 7, 1979.

the history of the WRRAIS's gain and voltage offsets was established as described in section B.4.

B&F Data Logger Stability. USBM gauges produced low-level strain gauge signals that were conditioned and fed into the full-scale WRRAIS and a B&F data logger. The B&F data logger provided internal storage for separate gain and voltage offsets for each channel. The long term stability of these stored constants is questionable; therefore, the B&F data were not used to analyze problems with the full-scale WRRAIS. Table B-17 illustrates large fluctuations in the B&F's readings of three relatively constant instrumentation power supply voltages.

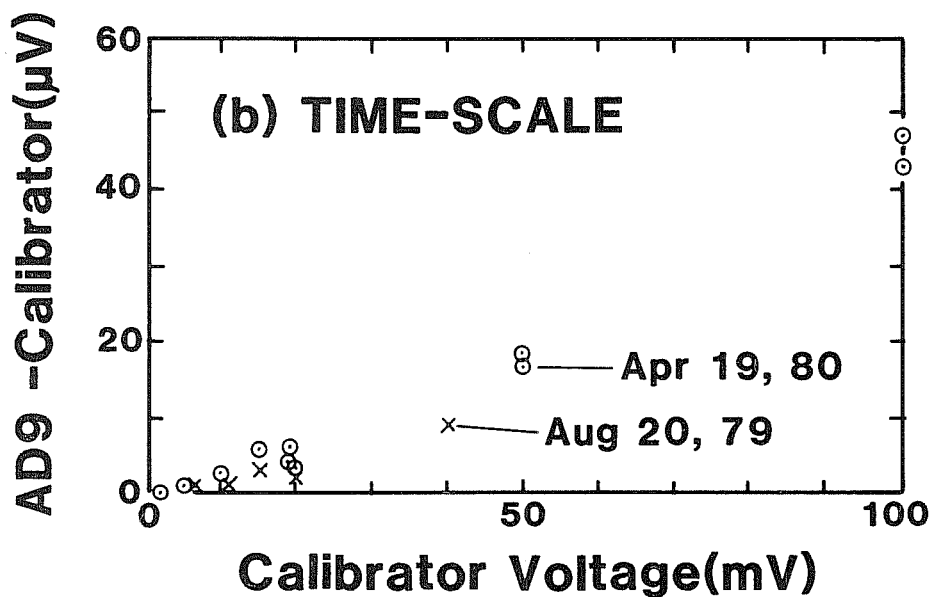
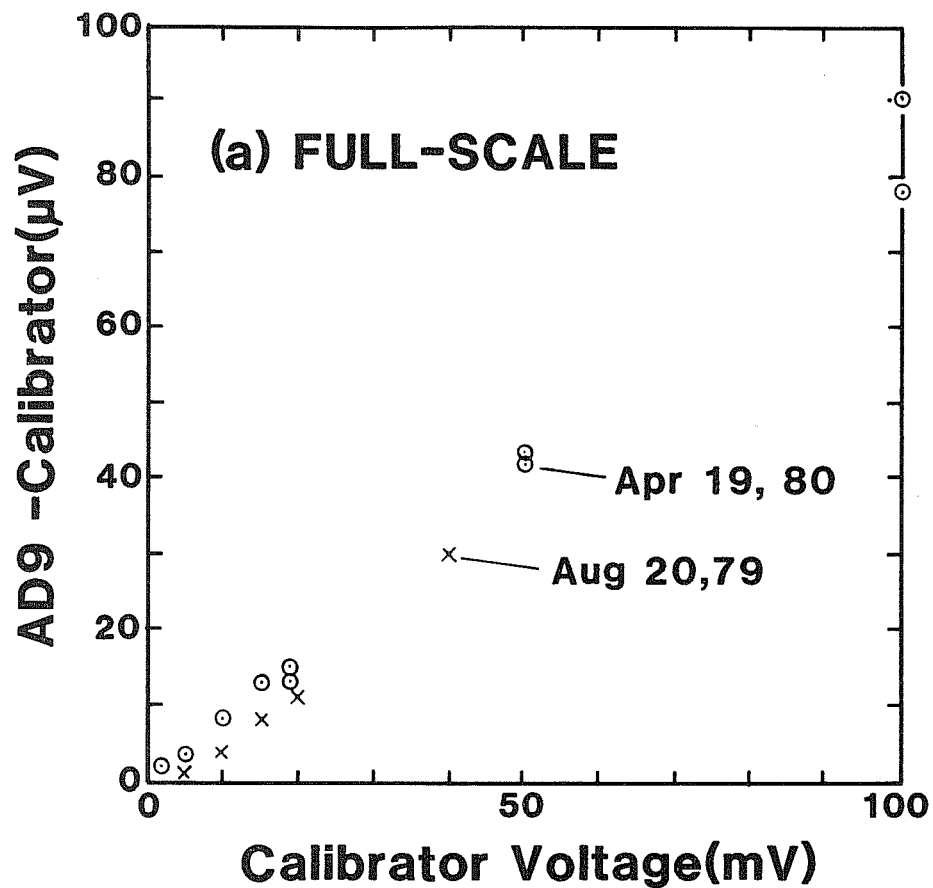
B.3.4 Calibration Results and Accuracies

AD-9 Calibration. Both the full-scale and time-scale AD-9s were calibrated in August 1979 and again in April and June 1980. In all three calibrations, the procedure was to monitor the input voltage with the Fluke 8500A DVM. Figure B-8 compares results from the first two calibrations over the range of zero to +100 mV. Several observations can be made from Fig. B-8:

1. Both AD-9s showed a positive deviation that increases almost linearly with the input voltage. The deviation of the full-scale AD-9 is almost twice as great as the time-scale AD-9.
2. The deviation has increased between the August 1979 and April 1980 dates. The direction of the deviation increase is the same as that shown in Fig. B.6.
3. The magnitude of the errors recorded on the calibrations in Fig. B-8 at +100 mV input is roughly the same as that indicated by the

Table B-17. B&F data logger voltage readings.

DATE Month/Day	Time	3 "Reference" Voltages		
		Strain Gauge Supply Voltage Ch 66 [V]	Extens. DCDT Voltage ~ ÷ 2 Ch 67 [V]	Isolated 2nd Extens. DCDT Voltage Ch 68 [V]
8/02/79	12:00	3.790	5.296	6.053
8/03	12:00	3.794	5.301	6.061
8/05	00:00	3.787	5.292	6.051
8/15	12:06	3.781	5.288	6.042
8/24	07:00	3.798	5.303	6.053
10/15	13:09	3.802	5.307	6.060
10/24	06:46	3.800	5.303	6.058
10/25	10:00	3.805	5.307	6.064
10/26	02:00	3.796	5.298	6.054
11/06	02:00	3.800	5.298	6.058
11/16	12:00	3.801	5.300	6.054
11/26	11:00	3.802	5.304	6.052
12/06	11:00	3.800	5.302	6.049
1/07/80	14:00	3.812	5.309	6.070
1/18	10:27	3.821	5.319	6.075
1/27	13:00	3.809	5.307	6.068
2/04	11:00	3.829	5.329	6.089
2/09	10:00	3.819	5.315	6.076
2/14	10:00	3.830	5.332	6.091
2/19	12:00	3.853	5.355	6.113
2/20	11:00	3.819	5.320	6.080
2/21	03:00	3.813	5.313	6.072



XBL 8011-7441

Fig. B-8. Calibrations of: (A) Full-scale and (B) Time-scale AD-9's in Aug. 79 and Apr. 80.

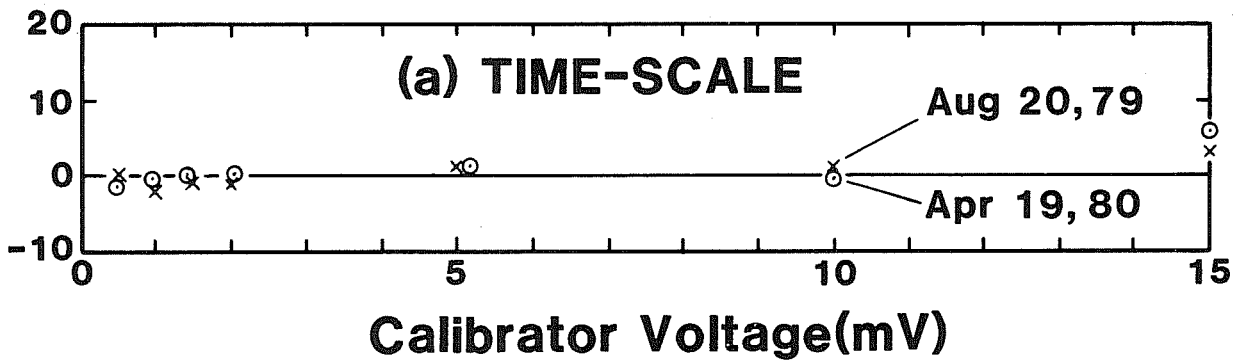
drift recorded using the reference voltage in Fig. B-6. That is, the 80 to 90 μV error found in the respective full-scale and time-scale AD-9s are roughly comparable to the 50 μV and 60 μV drifts found by monitoring the 112 mV reference voltages with the AD-9s and taking into account the 10 μV drift in the full-scale reference voltage. It should be noted that the full-scale AD-9 with the largest errors detected during calibrations was the older of the two data loggers and had been used for instrument calibrations in the United States during the year prior to installation in Sweden. The general agreement between the error found in calibrations and the drifts provides a reasonable basis for concluding that the AD-9s were responsible for the drifts shown in Fig. B-6.

These observations indicate that the drift of the AD-9 loggers is roughly proportional to the input voltage and will introduce a maximum error of about 0.1% over this range.

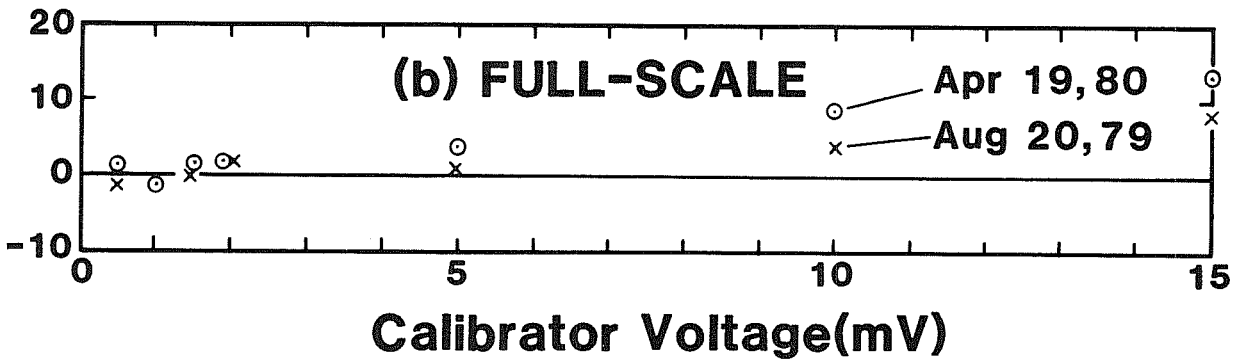
Fortunately, the 100 mV level was not used much in recording data at Stripa. Zero to +15 mV is the critical range for both thermocouples and USBM gauges; hence, Fig. B-9 displays the same calibration results for this range on an expanded scale. All deviations are less than 15 μV and decrease with decreasing input voltage. Such levels of error in these voltage ranges do not significantly affect the measurements at Stripa. Hence, the AD-9 data loggers were sufficiently accurate and stable so that their records were used to correct and compare the data acquired by the WRRAISs.

WRRAIS Calibration. Both the full-scale and time-scale WRRAISs were calibrated three times in Stripa in order to better understand problems that

AD9 - Calibrator(μ V)



AD9 - Calibrator(μ V)



XBL 8011-7442

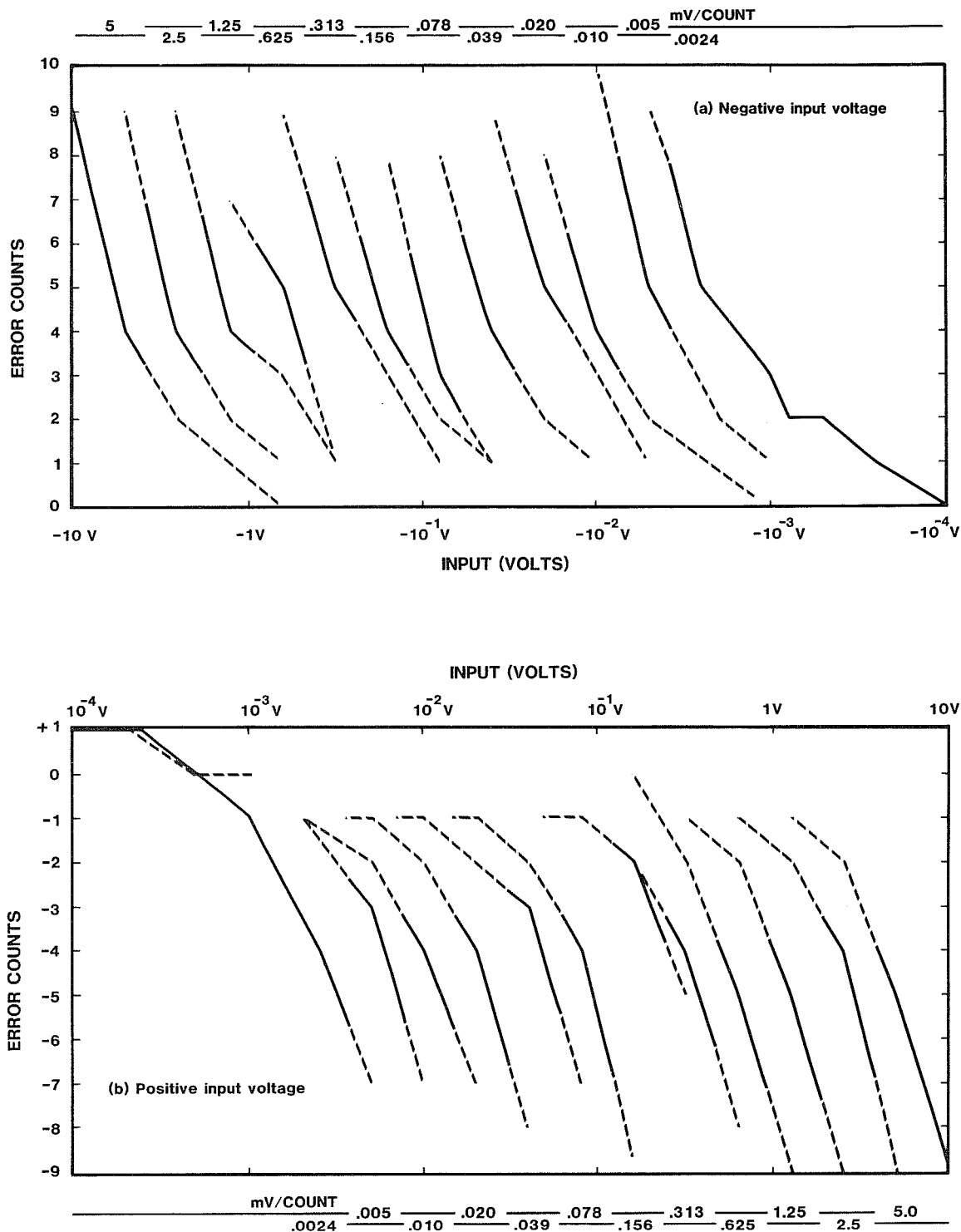
Fig. B-9. Expanded scale for calibration of: (A) Time-scale and (B) Full-scale AD-9's in Aug. 79 and Apr. 80.

occurred during data acquisition. Their calibrations took place in July 1979 and in February and June 1980. The calibration setups are shown in Fig. B-5.

These calibrations showed that the WRRRAISs were not functioning according to their specifications, listed in section B.3.2. The full-scale WRRRAIS was found to have particularly large voltage offsets and gain errors on all gains (as shown in Fig. B-10). Both the July '79 and February '80 calibration data were interpreted and an assessment made of the impact of the WRRRAIS's performance upon the temperature, displacement, and USBM gauge data. The IRAD channels bypass the WRRRAIS and are not relevant to its problems.

Most instrumentation was calibrated through the WRRRAIS; thus, those instrument calibrations incorporate the original WRRRAIS deviations. Only changes that occurred between the time of instrument calibration and subsequent WRRRAIS calibrations affected the data. Hence, the deviations plotted in the figures should represent maximums that occurred during the experiment.

A special computer program was written for the July 10, 1979 calibration of the WRRRAISs. The program requested manual entry of the Fluke DVM's reading. It then scanned full-scale WRRRAIS channel 345 and time-scale WRRRAIS channel 145 fifty times each and averaged those readings. Deviations between these averaged WRRRAIS readings and the fluke DVM's input readings were recorded. This procedure was repeated 16 to 20 times on each of the 12 gain ranges of the WRRRAIS. This same calibration test was repeated in February 1980.



XBL 8011-7443

Fig. B-10. Error counts vs: (A) Negative input voltages and (B) Positive input voltages for the full-scale WRR AIS with zero-offset board removed.

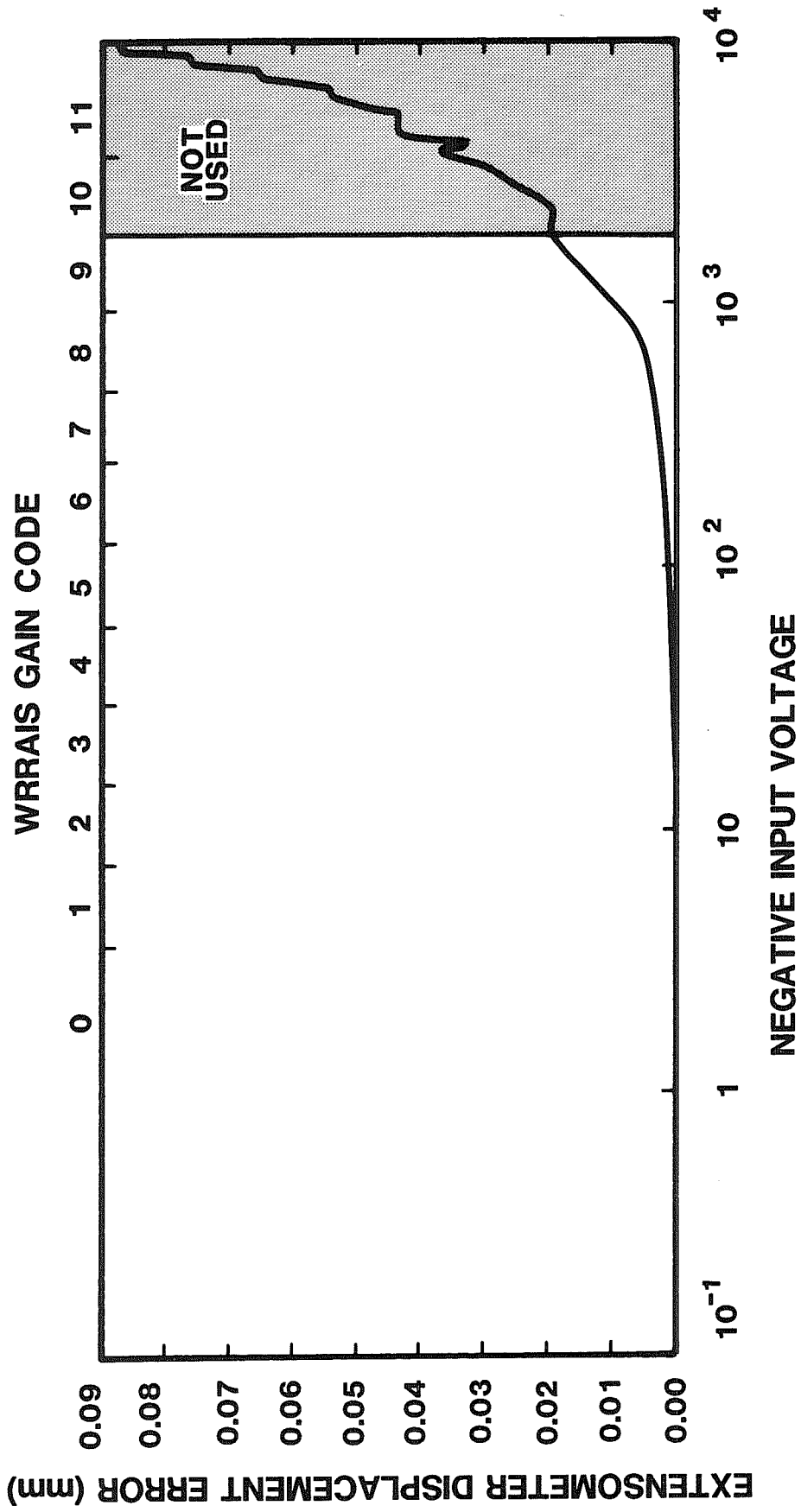
Figures B-11, B-12, and B-13 summarize the calibration errors of the full-scale WRRAISs in engineering units for three sensor types. In each case, the instrument error is obtained by multiplying the voltage deviation, found in the calibrations, by a scale factor for a representative sensor of that type.

- a. Extensometers. Figure B-11 shows the displacement errors (mm) computed from $\Delta E (\mu\text{m}) = 2.1669 \times \Delta V(\text{mV})$. The error climbs to almost 90 microns at the maximum voltage of -10 volts but is not significant because the operating range of the extensometers, as shown in Table B-3, does not include voltages that would require the use of gain ranges 10 and 11. Hence, it appears that any contribution of the WRRAIS to extensometer errors cannot exceed 20 microns, which is of little concern.
- b. USBM gauges. Calibrations for gain codes 0, 1, and 2, are plotted in Fig. B-12. The voltage deviation ranges from -25 to +75 μV , corresponding to borehole displacement errors computed from:

$$\Delta u (\mu\text{m}) = 64 \times \Delta V (\text{mV}).$$

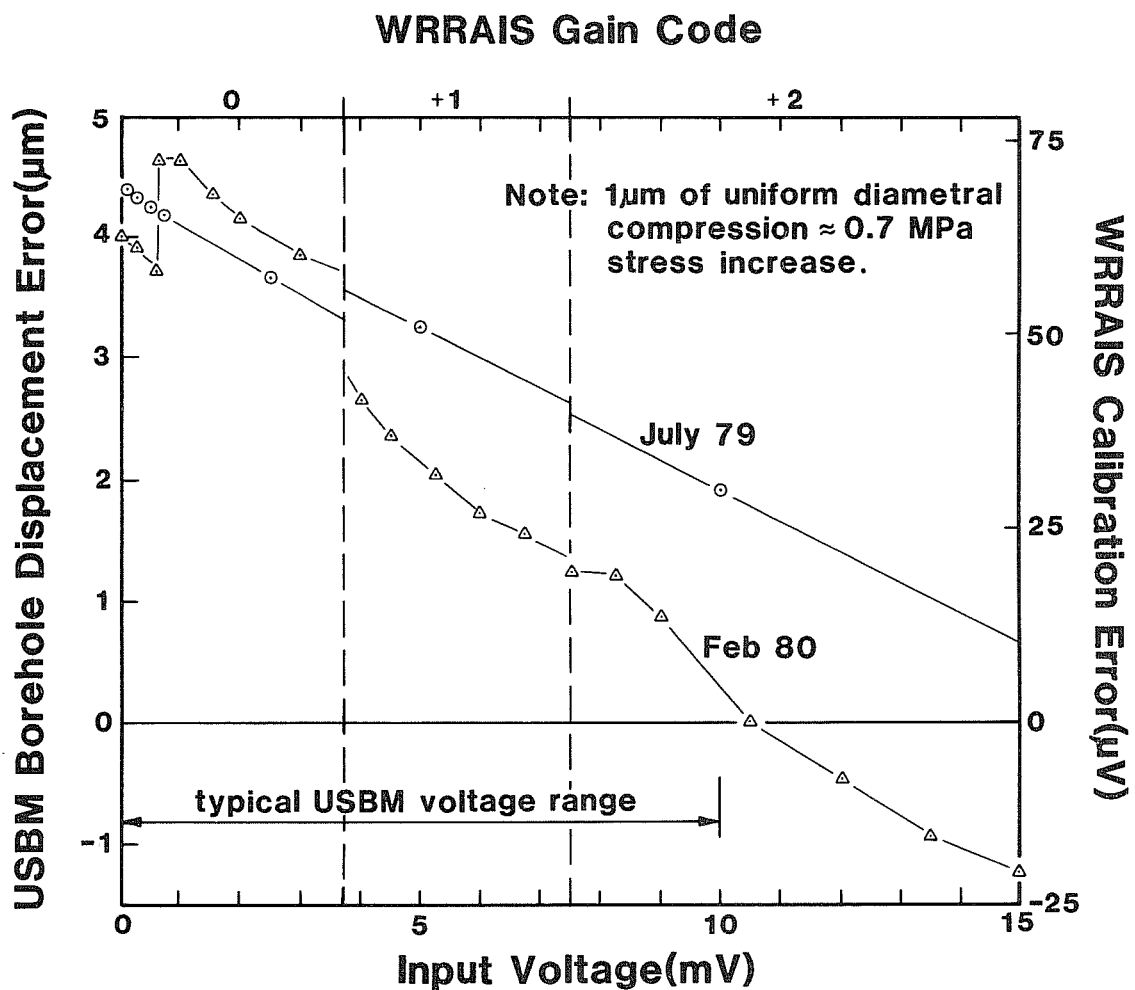
These errors range as high as 4 microns and are clearly a potential source of trouble for the USBM measurement. Especially troublesome is the difference between the two calibrations of July and February, which produce a 1.5 micron uncertainty. This uncertainty corresponds to a stress change of about 1 MPa, which is a precision needed from the stress gauges.

The February 1980 calibration on Fig. B-12 shows a jump of more than 10 μV in gain code 0 range. This offset is probably



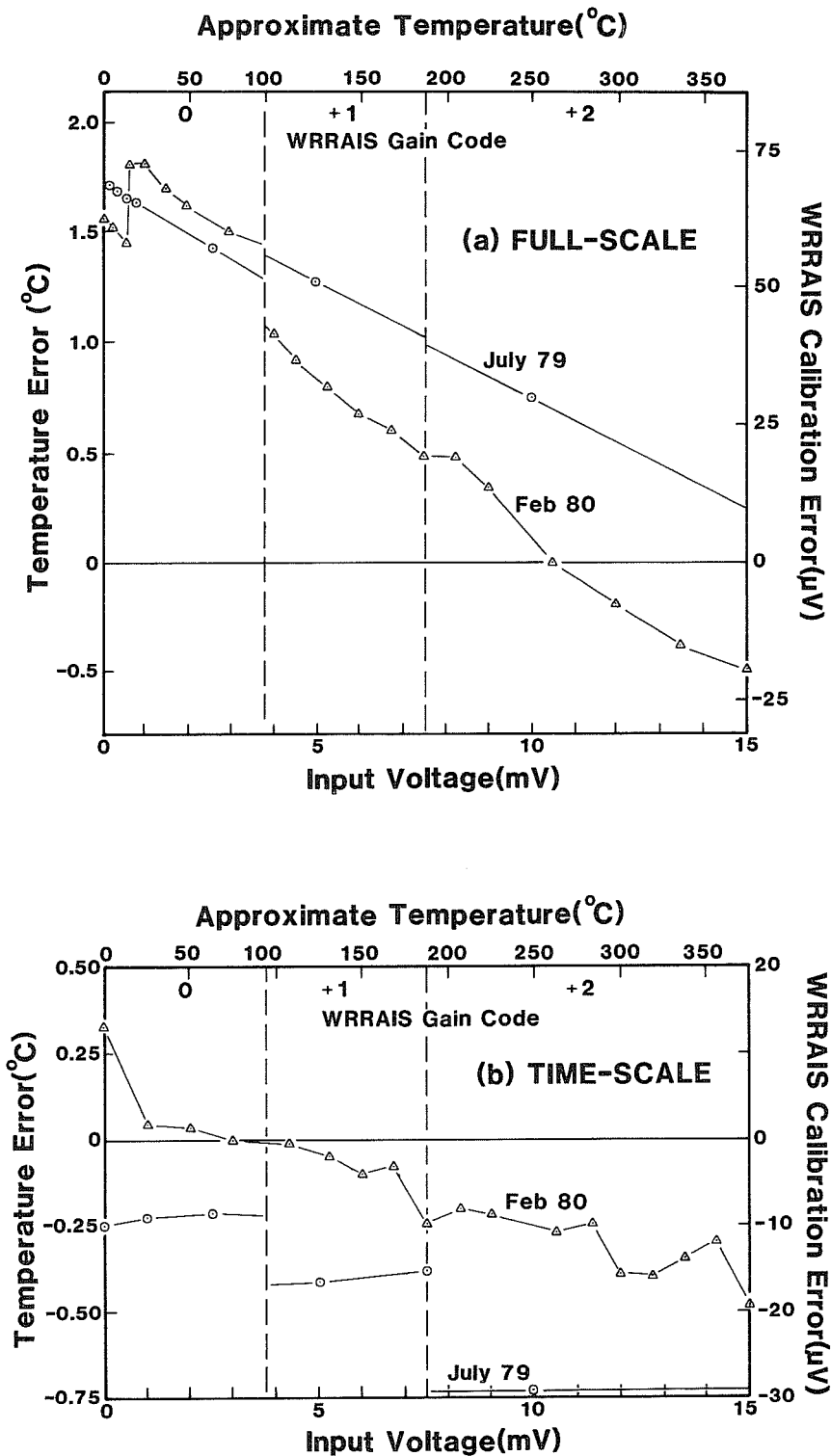
XBL 8011-7445

Fig. B-11. Extensometer displacement error due to full-scale WRRais error, Feb. 80.



XBL 8011-7446

Fig. B-12. USBM borehole deformation error due to the full-scale WRRAIS, for a typical (64 µm/mV) USBM gauge.



XBL 8011-7447

Fig. B-13. Temperature measurement errors due to: (A) Full-scale and (B) Time-scale WRRAIS errors, for a typical (25°C/mV) thermocouple.

caused by either the automatic gain change that occurs as the WRR AIS shifts between +0 to -0, or by the WRR AIS shift that results from close successive readings taken during the calibration procedure.

- c. Thermocouples. The same voltage plot shown in Fig. B-12 is repeated in Fig. B-13a, but with a temperature error scale computed from

$$T(^{\circ}\text{C}) = 25 \times V(\text{mV}).$$

Temperature errors are less severe than the USBM errors, but they still require further attention. The plot indicates that the WRR AIS shifts can easily generate 0.5 degrees of error, and possibly more. Fortunately, the most severe differences between the two calibration curves occur at the higher temperatures where less precision is required. Changes between gains 0 and +1 (around 90°C) may also be a problem, as the February 1980 calibration indicates about 0.5°C shift.

Results from calibrating the time-scale WRR AIS showed considerably smaller deviations on gain codes 0 and 1 than deviations from the full-scale WRR AIS (compare Figs. B-13 (a) and (b)). On numerically higher gain codes, the deviations are comparable to the full-scale WRR AIS but are constant across each individual gain range, rather than varying with the input voltage level. The effects of these deviations are:

- a. Extensometers. The largest excursions on gain code 9 were 5.0 mV, which corresponds to a displacement of only 12 microns. Hence, the effect of the WRR AIS deviations upon the extensometer measurements is unimportant in the time-scaled experiment as it was unimportant

- in the full-scale experiment.
- b. USBM gauges. There were no USBM gauges in the time-scaled experiment.
 - c. Thermocouples. Figure B-13(b) displays the deviation voltages in gain code ranges 0, 1 and 2 along with the corresponding temperature errors. Most thermocouples in the time-scaled experiment should have operated on the highest gain range (code 0) throughout the experiment, because temperatures did not exceed 50°C except in heater holes. Hence, measurements of rock temperature appear accurate to within $\pm 0.5^\circ\text{C}$, according to Fig. B-13(b). An exception to this occurs during the first six months of the experiments when the circuit boards were interchanged between the full-scale and time-scale WRAISs.

In summary, these calibration results indicate that WRAIS errors insignificantly perturbed extensometer measurements since the board changes should not have produced any errors greater than 20 microns. However, time-scale extensometer data shifts were observed at times when boards were changed, whereas the full-scale extensometers showed none. Errors in the temperature data (perhaps as much as 1.5°C) and in the USBM data (perhaps as much as 4 microns) are significant, are above the nuisance level, and motivated the data rescaling effort.

B.4 HISTORY OF THE WRAIS'S GAIN AND VOLTAGE OFFSETS

Time intervals, during which calibration of the WRAISs either remained constant or drifted linearly with time, were determined from Tables B.5 and B-6 and an inspection of Fig. B-4. Nine time intervals were established for full-scale and five for time-scale.

A suite of plots showing the difference between the WRR AIS and AD-9 voltages were compiled from thermocouple data for these time intervals. Figure B-14 shows the differences for full-scale and Fig. B-15 for time-scale. Voltages greater than 10 mV are usually from thermocouples in the heater holes where quite high temperatures were attained. The AD-9 data were taken from the paper tape records, and the WRR AIS data were selected from microfiche records to within ± 7.5 minutes of the AD-9's acquisition time. These deviation plots roughly obey an equation of the form,

$$V_m - V_a = V_o + (G - 1)V_a ,$$

where

V_m is the WRR AIS recorded voltage,

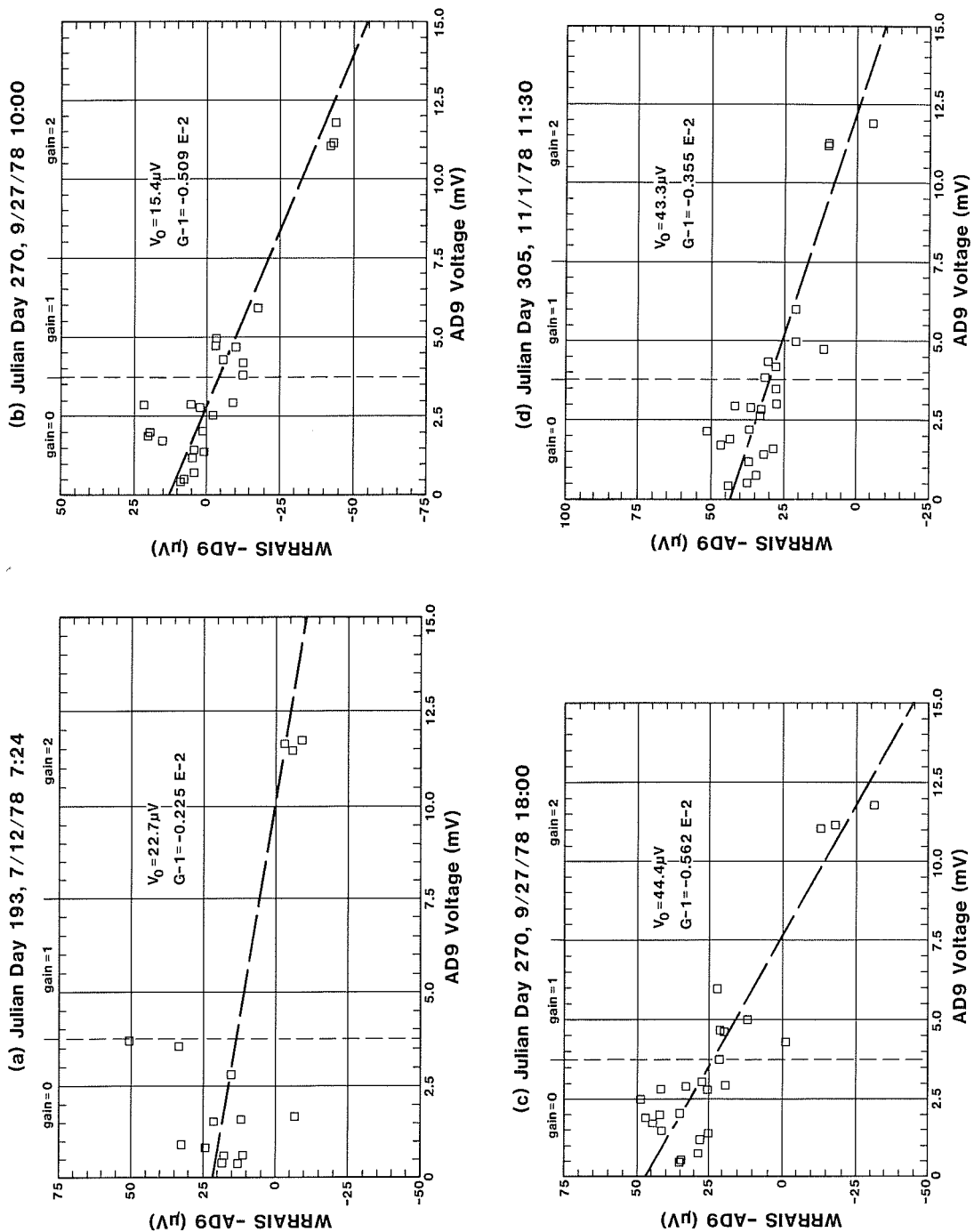
V_a is the AD-9 recorded voltage,

V_o is the WRR AIS offset voltage, and

G is the WRR AIS gain (nominally 1.00).

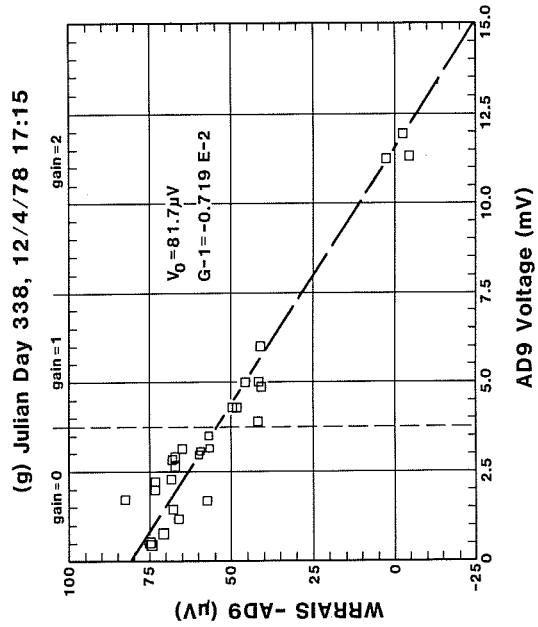
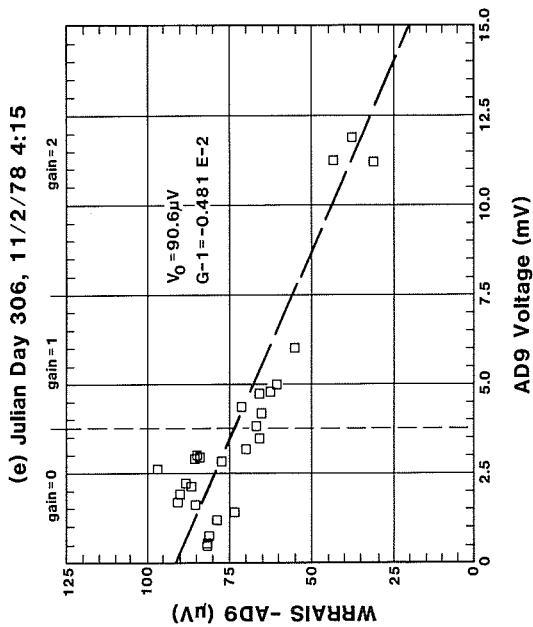
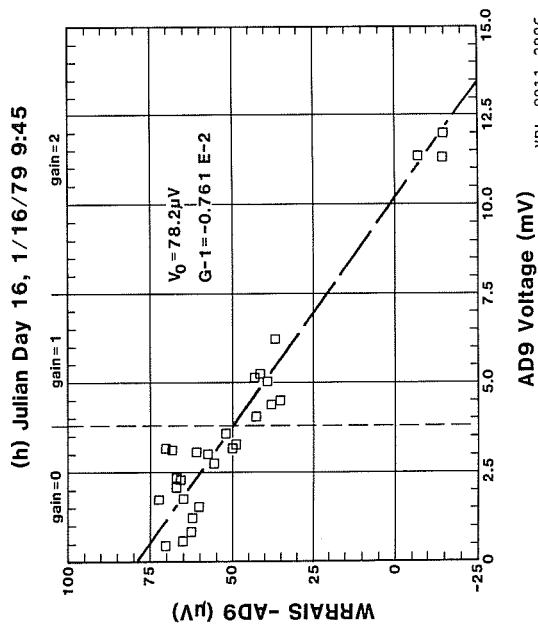
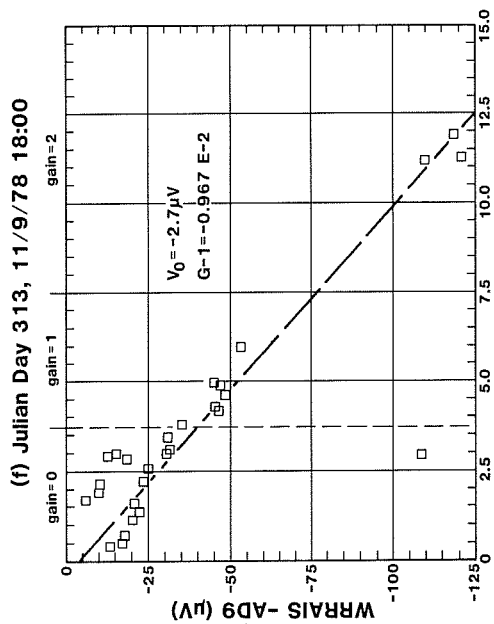
A least-squares straight line was fit to the data and is shown on the plots. This line determines an offset V_o and a gain factor $G - 1$ which are also given on each of the plots.

Offsets and gains were specified for time intervals that were chosen on the basis of Tables B-5 and B-6, and inspection of Fig. B-4. The results, for nine time intervals for full scale and five time intervals for time scale, are listed in Tables B-18 and B-19. During most of the time intervals the offsets and gains were taken to be constant. However, in several cases the offsets and gains changed between consecutive plots (see Figs. B-14 and B-15); therefore, it was decided to interpolate between the beginning and end points of those time intervals, such that the offsets and gains varied



XBL 8011-3995

Fig. B-14. Difference history between full-scale WRRAIS and AD-9 readings.



XBL 8011-3996

Fig. B-14 (continued).

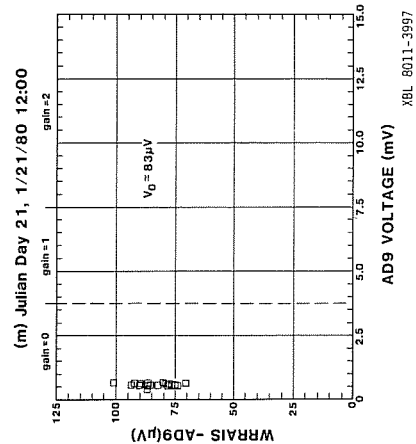
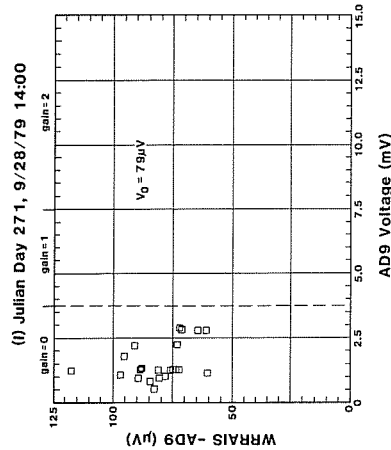
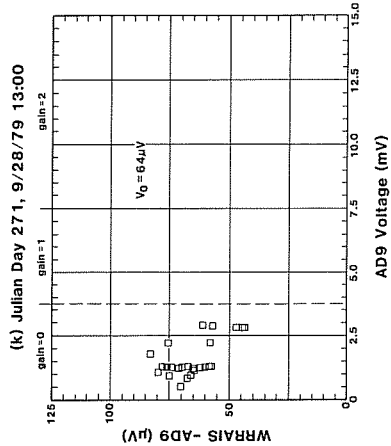
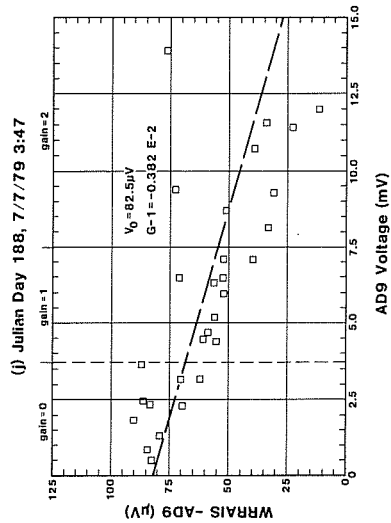
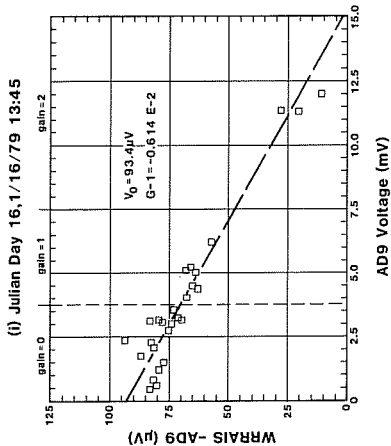
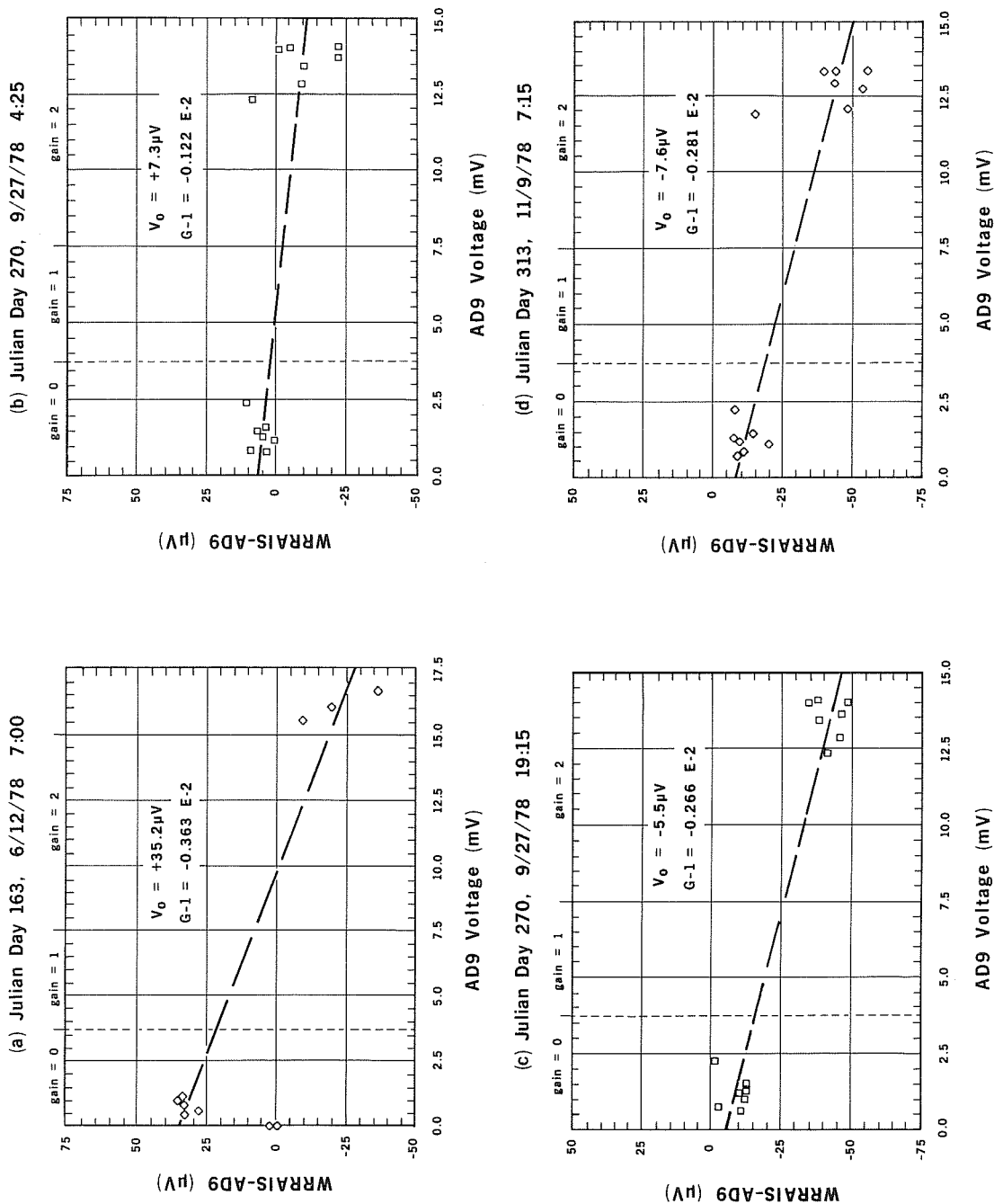
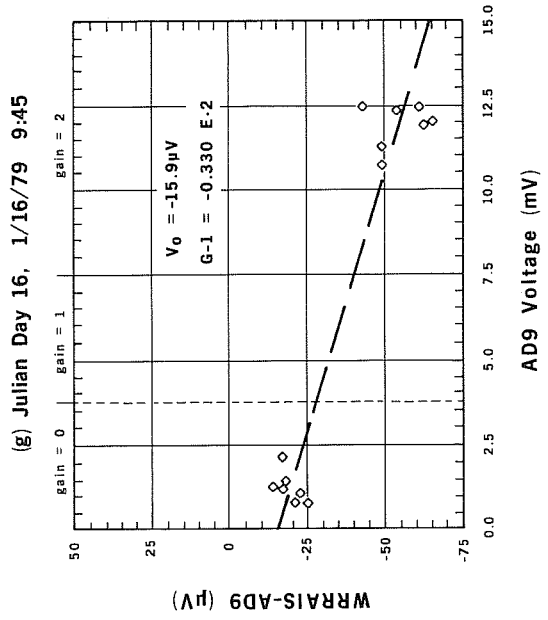
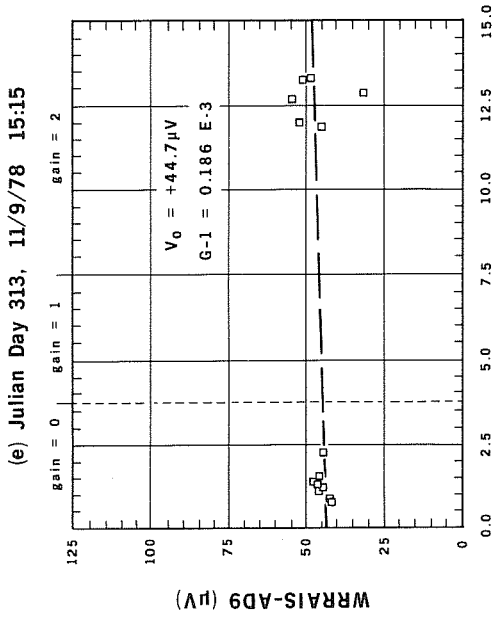
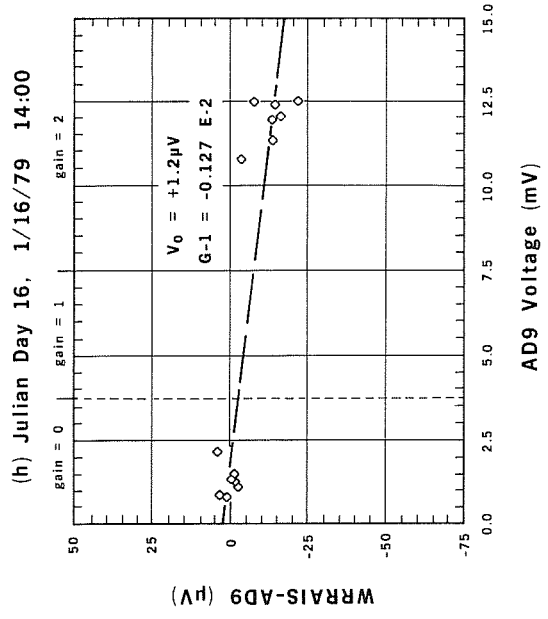
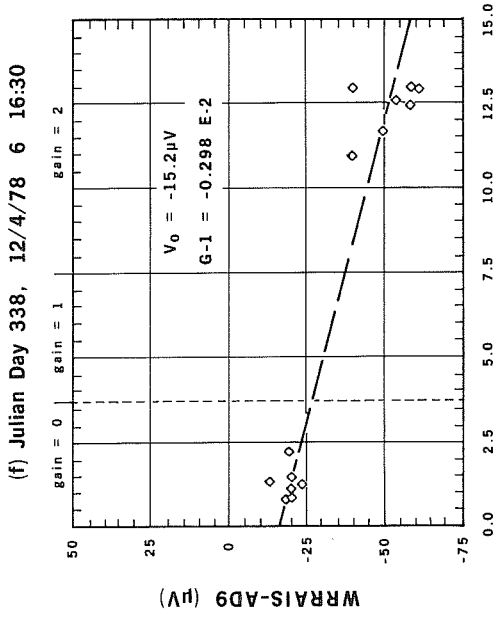


Fig. B-14 (continued).



XBL 8011-3992

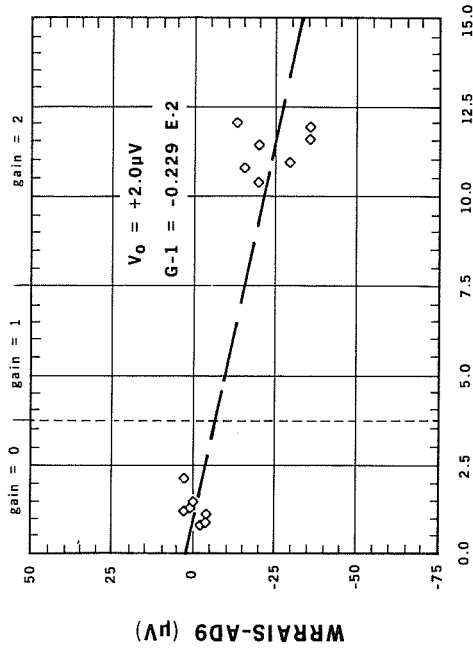
Fig. B-15. Difference history between time-scale WRRAIS and AD-9 readings.



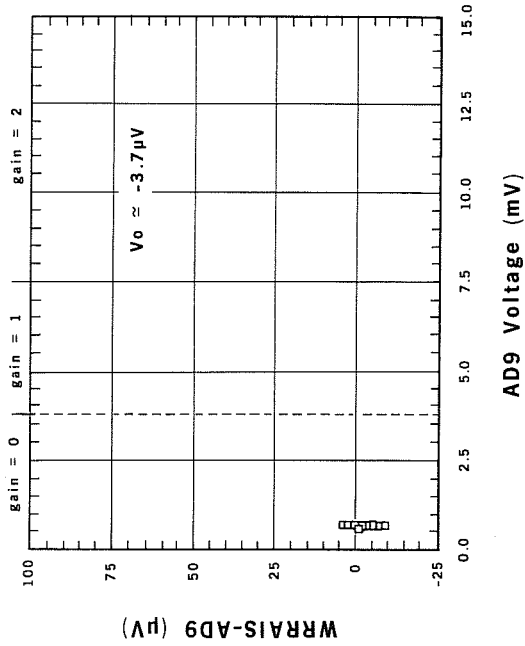
XBL 8011-3993

Fig. B-15 (continued).

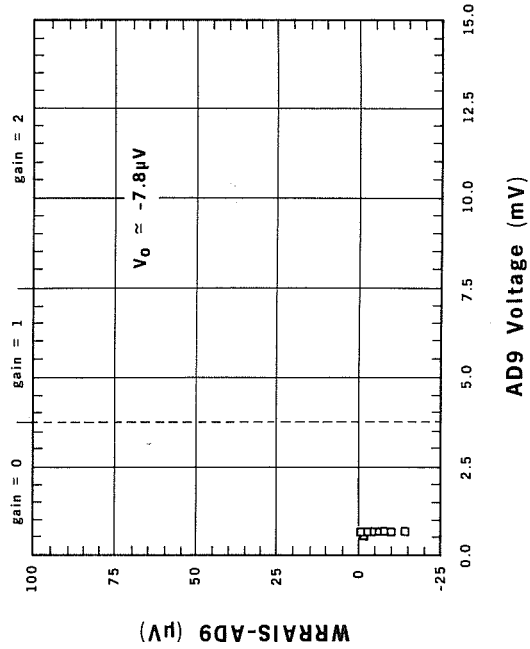
(i) Julian Day 86, 3/27/79 17:01



(j) Julian Day 271, 9/28/79 11:45



(k) Julian Day 271, 9/28/79 16:00



(l) Julian Day 337, 12/3/79 11:45

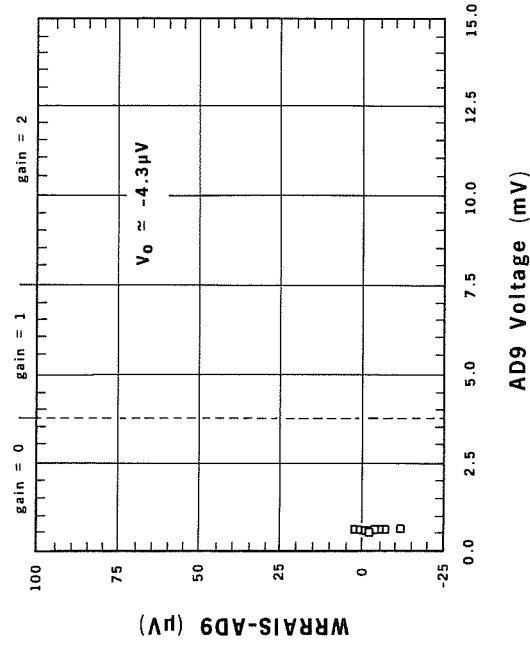


Fig. B-15 (continued).

Table B-18. Selected voltage offsets and gain factors used to correct the raw voltage data of the full-scale WRR AIS.

Time of First Point	Time of Last Point	V_o [Volts]	G-1
163 12:15 06/12/78	270 12:15 09/27/78	0.228 E-4 0.154 E-4	-0.225 E-2 -0.510 E-2
(Interpolate linearly between days 163 and 270)			
270 17:45 09/27/78	306 00:00 11/02/78	0.444 E-4 0.433 E-4	-0.562 E-2 -0.355 E-2
(Interpolate linearly between days 270 and 306)			
306 00:15 11/02/78	313 11:15 11/09/78	0.906 E-4	-0.481 E-2
313 11:45 11/09/78	338 13:15 12/04/78	-0.271 E-5	-0.967 E-2
338 13:45 12/04/78	016 11:00 01/16/79	0.800 E-4	-0.740 E-2
016 11:30 01/16/79	188 03:45 07/07/79	0.934 E-4 0.825 E-4	-0.614 E-2 -0.382 E-2
(Interpolate linearly between days 016 and 188)			
188 04:00 07/07/79	271 13:45 09/28/79	0.825 E-4 0.640 E-4	-0.382 E-2 -0.382 E-2
(Interpolate linearly between days 188 and 271)			
271 13:45 09/28/79	Last point . . .	0.810 E-4	-0.550 E-2

Table B-19. Selected voltage offsets and gain factors used to correct the raw voltage data of the time-scale WRR AIS.

Time of First Point			Time of Last Point			V_o	G-1
156	04:30	06/05/78	270	09:15	09/27/78	0.352 E-4	-0.363 E-2
						0.734 E-5	-0.122 E-2
<p>The offset and gain both changed gradually between day 156 and day 270. Interpolate linearly with time between the end values on days 156 and 270 to compute the offset and gain for any day during this time period.</p>							
270	17:45	09/27/78	313	10:45	11/09/78	-0.549 E-5	-0.266 E-2
						-0.763 E-5	-0.281 E-2
(Interpolate linearly between days 270 and 313)							
313	11:30	11/09/78	338	13:15	12/04/78	0.447 E-4	0.186 E-3
338	14:15	12/04/78	016	10:45	01/16/79	-0.155 E-4	-0.314 E-2
016	11:15	01/16/79	337	13:00	12/03/79	-0.180 E-5	-0.180 E-2

linearly with time.

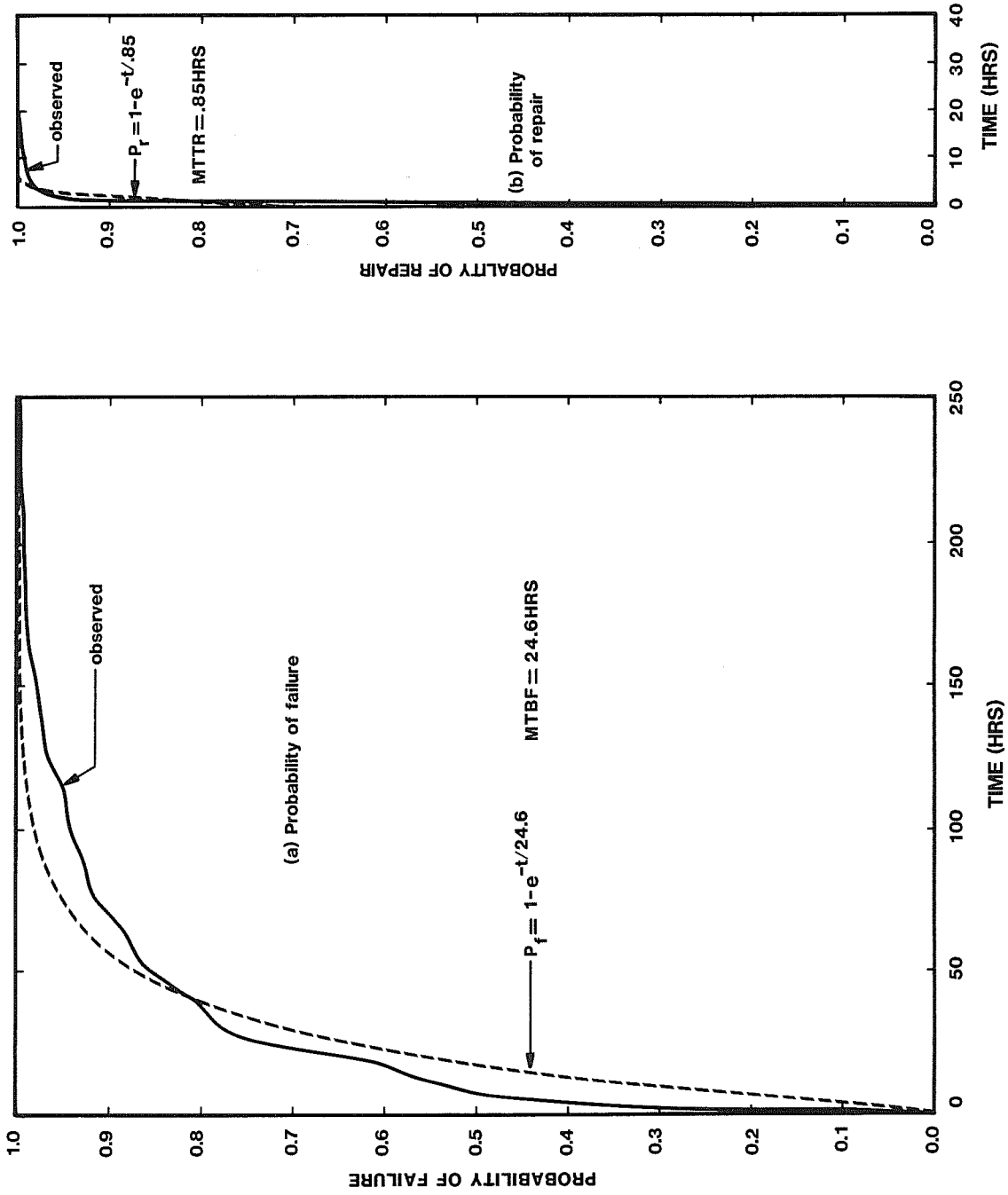
All data rescaling relied on the instrument calibrations done prior to the experiments because many of the thermocouples were grouted in-place and could not be recovered for a post-experiment calibration. The underlying assumption is that the initial calibrations were done with the WRAISS operating with offsets and gains specified for the first time intervals. This is correct only if no significant shifts occurred between the time of instrument calibration, during April and May 1978, and the time of the first AD-9 deviation plots in June and July 1978.

Details of the correction algorithm are given in section 6.1.

B.5 EVENT CHRONOLOGY

B.5.1 Reliability of the Data Acquisition System

The computer system was instrumented to maintain a history of the time when it was and was not functioning. The computer periodically read its battery powered real-time clock and recorded its "last active" time on disc. When re-booted, following a failure, it would also read its real-time clock to determine its "re-start" time. Both the last active time, which was the time of failure, and the re-start time were recorded and maintained in a Failure/Repair History log-file on disc. Time-between-failure intervals, derived from this file, are shown as "probability of failure" vs. time in Fig. B-16. Time-to-repair intervals, also derived from the file, are shown as "probability of repair" vs. time in Fig. B-16. The calculated Mean-Time-Between Failure (MTBF) is 24.6 hours and the Mean-Time-To-Repair (MTTR) is 51 minutes. Plots of exponential probability functions, based on these calculated MTBF and MTTR values, are overlaid to provide a comparison.



XBL 8011-7444

Fig. B-16. Observed: (A) Probability of failure and (B) Probability of repair vs. time for the MODCOMP computer system.

These poor MTBF results were not as troublesome as they appear. Several chronic problems, such as contention for memory and simultaneous access to the printer/plotter from separate devices, were most expeditiously "worked around" by halting the computer and re-booting from disc. The computer could be down for as much as 15 minutes without losing any raw data. The remoteness of Stripa from the system support available in Berkeley made it cost-effective to tolerate some of these chronic problems.

The data loggers were much more reliable than the computer system, mainly because of their increased use of large-scale integrated circuits, integrated packaging, minimal peripherals, and elementary software/firmware. One AD-9 was, however, down for repairs for several days in August 1978. While it was being repaired, some of its sensors were cross-connected to the AD-9 in the other instrument drift.

An ice-point reference also failed during August 1978. This failure was quickly detected due to the many software "data out of range" alarms. The failed unit was replaced with an on-site spare, which took several hours to install because of the numerous wire connections.

B.5.2 Data Gaps and Errors

Gaps in the computer-based magnetic tape records occurred often enough to be a nuisance. Power failures caused by either lightning storms or other outages in the local power service were common. Power outages and occasional software problems caused losses of only a few data points, however. More significant were hardware problems, usually with the disc drives or core memory, which produced data losses of hours to days.

Computer system failures lasting longer than 15 minutes caused gaps in the raw data file for all sensors. A list of gaps and errors was obtained by examining the raw data file history of two "stable" sensors. Full-scale thermocouple 478 and time-scale thermocouple 910 were used because they operated reliably throughout the experiment and were far removed from any heaters, thereby undergoing minimal temperature change during the heater experiments. Table B-20 shows these intervals of missing data along with explanatory comments from the Stripa log book and personal communications. Gaps occur between the times given on each line of Table B-20; a valid datum was collected at each of the stated times. Additional raw data gaps occurred at the beginning of the experiment. The time-scale heaters were turned-on June 1, 1978, but the raw data file begins at 11:00 a.m. on June 2, 1978. Longterm (time-averaged) data, however, are available for that period. Data overlaps (duplications) were removed and incorrect times (owing to 1980 being a leap year) have been corrected. The listed data gaps are identical for both the time-scale and full-scale sensors.

The raw data files for sensors 478 and 910 were also examined for "data flags." A $-.99999E+05$ flag signified that the raw data on the tape received from Stripa was invalid either because the gain code value was outside the range 0 to 11, or because the 4-bit BCD IRAD data character was not 0-9. For sensors 478 and 910, this data flag occurred only on 09/27/78. These invalid points are attributed to maintenance work undertaken on the WRAISSs. Sensors 478 and 910 were active throughout the experiment; hence, no inactive $-.12345E+05$ sensor flags were found. Any other "bad data" points (either 12,345 due to a deactivated sensor, or $-99,999$ due to a point out-of-range) occurring on any channel were probably caused by problems with equipment

Table B-20. Gaps in the "raw" data collected by the MODCOMP computer.

(Key: ne = no entry on computer log book; no expl = computer log book does have an entry but does not explain why data is missing.)

Time of Gaps (Julian day, hrs:mins, date)						No. Points Missing	Comments
from			to				
156	07.00	06/05/1978	156	07.30	06/05/1978	1	ne
159	07.00	06/08/1978	159	08.30	06/08/1978	5	ne
159	19.15	06/08/1978	159	19.45	06/08/1978	1	ne
165	14.00	06/14/1978	165	14.45	06/14/1978	2	ne
168	09.15	06/17/1978	168	10.30	06/17/1978	4	ne
172	12.30	06/21/1978	172	13.15	06/21/1978	2	ne
173	01.30	06/22/1978	173	02.45	06/22/1978	4	no expl
173	04.00	06/22/1978	173	04.30	06/22/1978	1	
176	00.00	06/25/1977	176	00.45	06/25/1978	2	ne
176	12.15	06/25/1978	178	11.00	06/27/1978	186	50 Hz diesel generator was off for repair
179	11.00	06/28/1978	179	12.15	06/28/1978	4	ne
183	20.45	07/02/1978	183	21.15	07/02/1978	1	ne
184	07.15	07/03/1978	184	09.00	07/03/1978	6	ne (H10 heater on at 9:00)
186	05.00	07/05/1978	186	05.30	07/05/1978	1	ne
187	10.30	07/06/1978	187	11.15	07/06/1978	2	ne
188	01.00	07/07/1978	188	01.30	07/07/1978	1	ne
189	19.45	07/08/1978	189	20.15	07/08/1978	1	ne
190	10.30	07/09/1978	190	11.00	07/09/1978	1	ne
193	09.00	07/02/1978	193	10.00	07/12/1978	3	ne
195	00.30	07/14/1978	195	01.00	07/14/1978	1	ne

(continued)

Table B-20. (continued).

Time of Gaps (Julian day, hrs:mins, date)						No. Points Missing	Comments
from			to				
201	09.00	07/20/1978	201	09.45	07/20/1978	2	no expl
203	14.00	07/22/1978	203	16.15	07/22/1978	8	Power outage stopped com- puters and T.S. Data logger
203	23.45	07/22/1978	204	00.15	07/23/1978	1	Bad disk 0 drive
204	13.15	07/23/1978	206	10.45	07/25/1978	181	repair of disc drive continued
206	11.30	07/25/1978	206	12/15	07/25/1978	2	
208	07.30	07/27/1978	208	08.15	07/27/1978	2	
208	14.15	07.27/1978	208	15.45	07/27/1978	5	no expl
209	14.45	07/28/1978	209	15.30	07/28/1978	2	ne
230	09.30	08/18/1978	230	11.45	08/18/1978	8	computer off for installation of remote restart chassis and hard- ware
236	20.30	08/24/1978	237	00.45	08/25/1978	16	power outage twice (H9 heater on at 14.00)
240	03.00	08/28/1978	240	03.30	08/28/1978	1	no expl
241	11.15	08/29/1978	241	12.45	08/29/1978	5	acquisition program ACQUIR stopped
242	00.00	08/30/1978	242	00.45	08/30/1978	2	computer stopped due to conflict in mid- night update program with plot data re- generation
243	10.30	08/31/1978	243	11.00	08/31/1978	1	ne
244	03.30	09/01/1978	244	04.00	09/01/1978	1	ne
264	22.15	09/21/1978	264	22.45	09/21/1978	1	no expl
265	14.30	09/22/1978	265	15.00	09/22/1978	1	ne

(continued)

Table B-20. (continued).

Time of Gaps (Julian day, hrs:mins, date)						No. Points Missing	Comments
from			to				
268	07.15	09/25/1978	268	07.45	09/25/1978	1	
268	11.15	09/25/1978	268	11.45	09.25/1978	1	no expl
268	14.30	09/25/1978	268	15.00	09/25/1978	1	
270	11.15	09/27/1978	270	11.45	09/27/1978	1	T.S. wide range had a bad analog power supply. Both T.S. and F.S. power were killed in order to repair. Hence no data acquisition.
270	12.15	09/27/1978	270	12.45	09/27/1978	1	
270	14.00	09/27/1978	270	14.30	09/27/1978	1	
270	14.30	09/27/1978	270	17.45	09/27/1978	12	
272	20.00	09/29/1978	272	21.00	09/29/1978	3	computer stopped due to insufficient memory for restart
273	00.00	09/30/1978	273	01.15	09/30/1978	4	computer stopped
277	00.00	10/10/1978	274	01.30	10/01/1978	5	ne
284	07.00	10/11/1978	284	07.45	10/11/1978	2	no expl
290	10.45	10/17/1978	290	11.15	10/17/1978	1	random MODCOMP com- puter memory problem and diagnostics
294	19.15	10/21/1978	294	19.45	10/21/1978	1	power glitch or wide range problems
297	20.00	10/24/1978	297	21.45	10/24/1978	6	fuses blew up on REMAC, Real time clock and asynch communication
301	08.00	10/28/1978	301	11.30	10/28/1978	13	
301	11.45	10/28/1978	301	12.45	10/28/1978	3	computer failure again due to bad bad fuses on REMAC and bad capacitors
301	13.15	10/28/1978	301	14.00	10/28/1978	2	
301	14.45	10/28/1978	301	16.15	10/28/1978	5	
305	10.30	11/01/1978	305	11.00	11/01/1978	1	no expl
307	14.15	11/03/1978	307	16.15	11/03/1978	7	switch to new power company
308	11.45	11/04/1978	308	13.15	11/04/1978	5	
319	13.45	11/15/1978	319	14.15	11/15/1978	1	no expl
334	13.15	11/30/1978	334	13.45	11/30/1978	1	wide range board change

(continued)

Table B-20. (continued).

Time of Gaps (Julian day, hrs:mins, date)						No. points Missing	Comments
from			to				
339	13.30	12/05/1978	339	14.45	12/05/1978	4	parity error problem with magnetic tape Drive 2
341	08.00	12/07/1978	341	08.45	12/07/1978	2	switch back to original power company
342	15.15	12/08/1978	342	16.45	12/08/1978	5	parity error on disc 0, history file partition DAQ went bad
345	09.00	12/11/1978	345	11.30	12/11/1978	9	
345	12.30	12/11/1978	345	13.15	12/11/1978	2	continued to repair disc 0 drive
345	13.15	12/11/1978	345	14.00	12/11/1978	2	
345	14.30	12/11/1978	345	16.30	12/11/1978	7	
346	10.15	12/12/1978	346	21.45	12/11/1978	45	disk 0 head alignment
347	11.30	12/13/1978	347	14.30	12/13/1978	11	trouble with disk 1, head alignment done
348	11.15	12/14/1978	348	11.45	12/14/1978	1	
348	13.00	12/14/1978	348	15.45	12/14/1978	10	disk 1 repair continued
352	08.45	12/18/1978	352	09.30	12/18/1978	2	
352	20.45	12/18/1978	352	22.00	12/18/1978	4	wide range bat wings
5	07.45	01/05/1979	10	02.45	01/10/1979	459	60 Hz converter off and consequent tape write problem
10	15.00	01/10/1979	10	16.30	01/10/1979	5	wide range off line due to parity error
14	14.30	01/14/1979	14	16.45	01/10/1979	8	
51	12.15	02/20/1979	51	15.15	02/20/1979	11	no expl
78	12.45	03/19/1979	86	15.15	03/27/1979	777	computer down, major failure!
89	05.45	03/30/1979	89	06.30	03/30/1979	2	computer off-line

(continued)

Table B-20. (continued).

Time of Gaps (Julian day, hrs:mins, date)						No. points Missing	Comments
from			to				
93	01.45	04/03/1979	93	02.15	04/03/1979	1	
93	02.15	04/03/1979	93	03.00	04/03/1979	2	
93	03.00	04/03/1979	93	03.30	04/03/1979	1	for several times on and off, computer off line; plane 2 memory was losing memory! Big trouble.
93	03.30	04/03/1979	93	04.00	04/30/1979	1	
93	05.00	04/03/1979	93	13.45	04/30/1979	34	
93	18.00	04/03/1979	93	19.00	04/30/1979	1	
93	21.15	04/30/1979	93	22.30	04/30/1979	4	
94	00.00	04/04/1979	94	01.00	04/04/1979	3	computer off line, lost memory
95	06.15	04/05/1979	95	06.45	04/05/1979	1	computer off line due to plot time span too long
96	11.45	04/06/1979	96	12.15	04/06/1979	1	switching memory plane 2 with that at the end of the memory line; ran diagnostics
96	12.15	04/06/1979	96	13.00	04/06/1979	2	
105	01.00	04/15/1979	105	01.30	04/15/1979	1	magnetic tape off line
109	09.30	04/19/1979	109	10.00	04/19/1979	1	core memory diag- nostics continue
109	11.00	04/19/1979	109	11.30	04/19/1979	1	
116	12.00	04/26/1979	116	12.45	04/26/1979	2	core memory replace- ment
123	17.15	05/03/1979	123	17.45	05/03/1979	-1	ne (data are identical)
126	19.30	05/06/1979	126	21.00	05/06/1979	5	ne
132	15.30	05/12/1979	132	16.00	05/12/1979	1	computer off line
141	08.30	05/21/1979	141	08.30	05/21/1979	-1	no expl (data are identical)
158	02.30	06/07/1979	158	04.15	06/07/1979	6	computer stopped running
161	04.45	06/10/1979	161	07.00	06/10/1979	8	computer stopped running (continued)

Table B-20. (continued).

Time of Gaps (Julian day, hrs:mins, date)						No. points Missing	Comments
from		to					
166	16.45	06/15/1979	166	07.00	06/15/1979	5	power failure
168	17.45	06/17/1979	168	19.45	06/17/1979	7	computer stopped
176	07.00	06/25/1979	176	07.45	06/25/1979	2	lightning storm caused computer power failure
178	17.00	06/27/1979	178	17.30	06/27/1979	1	no expl
179	08.00	06/28/1979	179	16.15	06/28/1979	32	computer off line due to bad capacitor in PIOP plane
180	19.45	06/29/1979	180	21.00	06/29/1979	4	disc 0 had bad capacitor
180	21.15	06/29/1979	180	23.30	06/29/1979	8	
180	23.30	06/29/1979	181	00.00	06/30/1979	1	power failure several times over the weekend
181	10.45	06/30/1979	181	12.45	06/30/1979	7	
181	23.45	06/30/1979	182	00.15	07/01/1979	1	
182	00.15	07/01/1979	182	01.00	07/01/1979	2	
186	01.00	07/05/1979	186	02.15	07/05/1979	4	computer stopped
191	01.00	07/10/1979	191	01.30	07/10/1979	1	wide range problems
192	12.30	07/11/1979	192	13.00	07/11/1979	1	didn't do reset on interface chasis after checking wide range
200	11.15	07/19/1979	200	14.00	07/19/1979	10	ne
203	17.45	07/22/1979	203	19.15	07/22/1979	5	power failure due to storm
208	15.15	07/27/1979	208	16.30	07/27/1979	4	power failure
209	14.00	07/28/1979	209	14.45	07/28/1979	2	power failure
221	05.15	08/09/1979	221	06.30	08/09/1979	4	several power failures due to storm
221	09.00	08/09/1979	221	09.45	08/09/1979	2	
226	13.45	08/14/1979	226	14.15	08/14/1979	1	no expl
230	14.00	08/18/1979	230	14.30	08/18/1979	1	ne

(continued)

Table B-20. (continued).

Time of Gaps (Julian day, hrs:mins, date)						No. points Missing	Comments
from			to				
245	22.00	09/02/1979	245	23.00	09/02/1979	3	power failure due to electrical storms 22.15 - 23.00
245	23.45	09/02/1979	246	00.15	09/03/1979	1	no expl
259	17.00	09/16/1979	259	19.45	09/16/1979	10	FS wide range parity error which stops pgm ACQUIR
274	10.45	10/01/1979	275	03.15	10/02/1979	65	raw tape missing due to subsequent power failure
276	15.45	10/03/1979	276	17.45	10/03/1979	7	power failure
311	02.15	11/07/1979	311	07.45	11/07/1979	21	disc 0 went to select lock mode, so no data acquired
311	07.45	11/07/1979	311	08.15	11/07/1979	1	
314	10.30	11/10/1979	314	12.30	11/10/1979	7	
314	16.00	11/10/1979	314	17.30	11/10/1979	5	weekend power surges due to power regulation on mine surface
314	21.45	11/10/1979	315	09.15	11/11/1979	45	
318	15.00	11/14/1979	318	16.00	11/14/1979	3	power failure
328	00.30	11/24/1979	328	01.45	11/24/1979	4	CPU hang
333	15.30	11/29/1979	333	15.30	11/29/1979	-1	ne (data are identical)
341	03.45	12/07/1979	341	03.45	12/07/1979	-1	ne (data are identical)
341	03.45	12/07/1979	341	04.15	12/07/1979	1	computer off line
343	00.15	12/09/1979	343	00.45	12/09/1979	1	no expl
343	02.30	12/09/1979	343	03.00	12/09/1979	1	no expl
343	21.15	12/09/1979	343	22.00	12/09/1979	2	computer off line
347	10.30	12/13/1979	347	11.00	12/13/1979	1	ne
359	08.15	12/25/1979	359	08.45	12/25/1979	1	ne
361	11.00	12/27/1979	361	11.30	12/27/1979	1	computer off line
363	12.00	12/29/1979	363	13.15	12/29/1979	4	power failure

(continued)

Table B-20. (concluded).

Time of Gaps (Julian day, hrs:mins, date)						No points Missing	Comments
from			to				
364	02.45	12/30/1979	and 364	10.00	12/30/1979	28	power failure, CPU hang
1	04.45	01/01/1980	1	09.45	01/01/1980	19	power failure
1	10.15	01/01/1980	1	11.30	01/01/1980	4	
2	12.00	01/02/1980	2	12.30	01/02/1980	1	power failure
7	17.45	01/02/1980	7	18.45	01/07/1980	3	power failure
10	13.00	01/10/1980	10	13.30	01/10/1980	1	ne
11	08.15	01/11/1980	12	10.45	01/12/1980	105	software changes in CKNAVG pgm System Parameter. File reloaded
12	21.00	01/12/1980	12	21.30	01/12/1980	1	ne
37	11.30	02/06/1980	37	13.45	02/06/1980	8	power failure caused by FS smoke alarm trip
58	03.30	02/27/1980	58	04.00	02/27/1980	1	disc pack meter problem
63	11.30	03/03/1980	64	11.45	03/04/1980	96	
65	11.30	03/05/1980	65	10.45	03/05/1980	-4	
65	10.45	03/05/1980	65	11.45	03/05/1980	3	hardware clock did not know it was a leap year
65	21.00	03/04/1980	65	22.15	03/04/1980	4	
66	07.45	03/06/1980	65	08.00	03/05/1980	-96	
66	11.30	03/06/1980	66	11.15	03/06/1980	-2	ne
66	11.15	03/06/1980	66	11.45	03/06/1980	1	ne
76	08.30	03/16/1980	78	11.15	03/18/1980	202	magnetic tape drive 1 problem
86	12.15	03/26/1980	86	12.45	03/26/1980	1	ne
98	10.30	04/07/1980	98	12.30	04/07/1980	7	computer off line, tape drive off
98	13.00	04/07/1980	98	14.45	04/07/1980	6	line

preceding the WRRAISSs, such as ice point references, transducer power supplies, and transducer failure.

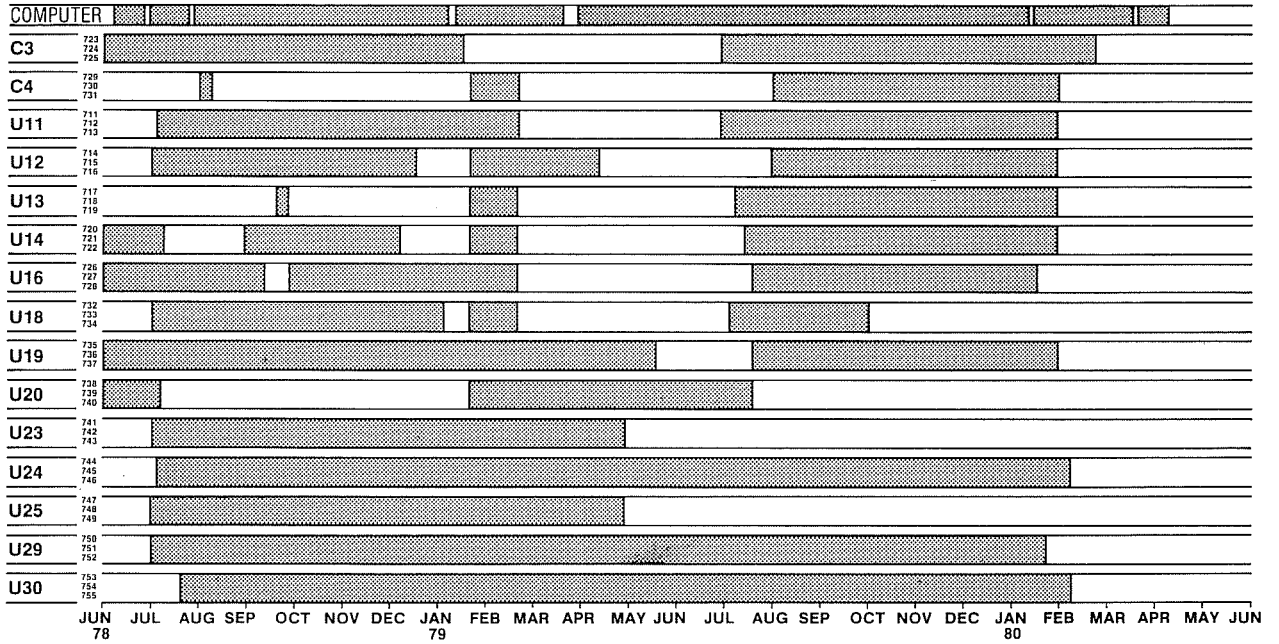
B.5.3 Instrument Operating History

Actual sensor performance, as determined from the data record, is shown graphically in Fig. B-17 for the 5 kW heater experiment, where temperatures were the highest and instrument failures the most severe. Stippled areas of the figures denote times where output voltages are within the capability of the transducer; open areas indicate that no valid data were acquired. In Fig. B-17(a), each of the boreholes C3 through U30 has one USBM gauge, each with three transducer outputs. Additional computer-related data losses that exceeded one day are shown in the top bar graph labeled "computer." Fortunately, none of these occurred at the critical times immediately following turn-off or turn-on of the heaters. Total losses amounted to 4% of the data record.

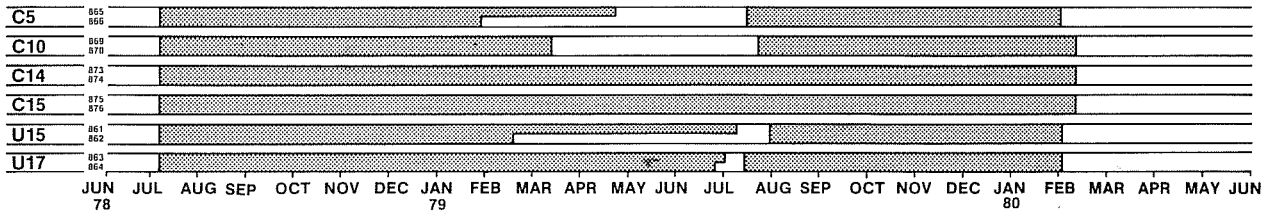
The 15 USBM borehole deformation gauges (Fig. B-17(a)) exhibited a high initial failure rate, followed by more failures after reinstallation in January 1979. These failures were caused by moisture infiltration that caused corrosion of components inside the gauge's body. The gauges were again removed, rebuilt and re-installed in July 1980, before the heater turnoff. This successfully eliminated the water problem, although some gauges failed subsequently due to lead breakage. At Stripa, the USBM gauges required more maintenance and modification than any other sensor type.

Moisture infiltrating the gauge's body also caused failures of some IRAD gauges (Fig. B-17(b)). A sectioned gauge revealed a badly rusted wire. Calibration was the main problem with the IRAD gauge since the slope of the

(a) USBM Gauges



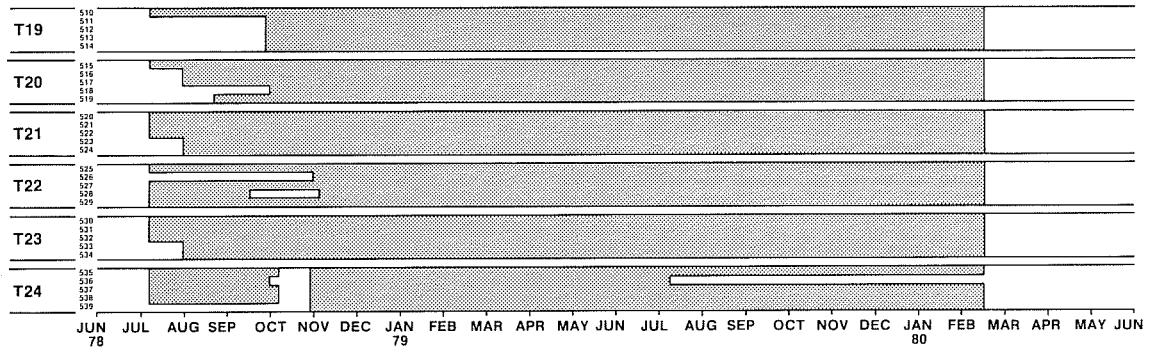
(b) IRAD Gauges



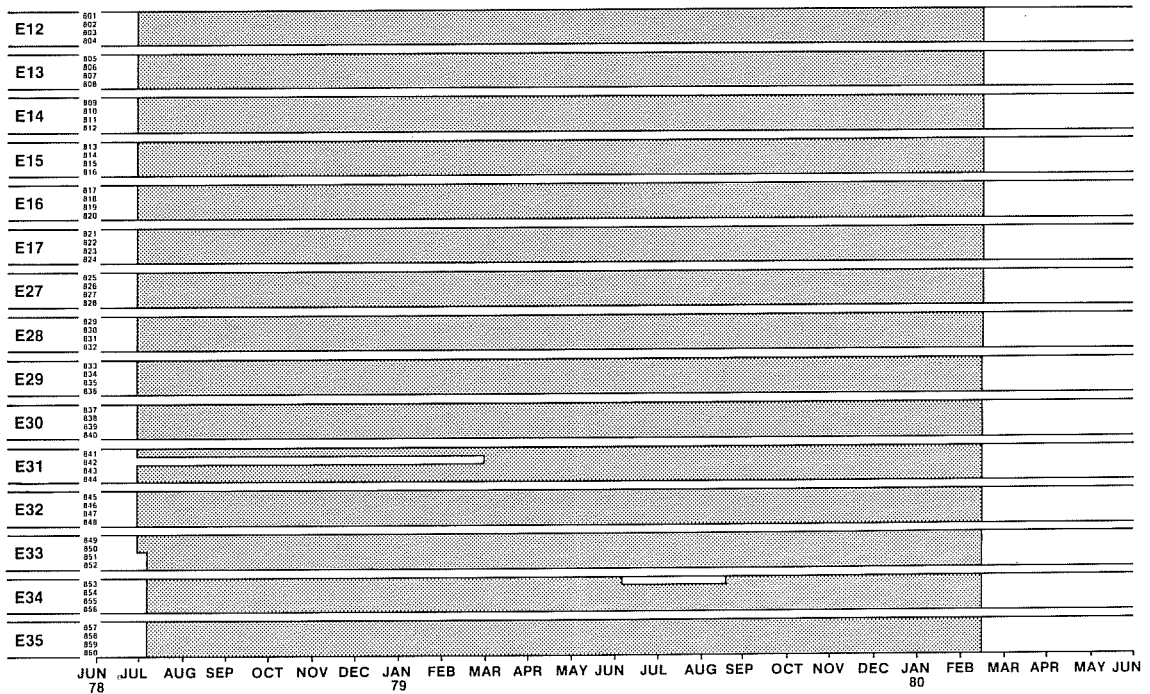
XBL 807-7230

Fig. B-17. Data collection periods (shaded regions) for H10: (A) USBM gauges, (B) IRAD gauges, (C) Thermocouples, and (D) Extensometers.

(c) Thermocouples



(d) Extensometers



XBL807-7227

Fig. B-17 (continued).

response curve (applied stress vs. the inverse square of the period) depended upon the setting period. Overall IRAD stability was good with most of the recovered gauges reading within ± 20 counts of their initial unloaded periods.

Thermocouple failures, shown in Fig. B-17(c), were largely restricted to those with stainless steel cladding, which corroded. Corrosion was accelerated both by the presence of moisture and by heat treatment prior to installation. Teflon-coated thermocouples--not shown in Fig. B-17(c)-- were used in lower temperature boreholes. They experienced some minor problems, caused by water infiltrating some of their junctions. Inconel-clad thermocouples, used in the high temperature environment, operated reliably but showed some signs of corrosion at the end of the experiments. Careful electrical grounding minimized other thermocouple problems.

The extensometers proved to be rugged and reliable instruments, as indicated by the low failure rate shown in Fig. B-17(d). Minor problems were experienced with the failure of one LVDT transducer, and with the accumulation of water in many of the horizontal and probably in some of the vertical extensometers. The main observable effect of the water was the corrosion of electrical connections at the heads. Soldering, waterproofing, and drainage helped. Water may also be corroding the elements down-hole over the long term, but there was no direct evidence for this.

Measured displacements on individual extensometer rods ranged from zero, observable on some of the outer horizontal rods, to 2120 microns gross displacement on one of the vertical rods. Incorporating the thermal expansion contribution of about 320 microns at 155°C results in a net rock displacement of 2440 microns. The high dynamic output of the displacement

transducers (2.1669 microns per millivolt) meant that the electronic voltage shifts in the WRRAIS's gain-ranging amplifiers did not noticeably affect the extensometer data.

Extensometer calibration stability was excellent. The original and final calibration constants generally agreed within $\pm 1\%$. Measurement sensitivity was limited by the least count of the analog-to-digital converter which was about three microns in the worst case. However, the interpretable limit will be determined by mechanical effects. After sticking caused by friction was identified as the source of step-like phenomena on the data records, extensometer heads were periodically thumped to release stored displacements, which were as large as 80 microns. Routine thumping is believed to have reduced the release magnitude, but a final assessment awaits the incorporation of bench test data with observed field results.

No problems were experienced with any of 18 electrical heaters throughout the experiments.

B.6 REFERENCES

- McEvoy, M.B. 1979. Data Acquisition, Handling, and Display for the Heater Experiments at Stripa. LBL-7062, SAC-14, UC-70. Berkeley, California: Lawrence Berkeley Laboratory.
- Schrauf, T., H. Pratt, E. Simonson, W. Hustrulid, P. Nelson, A. DuBois, E. Binnall, and R. Haught. 1979. Instrument Evaluation, Calibration, and Installation for the Heater Experiments at Stripa. LBL-8313, SAC-25, UC-70. Berkeley, California: Lawrence Berkeley Laboratory.

APPENDIX C. SENSOR PARAMETERS

Tables in this appendix summarize the calibration parameters used for converting the raw data to engineering units. These are identical to those contained in the SPF (sensor parameter file) on Tape 1 of the public-domain tapes.

Table C-1. Grouping of thermocouples by peak temperature.

Peak Temp (°C)	Sensor Number	Sensor Label
300-500	540, 541, 542 543, 544, 545 548, 549, 551, 552 554, 555, 557, 558 560, 561, 563, 564 566, 567, 569, 570 982, 983, 986, 987 990, 991, 994, 995 998, 999, 1002, 1003 1005, 1006, 1007 1009, 1010, 1011	TH10A, TH10B, TH10C TH10D, TH10E, TH10F TH11A, TH11B, TH12A, TH12B TH13A, TH13B, TH14A, TH14B TH15A, TH15B, TH16A, TH16B TH17A, TH17B, TH18A, TH18B TH1A, TH1B, TH2A, TH2B TH3A, TH3B, TH4A, TH4B TH5A, TH5B, TH6A, TH6B PROBE, TH7A, TH7B RACK, TH8A, TH8B
200-300	114, 115, 116 117, 118, 119 512, 522, 527 532, 537	TH9A, TH9B, TH9C TH9D, TH9E, TH9F T19C, T21C, T22C T23C, T24C
0-200	ALL THE REMAINING THERMOCOUPLES	

Table C-2. Thermocouple polynomial coefficients from NBS calibrations.

Temperature Range °C	Polynomial Coefficients				
	A	B	C	D	E
0-200	-.0544334	25.5679392	-.5652087	.08611938	-.00385947
200-300	.1139723	25.1789712	-.3857018	.05892778	-.0025899223
300-500	1.1004193	23.4824814	.2231085	-.015158225	.0002885662

Thermocouple Polynomial: $\text{Temperature} = A + BV + CV^2 + DV^3 + EV^4$
(V is corrected voltage in millivolts)

Table C-3. Sensor parameters for extensometers.

EXTENSOMETER SENSOR PARAMETERS FOR ENGINEERING CONVERSION (EXP 1)									
HOLE ID	SENSOR NUMBER	SENSOR LABEL	INITIAL VOLTAGE	CALIB CURVE SLOPE	HOLE ID	SENSOR NUMBER	SENSOR LABEL	INITIAL VOLTAGE	CALIB CURVE SLOPE
E6	291	E6A	-1.2350	2.2055	E19	321	E19A	-1.0950	2.1144
E6	292	E6B	-1.1638	2.1684	E19	322	E19D	-1.1963	2.1623
E6	293	E6C	-1.1313	2.1460	E20	323	E20D	-1.2075	2.1791
E6	294	E6D	-1.1688	2.1335	E20	324	E20C	-1.0575	2.1286
E7	295	E7A	-1.1613	2.1412	E20	325	E20B	-1.1363	2.1529
E7	296	E7B	-1.1338	2.1503	E20	326	E20A	-1.1325	2.1519
E7	297	E7C	-1.1013	2.1337	E21	327	E21D	-1.1650	2.1752
E7	298	E7D	-1.3363	2.2112	E21	328	E21C	-1.0875	2.1494
E8	299	E8A	-1.2913	2.2248	E21	329	E21B	-1.1213	2.1434
E8	300	E8B	-1.1625	2.1480	E21	330	E21A	-1.1663	2.1457
E8	301	E8C	-1.1913	2.1687	E22	331	E22D	-1.1125	2.1734
E8	302	E8D	-1.1113	2.1256	E22	332	E22C	-1.1225	2.1476
E9	303	E9A	-1.1413	2.1602	E22	333	E22B	-1.0913	2.1337
E9	304	E9B	-1.1213	2.1394	E22	334	E22A	-1.0925	2.1345
E9	305	E9C	-1.1313	2.1349	E22	335	E23D	-1.18875	2.1640
E9	306	E9D	-1.1438	2.1369	E23	336	E23C	-1.2263	2.1466
E10	307	E10A	-1.2263	2.1987	E23	337	E23B	-1.2300	2.1761
E10	308	E10B	-1.0150	2.1436	E23	338	E23A	-1.2400	2.1506
E10	309	E10C	-1.1400	2.1589	E24	339	E24B	-1.2138	2.1609
E10	310	E10D	-1.1238	2.1220	E24	340	E24C	-1.1200	2.1459
E11	311	E11A	-0.3734	2.3255	E24	341	E24D	-1.0750	2.1258
E11	312	E11B	-0.2771	2.4495	E24	342	E24A	-1.1050	2.1229
E11	313	E11C	-0.2051	2.2105	E25	343	E25D	-1.0750	2.1552
E11	314	E11D	-0.1033	2.5477	E25	344	E25C	-1.1263	2.1576
E18	315	E18D	-1.1525	2.1305	E25	345	E25B	-1.1063	2.1394
E18	316	E18A	-1.1400	2.1327	E25	346	E25A	-1.0563	2.1040
E18	317	E18B	-1.1338	2.1520	E26	347	E26D	-1.1250	2.1655
E18	318	E18C	-1.0363	2.1211	E26	348	E26C	-1.0825	2.1495
E19	319	E19C	-1.2350	2.1945	E26	349	E26B	-1.1313	2.1346
E19	320	E19B	-1.1950	2.1430	E26	350	E26A	-1.0725	2.1296

Table C-3. (continued).

EXTENSOMETER SENSOR PARAMETERS FOR ENGINEERING CONVERSION (EXP 2)

HOLE ID	SENSOR NUMBER	SENSOR LABEL	INITIAL VOLTAGE	CALIB CURVE SLOPE	HOLE ID	SENSOR NUMBER	SENSOR LABEL	INITIAL VOLTAGE	CALIB CURVE SLOPE
E12	801	E12B	-1.4300	2.1934	E28	831	E28B	-1.1100	2.1327
E12	802	E12C	-1.2540	2.1867	E28	832	E28A	-1.0075	2.0916
E12	803	E12D	-1.1038	2.1212	E29	833	E29D	--.85880	2.1442
E12	804	E12A	-.94380	2.1046	E29	834	E29C	-.84313	2.1291
E13	805	E13A	-1.1713	2.1781	E29	835	E29B	-.89688	2.1220
E13	806	E13B	-1.1500	2.15602	E29	836	E29A	-.81875	2.1074
E13	807	E13C	-1.0630	2.1359	E30	837	E30D	-1.2100	2.1806
E13	808	E13D	-1.0638	2.1266	E30	838	E30C	-1.1775	2.1808
E14	809	E14A	-1.0913	2.1816	E30	839	E30B	-1.18875	2.1477
E14	810	E14B	-1.0425	2.1243	E30	840	E30A	-1.16125	2.1451
E14	811	E14C	-.91690	2.1204	E31	841	E31D	-1.1350	2.1622
E14	812	E14D	-1.0263	2.1294	E31	842	E31B	-1.15875	2.1637
E15	813	E15A	-1.1063	2.1966	E31	843	E31A	-1.1475	2.1590
E15	814	E15B	-1.0680	2.1147	E31	844	E31C	-1.07875	2.1177
E15	815	E15D	-1.0363	2.1339	E32	845	E32D	-1.10125	2.1640
E15	816	E15D	-1.0050	2.1206	E32	846	E32C	-1.08625	2.1468
E16	817	E16A	-1.3513	2.2387	E32	847	E32B	-1.1200	2.1492
E16	818	E16B	-1.0900	2.1533	E32	848	E32A	-1.0400	2.1269
E16	819	E16C	-1.0975	2.1514	E33	849	E33D	-1.13875	2.1957
E16	820	E16D	-1.0650	2.1627	E33	850	E33C	-1.04375	2.1330
E17	821	E17A	-1.1213	2.1532	E33	851	E33B	-1.0300	2.1220
E17	822	E17B	-1.0300	2.1197	E33	852	E33A	-1.05125	2.1271
E17	823	E17C	-1.0300	2.1238	E34	853	E34D	-1.1875	2.1760
E17	824	E17D	-1.0550	2.1265	E34	854	E34C	-1.2000	2.1602
E27	825	E27D	-1.0963	2.1659	E34	855	E34B	-1.13125	2.1394
E27	826	E27C	-1.0825	2.1651	E34	856	E34A	-1.12125	2.2737
E27	827	E27B	-1.0600	2.1383	E35	857	E35D	-1.0425	2.1411
E27	828	E27A	-1.0788	2.1356	E35	858	E35C	-1.11125	2.1686
E28	829	E28D	-1.1625	2.1538	E35	859	E35B	-1.0375	2.1200
E28	830	E28C	-1.1938	2.1686	E35	860	E35A	-.97625	2.1086

EXTENSOMETER SENSOR PARAMETERS FOR ENGINEERING CONVERSION (EXP 3)

HOLE ID	SENSOR NUMBER	SENSOR LABEL	INITIAL VOLTAGE	CALIB CURVE SLOPE	HOLE ID	SENSOR NUMBER	SENSOR LABEL	INITIAL VOLTAGE	CALIB CURVE SLOPE
E1	1081	E1A	-1.2600	2.1642	E3	1091	E3C	-1.26125	2.1271
E1	1082	E1B	-1.2375	2.1209	E3	1092	E3D	-1.1850	2.0940
E1	1083	E1C	-1.2300	2.1293	E4	1093	E4A	-1.3200	2.1326
E1	1084	E1D	-1.24375	2.1114	E4	1094	E4B	-1.28125	2.0910
E2	1085	E2A	-1.41875	2.2026	E4	1095	E4C	-1.2300	2.1086
E2	1086	E2B	-1.2800	2.1301	E4	1096	E4D	-1.2300	2.1198
E2	1087	E2C	-1.2950	2.1089	E5	1097	E5A	-1.2525	2.1167
E2	1088	E2D	-1.3100	2.1091	E5	1098	E5B	-1.27625	2.1153
E3	1089	E3A	-1.23625	2.1224	E5	1099	E5C	-1.2300	2.1114
E3	1090	E3B	-1.2250	2.1116	E5	1100	E5D	-1.2050	2.0959

Table C-4 Sensor Parameter Records for USBM gauges. (a) Experiment 1 (H) Vertical USBM Gauges

Gauge Hole	Sensors	Date and Time		Temp at Time Zero C° (mV)	Zero Off-set	Rezero Offset	Calib. Curve Slope	USBM Temp Const	Sensor Label
		From	To						
U1-1	201	8/24/78	2/28/80	11.121	7.471	.106	.0686	-.320	U1A
U1-2	202	13:45	7:15		7.578	-.038	.0665	-.140	U1B
U1-3	203				10.732	2.445	.0662	.090	U1C
U2-1	204	8/24/78	9/17/80	10.440	5.571	.207	.0658	.0120	U2A
U2-2	205	13:45	10:45		5.947	.188	.0657	-.054	U2B
U2-3	206				6.772	.445	.0649	.012	U2C
U2-1	204	9/22/79	2/27/80	32.276	8.770	-.109	.0647	-.172	U2A
U2-2	205	16:45	12:00		8.535	-.028	.0645	.013	U2B
U2-3	206				7.295	-.275	.0656	.085	U2C
U3-1	207	8/24/78	2/21/79	10.793	7.041	-.110	.0645	.076	U3A
U3-2	208	13:45	11:30		7.627	2.140	.0656	0.047	U3B
U3-3	209				8.603	-.264	.0646	-.067	U3C
U4-1	210	8/24/78	2/25/80	11.550	7.666	.197	.0642	.242	U4A
U4-2	211	13:45	12:45		4.946	-.252	.0659	.231	U4B
U4-3	212				4.894	.397	.0655	0.0	U4C
U5-1	213	8/24/78	3/ 7/79	11.121	5.947	.299	.0651	.006	U5A
U5-2	214	13:45	12:00		5.561	-.235	.0658	.042	U5B
U5-3	215				7.891	2.750	.0637	.043	U5C
U5-1	213	9/11/79	2/25/80	26.913	7.715	.539	.0679	-.211	U5A
U5-2	214	14:45	8:15		8.672	-.641	.0672	-.142	U5B
U5-3	215				7.305	-.083	.0653	-.065	U5C
U6-1(C2)	216	8/24/78	10/ 4/78	11.222	6.143	.046	.0682	.029	U6A
U6-2(C2)	217	13:45	14:45		6.895	.362	.0661	-.017	U6B
U6-3(C2)	218				7.334	.304	.0653	.165	U6C
U6-1(C2)	216	8/10/79	2/26/80	48.567	8.984	1.111	.0658	.022	U6A
U6-2(C2)	217	12:45	7:45		6.680	-.053	.0648	-.060	U6B
U6-3(C2)	218				9.336	-.068	.0646	.011	U6C
U7-1	219	8/24/78	11/24/78	10.490	7.227	-.233	.0697	-.124	U7A
U7-2	220	13:45	9:45		8.193	-.038	.0632	-.208	U7B
U7-3	221				6.602	.631	.0668	-.039	U7C
U7-1	219	8/10/79	2/26/80	38.273	10.176	-.221	.0621	-.028	U7A
U7-2	220	12:45	12:15		9.346	-.049	.0650	-.122	U7B
U7-3	221				8.623	.636	.0677	.079	U7C
U8-1	222	8/24/78	10/11/78	10.440	8.281	.073	.0649	-.061	U8A
U8-2	223	13:45	14:30		8.623	.216	.0641	.058	U8B
U8-3	224				8.125	-.040	.0639	.048	U8C
U8-1	222	9/11/79	2/26/80	27.753	10.557	-.517	.0650	.090	U8A
U8-2	223	14:45	13:45		8.350	-.562	.0654	.003	U8B
U8-3	224				9.316	-1.617	.0647	.033	U8C
U9-1	225	8/25/78	4/10/79	11.045	5.244	-.463	.0581	.200	U9A
U9-2	226	13:45	9:00		7.334	-.033	.0695	.008	U9B
U9-3	227				7.529	.630	.0671	.093	U9C
U9-1	225	8/22/79	2/27/80	32.943	11.318	.421	.0570	.039	U9A
U9-2	226	19:15	9:00		9.092	-.230	.0646	-.130	U9B
U9-3	227				8.428	.049	.0655	.102	U9C
U10-1	228	8/24/78	2/27/80	10.919	4.844	.057	.0651	-.026	U10A
U10-2	229	13:45	7:15		5.020	-.154	.0662	.091	U10B
U10-3	230				6.563	.097	.0658	0.000	U10C

Table C-4(b) Experiment 1 (H9) Horizontal USBM Gauges.

Gauge Hole	Sensors	Date and Time		Temp at Time Zero C° (mV)	Zero Off-set	Rezero Offset	Calib. Curve Slope	USBM Temp Const	Sensor Label
		From	To						
U21-1	231	8/24/78	1/24/80	10.742	4.331	-.003	.0713	-.054	U21A
U21-2	232	13:45	15:00		3.716	-.258	.0694	-.074	U21B
U21-3	233				5.669	.003	.0667	-.252	U21C
U22-1	234	8/24/78	2/ 8/80	10.742	5.063	-.166	.0661	-.085	U22A
U22-2	235	13:45	8:15		4.971	-.418	.0673	.042	U22B
U22-3	236				4.248	-1.530	.0666	-.066	U22C
U26-1	237	8/24/78	2/ 7/80	10.187	5.537	.290	.0641	.055	U26A
U26-2	238	13:45	14:15		8.242	.763	.0655	-.006	U26B
U26-3	239				6.079	.242	.0643	.020	U26C
U27-1	240	8/24/78	2/ 8/80	10.313	4.643	.518	.0626	-.139	U27A
U27-2	241	13:45	8:45		5.337	.454	.0631	.026	U27B
U27-3	242				6.592	-.141	.0650	.130	U27C
U28-1	243	8/24/78	2/ 8/80	10.364	4.648	.079	.0625	-.158	U28A
U28-2	244	13:45	11:30		6.772	-1.580	.0663	-.113	U28B
U28-3	245				5.898	-.589	.0666	0.000	U28C

Table C-4(c) Experiment 2 (H10) Vertical USBM Gauges.

Gauge Hole	Sensors	Date and Time		Temp at Time Zero C° (mV)	Zero Off-set	Rezero Offset	Calib. Curve Slope	USBM Temp Const	Sensor Label
		From	To						
U11-1	711	7/ 3/78	2/20/79	11.745	7.617	.177	.0645	.033	U11A
U11-2	712	6:45	8:45		6.336	.262	.0656	-.058	U11B
U11-3	713				6.049	1.765	.0657	-.070	U11C
U11-1	711	6/27/79	1/28/80	116.142	10.342	-1.178	.0638	.059	U11A
U11-2	712	12:00	12:30		9.727	1.146	.0652	-.038	U11B
U11-3	713				9.863	.906	.0639	-.1127	U11C
U12-1	714	7/ 3/78	12/18/78	11.014	4.585	-.040	.0666	.057	U12A
U12-2	715	6:45	13:45		4.406	.118	.0650	-.214	U12B
U12-3	716				5.884	.021	.0657	-.171	U12C
U12-1	714	1/20/79	4/10/79	29.192	5.493	.075	.0676	.075	U12A
U12-2	715	12:45	9:00		6.489	.275	.0653	-.150	U12B
U12-3	716				7.207	.075	.0690	-.175	U12C
U12-1	714	7/29/79	1/28/80	53.677	8.623	.109	.0643	-.018	U12A
U12-2	715	14:45	8:15		8.926	-.595	.0653	.153	U12B
U12-3	716				7.246	-.308	.0696	-.114	U12C
U13-1	717	7/ 3/78	9/26/78	11.065	6.680	.113	.0650	.146	U13A
U13-2	718	6:45	8:45		9.170	-.010	.0645	-.650	U13B
U13-3	719				8.640	-.183	.0638	-.045	U13C
U13-1	717	1/20/79	2/20/79	43.641	4.873	.100	.0622	-.075	U13A
U13-2	718	12:45	8:45		6.123	-1.250	.0650	0.0	U13B
U13-3	719				5.396	-1.250	.0647	-.125	U13C
U13-1	717	7/ 9/79	1/28/80	86.406	8.760	.032	.0676	-.098	U13A
U13-2	718	9:30	11:45		9.150	1.113	.0641	-.022	U13B
U13-3	719				8.164	-1.107	.0657	.096	U13C
U14-1	720	7/ 3/78	7/ 3/78	11.065	5.629	.128	.0645	.136	U14A
U14-2	721	6:45	6:45		6.406	-.152	.0644	-.183	U14B
U14-3	722				6.712	-.190	.0643	-.025	U14C
U14-1	720	9/ 6/78	12/ 6/78	25.420	5.439	.405	.0629	-.156	U14A
U14-2	721	18:00	8:45		10.664	1.538	.0627	.087	U14B
U14-3	722				5.630	.237	.0638	-.042	U14C
U14-1	720	1/20/79	2/20/79	31.489	5.439	.110	.0643	-.160	U14A
U14-2	721	12:45	8:45		7.422	-.010	.0631	.060	U14B
U14-3	722				5.020	-.020	.0641	.150	U14C
U14-1	720	7/15/79	1/28/80	58.570	6.880	-.411	.0675	-.043	U14A
U14-2	721	10:00	10:45		10.147	-.496	.0645	.193	U14B
U14-3	722				9.395	.429	.0670	-.064	U14C
U15-1(C3)	723	7/ 3/78	1/15/79	11.115	4.671	-.190	.0666	-.086	U15A
U15-2(C3)	724	6:45	8:30		5.323	.105	.0683	.022	U15B
U15-3(C3)	725				6.703	.081	.0692	.208	U15C
U15-1(C3)	723	6/27/79	2/22/80	125.965	10.215	.158	.0647	-.050	U15A
U15-2(C3)	724	12:00	8:15		10.488	.070	.0648	.035	U15B
U15-3(C3)	725				9.805	-.001	.0616	-.037	U15C
U16-1	726	7/ 3/78	9/11/78	11.241	4.803	-1.354	.0657	-.146	U16A
U16-2	727	6:45	14:45		7.027	.066	.0691	.034	U16B
U16-3	728				5.611	.327	.0659	-.261	U16C
U16-1	726	9/26/78	2/20/79	30.586	9.434	.113	.0633	.146	U16A
U16-2	727	10:15	8:45		9.404	-.010	.0633	-.650	U16B
U16-3	728				7.588	-.183	.0634	-.045	U16C
U16-1	726	7/17/79	1/16/80	64.247	8.086	.402	.0672	.088	U16A
U16-2	727	12:00	11:00		9.941	.100	.0653	-.090	U16B
U16-3	728				10.293	.114	.0682	.112	U16C
U17-1(C4)	729	7/ 3/78	8/ 1/78	11.014	9.467	-.221	.0645	.038	U17A
U17-2(C4)	730	6:45	13:15		6.653	.117	.0655	.038	U17B
U17-3(C4)	731				7.770	-.079	.0635	-.117	U17C
U17-1(C4)	729	1/20/79	2/20/79	39.529	4.854	0.000	.0666	0.000	U17A
U17-2(C4)	730	12:45	8:45		7.607	.075	.0649	.050	U17B
U17-3(C4)	731				8.174	-.820	.0643	-.105	U17C
U17-1(C4)	729	7/29/79	1/28/80	77.950	8.623	.171	.0673	-.087	U17A
U17-2(C4)	730	14:45	14:15		9.072	.607	.0644	.076	U17B
U17-3(C4)	731				8.291	.215	.0677	.144	U17C
U18-1	732	7/ 3/78	1/ 3/79	11.745	6.264	.008	.0640	-.165	U18A
U18-2	733	6:45	11:45		6.360	.049	.0647	-.151	U18B
U18-3	734				6.244	-.485	.0645	-.120	U18C
U18-1	732	1/20/79	2/20/79	45.248	3.679	.040	.0693	-.115	U18A
U18-2	733	12:45	8:45		7.656	-.110	.0645	-.135	U18B
U18-3	734				8.301	-.200	.0647	-.125	U18C
U18-1	732	7/ 2/79	10/ 1/79	88.935	4.736	.001	.1757	-.007	U18A
U18-2	733	8:15	9:15		4.531	.120	.1764	.014	U18B
U18-3	734				4.800	.389	.1742	.006	U18C

Table C-4(c) (cont'd) Experiment 2 (H10) Vertical USBM Gauges (continued).

Gauge Hole	Sensors	Date and Time		Temp at Time Zero C° (mV)	Zero Off-set	Rezero Offset	Calib. Curve Slope	USBM Temp Const	Sensor Label
		From	To						
U19-1	735	7/ 3/78	5/15/79	11.745	4.826	-.100	.0637	-.049	U19A
U19-2	736	6:45	13:30		6.404	.331	.0656	-.149	U19B
U19-3	737				5.089	-.698	.0655	-.175	U19C
U19-1	735	7/17/79	1/28/80	56.163	7.920	-1.069	.0681	.009	U19A
U19-2	736	12:00	13:30		9.189	-.446	.0681	.297	U19B
U19-3	737				9.150	-.025	.0652	.008	U19C
U20-1	738	7/ 3/78	7/17/78	11.014	5.473	.065	.0655	.008	U20A
U20-2	739	6:45	6:45		5.735	.522	.0643	0.000	U20B
U20-3	740				5.711	-.052	.0666	.087	U20C
U20-1	738	1/20/79	7/17/79	25.675	8.184	-.050	.0655	-.300	U20A
U20-2	739	12:45	14:15		7.383	.100	.0698	.175	U20B
U20-3	740				7.891	.700	.0666	-.350	U20C

Table C-4(d) Experiment 2 (H10) Horizontal USBM Gauges.

Gauge Hole	Sensors	Date and Time		Temp at Time Zero C° (mV)	Zero Off-set	Rezero Offset	Calib. Curve Slope	USBM Temp Const	Sensor Label
		From	To						
U23-1	741	7/ 3/78	4/27/79	11.241	6.121	-.015	.0680	-.195	U23A
U23-2	742	6:45	8:45		8.389	1.560	.0667	.114	U23B
U23-3	743				7.374	.007	.0678	.020	U23C
U24-1	744	7/ 3/78	2/ 6/80	11.191	6.806	1.714	.0631	-.065	U24A
U24-2	745	6:45	15:00		3.287	-.283	.0638	-.186	U24B
U24-3	746				5.049	-.298	.0655	.101	U24C
U25-1	747	7/ 3/78	4/26/79	11.191	6.118	-.344	.0641	-.100	U25A
U25-2	748	6:45	8:15		7.169	.153	.0642	-.019	U25B
U25-3	749				5.427	-.898	.0648	-.032	U25C
U29-1	750	7/ 3/78	1/22/80	10.384	4.991	.369	.0674	-.024	U29A
U29-2	751	6:45	11:15		3.459	-.237	.0687	-.374	U29B
U29-3	752				4.812	.061	.0660	.205	U29C
U30-1	753	7/ 3/78	2/ 7/78	10.636	7.156	-.308	.0668	.128	U30A
U30-2	754	6:45	14:45		5.209	-.085	.0661	-.069	U30B
U30-3	755				8.918	-.347	.0687	.219	U30C

Table C-5 Time-Table for Bad* Data for USBM Gauges.

Sensor Number	Sensor Label	Date and Time			
		From		To	
206	U2C	7/30/79	14:31	9/18/79	00:00
221	U7C	1/24/80	11:34	2/27/80	00:00
233	U21C	2/21/79	08:04	1/25/80	00:00
740	U20C	5/ 4/79	08:38	7/18/79	00:00
752	U29C	4/ 9/79	13:33	1/22/80	00:00

*Bad data here means that one of the two components 2 and 3 (labeled B and C) of a USBM gauge is bad while the other component is good.

APPENDIX D. PLOTS AND LISTINGS OF ENGINEERING DATA ON MICROFICHE

This appendix consists of a set of microfiche which is available upon written request of

Earth Sciences Division
Lawrence Berkeley Laboratory
One Cyclotron Road
Bldg. 90; Room 1106
Berkeley, California 94720

(please specify LBL Report No. 11477, SAC-29; Appendix D). All time-averaged engineering data are plotted against experiment time on these microfiches. The listings are arranged in the same order as on the public-domain tape, as described in Section 8. The plots are in slightly different order, but each one is individually captioned.

Note that, on the power history plots for the peripheral heaters, some data were recorded before the heaters were turned on (experiment day 204). These are calibration data and should be ignored.

In plots for thermocouple temperatures for the time-scaled experiment, the data were cut off at 550 days (experiment time) because of computer memory limitations. Data beyond 550 days are calibration data only, and are of little interest for graphical presentation.

This report is part of a cooperative Swedish-American project supported by the U.S. Department of Energy and/or the Swedish Nuclear Fuel Supply Company. Any conclusions or opinions expressed in this report represent solely those of the author(s) and not necessarily those of The Regents of the University of California, the Lawrence Berkeley Laboratory, the Department of Energy, or the Swedish Nuclear Fuel Supply Company.

Reference to a company or product name does not imply approval or recommendation of the product by the University of California or the U.S. Department of Energy to the exclusion of others that may be suitable.

TECHNICAL INFORMATION DEPARTMENT
LAWRENCE BERKELEY LABORATORY
UNIVERSITY OF CALIFORNIA
BERKELEY, CALIFORNIA 94720

